Response to the review of J. Middelburg

The authors present a rather complex model allowing simulation of biogeochemical processes in coastal systems subject to seasonal anoxia. The paper has a few strengths and many weaknesses. Most numerical biogeochemical models focus ei- ther on the water column or on the sediments and very few couple these domains. The presented BROM model **does explicitly deal with the coupled system** and is therefore of value.

Strengths of this paper include the (a) coupling of pelagic and benthic modules, (b) the explicit resolution of the benthic boundary layer (BBL), (c) the focus on seasonal hypoxia and (d) its linkage to/integration with the Framework for Aquatic Biogeochemical Modeling. These characteristics make this an interesting paper and the presented model is potentially useful.

However, there are many issues to be resolved before publication of this paper and model. 1. The paper is poorly written in terms of organization, flow and **use of English**. A few examples of the latter (line 1: seawater and benthic sediments, benthic sys- tems or sediments are fine, but not benthic sediments; the use of the term protolithic processes: do you refer to stone age processes? or do you simply mean equilibrium processes, etc. etc.). There appear native speakers and/or UK/Canada based scientists among the authors: perhaps they should have another look at it. The text is also not prepared with utmost care: many typos, wrong equations etc. (see below in the list of detailed comments).

We apologize for the condition of the original submitted manuscript, and thank the Reviewer for nevertheless providing a detailed and constructive review which has contributed to a major improvement (in our opinion) in the model code and description. The new submission has been thoroughly revised to improve structure, language, and accuracy of the equations.

The model could be much better put in context and **existing literature** is poorly incorporated. I was missing references to other papers dealing with coupled benthic-pelagic models, the more simpler ones (Lancelot, Soetaert, Fennel, Reed and co-workers) and the highly complex ones from the ERSEM family. Soetaert and co-workers (Soetaert and Middelburg, 2009; Meire et al., 2013) have published on seasonal oxygen issues with coupled pelagic benthic models. There is also a large body of knowledge on the effect of oxygen in early diagenetic models; that literature is not covered. Extensive work on the role of sediments as moderating the timing of return fluxes (delay in return of N, P, Si after bloom) and the memory provided by stored reduced sulfur, iron and carbon in sediments is poorly covered (see work on Gulf of Mexico by Nancy Rabalais and co-workers).

We thank the reviewer for drawing our attention to this work, which is indeed highly relevant. The Background section has been extended to provide a more thorough summary of existing literature, including all of the models cited above. It remains, however, a summary and not an in-depth review; the latter is beyond our intended scope.

The model **description** is often incomplete and imprecise (see below for a far from complete list). The documentation is not sufficient. Boundary conditions of the model are not clearly described. Details about the coupling of the models are insufficient: e.g. the grid size is very likely changing, yet not provided. It is unclear whether particulate organic matter is modeled explicitly. Is it transported by bioturbation in the sediment. It is unclear how bio-irrigation and solid-phase mixing are treated.

Sometimes parameters are introduced in the text, but appear as fixed value (hard-coded) in the tables.

We acknowledge and apologize for these shortcomings. The new submission offers a much more thorough description. Boundary conditions are now described in a dedicated section 2.2.5. The BROM-transport grid, which combines water column and sediment subgrids, is now described in a dedicated section 2.2.3. Dead particulate organic matter is explicitly modeled, as is now stated clearly in section 2.1.2. Particulate variables are diffused in the sediment by bioturbation – this is now clarified in section 2.2.1 which describes the BROM-transport model formulation. In BROM-transport, bio-irrigation is treated as a non-local exchange process following (Boudreau, 1997; Schluter et al., 2000; Meile et al., 2001) (see section 2.2.1). Mixing of solid phase constituents is only by bioturbation in the sediments. Mixing of the solid phase as a whole (interphase mixing) in BROM-transport may occur only by bioturbation at the sediment-water interface. These processes are now clearly described in the new section 2.2.1.

The model is very complex and detailed (perhaps too much) in some aspects and very rudimentary in other aspects. Regarding the latter, many detailed Mn, Fe, S transformations are included, chemoautotrophy is resolved for aerobic and anaerobic microbes (or only bacteria?), but important processes such as methane generation and anaerobic methane oxidation coupled to sulfate reduction are ignored. Another example particle settling velocities is corrected for the formation of Mn-oxides in the water column but other carrier phases such as calcium carbonate are not resolved. Clearly, the presented model is a version 1.0 and represents a first step, but the priorities of the authors do not match those of the majority of the audience. At the minimum some motivation for their particular choice should be communicated to the audience.

The motivation for the complexity of BROM is discussed in the new text (section 2.1.1):

"The model has 33 state variables (Ci), described in Table 1. This includes frequently measured components such as hydrogen sulfide (H2S) and phosphate (PO4), as well as rarely measured variables such as elemental sulfur (S0), thiosulfate (S2O3), trivalent manganese species Mn(III), and bacteria. Variables of the latter category were included because their contribution to biogeochemical transformations is believed to be substantial. For instance, bacteria play an important role in many modelled processes and can consume or release nutrients in organic and inorganic forms (Canfield et al., 2005; Kappler et al., 2005). We acknowledge that for many of these additional variables, site-specific estimates of associated model parameters and initial/boundary conditions may be difficult or impossible to obtain, and may in practice require some crude assumptions and approximations (e.g. universal default parameter values, no-flux boundary conditions, initial conditions from a steady annual cycle). Nevertheless, we believe that for many applications this will be a price worth paying for the additional process resolution/realism provided by BROM for important biogeochemical processes in the BBL and sediments."

The definition of the “bacteria” model compartment is made precise in the new text:

"We divide all the living OM (biota) into Phy (photosynthetic biota), Het (non-microbial heterotrophic biota), and 4 groups of "bacteria" which may be considered to include microbial fungi."

The processes of methanogenesis and methane oxidation with oxygen have been added to BROM-biogeochemistry.

The effect of accelerated particle settling velocities has in fact been removed in the new code, and the text has been adjusted accordingly.

Section 3.1 on model output **discussion** needs major revision. The link with the figures is unclear and the organization is suboptimal. You discuss the oxygenated winter period and then link to later periods or a few days later in the section on oxygenated winter period. There is no **story**. Try **to limit yourself to a few findings and discuss those**. The reader now has to digest all the computer output her or himself.

Section 3 was shortened and re-structured. Following the reviewers' recommendations we now just focus on describing the ability of BROM to simulate changes in the redox conditions and illustrating the rates of processes and transport fluxes.

Section 3.2 is not useful or convincing. The link with data is very poor. This is indeed a difficult job, but here serious work has been done. A comparison with just three to four papers is made and the extensive databases on oxygen uptake, oxygen penetration depth etc are not consulted. A statement like line 10 on page 20: “further observations under anoxic and suboxic conditions are rare as field and experimental studies generally focus on oxic conditions” is close to unacceptable. Consider all the work done on the Eastern Pacific ocean margins (Washington and Oregon shelves, California basins, Mexico/Peru/Chile margin), Indian ocean and shelves and multiple European systems (Black Sea, Baltic Seas). There are nice seasonal time series in coastal systems with low-oxygen events during summer (Kiel bight, etc.)

Section 3.2. was removed from the text.

Minor issues:

Page 3: - Line 2: benthic sediments? –

Modified to "benthic systems"

Line 3: directly affect and are impacted by.. –

Sentence modified to:

"Benthic fluxes of chemical elements (C, N, P, O, Si, Fe, Mn, S) alter redox state and acidification (i.e. pH and carbonate saturation), which in turn affect the functioning of benthic and pelagic ecosystems."

Line 7: fuzzy writing, rewrite

Sentence modified to:

"The redox state of the near bottom layer in many regions can change with time, responding to the supply of organic matter, physical regime and coastal discharge."

Page 4: - Line 3: enrichment with OM or do you mean deposition of labile organic matter –

Sentence modified to:

"The sediment generally consumes oxygen due to deposition of labile OM and presence of reduced forms of chemical elements"

Line 26-27: animals can die, migrate or change their behavior: revise text accordingly

Modified to:

"This may lead to death, migration, or changed behavior of the benthic macro- and meiofaunal organisms responsible for bioturbation and bioirrigation…"

Page 5: - Line 4-15: **additional literature** incorporation required. How does your model differ from those. Where are the improvements etc.

Additional literature has been incorporated in the new Background section. The ways in which BROM differs from existing models are now explicitly listed in the final paragraph of this section.

- Line 22: the benthic boundary layer is a major strength. Introduce it better. Delineate the features, etc. –

The BBL is now better introduced in the second last paragraph of the Background:

"The BROM model described herein is a fully coupled benthic-pelagic model with a special focus on deoxygenation and redox biogeochemistry in the sediments and Benthic Boundary Layer (BBL). The BBL is "the part of the marine environment that is directly influenced by the presence of the interface between the bed and its overlying water" (Dade et al., 2001). Physical scientists tend to prefer the term "bottom boundary layer", but this is largely synonymous with the BBL (Thorpe, 2005). Within BROM, the term BBL is used to refer to the lower parts of the fluid bottom boundary layer where bottom friction strongly inhibits current speed and vertical mixing, hence including the viscous and logarithmic sublayers up to at most a few metres above the sediment. This calm-water layer plays a critical role in mediating the interaction of the water column and sediment biogeochemistry and in determining e.g. near-bottom oxygen levels, yet it remains poorly resolved in most physical circulation models. For BROM we have developed an accompanying offline transport module "BROM-transport" that uses output from hydrodynamic water column models but solves the advection-diffusion-reaction equations for a "full" grid including both water column and sediments. BROM-transport uses greatly increased spatial resolution near to the SWI, and thereby provides explicit spatial resolution of the BBL and sediments."

Line 24: at the BBL: do you exclude the sediments here?

Our BBL definition does exclude the sediments (see above), but the scope of BROM does not. This scope or goal is now better defined:

"The goal of this work was to develop a model that captures key biogeochemical processes in the water and sediment and to analyze the changes occurring in the BBL and SWI."

Page 6: - line 9-10: it is unclear whether organic C is also modeled or is it just inorganic

C. - Line 12: No nitrogen transformations?

Only inorganic C is explicitly modeled (state variable name DIC). Organic matter (dissolved and particulate) is modeled only in nitrogen currency (variable names DON and PON) so to derive organic C estimates from model output would require use of a stoichiometric ratio C:N. Nitrogen transformations are modelled. The new manuscript reads:

"BROM considers interconnected transformations of species of (N, P, Si, C, O, S, Mn, Fe) and resolves OM in nitrogen currency. OM dynamics include parameterizations of OM production (via photosynthesis and chemosynthesis) and OM decay via oxic mineralization, denitrification, metal reduction, sulfate reduction and methanogenesis."

Page 7: - Line 2: delete consists

Done

- Line 26 and all through: replace protolithic processes with **equilibrium processes/reactions or acid-base reactions**

Done

Page 8: - Line 11: provide the number of state variables to the reader

Done (33).

Page 9: - Line 1: chemoautotrophy is resolved, but overall **secondary production** is ignored. There may be good reasons for this, but communicate this then to the reader

Secondary production is resolved. The state variable 'Het' represents all non-microbial heterotrophs. These graze the phytoplankton as well as bacteria and detritus, and they reach significant concentrations in both pelagic and benthic parts of the model domain. The new section 2.1.2 reads:

"…We divide all the living OM (biota) into Phy (photosynthetic biota), Het (non-microbial heterotrophic biota), and 4 groups of "bacteria" which may be considered to include microbial fungi. These latter are: Baae (aerobic chemoautotrophic bacteria), Baan (anaerobic chemoautotrophic bacteria), Bhae (aerobic heterotrophic bacteria), and Bhan (anaerobic heterotrophic bacteria). OM is produced photosynthetically by Phy and chemosynthetically by bacteria, specifically by Baae in oxic conditions and by Baan in anoxic conditions. Growth of heterotrophic bacteria is tied to mineralization of OM, favouring Bhae in oxic conditions and Bhan in anoxic conditions. Secondary production is represented by Het which consumes phytoplankton as well as all types of bacteria and detritus…"

- Line 8-10: why is methanogenesis excluded? This is probably related to the way you model organic matter. Conceptually most simple is to turn all labile organic matter remaining after depletion of all oxidants into methane and carbon dioxide.

Methanogenesis is included in the new, modified version

- Line 15- 25: the alkalinity equations as given are wrong: the phosphate alkalinity term should include a H3PO4 term, the ammonium alkalinity term should not include NH4+, etc. Please check whether you have implemented it correctly into your model.

Checked and corrected.

Page 10:-Line 2: I guess you mean Atom was set to zero and not TOM.

Correct. In the new text, the TOM alkalinity is removed.

Page 11: -Line 1-10: quite a number of the reactions are not balanced and inconsistent with Table 2: e.g. denitrification with hydrogen sulfide and the line above represent two reactions of which the latter misses a two before OH-. Check carefully. -Line 11: Table 2 not 3.

Apologies for our sloppy editing. All equations have now been carefully checked and corrected.

Page 12: middle of page: a distinction is made between settling velocity of particulate matter and of particles with Fe and Mn oxides. Why not write particle settling velocities (w) as a sum of various contributing terms. Why the focus on Fe and Mn? Just a Black Sea model heritage?

In the new version, all the inorganic particles sink at the same constant velocity, and this velocity is larger than all organic matter sinking velocities.

Page 13: - Line 8: the eddy diffusion coefficient was assumed constant in the BBL. As a first coupled model that resolves the BBL **it may be done like this**, but given the **lognormal velocity profiles,** would one not expect a depth profile in Kz as well. This can be incorporated quite easily.

A good suggestion, thanks. In the new version, Kz (now D, to be more conventional) can have a linear depth variation either if it is treated dynamically or assuming a static log layer. This is now described in section 2.2.7:

"The vertical diffusivity needs a more careful treatment as it is the main defining characteristic of the pelagic vs. BBL vs. sediment environments. Within the water column, the total vertical diffusivity D = Dm + De for solutes and D = De for particulates, where Dm is a constant molecular diffusivity at infinite dilution, and De is the eddy diffusivity read from the input file for the pelagic water column. For the BBL, De can be defined as "dynamic", in which case it is linearly interpolated for each day between the deepest input forcing value above the SWI and zero at a depth h¬DBL above the SWI, where h¬DBL is the diffusive boundary layer (DBL) thickness (default value 0.5 mm). This option is likely appropriate for shallow water applications where De may be strongly time-dependent within the user-defined BBL (default thickness 0.5 m). Alternatively, a static, fixed profile D¬eBBL(z) may be more appropriate for deep water BBLs, where time dependence may be weak and deepest values from hydrodynamic models may be relatively far above the SWI. In this case, BROM-transport offers two options for D¬eBBL(z): 1) a constant value, dropping to zero in the DBL, or 2) a linear variation between a fixed value at the top of the BBL and zero at the top of the DBL. Option 1) defines a simplest-possible assumption, while option 2) corresponds to the assumption of a log layer for the current speed (e.g. Boudreau and Jorgensen, 2001). Eddy diffusivity is strictly zero in the DBL, on the SWI, and within the sediments. Diffusivity in the sediments is due to molecular diffusion and bioturbation and is parameterized as described in section 2.2.1."

- Line 15-20: the description of bioturbation/bioirrigation is difficult to follow. As written above are solid phase and solutes transported separately or together? This is unclear. Bioturbation depth are very shallow for fully oxic conditions.

This part of the model was significantly improved and is clearly described in the new section 2.2.1. Solid and liquid phases are diffused separately (intraphase mixing) except possibly at the sediment-water interface if the option to allow bioturbation across the SWI is enabled. Solute diffusivity in the sediments is a sum of molecular diffusivity, corrected for tortuosity and relative viscosity following Boudreau (1997), and bioturbation diffusivity, depending on a fixed vertical profile and a time-dependent oxygen status of the bottom layer of the water column (fluff layer). Particulate diffusivity in the sediments is just the bioturbation diffusivity. Solute burial velocity also now differs from particulate burial velocity due to the effects of compaction (Boudreau, 1997). Burial velocities now also depend on depth under an assumption of steady state compaction (Berner, 1970, 1981; Boudreau 1997; Meysman et al., 2005) and additional velocity components can optionally be added to account for modelled particulate fluxes to the SWI and particulate reactions in the sediments (see section 2.2.1 and Appendix B).

The current default "mixed layer" depth for bioturbation is 2 cm (cf. values 5 cm and 1 cm used by Soetaert and Middelburg (2009) for well-mixed and anoxic conditions respectively). The default decay scale for bioturbation diffusivity below the mixed layer is 1 cm, following Soetaert and Middelburg (2009). This information is now included in the run-time input file brom.yaml (see Appendix D). We agree that a 2 cm mixed layer may be too shallow for fully oxic conditions; in such cases the user should increase the mixed layer depth parameter in the brom.yaml file.

Section 2.3. The description of boundary conditions needs more attention. It appears that you use flux boundary conditions for the gases and constant or fixed (at least im- posed) boundary for the others. This may lead to mass balance issues. The boundary conditions at the bottom (depth 12 cm in sediments) are not described: no flux or **no gradient** or fixed concentration? The assumed sulfate concentration is either close to zero or do you mean 25 10-3M? Basically all external sources such as atmosphere and rivers are added to surface layer.

In the new BROM-transport code we allow four different options to define boundary conditions (upper and lower) for each variable. For the upper boundary (air-sea interface) the default option is no flux, unless the flux is specifically parameterized by the (FABM) biogeochemical model. For BROM-biogeochemistry this means that, by default, all variables have no flux surface boundary conditions except oxygen and DIC, which have fluxes parameterized using atmospheric oxygen and CO_2 levels prescribed in the brom.yaml file (see Appendix D). Optional fixed (Dirichlet) boundary conditions do indeed imply mass fluxes into or out of the modelled water column, but this need not be unrealistic. We have found in fjord and lake applications that fixed (possibly time-dependent) surface boundary condition can provide a way of modelling missing net influxes of nutrients from rivers. Boundary conditions at depth are no-gradient by default (advective outfluxes can still occur due to burial velocity). External sources (e.g. from rivers) can also be allowed to contribute directly to the model interior by setting the "horizontal mixing" forcings, rather than by setting boundary conditions. This all described in the new section 2.2.5:

"BROM-transport presently allows the user to chose between four different types of boundary condition for each variable and for upper and lower boundaries: 1) no-gradient at the bottom boundary (no diffusive flux) or no-flux at the surface boundary, except where parameterized by the FABM

biogeochemical model (i.e. for O2 and DIC in the case of BROM-biogeochemistry); 2) a fixed constant value; 3) a fixed sinusoidal variation in time defined by amplitude, mean value, and phase parameters; or 4) an arbitrary fixed variation in time read from the input netCDF file. All boundary condition options and parameters are set in the brom.yaml file (see Appendix D). Note that options 2-4 are Dirichlet boundary conditions which define implicit fluxes of matter into and out of the model domain, and that all boundary concentrations should be in units [mmol/m3 total volume (water+solids)]. The default option 1 is generally the preferred choice, but the Dirichlet options can also be useful to allow a simple representation of e.g. fluxes of nutrients into and out of the surface layer due to lateral riverine input. A possible alternative is to use the forcings parameters for horizontal mixing (see equation (1)) to specify horizontal exchanges or restoring terms to observed climatology (see section 2.2.7)."

For the sulfate upper and lower boundary conditions we have used Dirichlet conditions of 25000 uM (or mmol/m3) for both.

Section 3: I stop making detailed feedback because there are too many issues and the referee already spent double the amount of time normally needed for an evaluation.

Again we sincerely apologize for the condition of the original submitted manuscript. We are confident that the new version will not require so much correction.

p. 26, line 5-9: chemoautotrophy indeed involves CO2 consumption and thus has the potential to increase pH. However, the energy required for CO2 fixation is obtained from oxidation of reduced products: usually an acid producing process. With typical growth efficiencies one would produce more acid linked for the energy than consumption of acid by organic matter production. Cable-bacteria spatially disconnect half reactions and can therefore cause a real pH increase. Without detailed model investigations, I suggest removing these sentences. The authors might be right because of the com- plexity of reactions and the many buffering reactions, but it is not convincing as pre- sented here.

This part of discussions was removed from the modified version.

Table 1: it is stated that oxygen is presented in microM O, but sometimes it might be, at other places it is definitely in microM O2.

Corrected. O2 is now always present in microM O2.

Table 2: - Aerobic respiration and denitrification are treated different than Fe, Mn and sulfate reduction regarding DON and PON separation. - For Mn reduction where does the 0.5 come from (half saturation constant hard-coded?) - There are multiple typos which complicate checking. - Where is the (1+ftD(t)) term coming from. ftD is not defined. - Page 41: I guess that NO3 dependence should depend on nitrate and not on ammonia?

Apologies again. Table 2 has now been checked and corrected.

The factor 0.5 in the Mn reduction formulations is not a hard-coded half saturation constant (all half saturation constants are input parameters in fabm.yaml). It is rather there to ensure that the specific Mn reduction rates at high Mn concentration (tanh function tending to unity) and high H_2S concentration (Michaelis-Menten function tending to unity) are indeed set by the limiting rate parameters K_mn_rd1 and K_mn_rd2.

The variable ftD(t) and its corresponding dependence have been removed in the new version.

Apologies for the typo in NO3 dependence. This should have been a combined function of nitrate and ammonium (nitrate uptake suppressed at high ammonium concentrations). It is correct in the new Table 2.4.

Table 3: - I guess that K_Mn_rds should be K_Mnrd_HS? - There are many values assumed, some literature citations would be helpful. I guess that the model is rather insensitive to most of these parameters and their value should therefore be based on literature values.

Sorry, K_Mn_rds was a typo.

Literature citations have been added to the new tables. Table 3 has been checked, corrected, and divided into several tables.

- Why did you choose 2.7 for the Fe/P ratio and not the conventional 10?

Table 4: check carefully: e.g. for phosphate you have hard-coded 2.7 for Fe/P and 0.67 for Mn/P rather than a parameter. Taking stoichiometry as a constant is fine, but do not present

An explanation has been added to the text. We refer to assumptions and numerical experiments described in (Yakushev et al., 2007), where we aimed to analyze the reasons for formation of a typical "phosphate dipole" in the water column, with a minimum just above, and a maximum just beneath the hydrogen sulfide onset. We used extreme values of Fe/P and Mn/P to demonstrate that this phenomenon cannot be explained by Fe (even if Fe/P = 2.7, and not 10), but can be explained by Mn(III).

Table 5: this table is unuseful and I doubt whether the fluxes are all in the right units. Table 6: could be deleted.

Both tables have been deleted.

Figures. All captions need more documentation. For instance it is not even mentioned why some concentrations are presented on two different scales. As written above, reconsider to focus on a few results and elaborate the model results in another paper. The figures as presented now appear more like raw model output.

The figures has been redrawn and carefully selected. As recommended we focus on demonstrating of the model possibilities and not on analyzing the model results.

References

Berner, R.A. Principles of Chemical Sedimentology. McGraw-Hill. 1971.

Berner, R.A. .Early Diagenesis: A Theoretical Approach. Princeton Univ. Press. 1980.

Boudreau, B. P.: Diagenetic models and their implementation. Modelling transport and reactions in aquatic sediments., 1997.

Boudreau, B. P. and Jørgensen, B. B., eds.: The Benthic Boundary Layer : Transport Processes and Biogeochemistry, Oxford University Press, New York (NY), 2001.

1 Canfield, D. E., Kristensen, E. and Thamdrup, B.: Aquatic geomicrobiology., Adv. Mar. Biol., 48, 1–
2 599, doi:10.1016/S0065-2881(05)48011-6, 2005.

3 Dade, W. B., Hogg, A. J. and Boudreau, B. P.: Physics of Flow Above the Sediment- Water Interface,
4 in The Benthic Boundary Layer, editors B. P. Boudreau and B. B. Jorgensen, cc. 4–43, Oxford
5 University Press;, New York., 2001.

6 Kappler, A., Emerson, D., Edwards, K., Amend, J. P., Gralnick, J. A., Grathwohl, P., Hoehler, T. and
7 Straub, K. L.: Microbial activity in biogeochemical gradients - New aspects of research, Geobiology,
8 3(3), 229–233, doi:10.1111/j.1472-4669.2005.00053.x, 2005.

9 Meile, C., Koretsky, C.M., Cappellen, P.V. Quantifying bioirrigation in aquatic sediments: An inverse
10 modeling approach. Limnol. Oceanogr. 46(1), 164–177. 2001

11 Meysman, F.J.R., Boudreau, B.P. and J.J. Middelburg. Modeling reactive transport in sediments
12 subject to bioturbation and compaction. Geochimica et Cosmochimica Acta, Vol. 69, No. 14, pp.
13 3601–3617, 2005.

14 Schluter, M., Sauter, E., Hansen, H., Suess, E., Seasonal variations of bioirrigation in coastal
15 sediments: Modelling of field data. Geochimica et Cosmochimica Acta 64(5), 821–834. 2000.

16 Soetaert, K. and Middelburg, J. J.: Modeling eutrophication and oligotrophication of shallow-water
17 marine systems: The importance of sediments under stratified and well-mixed conditions,
18 Hydrobiologia, 629(1), 239–254, doi:10.1007/s10750-009-9777-x, 2009.

19 Thorpe, S. A.: The Turbulent Ocean, Cambridge University Press., 2005.

20 Yakushev, E. V., Pollehne, F., Jost, G., Kuznetsov, I., Schneider, B. and Umlauf, L.: Analysis of the
21 water column oxic/anoxic interface in the Black and Baltic seas with a numerical model, Mar. Chem.,
22 107(3), 388–410, doi:10.1016/j.marchem.2007.06.003, 2007.

23
24

Response to the review of O.P. Savchuk

Simulation of alternating oxic/anoxic conditions in coastal ecosystems on the fine spatio-temporal scales is useful for studies of specific questions, from an explicit description of the bottom boundary layer to a succession/alteration of multiple electron donor/acceptor agents to details of alkalinity composition and effects on the carbonate system, etc. Therefore the manuscript could be interesting to a wider audience and published also in the main body of Geoscientific Model Development papers. In that case, the manuscript demands a **major revision,** because both the form and content are rather sloppily observed and prepared. Many of specific issues and details of such revision have already been indicated by the first reviewer, Prof. J. Middelburg. I concur with almost all of them.

We apologize to the Reviewer for the poor condition of our submitted manuscript, and we thank the Reviewer for nevertheless providing a constructive review. We are confident that this review, in combination with the other two, has led to a major improvement in the model code and description.

However, while trying to further expand the list of questions, suggestions, and requests, I got substantial doubts in the suitability of this specific manuscript for this particular journal, based on the following:

Categorization of this manuscript as a "model description paper" requires a **comprehensive model description**, which internal consistency is verified by **demonstration of its capacities**, **rather than a detailed validation** of its implementation as would be ex- pected from a "model evaluation paper". The ambiguity of the paper's goals is reflected in repeating expressions like "to develop a model AND analyse seasonal effects". As it looks now, the manuscript describes a specific model implemented for studies of some particular biogeochemical questions rather than **presents some finished single product** that can be relatively straightforwardly borrowed and used by interested colleagues.

The text was extensively modified to become a comprehensive model description rather than a validation. We use an example of calculations to demonstrate the model capacity (this part was significantly reduced). The code was re-written in many parts and commented to facilitate its use by interested colleagues.

Such ambiguity starts already from rather inconsistent definition of objectives. The title announces "coupled benthic-pelagic model for simulation of seasonal anoxia", the abstract indicates the goal

as a capturing of “biogeochemical processes occurring at the bottom boundary layer (BBL) AND sediment-water interface (SWI)”, the last sentence of “Background” Section indicates the goal as a capturing of “key biogeochemical processes occurring at the bottom boundary layer” only. Even farther, “the main goal of the model was to reproduce the biogeochemical mechanism of transformation of oxic conditions into anoxic in the sediment–water interface”. Perhaps, such obscurity reflects also a story of development of BROM from ROLM by substantially expanding list of variables and their interactions. If, as it seems to me, the real focus and achievements lay in the “middle”, then almost a sole goal of the water column and sediment parts is to generate consistent boundary conditions for interacting BBL and SWI. From the manuscript it is also unclear, why the focus is on seasonal dynamics and what prevents the reproduction of sporadic short-term alterations or long-term persisting states.

The title and formulations of the goals in the abstract and text have been harmonized. A focus on seasonal dynamics was also deleted from the title following the Reviewer’s suggestions. For the example calculations we focus on a seasonal cycle because much of the strongest biogeochemical variability (including deoxygenation) typically occurs on this time scale. However, we are clear in the revised text that BROM can be applied to study variations on a broad range of time scales.

Then, for a further implementation in diverse geographical areas it should be stressed and clearly explained, where from should the user obtain the data about external inputs, internal dynamics and distribution on multiple forms of sulfur, man- ganese, iron, as well as on different functional groups of bacteria. At the least, recom- mendations should be given on some proxies that could be derived from the pelagic ecosystem models with less uncommon sets of variables and processes.

A step-by-step guide to applying the model in given geographical area has been added to the text (Appendix A: Running BROM step-by-step). The issue of missing model inputs/data is now clearly confronted in the General Description (section 2.1.1):

“The model has 33 state variables (Ci), described in Table 1. This includes frequently measured components such as hydrogen sulfide (H2S) and phosphate (PO4), as well as rarely measured variables such as elemental sulfur (S0), thiosulfate (S2O3), trivalent manganese species Mn(III), and bacteria. Variables of the latter category were included because their contribution to biogeochemical transformations is believed to be substantial. For instance, bacteria play an important role in many modelled processes and can consume or release nutrients in organic and inorganic forms (Canfield et al., 2005; Kappler et al., 2005). We acknowledge that for many of these additional variables, site-specific estimates of associated model parameters and initial/boundary conditions may be difficult or

impossible to obtain, and may in practice require some crude assumptions and approximations (e.g. universal default parameter values, no-flux boundary conditions, initial conditions from a steady annual cycle). Nevertheless, we believe that for many applications this will be a price worth paying for the additional process resolution/realism provided by BROM for important biogeochemical processes in the BBL and sediments."

Furthermore, there are several ad hoc features and patches pertaining, perhaps, only for this implementation that should be explicitly indicated for a prospective users, for instance, holding sea surface concentrations constant results in non-conservation; prescription constant coefficient of vertical transport in BBL, while arbitrarily modifying it by assumed bioturbation in the sediments; extensive use of squared availabilities (Nutrient/Biomass)^2 instead of concentrations N in nutrient limitation and trophic functions.

In the modified submission we have improved the flexibility of the model code and clarified the use of simplifying assumptions, including further comments and references in the text, Tables, model code, and input .yaml files (Appendices C and D). Regarding boundary conditions, the flexibility of the BROM-transport code has been improved and the options are now described and explained in section 2.2.5:

"BROM-transport presently allows the user to chose between four different types of boundary condition for each variable and for upper and lower boundaries: 1) no-gradient at the bottom boundary (no diffusive flux) or no-flux at the surface boundary, except where parameterized by the FABM biogeochemical model (i.e. for O2 and DIC in the case of BROM-biogeochemistry); 2) a fixed constant value; 3) a fixed sinusoidal variation in time defined by amplitude, mean value, and phase parameters; or 4) an arbitrary fixed variation in time read from the input netCDF file. All boundary condition options and parameters are set in the brom.yaml file (see Appendix D). Note that options 2-4 are Dirichlet boundary conditions which define implicit fluxes of matter into and out of the model domain, and that all boundary concentrations should be in units [mmol/m3 total volume (water+solids)]. The default option 1 is generally the preferred choice, but the Dirichlet options can also be useful to allow a simple representation of e.g. fluxes of nutrients into and out of the surface layer due to lateral riverine input. A possible alternative is to use the forcings parameters for horizontal mixing (see equation (1)) to specify horizontal exchanges or restoring terms to observed climatology (see section 2.2.7)."

Regarding vertical diffusivity, the variation in the BBL can now be parameterized in three ways, as described in section 2.2.1:

"Within the water column, the total vertical diffusivity $D = D_m + D_e$ for solutes and $D = D_e$ for particulates, where D_m is a constant molecular diffusivity at infinite dilution, and D_e is the eddy diffusivity read from the input file for the pelagic water column. For the BBL, D_e can be defined as "dynamic", in which case it is linearly interpolated for each day between the deepest input forcing value above the SWI and zero at a depth h_{DBL} above the SWI, where h_{DBL} is the diffusive boundary layer (DBL) thickness (default value 0.5 mm). This option is likely appropriate for shallow water applications where D_e may be strongly time-dependent within the user-defined BBL (default thickness 0.5 m). Alternatively, a static, fixed profile $D_{eBBL}(z)$ may be more appropriate for deep water BBLs, where time dependence may be weak and deepest values from hydrodynamic models may be relatively far above the SWI. In this case, BROM-transport offers two options for $D_{eBBL}(z)$: 1) a constant value, dropping to zero in the DBL, or 2) a linear variation between a fixed value at the top of the BBL and zero at the top of the DBL. Option 1) defines a simplest-possible assumption, while option 2) corresponds to the assumption of a log layer for the current speed e.g. (Boudreau and Jorgensen, 2001). Eddy diffusivity is strictly zero in the DBL, on the SWI, and within the sediments. Diffusivity in the sediments is due to molecular diffusion and bioturbation and is parameterized as described in section 2.2.1."

Regarding the use of squared availabilities an explanation has been added to section 2.1.2:

"The nutrient limitation and heterotrophic transfer functions are based on squared Monod laws for Nutrient/Biomass ratio, which also stabilizes the system compared with Michaelis-Menten and Ivlev formulations."

Fortunately, selected results, ideas and formulations can still be gratefully borrowed by interested colleagues with appropriate reference to the ever available discussion paper.

This is true, but we are confident that the revised paper meets all the requirements of a full, published model description paper in GMD.

Response to the review of G. Munhoven

General comments

Appreciation of the manuscript

In this paper, E. V. Yakushev and co-authors present a highly complex model suitable to study the coupled biogeochemical processes at the bottom boundary layer, the sediment-water interface and the surface sediment. The model appears to provide an extremely complete description, considering all the processes and primary and secondary chemical reactions that have been taken into account. It is integrated into the *Framework for Aquatic Biogeochemical Models*, FABM (Bruggeman and Bolding, 2014).

Although the model appears to have been skilfully designed and set up, the paper has, unfortunately, a number of weaknesses. It is not suitable for publication in *Geosci- entific Model Development* in its current form – it should nevertheless be possible to **reconsider it after a major revision**.

This paper would definitely have benefited from another round or two of rereading and proofreading. Not even the name of the model is unambiguously given: in the title, the name is *Bottom RedOx Model*, in the model presentation (p. 2, ll. 2–3) it is *Bottom RedOx Layer Model*. The English of the paper needs some thorough revision. There are parts that are acceptable and others that are almost unsuitable for review. I am not going to point out all the **English** errors that I found – they are simply to numerous to key them all in here. There is one British co-author and two co-authors with affiliations to institutions in English-speaking countries or regions: could they please have a look at the manuscript and help to correct it and rewrite where necessary! There are errors (spelling, grammar, syntax, style) on nearly every single page, but sections 3.2.4 (Manganese) and 3.3 (Carbonate system) require particularly close attention.

The paper has been submitted as a “model description paper”. Requirements for that type of paper are detailed in http://www.geoscientific-model-development.net/about/ manuscript_types.html#item1. Quite some requirements are not met in this paper.

We ask the Reviewer to accept our sincere apologies for the poor condition of the submitted manuscript. We also wish to convey our gratitude to the Reviewer for nevertheless providing a very detailed and constructive review. We feel confident that this review, in combination with the other two, has contributed to a major improvement in the model code and description.

The model description is not well contextualized. The application presented is for a shallow-water environment, but one may ask where else it could be applicable, and which extensions or adaptations would be required or which simplifications would be possible. The authors mention, e. g., a possible coupling to NEMO,which encompasses almost the complete range of marine environments that one can imagine.

The Background section has been extended to improve the model contextualization. The broad applicability of BROM is now clarified in our final paragraph of the Background, where the distinguishing features of BROM vs. other models are listed:

"The goal of this work was to develop a model that captures key biogeochemical processes in the water and sediment and to analyze the changes occurring in the BBL and SWI. As a result, BROM differs from existing biogeochemical models in several key respects. BROM features explicit, detailed descriptions of many chemical transformations under different redox conditions, and tracks the fate of several chemical elements (Mn, Fe, S) and compounds ($MnCO_3$, FeS, S0, S_2O_3) that rarely appear in other models. BROM also allows for spatially explicit representations of the vertical structure in the sediments and BBL. This distinguishes it from e.g. ERSEM (Butenschon et al., 2016) which has a more detailed representation of benthic biology (meiofauna and different types of macrofauna), but limits its chemistry to the dissolved phase to CO_2, O_2 and macronutrients, and its vertical structure of sediments to an implicit three-layer representation that relies on equilibrium profiles of solutes and idealized profiles of particulates. Third, BROM offers a near-comprehensive representation of all processes affecting oxygen levels in the BBL and sediments, and should therefore provide a useful tool for studies focused on deoxygenation in deep water and sediments. Finally, BROM is conceived and programmed as a flexible model that can be applied in a broad range of marine and lake environments and modelling problems. As a component of the Framework for Aquatic Biogeochemical Modelling (FABM, Bruggeman and Bolding, 2014), BROM can be very easily coupled online to any hydrodynamic model within the FABM, and can also be driven offline by hydrodynamic model output saved in netCDF or ascii format (using the purpose-built offline transport solver BROM-transport)."

The technical details of the implementation are incomplete, and therefore, the criterion of model reproducibility that the paper should aim for is not met. All to many details are not covered in the description.

The level of technical detail in the new manuscript has been substantially increased. BROM-transport is now described in much greater detail in the text. The BROM-biogeochemistry description has been reworked and the Tables now provide an accurate and exhaustive description of all parameterizations and parameter values. We have added an Appendix guide "Running BROM step-by-step" and have made the input files (netCDF, fabm.yaml, and brom.yaml) for the demonstration run available on the BROM-transport git repository so that these results can be exactly reproduced. The .yaml input files that contain further technical details of implementation have also been provided as Appendices.

1. The instructions about where to get the code are incomplete. Much guesswork is currently required to locate the relevant files inside the FABM distribution. This could easily be avoided by, say, three to five extra sentences.

This section has been improved and extended. We also added an Appendix “Running BROM step-by-step” to help the reader to run the model locally.

There does not seem to exist a way to permanently access the precise model version described in this paper.

Now we provide a permanent tags for both BROM and FAMB: BROM-transport tag v1.1. https://github.com/e-yakushev/brom-git.git and the BROM-biogeochemistry code in FABM tag v0.95.3 http://fabm.net.

Also now there is a Win32 executable file available at https://github.com/e-yakushev/brom-git/releases/tag/v1.1

The limitations of the model and the fundamental software requirements are not given: if the model described here is really BROM-transport (this is not a name found in the paper, but it is the name of the only sensible source code collection that I could find), then the paper needs to state right away that:

- the BROM source code can only be compiled with the Intel Fortran compiler for Windows
- the current version can only use hydrodynamic conditions derived from GOTM (according to the Wiki at https://sourceforge.net/p/fabm/wiki/BROM_ FABM).

Although it is reported on p. 16 (l. 5), that the model was run with the Intel compiler for Windows,[1] it is said nowhere that this is the only way to run it. This is obviously a extremely strongly limitation and I am wondering whether such a restriction is

fundamentally necessary. As far as I can see, FABM itself is written in standard- conforming Fortran 2003 in a portable manner (no hardcoded kind types, etc.) and does not seem to rely on a single compiler for a single platform.

[1] It would be useful to provide the version number of the compiler used. FABM and BROM require some specific Fortran 2003 features and the Intel compiler only offers full support for Fortran 2003 since version 15. However, a subset offered by earlier versions might be sufficient here.
I strongly encourage the authors to prepare a version of the source code that can be used on other platforms and with alternative compilers. It should be possible to do this quite rapidly by introducing a few pre-processor directives, which would switch off some extra functionality provided by the Intel Fortran compiler for Windows, but that is not fundamentally required for the model itself. This would increase the usefulness of BROM by orders of magnitude! Else, what is the point in emphasizing that the model code "[. . .] uses modern software standards: it is coded in object-oriented Fortran 2003, […]" (p. 27, ll. 17–18) if in the end, it only compiles with one single compiler on one single platform.

The new version of BROM is platform independent and is currently used by the co-authors under both Windows and Linux.

The model itself seems to be carefully designed and set up. There are a few assumptions regarding the physical environment that may be debatable and that would benefit from a few extra words of explanation (see specific comments below). The set of processes and coupled chemical reactions and equilibria that have been taken into account is extremely complex. It is not obvious if such a high degree of complexity is truly necessary. The model indeed seems to allow a rather accurate simulation of the environment chosen. However, to what extent does it contribute to improve our understanding of the way the environment evolves? It would be interesting to know which are the dominant actors of the system. Unfortunately, the paper does not address this kind of question at all.

The physical environment assumed by the offline 1D solver BROM-transport is now described and explained in much greater detail. Regarding model complexity, we state the philosophy behind BROM in the new section 2.1.1:

"The model has 33 state variables (Ci), described in Table 1. This includes frequently measured components such as hydrogen sulfide (H2S) and phosphate (PO4), as well as rarely measured variables such as elemental sulfur (S0), thiosulfate (S2O3), trivalent manganese species Mn(III), and bacteria. Variables of the latter category were included because their contribution to biogeochemical transformations is believed to be substantial. For instance, bacteria play an important role in many modelled processes and can consume or release nutrients in organic and inorganic forms (Canfield et al., 2005; Kappler et al., 2005). We acknowledge that for many of these additional variables, site-specific estimates of associated model parameters and initial/boundary conditions may be difficult or impossible to obtain, and may in practice require some crude assumptions and approximations (e.g. universal default parameter values, no-flux boundary conditions, initial conditions from a steady annual cycle). Nevertheless, we believe that for many applications this will be a price worth paying for the additional process resolution/realism provided by BROM for important biogeochemical processes in the BBL and sediments."

Regarding the contribution to understanding through model analysis: This is a very important message but we believe that it requires a special study that is beyond the scope of the present description paper. However, we do plan to perform such analysis with a model carefully validated to a natural system, as part of a separate publication.

2 Specific comments

2.1 Introduction

The scope of the model, i. e., the bottom boundary layer (BBL), (also known as the benthic boundary layer, or are there differences between those two BBLs?) deserves to be presented in more detail. What is its typical thickness? What influences that thickness? How does it change throughout the global ocean? What are the typical gradients across the BBL? Please do not forget that *Geoscientific Model Development* has a broad lectureship.

The BBL is indeed a focus of BROM, but it is not the only one: BROM also focuses on the upper layers of the sediment. Also, we are anxious not to lengthen the paper too much through extended discussion or literature review. BROM offers a novel and applicable tool to study water column plus sediment biogeochemistry in an integrated way and with a focus on redox chemistry and deoxygenation. We want readers to be able to quickly assess whether or not BROM will be useful to them, and to have a detailed documentation of the model if they decide to use it. Finally, BROM is not a specialized BBL model; it is rather a "benthic-pelagic" coupled model for the water column and sediments. As far as BROM is concerned, the BBL is simply a thin layer of calm water separating the "pelagic" water column from the sediments. The treatment of the BBL in the current version of BROM is quite simple: the vertical diffusivity is either set to a (low) constant value (the simplest assumption) or it increases linearly from the SWI (roughly corresponding to the assumption of a log layer for current speed, Boudreau and Jorgensen, 2001; Holtappels and Lorke, 2011). With these considerations and the comments of all reviewers in mind we have included the following paragraph in the new Background:

"The BROM model described herein is a fully coupled benthic-pelagic model with a special focus on deoxygenation and redox biogeochemistry in the sediments and Benthic Boundary Layer (BBL). The BBL is "the part of the marine environment that is directly influenced by the presence of the interface

between the bed and its overlying water" (Dade et al., 2001). Physical scientists tend to prefer the term "bottom boundary layer", but this is largely synonymous with the BBL (Thorpe, 2005). Within BROM, the term BBL is used to refer to the lower parts of the fluid bottom boundary layer where bottom friction strongly inhibits current speed and vertical mixing, hence including the viscous and logarithmic sublayers up to at most a few metres above the sediment. This calm-water layer plays a critical role in mediating the interaction of the water column and sediment biogeochemistry and in determining e.g. near-bottom oxygen levels, yet it remains poorly resolved in most physical circulation models. For BROM we have developed an accompanying offline transport module "BROM-transport" that uses output from hydrodynamic water column models but solves the advection-diffusion-reaction equations for a "full" grid including both water column and sediments. BROM-transport uses greatly increased spatial resolution near to the SWI, and thereby provides explicit spatial resolution of the BBL and sediments."

I am surprised to read that “the Bottom Boundary Layer (BBL) […] is still understudied” (p. 5, l. 22). On my shelf I have the fine book *The Benthic Boundary Layer: Trans- port Processes and Biogeochemistry* (Boudreau and Jørgensen, 2001). It is nearly 15 years old and BBL research has certainly not come to a rest since that book got published. Please reconsider that statement and provide a fair representation of the existing literature.

We have removed this statement. The summary of existing literature in the Background section has also been expanded to provide a fairer representation.

General model presentation

Scope of the model

In the end, it is not entirely clear what the exact scope of BROM is. In the abstract, BROM is introduced as a model for the biogeochemical process in the bottom boundary layer; in the model description though, we read that “[t]he water column considered in our model spans the sea surface (upper boundary) down to user’s defined sediment depth [. . .]”. This is to some extent contradicting as this domain largely exceeds the bottom boundary layer. Please clarify.

BROM was never intended to cover only the bottom boundary layer or to exclusively focus on this. We apologize for the lack of clarity in the original submission. In the new manuscript we have harmonized and clarified the stated goals and scope. In the new Abstract we have:

"The goal of this work was to develop a model that captures key biogeochemical processes in the water and sediments and that simulates the changes occurring in the bottom boundary layer and sediment-water interface."

then in the new Background section we have:

"The goal of this work was to develop a model that captures key biogeochemical processes in the water and sediment and to analyze the changes occurring in the BBL and SWI."

Computational aspects

It is stated that numerical integration was carried out with the Eulerian scheme (the explicit or the implicit variant? – the extremely short time-steps chosen make me guess it is the former, but it would be good to state this). Is the same Eulerian scheme used for both space and time dimensions? Please specify all the schemes used.

The numerical integration options of BROM transport are now described in a dedicated section 2.2.2. The new text reads:

"Equations (1-3) are integrated numerically over a single combined grid (water column plus sediments) and using the same model time step in both water column and sediments. All concentrations are stored internally and input/output in units [mmol/m^3 total volume]. Time stepping follows an operator splitting approach (Butenschon et al., 2012): concentrations are successively updated by contributions over one time step of diffusion, bioirrigation, reaction, and advection, in that order. If any state variable has any 'not-a-number' values at the end of the time step then the program is terminated.

Diffusive updates are calculated either by a simple forward-time central-space (FTCS) algorithm or by a semi-implicit, central-space algorithm adapted from a routine in the General Ocean Turbulence Model (GOTM, Umlauf et al., 2005). Bioirrigation and reaction updates are calculated as forward Euler time steps, using the FABM to compute R_i, and advection updates are calculated using a simple first-order upwind differencing scheme. After each update, Dirichlet boundary conditions (see below) are reimposed and all concentrations are low-bounded by a minimum value (default = 10^{-11} µM) to avoid negative values.

BROM-transport also provides the ability to divide the diffusion and advection updates into smaller time steps related to the sources-minus-sinks time step by fixed factors, since the physical transport processes are often numerically limiting (Butenschon et al., 2012). The default time step is 0.0025 days or 216 seconds, which is much longer than the characteristic equilibration timescale of the CO_2 kinetics (Zeebe and Wolf-Gladrow, 2001)."

Details about the pH solving algorithm can only be looked up in the code. The text only says that "[…] total pH was calculated using the Newton-Raphson method" (p. 11, ll. 20–21) and that "Carbonate system equilibration was parameterized using the standard approach (i.e. Lewis and Wallace, 1998)" (Table 2). This latter affirmation is meaningless: Lewis and Wallace (1998) neither provide information about the methods used in their program, nor do they define any standard approach. A few more details about how calculations are actually done in BROM would be of order here.

The carbonate system code was updated, in particular we added dependence of the carbonic acid constants on pressure, and we implemented the pH calculation method proposed by Munhoven (2013).

In the new text, the methods for calculating the carbonate system are described in section 2.1.4:

"Equilibration of the carbonate system was considered as a fast process occurring within a few seconds (Zeebe and Wolf-Gladrow, 2001). Accordingly, the equilibrium solution was calculated at every time step using an iterative procedure. The carbonate system was described using standard approaches

(Munhoven, 2013; Roy et al., 1993; Wanninkhof, 2014; Wolf-Gladrow et al., 2007; Zeebe and Wolf-Gladrow, 2001). The set of constants of (Roy et al., 1993) was used for carbonic acid. Constants for boric, hydrofluoric, and hydrogen sulfate alkalinity were calculated according to (Dickson, 1992), for silicic alkalinity according to (Millero, 1995), for ammonia alkalinity according to (Luff et al., 2001), and for hydrogen sulfide alkalinity according to (Luff et al., 2001) and (Volkov, 1984). The ion product of water was calculated according to (Millero, 1995). Total scale pH was calculated using the Newton-Raphson method with the modifications proposed in (Munhoven, 2013). Precipitation and dissolution of calcium carbonate were modelled following the approach of (Luff et al., 2001) (Table 2)."

In general, the text really ought to be more complete and informative about **numerical aspects of the model**. This is what *Geoscientific Model Development* readers expect.

We have addressed numerical aspects more thoroughly in the new text, including dedicated sections on numerical integration and numerical details on the carbonate system calculation (see above).

Rate law expressions

The tables that list all the processes considered in BROM and their rate laws, and that collect the different parameter values are among the most informative parts of the paper. They clearly represent one of its major strengths. Unfortunately no references are given for the parameter values presented in Table 3. There is a large variety of kinetic rate laws that are used in the model (Monod laws, squared Monod laws, laws in tanh, …). I think it would be good to have a few words of explanation about the choices operated. Please also complete the references where missing (Table 2, on pp. 41–43 and Table 3, throughout).

We have checked and completed the references in Table 2 and added references for the coefficient values in Table 3. Regarding the use of squared availabilities, an explanation has been added to the text:

"The redox-dependent switches are preferably based on hyperbolic functions that improve system stability compared with discrete switches. The nutrient limitation and trophic functions are preferably based on squared Monod laws for Nutrient/Biomass ratio, which also stabilizes the system compared with Michaelis-Menten and Ivlev formulations."

As mentioned in the general appreciation already, I really wonder if all that complexity is really necessary, or, put the other way around: which minimalist set of process would be sufficient to obtain realistic results?

Motivation for the complexity of BROM is provided in the Background section of the new text:

"The goal of this work was to develop a model that captures key biogeochemical processes in the water and sediment and to analyze the changes occurring in the BBL and SWI. As a result, BROM differs from existing biogeochemical models in several key respects. BROM features explicit, detailed descriptions of many chemical transformations under different redox conditions, and tracks the fate of

several chemical elements (Mn, Fe, and S) and compounds ($MnCO_3$, FeS, S0, S_2O_3) that rarely appear in other models. BROM also allows for spatially explicit representations of the vertical structure in the sediments and BBL. This distinguishes it from e.g. ERSEM (Butenschön et al., 2015), which has a more detailed representation of benthic biology (meiofauna and different types of macrofauna), but limits its chemistry to the dissolved phase to CO_2, O_2 and macronutrients, and its vertical structure of sediments to an implicit three-layer representation that relies on equilibrium profiles of solutes and idealized profiles of particulates. Third, BROM offers a near-comprehensive representation of all processes affecting oxygen levels in the BBL and sediments, and should therefore provide a useful tool for studies focused on deoxygenation in deep water and sediments. "

Further explanation of the BROM philosophy regarding model complexity has also been added to section 2.1.1:

"The model has 33 state variables (Ci), described in Table 1. This includes frequently measured components such as hydrogen sulfide (H_2S) and phosphate (PO_4), as well as rarely measured variables such as elemental sulfur (S0), thiosulfate (S_2O_3), trivalent manganese species Mn(III), and bacteria. Variables of the latter category were included because their contribution to biogeochemical transformations is believed to be substantial. For instance, bacteria play an important role in many modelled processes and can consume or release nutrients in organic and inorganic forms (Canfield et al., 2005; Kappler et al., 2005). We acknowledge that for many of these additional variables, site-specific estimates of associated model parameters and initial/boundary conditions may be difficult or impossible to obtain, and may in practice require some crude assumptions and approximations (e.g. universal default parameter values, no-flux boundary conditions, initial conditions from a steady annual cycle). Nevertheless, we believe that for many applications this will be a price worth paying for the additional process resolution/realism provided by BROM for important biogeochemical processes in the BBL and sediments."

Miscellanea

Denitrification is considered, and nitrification, but I could not find anything about how nitrogen fixation is dealt with. I would expect that this process is required to avoid an unrealistic drift in the nitrogen inventory.

Corrected.

Total alkalinity

This part of the paper (p. 9) is one of the most disappointing ones. It is very approxi- mate, completely overloaded with information that is ignored in the end. It furthermore contains several errors.

For clarity, it would be best to provide immediately the approximation actually used in the model, and not a hypothetical one, that could have been used. Alkalinity contribu- tions that are not included or that are set to zero should be omitted. The text will be considerably simplified.

Whatever the expression chosen for total alkalinity, it will anyway always remain only an approximation. But even approximations need to be factually correct. Unlike written in the paper, .

- ... H_3PO_4 is also part of alkalinity and $A_{TPO_4} = [HPO_4] + 2[PO_4] - [H_3PO_4]$ — interestingly this is correct in Table 6 (except for a typo) and also in the code;
- ... NH_4^+ is not part of alkalinity (it is the zero-level species) and thus $A_{TNH_3} = [NH_3]$;

- ... it is the total borate concentration that is estimated from salinity and not $[B(OH)_4^-]$ — $[B(OH)_4^-]$ is calculated from the state variables just like to others (this is correctly done in the code, fortunately);

- ... F^- is not part of alkalinity, only HF, so that $A_{THF} = [HF]$ — this is also wrong in Table 6 (at 68 μM, it would be barely negligible), but I suggest to discard the A_{THF} term from the alkalinity expression anyway, as it is not included in the model.

-

We apologize for these errors and lack of clarity in the submitted text. The total alkalinity formulation has now been corrected. We have chosen to retain the more general expression for total alkalinity as a starting point and then explicitly neglect the hydrogen sulfate, hydroflouric and nitrous acid terms. We feel that this helps to link our approach with the "classical" formulation.

Although it is specified later on that the stoichiometric constants of Roy et al. (1993) are used for the carbonate system, references for the other constants (e. g., dissociation constants for boric, phosphoric and silicic acids) required to solve the total alkalinity-pH equation are missing. Please provide references for those as well.

The references are now provided in the code (fabm.yaml) and the text:

"The set of constants of (Roy et al., 1993) was used for carbonic acid. Constants for boric, hydrofluoric, and hydrogen sulfate alkalinity were calculated according to (Dickson, 1992), for silicic alkalinity according to (Millero, 1995), for ammonia alkalinity according to (Luff et al., 2001), and for hydrogen sulfide alkalinity according to (Luff et al., 2001) and (Volkov, 1984). The ion product of water was calculated according to (Millero, 1995)."

Finally, the pH scale used in the paper turns out to be the total scale. This should be stated more clearly than it is currently done (at my third reading, I discovered on p. 11 (l. 20) that "total pH was calculated". Please state this more obviously.

We now specify total scale pH twice when the variable is first mentioned in section 2.1:

"Instead, the total scale pH is calculated as a diagnostic variable at every time step as a function of DIC and Alk (which are state variables). In turn, the total scale pH is used in calculations of the chemical equilibrium constants required to describe related processes (i.e. carbonate precipitation/dissolution, carbonate system parameters etc.)."

Physical environment

Porosity

Variable porosity is not included in the current version of BROM. The affirmation that "[. . .] its effect on [the] vertical transport is incorporated in[to] the values of Kz and Kz_{bio} , [...]" (p. 13, l. 17) is rather obscure. Kz_{mol} is actually constant so it is not clear how it could take porosity variations into account. I am furthermore not certain that this simplification is really necessary, given the complexity and detailed representation of the rest of the model. Variable porosity should not significantly increase the model's compleity.Furthermore, it appears that a tortuosity corresponding to the porosity value of 90%

was used, with reference to a “value from Boudreau, 1997” (p. 13, l. 22). This is not very meaningful. Boudreau (1997) lists eight theoretically based tortuosity-porosity relationships and three empirical ones. Please specify which one was used here and then cite the original reference.

We agree: this simplification was excessive. BROM-transport has received a major overhaul and now includes variable porosity as a fixed profile following the parameterization of Soetaert et al. (1996). Porosity now distinguishes the solute from particulate dynamics within the sediments assuming intraphase mixing (Boudreau 1997; see section 2.2.1); its effects are now treated explicitly and not folded into the vertical diffusivity (which in fact cannot fully account for porosity variations). The apparent or effective molecular diffusivity now varies with depth due to variable tortuosity. This is described in the new section 2.2.1:

"The total solute diffusivity $D_C = D_m + D_B$, where D_m is the apparent molecular/ionic diffusivity and D_B is the bioturbation diffusivity due to animal movement and ingestion/excretion. The apparent molecular diffusivity $D_m(z) = \theta^{-2} D_0 \frac{\mu_0}{\mu_{sw}}$ is derived from the infinite-dilution molecular diffusivity D_0 (an input parameter) assuming a constant relative dynamic viscosity $\frac{\mu_0}{\mu_{sw}}$ (default value 0.94, cf. Boudreau 1997, Table 4.10) and a tortuosity parameterized as: $\theta^2 = 1 - 2\ln\varphi$ from Boudreau (1997) Eqn. 4.120."

Boudreau (1997) is actually the original reference for this tortuosity parameterization. Boudreau himself refers to it as a "modified Weissberg" relation (Boudreau, 1997; Eqn. 4.119) but the empirical fit of the constant "b" is due to Boudreau (Boudreau, 1997; Table 4.12, Fig. 4.10).

Molecular diffusion

BROM uses a species-independent molecular diffusion coefficient. This consider- ably simplifies the advection-diffusion-reaction equations, as the total concentrations a, such as DIC and alkalinity can be transported directly. The reported value $K_{z\mathrm{mol}} = 1 \times 10^{-11}$ m^{2}s^{-1} is, however, almost two orders of magnitude lower than those for typ- ical ions: e. g., from Boudreau (1997, Table 4.8), we may calculate diffusion coeffi- cient values of 0.781×10^{-9} m^{2}s^{-1} for HCO^-, 0.632×10^{-9} m^{2}s^{-1} for CO^{2-}_3 and even 1.313×10^{-9} m^{2}s^{-1} for HS^- (each one for $t = 10\,^\circ$C). These are infinite dilution diffusion coefficients, but correcting them for tortuosity and for the dynamic viscosity of seawa- ter does not reduce these values by more than 15–20%. How would results change if these much higher values would be used?

We agree that the species-independent molecular diffusivity is a simplification, but as the reviewer states it does substantially simply matters in regard to composite variables. We have retained the species independence in the new code, although as it is now written the user would only have to make small modification to the code to allow species dependent diffusivity ($K_{z\mathrm{mol}}$ in the new code is actually stored as a matrix over depth and state variable, with zeros for particulate variables). We agree that the previous default value was too small, even if assumed to account for tortuosity and dynamic viscosity. In the new version, the default (single) value for infinite-dilution molecular diffusivity is 1×10^{-9} m^{2}s^{-1} based on the coefficients in Boudreau (1997, Table 4.8) (see brom.yaml in Appendix D). The user is free to change this parameter in the run-time brom.yaml file, where we also state the default value as well as a plausible range $(0.5\text{-}2.7) \times 10^{-9}$ m^{2}s^{-1} again derived from Boudreau (1997, Table 4.8). The default value of 1×10^{-9} m^{2}s^{-1} was used for the demonstration simulation in the new section 3 (see Appendix D).

2.3 Bioturbation

Biotubation is parametrized as a diffusive process, as is common usage. For the biod- iffusion coefficient, it is only stated that it takes a constant value over the top 2 cm and that it decreases

exponentially afterwards. However, I have not been able to find the length scale of this decrease anywhere in the text. Now, one may ask whether it is re- alistic to consider any bioturbation at all in anoxic parts of the sediment, the more since the text already indicates that the maximal bioturbation depth was only 0.5–2.2 cm (p. 13, ll. 15–16). How would this change your conclusions?

We apologize for making the reviewer search to no avail. The exponential decay scale is a user-defined parameter defined in the brom.yaml file (see Appendix D). Here we specify a default value of 1 cm, citing Soetaert and Middelburg (2009). In anoxic conditions, the entire profile of bioturbation diffusivity is scaled down by a Michaelis Menten function of oxygen concentration at the sediment surface. This is described in the new section 2.2.1:

"The bioturbation diffusivity $D_B(z,t)$ is modelled as a Michaelis-Menten function of the dissolved oxygen concentration in the bottom layer of the water column:

$$D_B(z,t) = D_{Bmax}(z)\frac{O_{2s}}{O_{2s}+K_{O2s}} \quad (5)$$

where $D_{Bmax}(z)$ is a constant over a fixed mixed layer depth in the surface sediments then decays to zero with increasing depth, and K_{O2s} is a half-saturation constant. The rationale for (5) is that the animals (worms etc.) that cause bioturbation require a source of oxygen at the sediment surface for respiration."

Bioirrigation

BROM takes the important process of bioirrigation into account. It is, however, represented as a purely diffusive process. Boudreau (1997) and Aller (2001) make a strong case that it would be more appropriate to represent bioirrigation as a non-local exchange process instead.

The simple possible parameterization, probably it is not enough… Of cource there are other approaches, but …

We agree. A more thorough examination of the literature shows little theoretical or observational support for a local diffusive parameterization of bioirrigation. In the new BROM-transport model, bioirrigation is modelled as a non-local exchange process as proposed in Boudreau (1997). This is described in the new section 2.2.1:

"Finally, the process of bioirrigation, whereby worms flush out their burrows with water from the sediment surface, is modelled as a non-local solute exchange following (Meile et al., 2001; Rutgers Van Der Loeff and Boudreau, 1997; Schlüter et al., 2000):

$$T_{birrC(i)} = \alpha\varphi\frac{O_{2s}}{O_{2s}+K_{O2s}}\left(\hat{C}_{f(i)} - C_i\right) \quad \text{(for solutes)} \quad (10)$$

where $\alpha(z)$ is the bioirrigation rate in oxic conditions, $\hat{C}_{f(i)}$ is the flushing concentration of solute in the fluff layer, and the Michaelis-Menten function again accounts for the suppression of worm activity in anoxic conditions. The oxic bioirrigation rate $\alpha(z)$ is parameterized as an exponential decay from the

sediment surface as in Schluter et al. (2000). The total mass transfer to/from the sediment column must be balanced by a flux into/out of the fluff layer (see equation (1)):

$T_{birr(i)} = \frac{1}{h_f}\frac{O_{2s}}{O_{2s}+K_{O2s}}\int_{z_{SWI}}^{z_{max}} \alpha\varphi\left(C_i - \hat{C}_{f(i)}\right) dz'$ (for solutes) (11)

where h_f is the thickness of the fluff layer and z_{max} is the depth of the bottom of the modelled sediment column. $T_{birrC(i)}, T_{birr(i)} = 0$ for all particulate variables."

Code

On p. 7 (ll. 24–25), it is said that BROM consists of three modules. I did not want to download and install the complete FABM, but nevertheless wanted to inspect the BROM code, to find out more about the technical details that were missing from the paper. This was, however, not entirely straightforward.

Accessibility

After having opened http://fabm.org (which redirects to the FABM project page on SourceForge), I started to search for references to BROM. After some searching around, I detected the first trace of BROM under the “Wiki” tab: section 7 of chap- ter 2 of the User’s Guide has the title “BROM-transport + FABM”. BROM-transport is most probably the transport model mentioned in the paper (p. 7, l. 2), but that is not clear, since the paper always mentions BROM only. That section provides at least the first useful hint about where to find the BROM biogeochemical modules: under src/models/niva/brom in FABM. Proceeding to the “Code” tab then allowed me to browse to the relevant files (under the indicated directory tree). BROM-transport, however, is not with FABM and must be retrieved from a different repository, located at https://github.com/e-yakushev/BROM-transport, not mentioned in the paper. I suggest that the authors give accurate and comprehensive instructions in the paper

about where the actual BROM source code files are located, both the biogeochemical ones and the main driver. And, please include also information about the license under which the code is distributed.

We apologize for the confusion and wild goose chase. In the new text we clarified and extended the section "Code Availability". It now reads:

"The model as presented consists of two components. The first is a set of biogeochemical modules (brom/redox, brom/bio, brom/carb, brom/eqconst), available as part of the official FABM distribution (http://fabm.net) (for a currently-functional direct link please see https://sourceforge.net/p/fabm/code/ci/master/tree/src/models/niva/brom/). The second is a hydrophysical driver (BROM-transport) that provides the 1D vertical context and resolves transport; this is available separately from https://github.com/e-yakushev/brom-git.git. When combined, the 1D BROM model as presented is obtained. Additionally, as BROM’s biogeochemical modules are built on FABM, they can be used from a wide range of 1D and 3D hydrodynamic models, including GOTM, GETM, MOM, NEMO and FVCOM (NEMO-FABM and FVCOM-FABM couplers have been developed by the Plymouth Marine Laboratory; contact J.B. for information).

BROM biogeochemical modules follow FABM conventions: they are coded in object-oriented Fortran 2003, have a build system based on CMake, and use YAML files for run-time configuration. The code is platform independent and only requires a Fortran-2003-capable compiler, e.g., gfortran 4.7 or

higher, or the Intel Fortran compiler version 12.1 or higher. The BROM-specific source code is located in the FABM code tree in directory src/models/niva/brom. The specific version used to produce the results described in this paper is associated with git commit 1581186939a0ff81a230468694bf909a42afc21e. However, we envisage the model to be further developed in a backward compatible manner, and encourage users to use the latest code version.

BROM-transport is coded in Fortran 2003. It includes facilities for producing results as NetCDF files, which can be read by a variety of software on different platforms. The reader should be able to reproduce the results shown in this paper using the BROM-transport and BROM-biogeochemistry code from the above repositories and the netCDF/.yaml input files found in the data/ folder of the BROM-transport repository. Step-by-step instructions for running BROM are found in Appendix A. BROM-transport as well as BROM biogeochemical modules are distributed under the GNU General Public License (http://www.gnu.org/licenses/)."

Code quality

The code is obviously “work in progress” and appears to undergo continuous changes. There are many lines of code that are commented out, some of them might be important. It is of not clear if they were also commented out when the results described in the paper were calculated.

The code quality and presentation have undergone a major overhaul. We have uploaded a finished, stable version with all commented-out code deleted. The reader should be able to reproduce the results shown in this paper using the BROM-transport and BROM-biogeochemistry code from the above repositories and the netCDF/.yaml input files found in the data/ folder of the BROM-transport repository (these .yaml files are also shown in Appendices C and D). Step-by-step instructions for running BROM are found in Appendix A.

I detected a few coding choices that put portability at risk. While REALs in the three biogeochemistry related modules are declared in a portable way with REAL(rk), where rk is an INTEGER parameter whose value gets derived from an appropriate SELECTED_REAL_KIND(...) call, there are some INTEGER(4) declarations that may lead to problems. In BROM-transport, there are numerous REAL(8) declarations, in different source code files. Kind type values – such as the ‘4’ of the INTEGER(4) or the ‘8’ of the REAL(8) declarations – are not standardized and may differ from one compiler to another. Programmers may not assume that they are equal to the ex- pected byte length and for portability reasons kind type values must therefore not be hard-coded.[2] Portable and reliable code would consistently follow the FABM approach, with the rk parameter derived from SELECTED_REAL_KIND(...)

All REAL(8)declarations in BROM-transport have now been changed to REAL(rk)where rk is inherited from the SELECTED_REAL_KIND(...)statement in the FABM code, using a command: use fabm_types, only: rk. All INTEGER(4)declarations have been replaced with INTEGER.

I have come across a few peculiarities or short-cuts in the code that may lead to seri- ous confusion: e. g., in the subroutine phIter in brom_carb.F90, the INTENT(IN) argument Sit_ (the total silicate concentration) is overridden by a local variable Sit,

[2]I know of one compiler where DOUBLE PRECISION is not REAL(8) but REAL(3).

which is set to zero, thus making the code ignore silicate alkalinity. The paper does, however, not state that silicate alkalinity is ignored.

The code has been significantly modified and the mentioned peculiarities have been removed.

The pH calculation routine is neither safeguarded nor does it include diagnostics for possible convergence failures or for early convergence: it simply executes 100 Newton- Raphson iterations, starting from a preset fixed starting value, that furthermore seems to require manual modification from time to time. No diagnostic is included, neither for possible convergence failures nor for early convergence. (Why carry out 100 iterations if convergence is reached after five of them already?)

There are now reliable methods to solve the alkalinity-pH equation, which are guaranteed to converge under any physically meaningful conditions, howsoever exotic, and usually in less than six iterations (**Munhoven**, 2013). These would be particularly recommended in the environments that BROM has been developed for, with complex alkalinity compositions and unusual total concentrations.

We are very grateful to the Reviewer for this suggestion, and have implemented the recommended methods to solve the alkalinity-pH equation. This has been very helpful in regard to computational efficiency.

Carbonate solubility constants do not take any pressure correction into account (the relevant lines are present, but commented out).

Corrected.

Finally, the comments in the code are not always correct, which also creates unnecessary confusion (e. g., the phosphoric alkalinity is not [H2PO4-] + 2.*[HPO4--] + 3.*[PO4-

--] as stated in a comment, but [HPO4--] + 2.*[PO4---] - [H3PO4]. Fortunately it is the latter that is implemented in the code.

Corrected.

Permanent access to the code for model version 1.0

As mentioned in the general appreciation, for model description papers there should exist a way to permanently access the precise model version described in the paper. The GitHub repository for BROM-transport includes a Ver. 1.0 directory, so for the transport model, this seems to be conceivable. The biogeochemical modules that are hosted in the FABM repository are however not clearly tied to version 1.0 of BROM.

It would thus be necessary to provide somehow tagged versions of the source code files for the model version 1.0 described here, or to provide copies of those files as a supplement to the paper.

The tag 1.1 for BROM transport is provided, https://github.com/e-yakushev/brom-git/releases/tag/v1.1

2.6 Tables

The tables contain a wealth of information and represent one of the most useful parts of the paper (with the exception of Table 6, which could be deleted without loss). Un- fortunately, Tables 1 and 4 are nearly unreadable because of the small font size. They would clearly benefit from a reorganization of their contents. Table 2 currently spans eight pages, Table 3 six pages. It would be useful to split them into smaller parts, with dedicated captions. While Table 2 still contains extensive references, Table 3 does not contain a single one. Readers ought to know where the adopted parameter values come from or how they have been derived.

The tables have been modified following the Reviewer's suggestions.

The second column of the row "Alkalinity changes" in Table 2 is completely overloaded. Please reorganize this information.

Corrected.

Table 6 is not essential for the paper and I suggest to delete it altogether. It also contains errors and except for Canfield et al. (2005), none of the references cited is in the reference list. A_{THF} is certainly not 68 μM, else it would not be negligible.

Table 6 has been deleted.

3 Technical comments

Throughout the paper: change "protolithic" to "protolitic" or "equilibrium" (depending on the context)

Corrected.

Throughout the paper: change "connected with" to "related to"

Corrected.

Throughout the paper: please check the usage of the word "parameterized" and "pa- rameterization". For example, in Table 2, it is said that the carbonate system equilibra- tion was parameterized. It were rather the stoichiometric constants that were parame- terized, as a function of temperature, salinity and pressure, but the carbonate system equilibration (it would be more correct to say speciation) was calculated.

Corrected.

p. 4, l. 26: “death or flight”? “death or migration” would perhaps be more appropriate

Corrected.

p. 7, l. 15: “changeable” is not appropriate in this context. Perhaps “varying”?

Corrected.

p. 9, ll. 20–25: it is common usage to speak about bor*ate*, phosph*ate* and silic*ate* alkalinity (as with *carbonate alkalinity*) and to reserve the terms bor*ic*, phosphor*ic* and silic*ic* for the corresponding acids (as in *carbonic acid*).

Corrected.

p. 11, l. 20: change “Roy’s constants” to “the set of constants of Roy et al.” – the co-authors will appreciate

Corrected.

p. 16, ll. 4–5: change “FORTRAN” to “Fortran 2003” (spelling and standard) and change “Intel FORTRAN for Windows Compiler” to “Intel Fortran Compiler for Win- dows”, which is the name of the product.

Corrected.

p. 16, l. 6: what is meant by “balanced distribution”?

We meant balanced fluxes in a quasi-stationary sense. This term has been deleted.

pp. 21–26 (section 3.2.4 – section 3.4): please check for the English and rewrite where necessary.

This has been done.

p. 39, rows 10 and 11: “sulfatereduction” should read “sulfate reduction”

Corrected.

p. 40, second-last row, right-hand column: should the “$CaCO_3$” on the last linee not read “caco3_diss−caco3_prec”?

Corrected. Note that in the new Table 2.3, "caco3_prec" has been replaced with "caco3_form".

p. 41, row 7: there is probably some “NO_3”-“NH_3” mismatch here

Corrected. The correct equation reads:

$$\mathrm{LimNO_3} = \frac{((\mathbf{NO_3}+\mathbf{NO_2})/\mathbf{Phy})^2}{\mathrm{K\_nox\_lim}^2+((\mathbf{NO_3}+\mathbf{NO_2})/\mathbf{Phy})^2}\exp(-\mathrm{K\_psi}\frac{(\mathbf{NH_4}/\mathbf{Phy})^2}{\mathrm{K\_nh4\_lim}^2+(\mathbf{NH_4}/\mathbf{Phy})^2})$$

p. 41, rows 7 and 8: the two trailing '2's in exponent seem to be misplaced (they probably belong to the second term in the denominator each time)

Corrected. Please forgive our sloppy editing.

p. 46, in the first row relative to a half-saturation for OM denitrification, "NO_2" should probably read "NO_3"

Corrected.

Table 6: "$[PO^{2-}]$" should read "$[PO^{3-}]$"

4 4

This table has been deleted.

References

Aller, R. C.: Transport and reactions in the bioirrigated zone, in: The Benthic Boundary Layer : Transport Processes and Biogeochemistry, edited by Boudreau, B. P. and Jørgensen, B. B., chap. 11, pp. 269–301, Oxford University Press, New York (NY), 2001.

Boudreau, B. P.: Diagenetic Models and Their Implementation, Springer-Verlag, Berlin, 1997.

Boudreau, B. P. and Jørgensen, B. B., eds.: The Benthic Boundary Layer : Transport Processes and Biogeochemistry, Oxford University Press, New York (NY), 2001.

Bruggeman, J. and Bolding, K.: A general framework for aquatic biogeochemical models, Env- iron. Model. Softw., 61, 249–265, doi:10.1016/j.envsoft.2014.04.002, 2014.

Lewis, E. and Wallace, D.: Program developed for CO_2 system calculations, Tech. Rep. 105, Carbon Dioxide Analysis Center, Oak Ridge National Laboratory, Oak Ridge (TN), available at http://cdiac.ornl.gov/oceans/co2rprt.html, 1998.

Munhoven, G.: Mathematics of the total alkalinity-pH equation – pathway to robust and uni- versal solution algorithms: the SolveSAPHE package v1.0.1, Geosci. Model Dev., 6, 1367– 1388, doi:10.5194/gmd-6-1367-2013, 2013.

Roy, R. N., Roy, L. N., Vogel, K. M., Porter-Moore, C., Pearson, T., Good, C. E., Millero, F. J., and Campbell, D. M.: The dissociation constants of carbonic acid in seawater at salinities 5 to 45 and temperatures 0 to 45 °C, Mar. Chem., 44, 249–267, doi:10.1016/0304-4203(93)90207-5, 1993.

Tracked changes in versions of paper:

Bottom RedOx Model (BROM, v.1.~~0~~1): a coupled benthic-pelagic model for simulation of ~~seasonal anoxia~~water and ~~its impact.~~ sediment biogeochemistry

E.V.Yakushev[1,2], E.A.Protsenko[2,1], J.Bruggeman[3], ~~R.G.J.Bellerby~~[4,1]P.Wallhead[4], S.V.~~Pakhomova~~[6,2], Pakhomova[5,2], S.Yakubov[2], R.G.J.Bellerby[6,4], R.-M. Couture[1,5], ~~S.Yakubov~~[27]

~~[1]{Norwegian~~[1]Norwegian Institute for Water Research (NIVA), Gaustadalléen 21, 0349 Oslo, Norway~~}~~,
~~[2]{P~~[2]P.P.Shirshov Institute of Oceanology RAS, Nakhimovskiy prosp. 36, 117991, Moscow, Russia~~}~~,
~~[3]{Plymouth~~[3]Plymouth Marine Laboratory, Prospect Place, The Hoe, Plymouth, United Kingdom~~}~~
~~[4]{State~~[4]Norwegian Institute for Water Research (NIVA Vest), Thormøhlensgate 53 D, 5006 Bergen, Norway
[5]Norwegian Institute for Air Research (NILU), P.O. Box 100, NO-2027 Kjeller, Norway
[6]State Key Laboratory for Estuarine and Coastal Research, East China Normal University, Shanghai, China~~}~~,
~~[5]{University~~[7]University of Waterloo, Earth and Environmental Sciences, Ecohydrology Group, 200 University Avenue West, N2L3G2, Canada~~}~~,
~~[6]{Norwegian Institute for Air Research (NILU), PO box 100, NO-2027 Kjeller, Norway}~~

Correspondence to: E.V. Yakushev (eya@niva.no)

Abstract

~~Interaction.~~ Interactions between seawater and benthic ~~sediments plays~~ systems play an important role in global biogeochemical cycling. Benthic fluxes of some chemical elements (e.g. C, N, P, O, Si, Fe, Mn, S) ~~directly affect~~ alter the redox state and ~~acidification~~ marine carbonate system (i.e. pH and carbonate saturation state), which in turn ~~determine~~modulate the functioning of ~~the~~ benthic and pelagic ecosystems. The redox state of the near bottom layer ~~can change and oscillate~~ in many regions can change with time, responding to the supply of organic matter, physical regime and coastal discharge. ~~The goal of this work was~~Due to ~~develop~~the high spatial and temporal variability of the drivers of pelagic-benthic exchange and its sensitivity to environmental and climate change it is difficult to represent these processes though observations alone. We developed a model ~~that captures~~(BROM) to represents key biogeochemical processes in the water and sediments and to simulate changes occurring ~~at~~in the bottom boundary layer~~ and sediment-water interface and analyze the changes that result from seasonal variability in redox conditions in the water column. We used a modular approach.~~ BROM consists of a transport module (BROM-transport) and several biogeochemical modules that are fully compatible with the Framework for the Aquatic Biogeochemical Models, allowing ~~the model to be coupled to existing~~ independent coupling to hydrophysical models in 1D, 2D or 3D.

~~The model~~ We demonstrate that BROM is capable ~~to simulate~~ of simulating the seasonality in production and ~~respiration~~mineralization of organic matter as well as ~~in mixing, that leads to variation of redox conditions in the~~

Formatted: Font: 17 pt
Formatted: MS title
Formatted: Font: 17 pt
Formatted: Font: 17 pt
Formatted: Font: 17 pt
Formatted: Superscript
Formatted: Not Highlight
Formatted: Not Highlight
Formatted: Affiliation
Formatted: Not Highlight
Formatted: Not Highlight
Formatted: Font: Italic
Formatted: Correspondence
Formatted: Font: Bold, English (U.S.)

~~bottom boundary layer. Production and reduction of organic matter and varying redox conditions in the bottom boundary layer affect the carbonate system and lead to changes in pH and alkalinity. Bacteria play a significant role in the fate of organic matter due to chemosynthesis (autotrophs) and consumption of organic matter (heterotrophs). Changes in the bottom boundary layer redox conditions modify the distribution of nutrients (N and P) and redox metals (Mn and Fe). The model~~the mixing that leads to variations in redox conditions. BROM can be used for analyzing and interpreting data on sediment-water exchange, and ~~estimating~~for simulating the consequences of ~~forcing~~forcings such as climate change, external nutrient loading, ocean acidification, carbon storage ~~leakages~~leakage, and point-source metal pollution.

Key Words – modeling; Bottom Boundary Layer; benthic fluxes; nutrient cycles; anoxic conditions; carbonate system.

1 Background

Oxygen depletion and anoxia are increasingly common features observed in the World Ocean, inland seas and coastal areas. ~~Observations show a decline in the dissolved oxygen concentrations at continental margins in many regions and these are related to both an increase in anthropogenic nutrient loadings and a decrease in vertical mixing e.g., (Diaz and Rosenberg, 2008; Rabalais et al., 2002; Richardson and Jørgensen, 1996). Although bottom waters may be permanently oxic or anoxic, they oscillate seasonally between these extremes in many water bodies (Morse and Eldridge, 2007). Such oscillations typically result from variation in the supply of organic matter (OM) to the sediment-water interface (SWI), from the hydrophysical regime (mixing/ventilation) and nutrient supply (river run-off) . Frequently, oxic conditions during periods of intense mixing are followed by near bottom suboxia or anoxia after the seasonal pycnocline forms, restricting aeration of the deeper layers. This occurs for instance in the Louisiana shelf (Morse and Eldridge, 2007; Yu et al., 2015), Corpus Christi Bay (McCarthy et al., 2008), the Sea of Azov (Debolskaya et al., 2008), and Elefsis Bay (Pavlidou et al., 2013).~~Observations show a decline in dissolved oxygen concentrations at continental margins in many regions and this has been linked to both an increase in anthropogenic nutrient loadings and a decrease in vertical mixing e.g. (Diaz and Rosenberg, 2008; Rabalais et al., 2002; Richardson and Jørgensen, 1996). Although bottom waters may be permanently oxic or anoxic, they oscillate seasonally between these extremes in many water bodies (Morse and Eldridge, 2007). Such oscillations typically result from variation in the supply of organic matter (OM) to the sediment-water interface (SWI), from the hydrophysical regime (mixing/ventilation), and from nutrient supply (river run-off). Frequently, oxic conditions during periods of intense mixing are followed by near-bottom suboxia or anoxia after the seasonal pycnocline forms, restricting aeration of the deeper layers. This occurs for instance on the Louisiana shelf (Morse and Eldridge, 2007; Yu et al., 2015) and in Corpus Christi Bay (McCarthy et al., 2008), the Sea of Azov (Debolskaya et al., 2008), and Elefsis Bay (Pavlidou et al., 2013).

~~The redox state and oxygenation of near bottom water is directly affected by transport of oxidized and reduced species across the SWI and, consequently, by biogeochemical processes occurring in the sediment itself (Cooper and Morse, 1996; Jorgensen et al., 1990; Roden and Tuttle, 1992; Sell and Morse, 2006). The sediment generally consumes oxygen due to enrichment with OM and presence of reduced forms of chemical elements. Its capacity~~

Formatted: Numbered + Level: 1 + Numbering Style: 1, 2, 3, … + Start at: 1 + Alignment: Left + Aligned at: 0,63 cm + Indent at: 1,27 cm

Formatted: Normal

~~to exchange oxygen with the pelagic is limited, as near bottom water is usually characterized by lowwater velocity and reduced mixing in the vicinity of the SWI (Glud, 2008). In combination, a high benthic oxygen demand (BOD) associated with local OM mineralization and low mixing rates can cause anoxia in the bottom water. This leads to the death or flight of benthic macro and meio faunal organisms responsible for bioturbation and bioirrigation (Blackwelder et al., 1996; Sen Gupta et al., 1996; Morse and Eldridge, 2007), which can greatly slow down the transport of solid and dissolved species inside the sediments and therefore rates of oxidative reactions there. Under such conditions, sedimentary sulphides can build up and dissolution of carbonate minerals may come to a halt (Morse and Eldridge, 2007).~~

~~A large number of studies demonstrate the capabilities of sophisticated reactive transport codes for integrated modelling of biogeochemical cycles in sediments e.g. (Paraska et al., 2014). However, few have directly investigated the influence of variable redox conditions in the water column on the depth distribution of biogeochemical processes (Katsev and Dittrich, 2013; Katsev et al., 2007) which thus remains an open question.~~

~~When oxic conditions return, there can be an "oxygen debt" of reduced species in the water column (Yakushev et al., 2011) and at the sediment–water interface this may buffer and delay the reestablishment of oxygenation to the sediments (Morse and Eldridge, 2007). In areas experiencing seasonal hypoxia/anoxia, the processes taking place in the water column and in the sediments are thus tightly coupled. Predicting the occurrence of hypoxia/anoxia thus requires a quantitative understanding of the dynamics of the network of physical, chemical and biological processes occurring in these environments, which drive oscillating redox conditions. Consequently, sophisticated fully coupled physical-biogeochemical models have established themselves as powerful tool to address this gap (Yu et al., 2015), although the tools are however often site-specific and complex to set up. Furthermore, the Bottom Boundary Layer (BBL) – a thin layer of water within which the steepest gradients and the greatest fluctuations in redox conditions are occurring, is still understudied.~~

~~The goal of this work was to develop a model that captures key biogeochemical processes occurring at the BBL and analyse the changes that result from seasonal variability in redox conditions in the water column.~~

~~2 Model description~~

~~Here we present the one-dimensional vertical transport and reaction model Bottom RedOx Layer Model, BROM. BROM builds on ROLM (RedOx Layer Model), a model constructed to simulate basic biogeochemical structure of the water column oxic/anoxic interface in the Black and Baltic Seas and fjords (Yakushev et al., 2006, 2007, 2009, 2011; He et al., 2012; Stanev et al., 2014). We extended the biogeochemical module of the model to consider an extensive list of compounds and processes (Figure 1), although this paper focuses on description of the fate of the species of the most important elements affected by the changes of the redox conditions – oxygen (O), nitrogen (N), sulphur (S), manganese (Mn), iron (Fe) – and describe the concurrent and resultant changes in the alkalinity and carbonate systems. The biogeochemical module of BROM includes parameterizations of OM production (via photosynthesis and chemosynthesis) and decay, and the transformation of phosphorus and silicate. BROM also includes a module describing the carbonate equilibria to account for the dynamic behavior of the components of total alkalinity significant in suboxic and anoxic conditions (i.e. speciation of S, N, Si, P).~~

~~The physical domain of the model~~The redox state and oxygenation of near-bottom water varies due to the transport of oxidized and reduced species across the SWI and biogeochemical processes occurring in the sediments (Cooper and Morse, 1996; Jorgensen et al., 1990; Roden and Tuttle, 1992; Sell and Morse, 2006). The sediments generally consume oxygen due to the deposition of labile OM and the presence of reduced forms of chemical elements. Their capacity to exchange oxygen with the pelagic layer is limited, as near bottom water

is usually characterized by low water velocity and reduced mixing in the vicinity of the SWI (Glud, 2008). In some cases, a high benthic oxygen demand (BOD) associated with local OM mineralization and low mixing rates can cause anoxia in the bottom water. This may lead to death, migration, or changed behavior of the benthic macro and meio faunal organisms responsible for bioturbation and bioirrigation (Blackwelder et al., 1996; Sen Gupta et al., 1996; Morse and Eldridge, 2007), which in turn can greatly slow down the transport of solid and dissolved species inside the sediments and therefore the rates of oxidative reactions. Under such conditions, sedimentary sulfides can build up, and dissolution of carbonate minerals may come to a halt (Morse and Eldridge, 2007). When oxic conditions return, there can be an "oxygen debt" of reduced species in the water column (Yakushev et al., 2011) which may buffer and delay reoxygenation of the sediments (Morse and Eldridge, 2007).

The processes taking place in the water column and in the sediments are therefore tightly coupled in areas experiencing seasonal hypoxia/anoxia, and an accurate understanding of physical, chemical, and biological processes driving changes in redox conditions is needed to predict the distribution of hypoxia/anoxia in a given environment. Also, the distinct environments of the water column and sediments may be strongly coupled by the exchange of matter on a range of time scales. This "benthic–pelagic coupling" is broadly defined by fluxes of OM to the sediments and return fluxes of inorganic nutrients to the water column. Variations in supply, dynamics and reactivity of OM affect the benthic communities (Pearson and Rosenberg, 1978), the sediment and porewater geochemistry (Berner, 1980), and the nutrient and oxygen fluxes at the SWI (Boudreau, 1997). The impact of OM on the benthos is generally more noticeable in shallow environments such as shelf seas, bays and lakes.

A number of recent studies demonstrate the capability of sophisticated reactive transport codes for integrated modelling of biogeochemical cycles in sediments (Boudreau, 1996; Van Cappellen and Wang, 1996; Couture et al., 2010; Jourabchi et al., 2005; Paraska et al., 2014; Soetaert et al., 1996). The water column redox interface was also specifically targeted in the models of (Konovalov et al., 2006; Yakushev et al., 2006, 2007). However, the process of integrating of such models with pelagic biogeochemical models to produce benthic-pelagic coupled models has only begun in recent years.

As of the year 2000, benthic-pelagic coupling was largely neglected or crudely approximated in many pelagic biogeochemical and early diagenetic models, which latter can in fact be regarded as benthic biogeochemical models (Soetaert et al., 2000). One of the first fully coupled physical–pelagic–benthic biogeochemical modes was developed for the Goban Spur shelf-break area to examine the impact of in-situ atmospheric conditions on ecosystem dynamics, to understand biogeochemical distributions in the water column and the sediments, and to derive a nitrogen budget for the area. This model was most suited to testing the impact of short-term physical forcing on the ecosystem (Soetaert et al., 2001).

Later, several coupled benthic-pelagic models were produced with an emphasis on studying eutrophication (Cerco et al., 2006; Fennel et al., 2011; Soetaert and Middelburg, 2009) or hypoxia in various locations including Tokyo bay (Sohma et al., 2008), the Baltic Sea (Reed et al., 2011), the North Sea Oyster Grounds (Meire et al., 2013) and Southern Bight (Lancelot et al., 2005). Another model was created to investigate early diagenesis of silica in Scheldt estuary, with benthic-pelagic coupling only of silica (Arndt and Regnier, 2007).

By coupling two quite sophisticated models ECOHAM1 and C.CANDI, a 3D model for the North Sea was created where pelagic model output was used as a forcing for a benthic biogeochemical module (Luff and Moll, 2004). Another physical-biological model for the North Sea, PROWQM, is more complex than ECOHAM1 and has been coupled to a benthic module to simulate seasonal changes of chlorophyll, nutrients and oxygen at the PROVESS north site, south–east of the Shetland Islands (Lee et al., 2002). (Brigolin et al., 2011) developed a spatially explicit model for the northwestern Adriatic coastal zone by coupling a 1D transient early diagenesis model with a 2D reaction-transport pelagic biogeochemical model. Currently, the most known and established coupled model is ERSEM – the European Regional Seas Ecosystem Model that was initially developed as a coastal ecosystem model for the North Sea and which has evolved into a generic tool for ecosystem simulations from shelf seas to the global ocean (Butenschön et al., 2015).

The BROM model described herein is a fully coupled benthic-pelagic model with a special focus on deoxygenation and redox biogeochemistry in the sediments and Benthic Boundary Layer (BBL). The BBL is "the part of the marine environment that is directly influenced by the presence of the interface between the bed and its overlying water" (Dade et al., 2001). Physical scientists tend to prefer the term "bottom boundary layer", but this largely synonymous with the BBL (Thorpe, 2005). Within BROM, the term BBL is used to refer to the lower parts of the fluid bottom boundary layer where bottom friction strongly inhibits current speed and vertical mixing, hence including the viscous and logarithmic sublayers up to at most a few meters above the sediment. This calm-water layer plays a critical role in mediating the interaction of the water column and sediment biogeochemistry and in determining e.g. near-bottom oxygen levels, yet it remains poorly resolved in most physical circulation models. For BROM we have developed an accompanying offline transport module "BROM-transport" that uses output from hydrodynamic water column models but solves the transport-reaction equations for a "full" grid including both water column and sediments. BROM-transport uses greatly increased spatial resolution near to the SWI, and thereby provides explicit spatial resolution of the BBL and sediments.

The goal of this work was to develop a model that captures key biogeochemical processes in the water and sediment and to analyze the changes occurring in the BBL and SWI. As a result, BROM differs from existing biogeochemical models in several key respects. BROM features explicit, detailed descriptions of many chemical transformations under different redox conditions, and tracks the fate of several chemical elements (Mn, Fe, and S) and compounds ($MnCO_3$, FeS, S0, S_2O_3) that rarely appear in other models. BROM also allows for spatially explicit representations of the vertical structure in the sediments and BBL. This distinguishes it from e.g. ERSEM (Butenschön et al., 2015), which has a more detailed representation of larger benthic organisms (meiofauna and different types of macrofauna), but limits its chemistry to the dissolved phase to CO_2, O_2 and macronutrients, its benthic bacteria to two functional groups, and its sedimentary vertical structure to an implicit three-layer representation that relies on equilibrium profiles of solutes and idealized profiles of particulates. Third, BROM offers a near-comprehensive representation of all processes affecting oxygen levels in the BBL and sediments, and should therefore provide a useful tool for studies focused on deoxygenation in deep water and sediments. Finally, BROM is conceived and programmed as a flexible model that can be applied in a broad range of marine and lake environments and modelling problems. As a component of the Framework for Aquatic Biogeochemical Modelling (FABM, Bruggeman and Bolding, 2014), BROM can be very easily coupled online

to any hydrodynamic model within the FABM, and can also be driven offline by hydrodynamic model output saved in NetCDF or text format using the purpose-built offline transport solver BROM-transport.

2 BROM description

Here we present the one-dimensional vertical transport and reaction model Bottom RedOx Model, BROM. It consists of two modules, BROM-biogeochemistry and BROM-transport. BROM-biogeochemistry is based on ROLM (RedOx Layer Model), a model constructed to simulate basic biogeochemical structure of the water column oxic/anoxic interface in the Black Sea, Baltic Sea, and Norwegian fjords (He et al., 2012; Stanev et al., 2014; Yakushev et al., 2009, 2006, 2007, 2011). In BROM–biogeochemistry we extended the list of modelled compounds and processes (Figure 1). BROM considers interconnected transformations of species of (N, P, Si, C, O, S, Mn, Fe) and resolves OM in nitrogen currency. OM dynamics include parameterizations of OM production (via photosynthesis and chemosynthesis) and OM decay via oxic mineralization, denitrification, metal reduction, sulfate reduction and methanogenesis. In order to provide a detailed representation of changing redox conditions, OM in BROM is mineralized by several different electron acceptors and dissolved oxygen is consumed during both mineralization of OM and oxidation of various reduced compounds. Process inhibition in accordance with redox potential is parameterized by various redox-dependent switches. BROM also includes a module describing the carbonate equilibria; this allows BROM to be used to investigate acidification and impacts of changing pH and saturation states on water and sediment biogeochemistry.

The physical domain of BROM-transport spans the water column, ~~the~~ BBL and ~~the~~ upper ~~layer~~layers of the sediments in a continuous fashion. ~~That allowed moving~~This allows for an explicit, high-resolution representation of the BBL and upper sediments, while also allowing the boundary conditions to be moved as far as possible from ~~the place~~these foci of interest~~, the sediment water interface,~~ i.e. to the ~~water~~/air ~~boundary~~ sea interface and to deep in the sediment.

~~To parameterize the water column, including temperature, salinity and turbulent diffusivity, we use results of a simulation of turbulent mixing performed using the General Ocean Turbulence Model (GOTM) (Bolding et al., 2002) for the North Sea. In the limits of the BBL, mixing was assumed to be constant. In the sediments, molecular diffusion and bioirrigation/bioturbation were parameterized.~~

BROM is built upon an existing modular platform (~~Framework for Aquatic Biogeochemical Modelling FABM, (Bruggeman and Bolding, 2014)) and present a mechanistic biogeochemical model that formalizes universal principles that apply throughout all three domains considered: pelagic, the BBL and upper sediment. BROM is written as~~FABM) and is therefore coded as a set of reusable "lego-brick" components, ~~consisting~~ consists of a ~~stand alone~~including the offline transport driver BROM-transport and separate modules for ecology, redox chemistry, and carbonate chemistry. ~~These modules are reusable: the~~ This means that BROM-transport ~~driver~~ can be used with all ~~other~~ biogeochemical ~~models~~modules available in FABM, including ~~the European Regional Seas Ecosystem Model (~~e.g. the modules comprising ERSEM~~),~~ and that BROM biogeochemical modules can be used in all other 1D and 3D hydrodynamic models supported by FABM (e.g., GOTM, GETM, MOM5, NEMO, FVCOM). Individual BROM modules can also be coupled to existing ecological models to expand their ~~feature~~

~~set~~scope, e.g.~~.~~. by providing ~~them with~~ descriptions of redox and carbonate chemistry. ~~Via~~Using the FABM~~, this approach allows~~ framework thus facilitates the transparent and consistent setup of ~~a~~ complex biogeochemical reaction ~~network~~networks for the prediction of hypoxia/anoxia while harnessing the capabilities of various hydrophysical drivers. ~~This allows an investigation of the dynamics of interfaces in the water column-sediment continuum that is critical for ecosystem functioning, yet hard-to-reach for in-situ exploration.~~

~~1 This presented model application can be considered as rather theoretical one aiming in analyses of the potential influence of the changeable redox conditions on the properties distributions and processes rates. Here we present model results for the seasonal variability of biogeochemical variables, emerging from the interplay of modelled biogeochemical processes, the variability in environmental conditions (temperature, salinity, turbulent mixing), and the imposed boundary conditions (prescribed constant concentrations or fluxes for selected variables).~~**Biogeochemical module**

~~4~~2.1.1 General description

BROM ~~contains~~ biogeochemistry consists of 3 biogeochemical ~~modules~~submodules: BROM_bio (ecological model), BROM_redox (redox processes) and BROM_carb (carbonate system).

In BROM, reactions are either defined as kinetic processes (e.g. ~~organic matter~~OM degradation) or ~~protolithic~~equilibrium processes (e.g. carbonate system equilibration) (Boudreau, 1996; Jourabchi et al., 2008; Luff et al., 2001). In general, the ~~protolythic~~redox reactions are fast ~~compared to~~in comparison with the other ~~kinetic processes~~reactions and ~~compared to~~with the time step at which the model is typically integrated. Therefore, equilibrium concentrations of the chemical element species involved in such reactions can be calculated using mass action laws and equilibrium constants for ~~the~~ seawater (Millero, 1995). ~~That takes away~~This eliminates the need to include a separate state variable ~~for~~ e.g. for pH~~, which instead~~. Instead, the total scale pH is calculated as a diagnostic variable at every time step as a function of DIC and Alk (~~that~~which are state variables). In turn, the total scale pH is ~~then~~ used in calculations of the chemical equilibrium constants required to describe related processes (i.e. carbonate precipitation/dissolution, carbonate system parameters etc.).

The model has 33 state variables, described in Table 1. This includes frequently measured components such as hydrogen sulfide (H_2S) and phosphate (PO_4), as well as rarely measured variables such as elemental sulfur (S^0), thiosulfate (S_2O_3), trivalent manganese species Mn(III), and bacteria. Variables of the latter category were included because their contribution to biogeochemical transformations is believed to be substantial. ~~The model state variables (C_i) are described in (Table 1).~~

~~The simplified ecological model of BROM reflects main functional groups of organisms (i.e. phytoplankton, heterotrophs, 4 functional groups of bacteria (aerobic heterotrophic, aerobic autotrophic, anaerobic heterotrophic, anaerobic autotrophic) and parameterizes the key features of organic matter~~For instance, bacteria play an important role in many modelled processes and can consume or release nutrients in organic and inorganic forms (Canfield et al., 2005; Kappler et al., 2005). We acknowledge that for many of these additional variables, site-specific estimates of associated model parameters and initial/boundary conditions may be difficult

Formatted: Font: Bold, English (U.S.), Hidden

Formatted: List Paragraph, Level 2, Space Before: 10 pt, Line spacing: Multiple 1,15 li, Outline numbered + Level: 1 + Numbering Style: 1, 2, 3, … + Start at: 1 + Alignment: Left + Aligned at: 0 cm + Tab after: 0,76 cm + Indent at: 0,76 cm

Formatted: Left, Space Before: 10 pt, After: 0 pt, Line spacing: Multiple 1,15 li, Don't keep with next

Formatted: Font: 10 pt

Field Code Changed

Field Code Changed

or impossible to obtain, and may in practice require some crude assumptions and approximations (e.g. universal default parameter values, no-flux boundary conditions, initial conditions from a steady annual cycle). Nevertheless, we believe that for many applications this will be a price worth paying for the additional process resolution/realism provided by BROM for important biogeochemical processes in the BBL and sediments. The equations and parameters employed in BROM are given in Tables 2 and 3, and a flow chart is shown in Figure 1.

2.1.2 Ecosystem and redox models

The BROM modules for ecosystem and redox processes are equivalent to those featured in ROLM. The overall goal of the ecosystem representation is to parameterize the key features of OM production and decomposition, which is based on Redfield and Richards stoichiometry (Richards, 1965).

~~The model contains frequently measured components such as sulfides (H_2S) and phosphate (PO_4) whose spatial and temporal variability is generally known, as well as rarely measured variables such as elemental sulfur (S^0), thiosulfate (S_2O_3), trivalent manganese species Mn(III) and bacteria.~~ We divide all the living OM (biota) into Phy (photosynthetic biota), Het (non-microbial heterotrophic biota), and 4 groups of "bacteria" which may be considered to include microbial fungi. These latter are: Baae (aerobic chemoautotrophic bacteria), Baan (anaerobic chemoautotrophic bacteria), Bhae (aerobic heterotrophic bacteria), and Bhan (anaerobic heterotrophic bacteria). OM is produced photosynthetically by Phy and chemosynthetically by bacteria, specifically by Baae in oxic conditions and by Baan in anoxic conditions. Growth of heterotrophic bacteria is tied to mineralization of OM, favouring Bhae in oxic conditions and Bhan in anoxic conditions. Secondary production is represented by Het which consumes phytoplankton as well as all types of bacteria and dead particulate organic matter (detritus, which is also explicitly modelled). ~~Variables of the latter category were included because their contribution to biogeochemical transformations is believed to be substantial. For instance, bacteria play an important role in many of the processes modelled and can consume or release nutrients as in both the organic and inorganic form (Canfield et al., 2005; Kappler et al., 2005) . The equations and parameters employed in BROM are given in Tables 2 and 3, a flow chart is shown in Figure 1.~~

~~4.1.1 **Ecosystem and redox model**~~

~~The BROM model of ecosystem and redox processes are equivalent to those featured in ROLM. The main goal of the ecosystem parameterization is to describe the fate of OM. OM is produced photosynthetically by phytoplankton and chemosynthetically by bacteria, specifically by aerobic autotrophic bacteria in oxic conditions and by anaerobic autotrophic bacteria in anoxic conditions. Growth of heterotrophic bacteria is tied to mineralization of OM, favouring aerobic bacteria in oxic conditions and anaerobic bacteria in anoxic conditions. Heterotrophs consume phytoplankton, all types of bacteria and detritus.~~ The effect of suboxia and anoxia is parameterized by letting the mortality of aerobic organisms depend on the oxygen availability. ~~Mineralization of OM leads to a consequent depletion of oxygen, nitrate, oxidized Mn, oxidized Fe and sulfate. The redox processes that affect reduced and oxidized inorganic species of nitrogen, sulphur, manganese and iron, and phosphorus species are also parameterized. A detailed description of this processes and parameterizations is given in Yakushev at al. (2007, 2013).~~

As was mentioned before, BROM is based on ROLM which was designed to simulate redox processes that affect inorganic species of nitrogen, sulfur, manganese, iron, and phosphorus. Their detailed description is given in (Yakushev et al., 2007, 2013a) but the process parametrization, chemical reactions, rate and stoichiometric

Field Code Changed

Formatted: English (U.S.)

constants values are summarized in Tables 2-4. Table 2 also describes the redox-dependent switches, nutrient limitation and heterotrophic transfer functions. The redox-dependent switches are mostly based on hyperbolic tangent functions which improve system stability compared with discrete switches. The nutrient limitation and heterotrophic transfer functions are based on squared Monod laws for Nutrient/Biomass ratio, which also stabilizes the system compared with Michaelis-Menten and Ivlev formulations. Here we describe the parameterization of carbon that was not considered in ROLM and was not described in (Yakushev, 2013).

~~5~~2.1.3 Total alkalinity

Total alkalinity, A_T, is a model state variable. Following the formal definition of A_T (Dickson, 1992; Wolf-Gladrow et al., 2007; Zeebe and Wolf-Gladrow, 2001) ~~-~~the following alkalinity components ~~are~~were considered:

~~$A_T = A_{TCO2} + A_B + A_{TPO4} + A_{Si} + A_{TNH3} + A_{TH2S} + [A_{NH3} + A_{H2S} + [OH^-] - A_{THF} - A_{THNO3} - A_{TSO4} A_{SO4} - A_{HF} - A_{HNO3} - [H^+] + A_{TOM}$~~

where the carbonate alkalinity~~,~~ $A_{TCO2} = [HCO_3^-] + 2[CO_3^{2-}]$, ~~the~~ phosphoric alkalinity~~,~~ $A_{TPO4} = [HPO_4^{2-}] + 2[PO_4^{3-}]$~~,~~ ~~the ammonia alkalinity, $A_{TNH3} = [NH_3] + [NH_4^+]$, the~~ $-[H_3PO_4]$, silicic alkalinity $A_{Si} = [H_3SiO_4^-]$, ammonia alkalinity $A_{NH3} = [NH_3]$, and ~~the~~ hydrogen ~~sulphide~~sulfide alkalinity~~, A_{TH2S}~~ $A_{H2S} = [HS^-]$~~, are~~ were calculated from the corresponding model state variables (Table 1) according to (Luff et al., 2001; Volkov, 1984). ~~The boric alkalinity, $A_B = [B(OH)_4^-]$, is estimated from salinity. Hydrogen sulfate alkalinity, $A_{TSO4} = [HSO_4^-]$, nitrous acid alkalinity $A_{THNO3} = [HNO_2]$ and the hydrofluoric alkalinity, $A_{THF} = [F^-] + [HF]$, were ignored due to their insignificant role to the A_T variations in this study . A_{TOM}, the alkalinity connected with total (dissolved and particulate) organic matter, TOM, was assumed set to 0~~The boric alkalinity $A_B = [B(OH)_4^-]$ was estimated from salinity. $[OH^-]$ and $[H^+]$ were calculated using the ion product of water (Millero, 1995). The hydrogen sulfate alkalinity $A_{SO4} = [HSO_4^-]$, hydrofluoric alkalinity $A_{HF} = [HF]$, and nitrous acid alkalinity $A_{HNO3} = [HNO_2]$ were ignored due to their insignificant impact on A_T variations in most natural marine and freshwater systems.

~~Biogeochemical processes can affect alkalinity via the 'nutrient H^+ compensating principle' formulated by Wolf-Gladrow et al. (2007): during uptake or release of charged nutrient species, electroneutrality is maintained by consumption or production of proton (i.e. during uptake of nitrate for photosynthesis or denitrification, or production of nitrate by nitrification). Besides these, the biogeochemical process can lead to either increase or decrease of alkalinity, and alkalinity can be used as~~Biogeochemical processes can lead to either increase or decrease of alkalinity, and alkalinity can be used as an indicator of specific biogeochemical processes (Soetaert et al., 2007). Organic matter production can affect alkalinity via the 'nutrient-H^+ compensating principle' formulated by Wolf-Gladrow et al. (2007): during uptake or release of charged nutrient species, electroneutrality is maintained by consumption or production of a proton (i.e. during uptake of nitrate for photosynthesis or denitrification, or production of nitrate by nitrification).

Formatted: Font: 10 pt
Formatted: Left, Space Before: 10 pt, After: 0 pt, Line spacing: Multiple 1,13 li, Don't keep with next
Field Code Changed
Formatted: Font: Cambria Math, 10 pt, Italic
Formatted: Font: Cambria Math, 10 pt, Italic
Formatted: Font: Cambria Math, 10 pt, Italic
Formatted: Font: Cambria Math, 10 pt, Italic
Formatted: Font: Cambria Math, 10 pt, Italic
Formatted: Font: Cambria Math, 10 pt, Italic
Formatted: Pattern: Clear (White)
Field Code Changed
Field Code Changed

~~The~~BROM also considers the effect on alkalinity of the following redox reactions occurring in suboxic and anoxic conditions via production or consumption of [OH^-] and [H^+] ~~or~~and changes ~~of~~in other "standard" alkalinity components ~~was explicitly considered in the model:~~A_{TCO2} and A_{H2S} (see bold font):

$4Mn^{2+} + O_2 + \mathbf{4H^+} \rightarrow 4Mn^{3+} + 2H_2O$

$2Mn^{3+} + 3H_2O + 0.5O_2 \rightarrow 2MnO_2 + \mathbf{6H^+}$

$2MnO_2 + \mathbf{7H^+} + \mathbf{HS^-} \rightarrow 2Mn^{3+} + 4H_2O + S^0$

$2Mn^{3+} + \mathbf{HS^-} \rightarrow 2Mn^{2+} + S^0 + \mathbf{H^+}$

$Mn^{2+} + \mathbf{HS^-} \leftrightarrow MnS + \mathbf{H^+}$

$Mn^{2+} + \mathbf{CO_3^{2-}} \leftrightarrow MnCO_3$

$2\ MnCO_3 + O_2 + 2H_2O \rightarrow 2MnO_2 + \mathbf{2HCO_3^-} + \mathbf{2H^+}$

$4Fe^{2+} + O_2 + 10H_2O \rightarrow 4Fe(OH)_3 + \mathbf{8H^+}$

$2Fe^{2+} + MnO_2 + 4H_2O \rightarrow 2Fe(OH)_3 + Mn^{2+} + \mathbf{2H^+}$

$2Fe(OH)_3 + \mathbf{HS^-} + \mathbf{5H^+} \rightarrow 2Fe^{2+} + S^0 + 6H_2O$

$Fe^{2+} + \mathbf{HS^-} \leftrightarrow FeS + \mathbf{H^+}$

$FeS + 2.25O_2 + 2.5H_2O \rightarrow Fe(OH)_3 + \mathbf{2H^+} + SO_4^{2-}$

$FeS_2 + 3.5O_2 + H_2O \rightarrow Fe^{2+} + 2SO_4^{2-} + \mathbf{2H^+}$

~~$4S^0 + 3H_2O \rightarrow 2H_2S + S_2O_3^{2-} + 2H^+$~~

$Fe^{2+} + \mathbf{CO_3^{2-}} \leftrightarrow FeCO_3$

$NH_4^+ + 1.5O_2 \rightarrow NO_2^- + \mathbf{2H^+} + H_2O$

$0.75CH_2O + \mathbf{H^+} + NO_2^- \rightarrow 0.5N_2 + 1.25H_2O + 0.75CO_2$

$4S^0 + 3H_2O \rightarrow 2H_2S + S_2O_3^{2-} + 2\mathbf{H^+}$

$2S^0 + O_2 + H_2O \rightarrow S_2O_3^{2-} + 2\mathbf{H^+}$

$4S^0 + 3NO_3^- + 7H_2O \rightarrow 4SO_4^{2-} + 3NH_4^+ + 2\mathbf{H^+}$

$S_2O_3^{2-} + 2O_2 + \mathbf{2OH^-} \rightarrow 2SO_4^{2-} + H_2O$

~~$3H_2S + 4NO_3^- + 6\mathbf{OH^-} \rightarrow 3SO_4^{2-} + 2N_2$~~ $5H_2S + 8NO_3^- + \mathbf{2OH^-} \rightarrow 5SO_4^{2-} + 4N_2 + 6H_2O$

$Ca^{2+} + \mathbf{CO_3^{2-}} \leftrightarrow CaCO_3$

~~There were also parameterized changes in the "standard"~~Standard alkalinity components ~~(i.e. A_{TNH3}, A_{TH2S}) followed from these reactions and all the~~were also affected by other reactions considered in the model (see Table ~~3~~2).

~~6~~2.1.4 Carbonate system

Equilibration of the carbonate system was considered as a fast process occurring ~~in less than several~~within a few seconds ~~(protolithic reactions)~~ (Zeebe and Wolf-Gladrow, 2001)~~. Accordingly, the equilibrium solution was calculated at every time step using an iterative procedure. That was needed to model the fate of, for example, calcium carbonate that is involved in both protolithic reactions and with transport processes. The carbonate system was described using standard approaches (Lewis and Wallace, 1998; Roy et al., 1993; Wanninkhof,~~

Formatted ... (×36)
Field Code Changed ...

~~2014; Wolf-Gladrow et al., 2007; Zeebe and Wolf-Gladrow, 2001). We used Roy's set of constants (Roy et al, 1993), total pH was calculated using the Newton-Raphson method. Precipitation and dissolution of calcium carbonate were modeled following an approach of (Luff et al., 2001) (Table 2).~~

~~6.1 Physical environment~~

~~The 1-dimensional model domain spans the water column, the Bottom Boundary Layer (BBL) and the upper layer of the sediments.~~

~~The water column extends from 0 to 90 m (with a spatial resolution of 5 m), the BBL from 90 to 90.5 m (with a spatial resolution of 2.5 cm) and the upper layer of sediments from 90.5 to 90.62 m (with a spatial resolution of 2 mm). This rather thick BBL was taken to illustrate the peculiarities of the biogeochemical structure above the bottom in case of bottom anoxic formation.~~

. Accordingly, the equilibrium solution was calculated at every time step using an iterative procedure. The carbonate system was described using standard approaches (Lewis and Wallace, 1998; Munhoven, 2013; Roy et al., 1993a; Wanninkhof, 2014; Wolf-Gladrow et al., 2007; Zeebe and Wolf-Gladrow, 2001). The set of constants of (Roy et al., 1993a) was used for carbonic acid. Constants for boric, hydrofluoric, and hydrogen sulfate alkalinity were calculated according to (Dickson, 1992), for silicic alkalinity according to (Millero, 1995), for ammonia alkalinity according to (Luff et al., 2001), and for hydrogen sulfide alkalinity according to (Luff et al., 2001) and (Volkov, 1984). The ion product of water was calculated according to (Millero, 1995). Total scale pH was calculated using the Newton-Raphson method with the modifications proposed in (Munhoven, 2013). Precipitation and dissolution of calcium carbonate were modelled following the approach of (Luff et al., 2001) (Table 2).

2.2 Physical environment

As mentioned above, BROM-biogeochemistry can be very simply coupled "online" to any hydrodynamic model with FABM support. Typically, however, such couplings only cover biogeochemistry within the interior of the water column; the hydrodynamic model code may require extensive adaptation to resolve the BBL and upper sediments. We therefore developed a simple 1D offline transport-reaction model, BROM-transport, whose model domain spans the water column, BBL, and upper layers of the sediments, with enhanced spatial resolution in the BBL and sediments. All options and parameter values for BROM-transport are specified in a run-time input file brom.yaml. A step-by-step guide to running BROM-transport is provided in Appendix A.

2.2.1 BROM-transport model formulation

The time space evolution of ~~the BROM biogeochemical~~state variables in BROM-transport is described by a system of ~~horizontally integrated vertical diffusion~~1D transport-reaction equations ~~for non-conservative substances:~~

$$\frac{\partial C_i}{\partial t} = \frac{\partial}{\partial z} K_z \frac{\partial C_i}{\partial z} - \frac{\partial (W_{Ci} + W_{Me}) C_i}{\partial z} + R_{C_i} \quad (1)$$

where C_i – concentration of a model compounds; K_z – vertical transport coefficient; W_{Ci} – is in Cartesian coordinates. In the sinking rate of the particulate matter; W_{Me} – sinking rate of particles with settled Mn and Fe hydroxides; $R_{C_i} = \sum_j R_{B_j C_i}$ – combined sources minus sinks of a substance (rates of transformation), being an algebraic sum of terms associated with specific biogeochemical processes ($R_{B_j C_i}$).

To evaluate the behaviour of the model under realistic forcing we use North Sea data (Bolding et al., 2002) to parameterize water column characteristics and to test on an independent subset of the data results of the biogeochemical model. Data for water column parameterization include initial profiles of temperature and salinity, external pressure gradients (e.g., tidal constituents), and surface forcing. Data used to evaluate model results include the fluxes and concentrations in the sediments, as well as additional observations (i.e. local presence of the bacterial mats). The mathematical parameterization of the vertical exchange treats K_z as the turbulent diffusion coefficient in the water column and molecular diffusion coefficient in the sediments. Bioirrigation and bioturbation can also be parameterized as modifiers of the value of K_z the dynamics are:

To the water column K_z is provided by the results of the 1D General Ocean Turbulence Model (GOTM) simulations for the Northern North Sea, described in (Bolding et al., 2002) http://www.gotm.net/index.php?go=software&page=testcases. We aimed for a solution representative for "present day", and we are thus treating the GOTM setup incl. forcing as representative for a "normal year".

For the BBL K_z was assumed to be constant with value 0.5×10^{-6} $m^2 s^{-1}$.

In the sediments, K_z was parameterized as a sum of the pore water molecular diffusion coefficient K_{z_mol}=1×10^{-11} $m^2 s^{-1}$ and bioirrigation/bioturbation coefficient.

Bioturbation activity (i.e. mixing of sediment particulates by burrowing infauna) and bio irrigation (i.e. flushing of benthic sediment by burrowing fauna through burrow ventilation) were parameterized in the model. In mesocosm experiments with North Sea sediments (Queirós et al., 2014) the biodiffusion coefficient was found to be 2 – 5 $cm^2 yr^{-1}$ (0. 6 – 1.6 10^{-11} $m^2 s^{-1}$) and the maximum bioturbation depth was 0.5–2.2 cm. In current version of model sediment porosity is not explicitly considered, but its effect on vertical transport is incorporated in the values of K_z and K_{z_bio}, which together control the vertical diffusion in the sediment. K_z is set to a constant value of 1.10^{-11} $m^2 s^{-1}$, it was calculated using averaged substance dependent diffusion coefficient (Boudreau, 1997) adjusted by assuming a constant porosity of 90% (applicable for upper 10 cm of sediment (Vershinin, Rozanov, 2002) and by a tortuosity corresponding to this porosity value (value from (Boudreau,1997). K_{z_bio} is a value of biodiffusion coefficient, it is constant for upper 2 cm of sediment ($K_{z\_bio\_max}$= 1.10^{-11} $m^2 s^{-1}$) and further exponentially decrease with depth. K_{z_bio} is further scaled with a Michaelis-Menten function of the oxygen concentration.

$$K_{z\_bio} = K_{z\_bio\_max} \frac{O_{2s}}{O_{2s} + K_{O2s}} \quad \frac{\partial \hat{C}_i}{\partial t} = \frac{\partial}{\partial z} D \frac{\partial \hat{C}_i}{\partial z} - \frac{\partial}{\partial z} v_i \hat{C}_i + \varepsilon_h (\hat{C}_{0i} - \hat{C}_i) + T_{birr(i)} + R_i$$

(1)

where $\hat{C}_i$ is the concentration in units [mmol/m^3 total volume] of the i^{th} state variable, $D(z,t)$ is the vertical diffusivity, v_i is the settling or sinking velocity, $\varepsilon_h(z,t)$ is a rate of horizontal mixing with an external concentration $\hat{C}_{0i}(z,t)$ (or alternatively, a restoring rate to a climatological concentration), $T_{birr(i)}$ is a tendency due to bioirrigation (only non-zero for dissolved substances in the bottom layer of the water column, see below), and R_i is the combined sources-minus-sinks (in this study provided by BROM-biogeochemistry, but in principle any biogeochemical model in FABM could be used). Values for D, ε_h, $\hat{C}_{0i}$, and other forcings used by R_i are configured at run time through input files (see section 2.2.7). Sinking velocities v_i are non-zero only for particulate (non-dissolved) variables and are determined at each time step by the biogeochemical module (through FABM). BROM-biogeochemistry assumes constant sinking velocities for phytoplankton, zooplankton, bacteria, detritus, and inorganic particles (Table 3.5).

In the sediments, dissolved substances or solutes obey the dynamics:

$$\varphi \frac{\partial C_i}{\partial t} = \frac{\partial}{\partial z}\varphi D_C \frac{\partial C_i}{\partial z} - \frac{\partial}{\partial z}\varphi u C_i + T_{birrC} + R_i \qquad (2)$$

where φ is the porosity, assumed constant in time, D_C is the total solute diffusivity, u is the solute burial velocity, and C_i is the porewater concentration in units [mmol/m^3 porewater]. Particulate substances become part of the solid matrix in the sediments. These obey:

$$(1-\varphi)\frac{\partial B_i}{\partial t} = \frac{\partial}{\partial z}(1-\varphi) D_B \frac{\partial B_i}{\partial z} - \frac{\partial}{\partial z}(1-\varphi) w B_i + R_i \qquad (3)$$

where D_B is the particulate (bioturbation) diffusivity, w is the particulate burial velocity, and B_i is the particulate concentration in units [mmol/m^3 total solids].

The porosity $\varphi(z)$ in (2) and (3) is prescribed as an exponential decay, following (Soetaert et al., 1996):

$$\varphi = \varphi_\infty + (\varphi_0 - \varphi_\infty) e^{-\frac{(z - z_{SWI})}{\delta}} \qquad (4)$$

where φ_∞ is the deep (compacted) porosity, φ_0 is the sediment surface porosity, z_{SWI} is the depth of the SWI, and δ is a decay scale defining the rate of compaction.

Diffusion within the sediments is assumed to be strictly "intraphase" (Boudreau, 1997), hence the Fickian gradients in (2) and (3) are formed using the concentration per unit volume porewater for solutes and per unit volume total solids for particulates. The total solute diffusivity $D_C = D_m + D_B$, where D_m is the apparent molecular/ionic diffusivity and D_B is the bioturbation diffusivity due to animal movement and ingestion/excretion. The apparent molecular diffusivity $D_m(z) = \theta^{-2} D_0 \frac{\mu_0}{\mu_{sw}}$ is derived from the infinite-dilution molecular diffusivity D_0 (an input parameter) assuming a constant relative dynamic viscosity $\frac{\mu_0}{\mu_{sw}}$ (default value 0.94, cf. (Boudreau, 1997), Table 4.10) and a tortuosity parameterized as: $\theta^2 = 1 - 2\ln\varphi$ from (Boudreau, 1997)Eqn. 4.120. The bioturbation diffusivity $D_B(z,t)$ is modelled as a Michaelis-Menten function of the dissolved oxygen concentration in the bottom layer of the water column:

$$D_B(z,t) = D_{Bmax}(z)\frac{O_{2s}}{O_{2s} + K_{O2s}} \qquad (5)$$

~~Where O_{2s} is the concentration of dissolved oxygen at the sediment surface, $K_{z\_bio\_max}$ is maximum bioturbation/bioirrigation coefficient and~~ where $D_{Bmax}(z)$ is a constant over a fixed mixed layer depth in the surface sediments then decays to zero with increasing depth, and K_{O2s} ~~= 1 µM is a constant.~~

Formatted: Justified, Indent: First line: 0 cm

Field Code Changed

Constant W_{Cr} values were assumed for phytoplankton, zooplankton, bacteria, and detritus (Table 3). In addition, the effect of increased sinking rates due to the formation of Mn(IV) and Fe(III) oxides and their association with particulate organic matter (POM) was parameterized. It was found that the precipitation of particulate Mn oxide significantly increases the flux of sinking particles, which, in turn, affects the overall distribution of particles (Yakushev and Debolskaya, 1998):

$$W_{Me} = W_{Me}^{\max} \frac{Mn(IV)}{Mn(IV) + K_{Me}} \quad (3)$$

Coefficients W_{Me}^{max} and K_{Me} are given in Table 3.

6.2 Boundary Conditions

The water column considered in our model spans the sea surface (upper boundary) down to user's defined sediment depth (12 cm depth in this application) as a lower boundary. At the upper boundary, fluxes of the modeled chemical constituents are assumed to be zero, with the exception of O_2, CO_2, PO_4, inorganic nitrogen compounds and Fe and Mn oxides.

For oxygen, the surface flux represents exchange with the atmosphere. This is given by the flux equation:

$$Q_{O_2} = k_{660} (Sc/660)^{-0.5} (Oxsat - O_2), \quad (4)$$

where *Oxsat* is equal to oxygen saturation as a function of temperature and salinity, according to UNESCO (1986); *Sc* is the Schmidt number; k_{660} is the reference gas-exchange transfer velocity. To describe k_{660} as a function of wind speed, the following equation is used:

$$k_{660} = 0.365 \cdot u^2 + 0.46 \cdot u \quad (A5)$$

Simulations are carried out using a mean wind speed $u = 5\ m*s^{-1}$.

CO_2 exchange was parameterized in a same way as for oxygen, with atmospheric CO_2 equal 400 ppm during all the seasons, but with a different Sc.

Inputs of phosphorus, nitrogen, iron and manganese from atmospheric precipitates and rivers were taken into account by prescribing concentrations at the sea surface. For phosphorus (Q_P) and nitrogen (Q_N), the seasonality in these inputs was considered by imposing time-varying surface concentrations:

$$Conc(PO4) = (1 + sin(2\pi * (julianday + 55)/365)) * 0.9 \quad (6)$$

$$Conc(NO3) = (1 + sin(2\pi * (julianday + 55)/365)) * 7 \quad (7)$$

~~where *julianday* is the Julian day number.~~

~~Constant surface concentrations were prescribed for the following variables: SO_4 (25×10^{-3} µM), Alk (2250 µM), Mn(IV) (1×10^{-4} µM), Fe (III) (5×10^{-5} µM). At the lower boundary we assumed constant concentrations of SO_4 (25×10^{-3} µM). Therefore, the model biogeochemistry was predominantly forced by the upper boundary conditions; the concentrations at the lower boundary emerge as a result of processes occurred in the water column, BBL and upper sediment. The boundary conditions for the physical parameters used in the model were those described in (Bolding et al., 2002). Irradiance was calculated as described in Table 3.~~

~~6.3 Computational aspects~~

~~Numerical~~is a half-saturation constant. The rationale for (5) is that the animals (worms etc.) that cause bioturbation require a source of oxygen at the sediment surface for respiration.

Diffusion between the sediments and water column, i.e. across the SWI, raises a subtle issue in regard to particulates. Here any diffusive flux cannot be strictly intraphase, because particulates are modelled as [mmol/m^3 total solids] in the sediments but as [mmol/m^3 total volume] in the water column. In BROM-transport, the bottom layer of the water column is considered a "fluff layer"; particles enter through the upper interface at their sinking velocity and leave through the layer interface (SWI) at the particulate burial velocity. It follows that a portion of the particulate matter in the fluff layer must be considered as settled fluff, but that portion is not predicted by the model. BROM-transport therefore offers two options. In the first approach, the bioturbation diffusivity is set to zero on the SWI, so that only solutes can diffuse across the SWI by molecular diffusion. Since the present version of BROM-transport does not parameterize resuspension through the SWI due to fluid turbulence, the SWI thus becomes a one-way street for particulate matter, whose components can only reenter the water column after dissolution. In the second approach, the bioturbation diffusivity is given by (5) on the SWI, but the bioturbation flux is interphase, mixing concentrations in units [mmol/m^3 total volume] for both solutes and particulates. This option is appropriate if bioturbation can be assumed to exchange fluff and sediment, or if it contributes significantly to particulate resuspension.

The burial velocities u and w in (2) and (3) can be inferred from the porosity profile under the assumptions of steady state compaction (φ constant in time) and no externally-impressed porewater flow (Berner, 1971, 1980; Boudreau, 1997; Meysman et al., 2005). Here, BROM-transport again offers two approaches. In the first approach, the reactions of particles in the sediments are assumed to have negligible impact on the volume fraction of total solids, and the deep particulate burial velocity w_∞ in compacted sediments (where $\varphi = \varphi_\infty$) is assumed to be a known constant $w_{b\infty}$ (an input parameter). Since compaction ceases at this (possibly infinite) depth, the solute burial velocity must here equal the particulate burial velocity ($u_\infty = w_{b\infty}$). Steady state then implies the following burial velocities (Appendix B):

$$w = \frac{(1-\varphi_\infty)}{(1-\varphi)} w_{b\infty} - \frac{1}{(1-\varphi)} D_B^{inter} \frac{\partial \varphi}{\partial z} \quad (6)$$

$$u = \frac{\varphi_\infty}{\varphi} w_{b\infty} + \frac{1}{\varphi} D_B^{inter} \frac{\partial \varphi}{\partial z} \quad (7)$$

where D_B^{inter} is the interphase bioturbation diffusivity, non-zero only at the SWI and only if bioturbation across the SWI is enabled. In the second approach, the reactions of the modelled particulate substances in the sediments modify the total solid volume fraction, and the modelled sinking fluxes from the water column modify the flux of solid volume at the SWI. The velocities in (6, 7) then define background velocities (w_b, u_b) due to non-modelled particulates. Again assuming steady state compaction leads to the following corrections to the background burial velocities (see Appendix B):

$$w' = \frac{1}{(1-\varphi)} \sum_i^{N_p} \frac{1}{\rho_i} \left[v_{f(i)} \hat{C}_{sf(i)} + \int_{z_{SWI}}^{z} R_i(z') dz' \right] \quad (8)$$

$$u' = \frac{1}{\varphi} (w'_\infty - (1-\varphi) w') \quad (9)$$

where $w' = w - w_b$, $u' = u - u_b$, N_p is the number of particulate variables, ρ_i is the density of the i^{th} particle type, $v_{f(i)}$ is the sinking velocity in the fluff layer, $\hat{C}_{sf(i)}$ is the suspended particulate concentration in the fluff layer, R_i is the particulate reaction term, and w'_∞ is the correction to the deep particulate burial velocity, in practice approximated by the deepest value of w'. Since the suspended portion $\hat{C}_{sf(i)}$ is not explicitly modelled, it is approximated as the minimum of the particulate concentrations in the fluff layer and the layer immediately above. In our applications we have found that (8) and (9) can improve the realism of sediment organic matter distributions, mainly by increasing the burial rate following pelagic production and export events such as the spring bloom.

Finally, the process of bioirrigation, whereby worms flush out their burrows with water from the sediment surface, is modelled as a non-local solute exchange following (Meile et al., 2001; Rutgers Van Der Loeff and Boudreau, 1997; Schlüter et al., 2000):

$$T_{birrC(i)} = \alpha \varphi \frac{O_{2s}}{O_{2s} + K_{O2s}} \left(\hat{C}_{f(i)} - C_i \right) \quad \text{(for solutes)} \quad (10)$$

where $\alpha(z)$ is the bioirrigation rate in oxic conditions, $\hat{C}_{f(i)}$ is the flushing concentration of solute in the fluff layer, and the Michaelis-Menten function again accounts for the suppression of worm activity in anoxic conditions. The oxic bioirrigation rate $\alpha(z)$ is parameterized as an exponential decay from the sediment surface as in Schluter et al. (2000). The total mass transfer to/from the sediment column must be balanced by a flux into/out of the fluff layer (see equation (1)):

$$T_{birr(i)} = \frac{1}{h_f} \frac{O_{2s}}{O_{2s} + K_{O2s}} \int_{z_{SWI}}^{z_{max}} \alpha \varphi \left(C_i - \hat{C}_{f(i)} \right) dz' \quad \text{(for solutes)} \quad (11)$$

where h_f is the thickness of the fluff layer and z_{max} is the depth of the bottom of the modelled sediment column. $T_{birrC(i)}, T_{birr(i)} = 0$ for all particulate variables.

2.2.2 BROM-transport numerical integration ~~was conducted with the Eulerian scheme and by process~~

Equations (1-3) are integrated numerically over a single combined grid (water column plus sediments) and using the same model time step in both water column and sediments. All concentrations are stored internally and input/output in units [mmol/m^3 total volume]. Time stepping follows an operator splitting ~~(i.e., separate treatment of~~approach (Butenschön et al., 2012): concentrations are successively updated by contributions over one time step of diffusion, bioirrigation, reaction, and sedimentation, in that order. If any state variable has any 'not-a-number' values at the end of the time step then the program is terminated.

Diffusive updates are calculated either by a simple forward-time central-space (FTCS) algorithm or by a semi-implicit, central-space algorithm adapted from a routine in the General Ocean Turbulence Model, GOTM (Umlauf et al., 2005). Bioirrigation and reaction updates are calculated as forward Euler time steps, using the FABM to compute R_i, and sedimentation updates are calculated using a simple first-order upwind differencing scheme. After each update, Dirichlet boundary conditions (see below) are reimposed and all concentrations are low-bounded by a minimum value (default = 10^{-11} µM) to avoid negative values. Maximum diffusive and advective Courant numbers can optionally be output after every time step or when/if a 'not-a-number' value is detected. Before starting the integration, the program calculates Courant numbers due to eddy/molecular diffusion~~, advection/sinking and reaction/source-sink terms). Time steps were set to 2.5×10^{-3} d for biogeochemical processes and sinking and 6.25×10^{-4} d for~~ and returns a warning message if the maximum value on high on any given day and the FTCS option is selected.

BROM-transport also provides the ability to divide the diffusion~~, that is 54~~ and sedimentation updates into smaller time steps related to the sources-minus-sinks time step by fixed factors, since the physical transport processes are often numerically limiting (Butenschön et al., 2012). The default time step is 0.0025 days or 216 seconds, ~~a~~which is much ~~larger number that~~longer than the characteristic ~~scale~~equilibration timescale of the CO_2 kinetics (Zeebe and Wolf-Gladrow, 2001)~~. The initial calculations assume a vertically homogenous distribution of all biogeochemical variables, with compound specific initial concentrations. To subsequently resolve spatial and temporal variation in the biogeochemical components, calculations are repeated with seasonal changes of temperature, salinity, vertical turbulence in the water column (calculated with GOTM) and irradiance until a quasi stationary solution with seasonal forced oscillations of the biogeochemical variables is reached. The code is written in FORTRAN and was run with the Intel FORTRAN for Windows Compiler.~~

~~To determine the vertically balanced distribution, the calculations were repeated with seasonal changes of temperature, salinity, vertical turbulence in the water column (calculated with GOTM) and irradiance until a quasi stationary solution with seasonal forced oscillations of the biogeochemical variables was reached. That is, there were no changes in the year-averaged concentrations of the variables for at least 100 model years.~~

~~7 Model Output Discussion~~

~~In this work we used a simplified hydrodynamic scenario, since the main goal of the model was to reproduce the biogeochemical mechanism of transformation of oxic conditions into anoxic in the sediment-water interface. The model biogeochemical modules consider relatively fast processes, (seasonal and shorter), and therefore exclude longer time scale processes, occurring on e.g. geological time scales. Additionally, the model was forced only at the sea surface and did not include fluxes of reduced components (i.e. hydrogen sulphide, Mn(II), MnS, FeS)~~

Formatted: Indent: First line: 0 cm

Field Code Changed

~~across the low boundary of the model, in order to focus exclusively on the consequences of supply of the fresh organic matter as a main reducer in the water column and in the sediments.~~

~~**7.1 Test Case Simulations**~~

2.2.3 ~~The model shows a possibility of the~~ BROM-transport vertical grid

The vertical grid in BROM-transport is divided into the pelagic water column, the BBL, and the sediments. The pelagic water column grid is either set as uniform with height/spacing set by the brom.yaml file (see Appendix C), or it is read from the NetCDF forcing input file (see below), with an option to decrease resolution by subsampling. In principle, the NetCDF input from the hydrodynamic model may already include a fully-resolved BBL, but in practice we find this is rarely the case. BROM-transport therefore allows the user to "insert" a high-resolution BBL into the bottom of the input water column. This BBL has non-uniform grid spacing with layer thickness decreasing geometrically towards the SWI, reaching 2(cm) thickness for the fluff layer, based on parameters from the brom.yaml file. For the upper sediments, the layer thickness is increased geometrically moving down from the SWI, from 0.5(mm) thickness in the surface layer to 1(cm) thickness deeper in the sediments, again based on brom.yaml parameters. The result is a full grid with non-uniform spacing and maximum resolution near the SWI. As in many ocean models (e.g. ROMS, GOTM) the vertical grid in BROM-transport is staggered: temperature, salinity, and biogeochemical concentrations are defined at layer midpoints, while diffusivities, sinking/burial velocities, and resulting transport fluxes are all defined on layer interfaces.

2.2.4 BROM-transport initial conditions

Initial conditions for all concentrations in equations (1-3) can be provided by either using the initialization values defined in the fabm.yaml file (see Appendix D) as uniform initial conditions for each variable, or by providing the initial conditions for all variables at every depth in a text file with a specific format. Typically these initial condition text files are generated by running the model to a steady state annual cycle and saving the final values as the desired start date. Alternatively they could be generated by interpolating /smoothing data, in which case the user should note that the input concentrations must be in units [mmol/m^3 total volume].

2.2.5 BROM-transport boundary conditions

BROM-transport presently allows the user to choose between four different types of boundary condition for each variable and for upper and lower boundaries: 1) no-gradient at the bottom boundary (no diffusive flux) or no-flux at the surface boundary, except where parameterized by the FABM biogeochemical model (i.e. for O_2 and DIC in the case of BROM-biogeochemistry); 2) a fixed constant value; 3) a fixed sinusoidal variation in time defined by amplitude, mean value, and phase parameters; or 4) an arbitrary fixed variation in time read from the input NetCDF file. All boundary condition options and parameters are set in the brom.yaml file (see Appendix C). Note that options 2-4 are Dirichlet boundary conditions which define implicit fluxes of matter into and out of the model domain, and that all boundary concentrations should be in units [mmol/m^3 total volume (water+solids)]. The default option 1 is generally the preferred choice, but the Dirichlet options can also be useful to allow a

simple representation of e.g. fluxes of nutrients into and out of the surface layer due to lateral riverine input. A possible alternative is to use the forcings parameters for horizontal mixing (see equation (1)) to specify horizontal exchanges or restoring terms to observed climatology (see section 2.2.7).

Under option 1, and using BROM-biogeochemistry, a surface O_2 flux representing exchange with the atmosphere is parameterized as:

$$Q_{O_2} = K_{660} * \left({Sc}/{660}\right)^2 * (Oxsat - O_2) \quad (12)$$

where Oxsat is the oxygen saturation as a function of temperature and salinity, according to UNESCO (1986), Sc is the Schmidt number, and k_{660} is the reference gas-exchange transfer velocity, parameterized as $k_{660} = 0.365u^2 + 0.46u$ where u is the wind speed 10 m above the sea surface [m s^{-1}]. Air-sea exchange of CO_2 in BROM-biogeochemistry is parameterized using the differences of the particle pressures in water (pCO_2^{water}) and air pCO_2^{air}). The formulation and coefficient were those used in ERSEM (Butenschön et al., 2016)

Field Code Changed

$$Q_{O_2} = F_{wind} * \left(pCO_2{}^{air} - pCO_2{}^{water}\right) \quad (13)$$

where $F_{wind} = (0.222u^2 + 0.333u)(Sc/660)^{-0.5}$ is a wind parameter, u is the wind speed, and Sc is a Schmidt number.

2.2.6 BROM-transport irradiance model

BROM-transport includes two simple Beer-Lambert attenuation models to calculate in situ 24-hour average photosynthetically active radiation (PAR) as needed by BROM-biogeochemistry and many other biogeochemical models. The first is derived from the current ERSEM default model (Blackford et al., 2004; Butenschön et al., 2016) and models the total attenuation as:

$$k_t = k_0 + k_{Phy}Phy + k_{PON}PON + k_sS \quad (14)$$

where k_0 is the background attenuation of seawater, k_{Phy} , k_{PON} are the specific attenuations due to phytoplankton and detritus respectively, and k_s is the specific attenuation due "other" optically active substances with concentration *S* (currently a constant input parameter). The second model includes attenuation due to other optically active concentrations that are modelled by BROM-biogeochemistry:

$$k_t = k_0 + k_{Phy}Phy + k_{PON}PON + k_{Het}Het + k_{DON}DON + k_{PB}B + k_{PIV}PIV + k_sS \quad (15)$$

where *B* is the total bacterial concentration (= *Baae* + *Baan* + *Bhae* + *Bhan*) and *PIV* is the total volume fraction of modelled inorganic particles, calculated from the concentrations using input densities of each inorganic solid. The final irradiance is scaled by a constant parameter representing either the photosynthetically active fraction of the in situ irradiance or the relationship between surface PAR in water and the forcing surface

irradiance (Mobley and Boss, 2012). The forcing surface irradiance $Eair(t)$ can be read from NetCDF input or otherwise calculated using a sinusoidal function (Yakushev et al., 2013b). In addition, the surface attenuation due to ice cover can be accounted for as a simple linear function of a NetCDF input ice thickness variable $hice(t)$.

2.2.7 BROM-transport input forcings

BROM-transport requires forcing inputs at least for temperature, salinity, and vertical diffusivity at all depths in the pelagic water column and for each day of the simulation. These may be provided from an input subroutine that creates simple, hypothetical profiles, or from text/NetCDF files containing data from interpolations of measurements or hydrodynamic model output. Forcing time series of surface irradiance and ice thickness may also be read as NetCDF input. BROM-transport then uses these inputs in combination with parameters set in the run-time input file brom.yaml (see Appendix C) to solve the transport-reaction equations on a "full" vertical grid including pelagic water column, BBL, and sediment subgrids.

In order to run, BROM-transport must extend the input pelagic (temperature, salinity, diffusivity) forcings over the full grid. Temperature and salinity in the BBL and sediments are set as uniform and equal to the values at the bottom of the input pelagic water column for each day. The vertical diffusivity needs a more careful treatment as it is the main defining characteristic of the pelagic vs. BBL vs. sediment environments. Within the water column, the total vertical diffusivity $D = D_m + D_e$ for solutes and $D = D_e$ for particulates, where D_m is a constant molecular diffusivity at infinite dilution, and D_e is the eddy diffusivity read from the input file for the pelagic water column. For the BBL, D_e can be defined as "dynamic", in which case it is linearly interpolated for each day between the deepest input forcing value above the SWI and zero at a depth h_{DBL} above the SWI, where h_{DBL} is the diffusive boundary layer (DBL) thickness (default value 0.5 mm). This option is likely appropriate for shallow water applications where D_e may be strongly time-dependent within the user-defined BBL (default thickness 0.5 m). Alternatively, a static, fixed profile $D_{eBBL}(z)$ may be more appropriate for deep water BBLs, where time dependence may be weak and deepest values from hydrodynamic models may be relatively far above the SWI. In this case, BROM-transport offers two options for $D_{eBBL}(z)$: 1) a constant value, dropping to zero in the DBL, or 2) a linear variation between a fixed value at the top of the BBL and zero at the top of the DBL. Option 1) defines a simplest-possible assumption, while option 2) corresponds to the assumption of a log layer for the current speed e.g. (Boudreau and Jorgensen, 2001). Eddy diffusivity is strictly zero in the DBL, on the SWI, and within the sediments. Diffusivity in the sediments is due to molecular diffusion and bioturbation and is parameterized as described in section 2.2.1.

Optional forcings for BROM-transport include 24-hour average surface irradiance $Eair(t)$, which is often supplied by hydrodynamic models (e.g. ROMS), a surface ice thickness forcing $hice(t)$, and depth-time arrays of horizontal mixing rates $\varepsilon_h(z,t)$ and horizontal mixing concentrations $\hat{C}_{0i}(z,t)$ (see equation (1)). Horizontal mixing rates within the inserted BBL and sediments are set to zero. Note that these horizontal mixing forcings can also be used to define relaxation or restoring fluxes to climatological values within the pelagic water column, which may in some cases provide a valid means of accounting for horizontal flux divergence effects that are missing in the 1D model.

3 BROM demonstration run

3.1 Model setup

A North Sea hydrodynamic scenario was used to demonstrate the ability of BROM to reproduce the biogeochemical mechanisms of oxic/anoxic transformations. Complete lists of the model options and parameter values used are given in Appendix C (brom.yaml input file for BROM-transport) and Appendix D (fabm.yaml input file for BROM-biogeochemistry).

The BROM-transport water column extended from 0 to 110 m, with a pelagic spatial resolution of 1 m inherited from the GOTM hydrodynamic model used to provide forcings. A high-resolution BBL was inserted from 109.5 to 110 m, with layer thickness decreasing from approximately 25 cm to 3 cm in the fluff layer. Sediment grid points were added to cover the upper 10 cm of sediments with layer thickness increasing from 0.5 mm in the surface layer to 1 cm at depth. The model time step for BROM-transport was set to 0.0025 days (216 seconds).

Upper boundary conditions included sinusoidal, time-varying Dirichlet boundary conditions for nitrate, phosphate and silicate, implying net influxes and outfluxes of surface nutrients, as well as the default parameterized air-sea fluxes of O_2 and DIC (see Appendix C). Lower boundary conditions assumed (by default) zero diffusive flux for all reduced components (i.e. hydrogen sulfide, solid phase concentrations of metal sulfides and carbonates, silicon and OM). The simulation therefore focuses on the consequences of the supply of fresh OM as a main reducer in both water column and sediments.

The pelagic water column was forced by output from a GOTM hydrodynamical simulation for temperature, salinity, and vertical diffusivity (taken from the salinity diffusivity) and surface irradiance calculated using the sinusoidal option. We aimed for a solution representative for "present day" and therefore treated the GOTM forcing as representative for a "normal year". BROM-transport was spun up from vertically-homogeneous initial conditions for 100 model years with repeated-year forcings and boundary conditions. After this time, a quasi-stationary solution with seasonally forced oscillations of the biogeochemical variables had been reached.

The results of these calculations were written to an output file in NetCDF format, including the daily vertical distributions of model state variables, diagnostic rates of biogeochemical transformations, and fluxes associated with diffusion and sedimentation. This output can be visualized by any NetCDF-compatible software.

3.2 Results

The model simulated the periodic replacement of oxic ~~conditions~~ with anoxic~~, which leads to changes~~ conditions in the ~~vertical distributions of~~BBL following seasonal mixing and OM production. The simulation demonstrates the ~~biogeochemical variables (Figures 2-6) and their fluxes (Figure 7). These simulations revealed a number of~~ characteristic features of ~~the sediment-water interface biogeochemistry.~~biogeochemical profiles in the water column, BBL and upper sediments, as well as their variability under changing redox conditions (Figs. 2-4).

~~**In the**~~During intensive mixing conditions in winter, the water column is well, oxygenated ~~**winter period**~~and the oxic/anoxic interface ~~was positioned~~is located at several ~~millimeters~~centimeters depth in the sediments (~~see also Figure~~Figs. 2~~). Deposition~~, 3). In summer, just after the spring bloom, an enrichment of ~~large amounts of~~the sediment surface with fresh OM ~~to the bottom under~~and a restricted oxygen supply leads to ~~a shift of this interface toward the sediment surface, due to consistent~~the consumption of O_2~~, NO_3, Mn(IV), Mn(III), Fe(III)~~

Formatted: Font: Not Bold

~~and SO_4 for the~~ by OM mineralization ~~(Figure 4). In the BBL O_2 started to disappear in the middle of summer, accompanied by slower remineralization of OM and slower oxidation of~~and close to suboxic conditions (Fig. 2). The second bloom in the autumn leads to a further decrease of oxygen concentrations to complete depletion. There is a concomitant increase in reduced forms of ~~Mn, N, Fe and S. After O_2 consumption, NO_3 became a dominant oxidizer, which was then also rapidly depleted.~~

~~**After the decrease of oxygen at the sediment water interface to 5 µM**, the release from the bottom of S_2O_3 and S^0 starts;~~N, Mn, Fe and finally of hydrogen ~~sulphide initially remains in the sediments, only to enter the water column several days later (Figure 4). This is explained by the significant concentrations of Mn and Fe oxides in the upper millimeters of the sediments which prevented the immediate release of H_2S. Mn and Fe oxides react with hydrogen sulphide producing S_2O_3 and S^0. The modelled order of appearance in the water column of the intermediate sulphur species (first S_2O_3, then S^0 and then H_2S) corresponds to their typical order of appearance at real water column redox interfaces (Kamyshny et al., 2013). The delayed release of H_2S allowed the bottom surface and the BBL to be in suboxic conditions, allowing the accumulation of Mn(III).~~ sulfide in the bottom water (Figs. 2, 4). The redox interface thus moves from the sediment to the BBL.

~~Total dissolution of Fe and Mn oxides in late summer leads to a release of the H_2S from the sediments and an upward shift of the oxic/anoxic interface into the water column (Figure 6). This is accompanied by the disappearance of the phosphate minimum at the sediment surface (connected with trapping by the metal oxides) and sudden influx of phosphate from the sediment into the water. The calculated seasonal variability of the vertical fluxes (Figure 7) illustrates this behavior and allows us to compare roles of different species affecting the position of the redox interface.~~

~~**During the anoxic period**, H_2S, Mn(II), PO_4, Fe(II), S_2O_3 and NH_4 move upward in the water sediment column (Figure 7).~~

~~The majority of occurring redox processes is microbially mediated, leading to bacterial growth (both heterotrophs and autotrophs) and production of new OM (by autotrophs). This forms a positive feedback that accelerates the consumption of oxidizing compounds.~~

~~After the formation of suboxic and anoxic conditions in the BBL, aerobic heterotrophic bacteria disappear and an increase of the aerobic autotrophic and anaerobic heterotrophic bacteria is seen. This modelled increase of the bacterial concentrations at the sediment surface could hint at the presence of bacterial mats, which are known to occur under hypoxic/anoxic conditions [REF].~~

~~**Winter flushing events** lead to an abrupt increase of O_2 above the bottom, the appearance of Mn(IV), Mn(III) and Fe(III) in the water column, and their accumulation at the sediment surface (Figure 5). This is followed by a deepening of the oxic /anoxic interface inside the sediments during the winter.~~

~~The model clearly demonstrates the presence of a fine vertical biogeochemical structure in the near bottom water, especially under suboxic and anoxic conditions (Figure 2, Figure 3, and Figure 4). That means that the concentrations and fluxes change over every cm of the BBL and also temporally during the year. This should be taken into account while analyzing the data of observations and experiments, since the methods applied usually don't allow for fine-structure sampling. For example, in the standard methods of the sediment – water flux measurements with the box corers or benthic chambers, this fine structure is destroyed.~~

7.2 Comparison with data

Validation of the present complex multi component model against data is not trivial, because it is hard to assemble a comprehensive dataset against which to calibrate the model components at a vertical resolution and temporal frequency that captures to the fine scale vertical structure and rapid temporal variation characteristic of the system. Even though such dataset is not yet assembled, we believe it is a worthy exercise to present a model that captures a wide range of processes, thus providing a platform to test hypothesis and affine our conceptual understanding of anoxia.

Here we will provide relevant examples from regions with contrasting redox conditions where the model can be potentially use. Given that the water column model was parameterized for the Northern North Sea, we can compare our results against observations of the BBL under oxic conditions, collected recently in the Sleipner area (Linke et al., 2014; Queirós et al., 2014). Besides this, we can use the literature data on typical values or distributions collected in the other regions with suboxic and anoxic conditions.

For example the model is able to simulate the periodic succession of oxic, hypoxic and anoxic bottom waters following winter oxygenation that is documented for many years with very rare (4 times a year) observations for the Elefsis Bay in the Aegean Sea (Pavlidou et al., 2013).

The modelled concentrations and vertical distributions of dissolved oxygen, inorganic nitrogen species (nitrate, nitrite, ammonia), silicates, phosphates and iron and manganese species (Fe(II), Fe(III), Mn(II), Mn(III), and Mn(IV)) in the water column, BBL and porewater of upper sediment layer as well as range of its benthic fluxes values are in good agreements with the measured data (Table 5) (Pakhomova et al., 2007; Almroth et al., 2009; Queirós et al., 2014).

7.2.1 Dissolved oxygen

The model reproduces changes of oxygen concentrations at the sediment-water interface from 200 μM in oxygenated period to 0 μM during the anoxia. The field data in the Sleipner area show DO oscillations from 160 to 360 μM in the bottom water during observations taken over a two-month period (Linke et al., 2014) . The modeled downward vertical flux of oxygen was found to the highest in the water column below the euphotic zone in winter and early spring, it and sporadically exceeds 200 mmol $m^{-2} \cdot d^{-1}$, in connection with the mixing intensity changes (Figures 6, 7). In the limits of the BBL oxygen flux decreases from about 10 to 0 mmol $m^{-2} \cdot d^{-1}$, corresponding to the typical values of the oxygen flux that can be received in the field and laboratory experiments. For example, during the chamber experiments there was measured sediment oxygen consumption in the range 3.9-4.6 mmol $m^{-2} \cdot d^{-1}$ in the Sleipner area. (Queirós et al., 2014) and 5-13 mmol $m^{-2} \cdot d^{-1}$ in the Gulf of Finland, Vistula Lagoon, and shelf Black Sea (Almroth et al., 2009; Pakhomova et al., 2007). While in organic rich sediments, oxygen flux could reach up to 70 mmol $m^{-2} \cdot d^{-1}$ (Pakhomova et al., 2004, 2003).

The sediment pore water profile measured during the laboratory experiment shows oxygen depletion at 9 mm depth in oxic conditions and at 3 mm depth in hypoxic conditions (Queirós et al., 2014). That corresponds well with the modeled distribution of oxygen (Figure 2).

Unfortunately, further observations under anoxic and suboxic conditions are rare, as field and experimental studies generally focus on oxic conditions. While the model can describe the biogeochemistry of the bottom

areas with the restricted aeration, i.e. trenches and methane sips where hypoxia and anoxia can occur, lack of observations make it difficult to validate the corresponding model predictions, e.g., the disappearance of oxygen in the sediments, and in the near-bottom water during the stagnation period (Figure 3, Figure 4).

7.2.2 Nitrogen

The modelled concentrations of nitrate in the water column correspond to the climatic values (National Oceanographic Data Center (NODC) http://www.nodc.noaa.gov/). The flux of NO_3 changed its direction (Figure 7). In oxic conditions an upward flux of nitrate exists in the limits of the BBL and in the water column, compensating the loss of nitrate for photosynthesis production. In suboxic conditions there is a downward flux of nitrate connected with denitrification. The modelled upward values of the nitrate flux in the BBL (0.5 -2 mmol $m^{-2} d^{-1}$ in oxic period are within the range of measured values (from 0.5 to 2.5 mmol $m^{-2} d^{-1}$) (Almroth et al., 2009; Queirós et al., 2014).

In the sediments the modelled nitrogen was represented by ammonia with concentrations 250 μM, that is 2 times higher than measured during the experiments for nonsulphydic sediments, 120 μM, (Queirós et al., 2014) but is typical for sulphidic sediments (Almroth et al., 2009). The flux of ammonia is directed upward throughout the year, and changes from 0.03 mmol $m^{-2} d^{-1}$ during the oxic period to more than 1 mmol $m^{-2} d^{-1}$ during the anoxic period. The measured ammonia flux was in the range from 1 to 6 mmol $m^{-2} d^{-1}$ (Almroth et al., 2009; Queirós et al., 2014) was highest for anoxic sediments.

Figure 5 shows the rate of OM mineralization with a variety of electron acceptors. Oxygen is consumed during OM mineralization in summer and autumn and, after its complete depletion, denitrification dominates, with both nitrate reduction and nitrite reduction playing significant roles. The rate of mineralization of OM with Mn and Fe oxides is small, but as these processes prevent mineralization with sulfate, they cause a lag of a few days between the depletion of oxygen and the appearance of hydrogen sulfide in the water column (Figs. 2, 5). The amount of labile degradable OM is relatively small and mineralization with sulfate completely removes the remaining OM, thus preventing methanogenesis (Fig. 5).

The seasonal variability of the sediment-water fluxes clearly demonstrates the appearance in the bottom water of reduced forms of N, Mn, Fe and phosphate (Fig 6).

Generally, the concentrations, vertical distributions and benthic-pelagic fluxes of the parameters considered in the model are reasonable and are within observed ranges for the North Sea (Queirós et al., 2014) and some other regions with temporary bottom anoxia (Almroth et al., 2009; McCarthy et al., 2008; Morse and Eldridge, 2007; Pakhomova et al., 2007; Queirós et al., 2014; Yu et al., 2015).

4 Conclusion and future work

This paper presents a description of BROM, a fully-coupled pelagic-benthic model that provides a integrated framework to study the biogeochemistry of a water column and upper sediments. BROM simulates changes in redox conditions and their impact on the distributions of a wide range of biogeochemical variables. In particular, BROM provides a detailed description of the fate and availability of dissolved oxygen and hydrogen sulfide, the

former essential for macroscopic marine life, the latter highly toxic to it. BROM can therefore provide valuable information to ecological studies, particularly in the context of multistressor impacts. The model suggests that the timing of hydrogen sulfide release into the pelagic is linked to the dynamics of several electron acceptors that are themselves of limited interest for biogeochemical and ecological purposes, and that are therefore rarely included in models. The ability of BROM to simulate and forecast H_2S toxicity is in fact the direct result of its inclusion of several of these rarely modelled chemical compounds (e.g., Mn(IV), Fe(III)).

This paper was not devoted to a detailed validation of BROM with in situ data; we plan to explore this in future work. A qualitative analysis of the model results (Chapter 3) suggests that the model can produce realistic distributions and fluxes of key biogeochemical variables during periodic changes in redox conditions. More detailed evaluations of the model will be presented in the separate papers devoted to the studies in the selected regions, namely, for the Lagoon Berre, Fjord Sælenvatnet , and for the Gulf of Finland (in preparation).

In summary, we present a new benthic-pelagic biogeochemical model (BROM) that combines a relatively simple pelagic ecosystem model with a detailed biogeochemical model of the coupled cycles of (N, P, Si, C, O, S, Mn, Fe) in the water column, benthic boundary layer, and sediments, with a focus on oxygen and redox state. BROM should be an interesting tool for the study of benthic nutrient recycling, redox biogeochemistry, eutrophication, industrial pollution from mineral effluent and organic loading, deoxygenation, acidification, and the potential associated release of contaminants such as hydrogen sulfide in marine and freshwater environments.

~~7.2.3 **Phosphorus**~~

~~The modelled concentrations of phosphate increased from 0-2 µM in the the water column to around 4 µM in the BBL, which is higher than typical measured at oxic conditions values but could be found above the sulphidic sediments. Modelled phosphate concentrations in the upper sediments (up to 30-35 µM) were higher than the measured values of around 5 µM for nonsulphidic sediment (Queirós et al., 2014) but of the same level as for sulphidic sediment (15-50 µM, (Almroth et al., 2009)). Modelled phosphate fluxes in the BBL were less than 0.01 mmol m^{-2} d^{-1} in oxic conditions, increasing to 0.01 mmol m^{-2} d^{-1} in anoxic; these are comparable with measured values ranging from 1 to 0.9 mmol m^{-2} d^{-1} for oxic sediment (Queirós et al., 2014) but are lower than for sulphidic sediments (1.5 mmol m^{-2} d^{-1}, (Almroth et al., 2009)).~~

~~7.2.4 **Manganese**~~

~~Under oxic conditions the modelled manganese content was negligible in the water column and the sediment-water interface was characterized by an accumulation of Mn(IV). Beneath the maximum of Mn(IV) a peak of Mn(III) is formed, followed by a Mn(II) maximum and finally by a $MnCO_3$ and MnS increase, in agreement with the modern paradigm of Mn species distributions in the sediments (Madison et al., 2013). From qualitative point of view the modelled Mn(II) concentrations in the upper sediment (8-20 µM) were about the same level obtained for sulphidic sediments (5-30 µM in the coastal Black Sea, 25-50 µM in the Gulf of Finland,~~

(Pakhomova et al., 2007)) and lower than for nonsulphidic sediments (over 100 μM,(Pakhomova et al., 2007; Queirós et al., 2014)).

The model predicted the observed small concentrations of Mn(III) and Mn(II) in the bottom water during the stagnation period, but the modelled concentrations of Mn(II) were much smaller than observed . Modelled fluxes of Mn(IV), Mn(III) and Mn(II) were negligible (less than 0.1 mmol m^{-2} d^{-1}) while the measured fluxes varied from 3 to 20 mmol m^{-2} d^{-1} (Pakhomova et al., 2007; Queirós et al., 2014). To our knowledge, this is the first time that the distributions of Mn(III), a form of Mn that has only recently been considered (Madison et al., 2013), is included in a reaction network for sediment biogeochemistry.

The modelled concentration of Mn as solid $MnCO_3$ in upper sediment layers reached up to 11 μM that corresponds to 0.04% of Mn in the sediment (using transformation coefficient between dissolved and solid phases, F=0.66). The same average level of Mn is observed in sulphidic sediments 0.01 1% (Calvert and Pedersen, 1993; Pakhomova et al., 2007). Simulated by the model negligible concentrations of MnS in upper sulphidic sediment were is in agreement with field observation in many regions.

7.2.5 Iron

The distributions and variability of iron species were similar to those of manganese. As for Mn(II) the maximum modelled concentrations of Fe(II) in pore water (8-40 μM) were smaller than measured for nonsulphidic sediments (over 100 μM) (Pakhomova et al., 2007; Queirós et al., 2014) but slightly higher level than for sulphidic sediments (0.5-7 μM, (Pakhomova et al., 2007). Modelled fluxes of Fe(III) and Fe(II) (up to 0.1 mmol m^{-2} d^{-1}) were the same order of magnitude as average measured fluxes for sulphidic sediments, 0.04 and 0.3 mmol m^{-2} d^{-1} for Fe(III) and Fe(II) respectively. Both modelled and measured Fe(II) fluxes were highest at suboxic conditions in bottom water while measured Fe(II) fluxes could reach 1 mmol m^{-2} d^{-1} (Pakhomova et al., 2007).

7.3 Carbonate system

The modelled distributions of the carbonate system, their variability and fluxes are shown in Figure 5-7.

In the upper water layer pH values are high (8.10 in winter and 8.23 in summer), the values of pCO_2 are close to the equilibrium with the atmosphere (about 400 ppm). Calcium carbonate is oversaturated (about 2.5 for aragonite and about 3.5 for calcite). The values of total alkalinity (2300 μM) and DIC (2200 μM) are close to the typical values for the open ocean.

In the seasonally anoxic deep water layer and the BBL pH oscillated from 7.6 in oxygenated period to 7.1 during anoxia. pCO_2 varies from to 1200-1500 ppm to 2500-2800 ppm. Aragonite and calcite saturations change from 0.6 and 1.0 in oxic conditions to 0.2 and 0.4 in anoxic conditions, respectively. Total alkalinity and DIC are lower under oxic conditions (2200-2300 μM and 2200 μM) and larger values during anoxic conditions (2400 μM and 2500 μM).

In the upper 12 cm of the sediment pH decreases from 7.1-7.4 to 6.6, and pCO_2 increases from 2500-4000 ppm to is about 17000-23000 ppm. The performed calculations show that, under natural conditions, there are significant season variations in the carbonate saturation and pH values in the BBL. Modelled $CaCO_3$ was present in small concentrations (0.5 µM)at the SWI only in the oxygenated period (Figure 5).

It is known that the processes connected with changes of redox conditions represent an important factor of influence on the carbonate system and alkalinity. For example, pH dynamics caused by OM degradation are buffered by precipitation and dissolution of carbonates (Luff et al., 2001), sulphate reduction produces large amount of bicarbonate ion (Boudreau, 1996), Mn reduction increases alkalinity by producing bicarbonate and consuming protons (Sternbeck, 1996) , and Fe reduction leads to a consumption of protons (Luff et al., 2001).
The potential role of a such processes in the pH and alkalinity changes was analyzed by (Soetaert et al., 2007). In this model we simulate the combined effect of the mentioned processes in a scenario of variations of the bottom redox conditions from oxic into anoxic.
The comparison between the main seawater alkalinity components shown in Table 6 demonstrates that even in the anoxic conditions the contributions of such components A_{TPO4}, A_{Si}, A_{TNH3}, A_{TH2S} remain small compared with the carbonate alkalinity. The modeled mechanism of significant alkalinity changes is connected with redox processes (listed in chapter 2.1.1) that produce or remove H^+ or OH^- and the redox processes connected with OM mineralization (i.e. sulphate reduction, Mn reduction and Fe reduction). Because the protolithic reactions are very fast the results of these processes reflects in the ratio between carbonate and bicarbonate in a larger degree than in production/consumption of the forms of alkalinity that increases in anoxic conditions (i.e. A_{TPO4}, A_{Si}, A_{TNH3}, A_{TH2S}).
According to the model, at the sediment surface this resulted in a decrease of pH from 7.6 in oxic period to 7.1 in anoxic (Figure 5). In the sediments, pH decreased with depth to 6.6-6.7 at 12 cm. During the stagnation period, a pH minimum could be marked out at 1 cm depth where there was also a maximum of H_2S (Figure 4) and maximum of pCO_2, A_t and DIC. All this hints at a dominant role for sulfate reduction, which particularly affects the ratio between DIC and A_t that determines pH (i.e. analyzed by (Luff et al., 2001)). The upper sediment alkalinity maximum during the anoxic period subsequently smoothes and propagates into the deeper layers, leading to lower alkalinity during the oxic period. At the boundary between the BBL and the water column the alkalinity flux changes its direction from downward in oxic conditions to upward in anoxic conditions. At the SWI the alkalinity flux is directed upward with much smaller values in oxic than in anoxic conditions (Figure 7).
The bottom water is close to saturation regarding calcite and undersaturation regarding aragonite during the oxygenated period, and is undersaturated regarding both calcite and aragonite during the anoxic period. Deeper in the sediment aragonite (to a larger degree) and calcite (to a smaller degree) are always undersaturated. Note that according to the model assumption the sediment carbonate system processes were forced by the upper boundary.
The model calculations clearly demonstrates the impact of redox conditions on the carbonate system (and alkalinity and consequently, their role in regulating carbon transformation and transport.

~~7.4 Modeling analyses of the role of chemosynthesis and bioturbation~~

~~The model allows a quantitative analysis of how the processes interact and combine. It is possible to "unlock" or accelerate certain processes and to demonstrate their specific significance. Here we demonstrate this possibility on assessing of a role of chemosynthesis and bioturbation in the bottom biogeochemistry.~~

~~**For baseline simulations, we assumed the following parameters values: $k_{\_Baan\_gro}$ = 0.012 d^{-1} for anaerobic autotrophs chemosynthesis specific growth rate, and $K_{z\_bio\_max}$=1×10^{-11} m^2s^{-1} for maximum bioturbation/bioirrigation coefficient.**~~

~~**To assess an effect of chemosynthesis and bioturbation on the distribution of the model variables was calculated with varying $k_{\_Baan\_gro}$: A) $k_{\_Baan\_gro}$ = 0.012 d^{-1} (baseline) and B) $k_{\_Baan\_gro}$ = 0.060 d^{-1} and $K_{z\_bio\_max}$: I) $K_{z\_bio\_max}$ =0 m^2s^{-1}, II) $K_{z\_bio\_max}$ =1×10^{-11} m^2s^{-1} (baseline) and $K_{z\_bio\_max}$ =10×10^{-11} m^2s^{-1}. The results are shown in Figure 8.**~~

~~The model experiment showed that bioturbation affects the depth of oxygen penetrations. In case of an absence of bioturbation that is less than 1 mm (AI), in case of a baseline bioturbation it is 2-4 mm (AII). In case of an increased bioturbation (AIII), oxygen penetration increases to 8-10 mm in the sediment column (Figure 8). In this case, the model predicts a pH minimum at the vicinity of depth of oxygen penetration. This is consistent with oxygen consuming reactions by reduced forms of S, N, Mn, Fe which consumes proton.~~

~~An increase of the chemosynthesis rate (Figure 8, column B) leads to a formation of a pH maximum just below the SWI that is connected with the consumption of CO_2, affecting the ratio between DIC and A_t. This maximum is more pronounced in the absence of bioturbation (BI) and is not pronounced under high bioturbation (BIII). This pH maximum produces a maximum in calcite saturation, which could favor the organisms with carbonate skeletons.~~

~~The pH distributions with a maximum below the SWI is usually explained by an electron transfer by long filamentous bacteria or grain to grain contacts between conductive materials (Meysman et al., 2015; Nielsen et al., 2010), but this model shows that chemosynthesis can have a similar effect.~~

Formatted: No bullets or numbering

~~8~~ Code availability

The ~~BROM~~ model ~~source code is publicly~~as presented consists of two components. The first is a set of biogeochemical modules (brom/redox, brom/bio, brom/carb, brom/eqconst), available as part of the official FABM distribution ~~at http://fabm.net. Being a part of FABM, BROM uses modern software standards: it~~(http://fabm.net); BROM-specific files are located in subdirectory src/models/niva/brom). The second is a hydrophysical driver (BROM-transport) that provides the 1D vertical context and resolves transport; this is available separately from https://github.com/e-yakushev/brom-git.git. When combined, the 1D BROM model as presented is obtained.

Both FABM and BROM-transport are coded in object-oriented Fortran 2003, ~~has~~have a build system based on CMake~~, and uses~~ (https://cmake.org), and use YAML files (http://yaml.org) for run-time configuration. The code is platform independent and only requires a Fortran 2003-capable compiler, e.g., gfortran 4.7 or higher, or the Intel Fortran compiler version 12.1 or higher. BROM-transport includes facilities for producing results as NetCDF files, which can be read by a variety of software on different platforms.

~~9 Summary and Conclusion~~

~~This paper presents a coupled benthic-pelagic model that reproduces different redox conditions and their impact on the distributions of a wide range of biogeochemical variables.~~

~~The comparison with the available data allows us to conclude that the model reproduces distributions and fluxes of key biogeochemical variables during the periodic change of redox conditions. That allows us to conclude the following:~~

- ~~The main driver of the redox state at the SWI is the formation of anoxia in the water column. That arises by an imbalance between the supply of OM and dissolved oxygen to the bottom water, which in turn is due to seasonality in production and consumption of OM, as well as mixing.~~
- ~~The model captures the time lag between disappearance of dissolved oxygen and appearance of H_2S in the bottom water. That is connected with Mn and Fe oxides, which buffer the H_2S efflux from the sediments after complete oxygen consumption. These oxides acts as "batteries", that are using up in anoxic periods and accumulates during oxic periods.~~
- ~~The model also demonstrates that redox conditions have a pronounced impact on the carbonate system and on alkalinity, which in turn affects carbon transformation and transport. It is shown that in anoxic conditions the total alkalinity changes in a larger degree because of variation of the ratio between carbonate and bicarbonate due to fast redox reactions producing or consuming proton, than because of and an increase or decrease of other alkalinity components (i.e. A_{TPO4}, A_{Si}, A_{TNH3}, A_{TH2S}).~~
- ~~Bacteria play a significant role in the fate of OM due to chemosynthesis (autotrophs) and consumption of DOM (heterotrophs). In particular, in certain conditions, the consumption of CO2 in chemosynthesis can lead to the formation of a pH maximum below the SWI.~~

~~In summary, the capability of BROM to reproduce seasonal variations in oxygen concentration and redox state, to resolve fine scale structure of the water column, BBL and sediment and to capture the time lags associated with rarely modelled compounds (e.g., Mn and Fe oxides role in securing of the H_2S efflux, pH, alkalinity, carbonate saturation change) presents a wide range of possibilities for use in applications.~~

As BROM's biogeochemical modules are built on FABM, they can be used from a wide range of 1D and 3D hydrodynamic models, including GOTM, GETM, ROMS, MOM, NEMO and FVCOM (a ROMS-FABM coupler has been developed by P.W.; NEMO-FABM and FVCOM-FABM couplers have been developed by the Plymouth Marine Laboratory; contact J.B. for information).

Results shown in this paper were produced with BROM-transport tag v1.1. and the BROM-biogeochemistry code in FABM tag v0.95.3, available from the above repositories. The simulation was run using the netCDF/.yaml input files found in the data/ folder of the BROM-transport repository. However, we envisage BROM to be further developed in a backward compatible manner, and encourage users to adopt the latest version of the code. Step-by-step instructions for running BROM are found in Appendix A. Both FABM and BROM-transport are distributed under the GNU General Public License (http://www.gnu.org/licenses/).

Author contributions: Development of the model code was made by EY, EP, JB, PW, SY, analyses of the model results and discussions were conducted by RB, RC and SP, and all authors contributed to the writing of the manuscript.

Formatted: Font: Times New Roman

Formatted: Font: Times New Roman

Formatted: Font: Times New Roman

Formatted: Heading 1;Kap. 1.

Acknowledgements

We wish to thank J. Middelburg, O.P. Savchuk, and G. Munhoven for detailed and constructive reviews that ultimately led to a major improvement in the manuscript. We acknowledge funding from the EC 7th Framework Program (FP7/2007-2013) under grant agreement no 265847 ('Sub-seabed CO2 Storage: Impact on Marine Ecosystems', ECO2) and 240837 ('Research into Impacts and Safety in CO2 Storage', RISCS), with additional development funds from FME SUCCESS, CO2Base, EEA CO2MARINE, Norwegian Research Council project no. 236658 ('New knowledge on sea deposits' NYKOS), the Research Council of Norway through its Centers of Excellence funding scheme, project number 223268/F50 (CERAD), contract no. 208279 (NIVA Strategic Institute Initiative "Climate effects from Mountains to Fjords"), NIVA OASIS, and VISTA – a basic research program and collaborative partnership between the Norwegian Academy of Science and Letters and Statoil, project no.6164. The work of J.B. was funded by NERC National Capability in Marine Modelling.

Appendix A: Running BROM step-by-step

1. Installation. A Fortran-2003-capable compiler, e.g., gfortran 4.7 or higher, or the Intel Fortran compiler version 12.1 or higher should be installed. In our demonstration we used the Intel Fortran Compiler version 15.0.4.221. Additionally, a NetCDF library compatible with the chosen Fortran compiler is required. CMake software should be installed. After ensuring these prerequisites are in place, create a directory to hold the BROM model code and associated input and output files. Detailed instructions for installation are provided at BROM repository https://github.com/e-yakushev/brom-git.git

2. Preparation of input files. The model reads two .yaml files with the model parameters (fabm.yaml and brom.yaml), as well as a NetCDF or text file with the hydrophysical forcing data. Optionally the biogeochemical initial conditions can be read from an text file **start.dat**; this may be a file written by a previous simulation (the final model state is written to a file named **finish.dat** at the end of every simulation).

i. brom.yaml (see Appendix C). This file specifies the values of transport model parameters as well as various option switches and input/output file and variable names. Text comments provide guidance and references for setting parameter values. If using NetCDF input the user should pay careful attention to the NetCDF input parameters and names, ensuring that this information is consistent with the input NetCDF file. The selected year parameter year must refer to a year that is covered by the input forcing data.

ii. fabm.yaml (see Appendix D). This file specifies the values of biogeochemical model parameters , default initial values for state variables, and the coupling of FABM modules. Text comments provide annotation and references.

iii. nns_annual.nc (in the example). This file contains input forcing data that may be derived from observations or hydrodynamical model output (GOTM in our demonstration). It can be replaced by a text (.dat) file if this is the format of the hydrodynamical model output.

iv. start.dat. Text file with initial values for model state variables at every depth. This file may be created by renaming the output of a previous simulation (finish.dat: the state at the 1st of January of the last modeled year).

3. Output files. These are NetCDF and headed text files generated automatically by the model during the simulation. Output files can be readily imported into various software packages for visualization and further analysis. Certain output files (Vertical_grid.dat and Hydrophysics.dat) are generated early in the simulation and should be checked by the user to ensure that the model grid and hydrophysical forcings are set up as intended.

i. Vertical_grid.dat. Text file with model layer indices, midpoint depths, increments between midpoint depths, and thicknesses.

ii. Hydrophysics.dat. Text file with daily profiles of hydrophysical variables (temperature, salinity, diffusivity, porosity, tortuosity, burial velocities).

iii. finish.dat. Text file with the state variables for the 1st of January of the last modeled year. Can be used for visualization or as initial conditions for further calculations.

iv. output_NNday.dat. Optional text file with the state variables and diagnostic variables for day NN to make plots of vertical distributions (e.g. Fig. 3)

v. BROM_out.nc. NetCDF file with daily profiles of state variables, rates of biogeochemical transformations, vertical fluxes.

4. Visualization. For NetCDF output file can be used any software with NetCDF input. In the example we used PyNcView. To visualize vertical distributions from text files we used the Python script available at https://github.com/lisapro/_brom-pics.git

Appendix B: Derivation of burial velocities

The conservation equations for liquid and total solid volume fractions in the sediments can be written as:

$$\frac{\partial \varphi}{\partial t} = \frac{\partial}{\partial z} D_B^{inter} \frac{\partial \varphi}{\partial z} - \frac{\partial}{\partial z} u\varphi - \sum_{i=1}^{N_p} \rho_i^{-1} R_i \quad \text{(B1)}$$

$$\frac{\partial (1-\varphi)}{\partial t} = \frac{\partial}{\partial z} D_B^{inter} \frac{\partial (1-\varphi)}{\partial z} - \frac{\partial}{\partial z} w(1-\varphi) + \sum_{i=1}^{N_p} \rho_i^{-1} R_i \quad \text{(B2)}$$

where D_B^{inter} is the interphase bioturbation diffusivity (possibly non-zero only at the SWI), ρ_i is the density of the i^{th} particulate substance, and R_i is the corresponding reaction term. Equations (B1) and (B2) assume that the densities of liquid and total solid are both constant, and they retain the net contributions of reactive terms although these are often considered negligible e.g. (Boudreau, 1997; Meysman et al., 2005). Summing (B1) and (B2) and integrating over depth gives a useful and quite general relationship:

$$\varphi u + (1-\varphi) w = U \quad \text{(B3)}$$

where $U(t)$ is only a function of time. If we now assume no externally impressed porewater flow, it follows that at some (possibly infinite) depth where compaction ceases ($\frac{\partial \varphi}{\partial z}$=0, $\varphi = \varphi_\infty$), the solute burial velocity u must here equal the particulate burial velocity w, hence $u_\infty = w_\infty$. Equation (B3) becomes:

$$\varphi u + (1-\varphi) w = w_\infty \quad \text{(B4)}$$

Now assuming steady state compaction ($\frac{\partial \varphi}{\partial t}$=0), equation (B2) can be integrated from the SWI to a depth z within the sediments:

$$(1-\varphi) w + D_B^{inter} \frac{\partial \varphi}{\partial z} = (1-\varphi_{SWI}) w_{SWI} + D_{BSWI}^{inter} \frac{\partial \varphi}{\partial z}_{SWI} + \sum_i^{N_p} \frac{1}{\rho_i} \int_{z_{SWI}}^{z} R_i(z') dz' \quad \text{(B5)}$$

To determine the first term on the RHS of (B5), we assume that the total solid volume flux across the SWI is equal to the total solid volume flux from the sinking of suspended particulate matter in the fluff layer:

$$(1-\varphi_{SWI}) w_{SWI} + D_{BSWI}^{inter} \frac{\partial \varphi}{\partial z}_{SWI} = F_b + \sum_i^{N_p} \frac{1}{\rho_i} v_{f(i)} \hat{C}_{sf(i)} \quad \text{(B6)}$$

where F_b defines a constant background solid volume flux due to non-modelled particles, $v_{f(i)}$ is the sinking velocity in the fluff layer, and $\hat{C}_{sf(i)}$ is the suspended particulate concentration in the fluff layer. Substituting into (B5) we have:

$$(1-\varphi) w + D_B^{inter} \frac{\partial \varphi}{\partial z} = F_b + \sum_i^{N_p} \frac{1}{\rho_i} \left[v_{f(i)} \hat{C}_{sf(i)} + \int_{z_{SWI}}^{z} R_i(z') dz' \right] \quad \text{(B7)}$$

Since $D_B^{inter} \frac{\partial \varphi}{\partial z}$ is zero at depth, the constant surface flux term is given by $F_b = (1-\varphi_\infty) w_{b\infty}$, where both φ_∞ and $w_{b\infty}$ are input parameters. Hence we have:

$$(1-\varphi) w + D_B^{inter} \frac{\partial \varphi}{\partial z} = (1-\varphi_\infty) w_{b\infty} + \sum_i^{N_p} \frac{1}{\rho_i} \left[v_{f(i)} \hat{C}_{sf(i)} + \int_{z_{SWI}}^{z} R_i(z') dz' \right] \quad \text{(B7)}$$

Equation (6) directly follows from (B7) by neglecting the modelled settling flux and reaction terms, then equation (7) follows by application of (B4). Equations (8) and (9) follow by considering the additional particulate burial velocity due to modelled fluxes and reactions (from the last term in B7) and applying

(B4) to obtain the additional solute burial velocity.Appendix C: run-time input file for BROM-transport (brom.yaml)

```
# IMPORTANT !!!!    <TAB> is NOT allowed here, used <Space> only !!!!
# Each entry must have 6 spaces before the parameter name
instances:
  brom:
    initialization:
##---Paramters for grid-------(see io_ascii.f90/make_vert_grid for a grid diagram)-----------------
      water_layer_thickness: 95.  # Thickness of the water column [m] (may overriden by netCDF input, see below)
      k_wat_bbl: 18             # Number of levels above the water/BBL boundary  (may be overriden by netCDF input, see
below)
      bbl_thickness: 0.5        # Thickness of the high-resolution layer overlying the sediments (model "benthic boundary
layer") [m] (default = 0.5 m)
                                #   This should be thinner than the full viscous+logarithmic layer, but thicker than the viscous layer
                                #   Typical thicknesses for full viscous+logarithmic layer are 1 m and 10 m for deep sea and shelf
respectively (Wimbush 2012)
      hz_bbl_min: 0.02          # Minimum allowed layer thickness in the BBL near the SWI [m] (default = 0.02 m)
      hz_sed_min: 0.0005        # Minimum layer thickness in the sediments near the SWI [m] (default = 0.0005 m)
      hz_sed_max: 0.01          # Maximum layer thickness deeper in the sediments [m] (default = 0.01 m)
      k_min: 1                  # Minimum k number defining the layer that is in contact with the atmosphere (default = 1)
      k_points_below_water: 17    # Number of levels below the water/BBL boundary (default = 20)
      i_min: 1                  # Minimum i number (default = 1)
      i_water: 1                # Number of i for water column (default = 1)
      i_max: 1                  # Maximum i number  (default = 1)
#Note: (i_min,i_water,i_max) should be (1,1,1) for 1D applications
#
#
##---Boundary conditions-----------------------------------------------------------------------
#
#Here we set the type of boundary condition using bctype_top_<variable name> and bctype_bottom_<variable name>
#     0 to use surface fluxes from FABM where parameterized, otherwise no flux (default, does not need to be explicitly set)
#     1 for constant Dirichlet, specified by bc_top_<variable name> or bc_bottom_<variable name>
#       E.g. bctype_bottom_niva_brom_bio_O2: 1
#            bc_bottom_niva_brom_bio_O2: 0.
#     2 for sinusoidal Dirichlet, specified by bcpar_top_<variable name> or bcpar_bottom_<variable name>
#            The model is: phi(t) = a1 + a2*sin(omega*(day-a3)) where omega = 2*pi/365
#                                  => max(phi(t)) = a1+a2, min(phi(t)) = a1-a2, mean(phi(t)) = a1, peak at 91.25+a3 days
#            Model parameters are specified by a1top_<variable name> etc.
#       E.g. bctype_top_niva_brom_bio_NO3: 2
#            a1top_niva_brom_bio_NO3: 3.0
#            a2top_niva_brom_bio_NO3: 3.0
#            a3top_niva_brom_bio_NO3: 60.
#     3 for arbitrary Dirichlet, read from netCDF file (see I/O options to specify netCDF variable names)
#
#     bctype_bottom_niva_brom_bio_O2: 1
#     bc_bottom_niva_brom_bio_O2: 0.
#
      bctype_top_niva_brom_redox_SO4: 1
      bc_top_niva_brom_redox_SO4: 25000.
      bctype_bottom_niva_brom_redox_SO4: 1
      bc_bottom_niva_brom_redox_SO4: 25000.
#
      bctype_top_niva_brom_redox_Mn4: 1
      bc_top_niva_brom_redox_Mn4: 20.E-4
#
      bctype_top_niva_brom_redox_Fe3: 1
      bc_top_niva_brom_redox_Fe3: 5.E-4
#
      bctype_top_niva_brom_carb_Alk: 1
      bc_top_niva_brom_carb_Alk: 2200.
#     bctype_bottom_niva_brom_carb_Alk: 1
#     bc_bottom_niva_brom_carb_Alk: 3200.
```

```
#
#     bctype_bottom_niva_brom_carb_DIC: 1
#     bc_bottom_niva_brom_carb_DIC: 2850.
#
#     bctype_bottom_niva_brom_bio_NH4: 1
#     bc_bottom_niva_brom_bio_NH4: 10.
#
     bctype_top_niva_brom_bio_NO3: 2
     a1top_niva_brom_bio_NO3: 1. # 3
     a2top_niva_brom_bio_NO3: 1.
     a3top_niva_brom_bio_NO3: 320.
     bctype_bottom_niva_brom_bio_NO3: 1
     bc_bottom_niva_brom_bio_NO3: 0.
#
     bctype_top_niva_brom_bio_PO4: 2
     a1top_niva_brom_bio_PO4: 0.7 #0.8
     a2top_niva_brom_bio_PO4: 0.7
     a3top_niva_brom_bio_PO4: 320. #60.
#     bctype_bottom_niva_brom_bio_PO4: 1
#     bc_bottom_niva_brom_bio_PO4: 10.
#
     bctype_top_niva_brom_redox_Si: 2
     a1top_niva_brom_redox_Si: 1.5
     a2top_niva_brom_redox_Si: 1.5
     a3top_niva_brom_redox_Si: 320.
#     bctype_bottom_niva_brom_redox_Si: 1
#     bc_bottom_niva_brom_redox_Si: 100.
#
#
##---Horizontal mixing parameters------------------------------------------------------------
#
#Here we specify horizontal mixing model using hmix_<variable name>
#     0 to assume no horizontal mixing (default, does not need to be explicitly set)
#     1 for "box model" mixing model: hmix = hmix_rate*(X_0 - X) with X_0 specified by netCDF input file and hmix_rate
specified here
#
     hmix_niva_brom_bio_NO3: 0
     hmix_niva_brom_bio_NH4: 0
     hmix_niva_brom_bio_PO4: 0
     hmix_niva_brom_redox_Si: 0
     hmix_niva_brom_bio_O2: 0
#
#
##---Ice model parameters--------------------------------------------------------------------
     use_hice: 0        # 1 to use ice thickness forcing "hice" from netCDF input
#
#
##---Constant forcings-----------------------------------------------------------------------
     density: 1000.
     wind_speed: 8.     # Wind speed 10 m above sea surface [m/s] (default = 8 m/s)
     pco2_atm: 380.     # Atmospheric partial pressure of CO2 [ppm] (default = 380 ppm)
#
#
##---Surface irradiance model parameters-----------------------------------------------------
     use_Eair: 0        # 1 to use 24-hr average surface downwelling shortwave irradiance in air from netCDF input
     lat_light: 50      # Latitude of modelled site [degrees north], e.g. Hardangerfjord station H6 is at 60.228N; Sleipner=50N;
Saelen=60.33N
     Io: 80.            # Theoretical maximum 24-hr average surface downwelling shortwave irradiance in air [W/m2] (default =
80 W/m2)
                        #   This should include that effect of average cloud cover (local)
     light_model: 0     # Specify light model: 0 for simple model based on ersem/light.f90
                        #                      1 for extended model accounting for other particulates in BROM
#
```

```
#
##---Light absorption model parameters ----------------------------------------------------------
    Eair_to_PAR0: 0.5  # Factor to convert input or calculated surface downward irradiance Eair to surface PAR in water
(default = 0.5, units dependent on Eair)
                #   Factor of ~0.48 to convert shortwave (0.3-4 um) to PAR-band (0.4-0.7 um) in [W/m2]
                #   Further factor of 0.8-0.95 to convert downward-in-air to net-in-water (Mobley and Boss, 2012, Figs. 2c,
4b, 8a)
                #   Latter factor becomes 0.45-0.55 if modelling PAR in terms of photon flux (Mobley and Boss, 2012, Figs.
5b, 8b)
    k0r:  0.04        # Background PAR attenuation [m-1] (default = 0.04 m-1, from ERSEM shortwave attenuation default)
    kESS: 4e-05       # Specific PAR attenuation by silt [m^2/mg] (default = 4e-05 m^2/mg, from ERSEM shortwave
attenuation default)
    ESS:  0.          # Assumed (constant) concentration of silt [mg/m^3] (default = 0. mg/m^3, from ERSEM shortwave
attenuation default)
    kPhy: 0.00023     # Specific PAR attenuation by phytoplankton [m^2/mg N] (default = 0.0023 m^2/mg N, from ERSEM
shortwave attenuation default)
                #   From ERSEM Blackford (P1-P4), default = 0.0004 m^2/mg C * 5.68 mg C/mg N (Redfield ratio 106/16
mol/mol)
                #   Note misprint "e-3" instead of "e-4" in Blackford et al. (2004) Table 1
    kPON: 0.          # Specific PAR attenuation due to PON [m^2/mg N] (default = 0. m^2/mg N)
# The following are only used if light_model = 1
    kHet: 0.          # Specific PAR attenuation due to zooplankton [m^2/mg N] (default = 0. m^2/mg N)
    kDON: 0.          # Specific PAR attenuation due to DON [m^2/mg N] (default = 0. m^2/mg N)
    kB:   0.          # Specific PAR attenuation due to bacteria [m^2/mg N] (default = 0. m^2/mg N)
    kPIV: 0.          # Specific PAR attenuation due to total particulate inorganic volume fraction (default = 0. m^-1)
#
#
##---Assumed densities for particles in the model (may be used in light/sedimentation models)------
#
# Densities are specified by rho_<full variable name> and in same units as the model concentration
# Any missing values will use the default density rho_def
    rho_def:   3.0E7                  # Default density of solid particles [mmol/m3]
    rho_niva_brom_bio_Phy: 1.5E7        # Density of (living) phytoplankton [mmolN/m3] (default = 1.4E6 mmolN/m3 from
PON default)
    rho_niva_brom_bio_PON: 1.5E7        # Density of (dead) particulate organic matter [mmolN/m3] (default = 1.4E6
mmolN/m3, from: 1.23 g WW/cm3 (Alldredge, Gotschalk, 1988), mg DW/mg WW=0.18 and mg DW /mg C=2 (Link et
al.,2006))
    rho_niva_brom_bio_Het: 1.5E7        # Density of (living) non-bacterial heterotrophs [mmolN/m3] (default = 1.4E6
mmolN/m3 from PON default)
    rho_niva_brom_redox_Baae: 1.5E7     # Density of (living) aerobic autotrophic bacteria [mmolN/m3] (default = 1.4E6
mmolN/m3 from PON default)
    rho_niva_brom_redox_Bhae: 1.5E7     # Density of (living) aerobic heterotrophic bacteria [mmolN/m3] (default = 1.4E6
mmolN/m3 from PON default)
    rho_niva_brom_redox_Baan: 1.5E7     # Density of (living) anaerobic autotrophic bacteria [mmolN/m3] (default = 1.4E6
mmolN/m3 from PON default)
    rho_niva_brom_redox_Bhan: 1.5E7     # Density of (living) anaerobic heterotrophic bacteria [mmolN/m3] (default =
1.4E6 mmolN/m3 from PON default)
    rho_niva_brom_redox_CaCO3: 2.80E7    # Density of calcium carbonate [mmolCa/m3] (default = 2.80E7 mmolCa/m3)
    rho_niva_brom_redox_Fe3: 3.27E7     # Density of Fe3 [mmolFe/m3] (default = 3.27E7 mmolFe/m3)
    rho_niva_brom_redox_FeCO3: 2.93E7    # Density of FeCO3 [mmolFe/m3] (default = 2.93E7 mmolFe/m3)
    rho_niva_brom_redox_FeS: 5.90E7     # Density of FeS [mmolFe/m3] (default = 5.90E7 mmolFe/m3)
    rho_niva_brom_redox_FeS2: 4.17E7     # Density of FeS2 [mmolFe/m3] (default = 4.17E7 mmolFe/m3)
    rho_niva_brom_redox_Mn4: 5.78E7      # Density of Mn4 [mmolMn/m3] (default = 5.78E7 mmolMn/m3)
    rho_niva_brom_redox_MnCO3: 3.20E7    # Density of MnCO3 [mmolMn/m3] (default = 3.20E7 mmolMn/m3)
    rho_niva_brom_redox_MnS: 4.60E7      # Density of MnS [mmolMn/m3] (default = 4.60E7 mmolMn/m3)
    rho_niva_brom_redox_S0: 6.56E7       # Density of S0 [mmolS/m3] (default = 6.56E7 mmolS/m3)
    rho_niva_brom_redox_Sipart: 4.40E7   # Density of particulate silicate [mmolSi/m3] (default = 4.40E7 mmolSi/m3)
#
#
##---Time stepping parameters----------------------------------------------------------------------
    dt:         0.0025      # Time step in [days] (default = 0.0025 days)
    freq_turb:  1           # Physical mixing time step = dt/freq_turb (default = 1)
    freq_sed:   1           # Sinking / bhc frequency (default = 1)
```

```
    year:       1998       # Selected year (for reading netCDF inputs) WARNING: This must be a year present in the netCDF
file, and nc_year0 must be correctly specified below
    days_in_yr:  365       # Number of days in repeated period (typically 365 or 366, default = 365)
    last_day:   3650       # Last day in simulation (~ days_in_yr * no. repeated years, default = 365)
    cc0:        1.0E-11    # Resilient (minimum) concentration for all variables [mmol/m3] (default = 1.0E-11 mmol/m3)
    surf_flux_with_diff: 0   # 1 to include surface fluxes in diffusion update, 0 to include in biogeochemical update (default =
0)
#
#
##---Vertical diffusivity parameters----------------------------------------------------------------
    diff_method:    1      # Numerical method to treat vertical diffusion (default = 1):
                           #   0 for FTCS approach (Forward-Time Central-Space scheme)
                           #   1 for GOTM approach (semi-implicit in time) using diff_center from GOTM lake (converting
input/output units)
                           #   2 for GOTM approach (semi-implicit in time) using modified version of original GOTM diff_center
(no units conversion required, should give very similar results to diff_method = 1)
                           #   Note: If diff_method>0 and bioturb_across_SWI = 1 below, only one modified GOTM subroutine can
be used (diff_center2)
    cnpar:          0.6    # "Implicitness" parameter for GOTM vertical diffusion (default = 0.6):
                           #   0 => Forward Euler  (fully explicit, first-order accurate)
                           #   1 => Backward Euler (fully implicit, first-order accurate)
                           #   0.5 => Crank-Nicolson (semi-implicit, second-order accurate)
    dynamic_kz_bbl: 0      # 1 for dynamic (time-dependent) kz_bbl, 0 for static kz_bbl (default = 0)
                           #   For deep water (e.g. >500 m) a static kz_bbl may be a reasonable approximation.
                           #   For shallower water, probably better to set dynamic_kz_bbl = 1; kz in the BBL is then determined by
linearly interpolating between zero at the SWI and the value at the bottom of the hydrodynamic model input water column
    kz_bbl_type:    1      # Type of variation of eddy diffusion kz(z) assumed over the benthic boundary layer:
                           #   0 => constant = kz_bbl_max, 1 => linear (~=> log-layer for velocity, Holtappels & Lorke, 2011)
                           #   This is only used if assuming a static kz_bbl (dynamic_kz_bbl = 0)
    kz_bbl_max:    5.E-6   # Maximum eddy diffusivity in the benthic boundary layer [m2/s] (default = 1.0E-5 m2/s)
                           #   This is only used if assuming a static kz_bbl (dynamic_kz_bbl = 0)
    dbl_thickness:  0.0005  # Thickness of the diffusive boundary layer [m] (default = 0.0005 m = 0.5 mm)
                           #   Jorgensen and Revsbech (1985) quote a range 1-2 mm over the deep sea floor (Boudreau and
Guinasso, 1982, Wimbush 1976)
                           #   and down to 0.1-0.2 mm over more exposed sediments (Santschi et al., 1983)
                           #   All layers within the DBL (midpoint height above SWI < dbl_thickness) have kz = kz_mol0 (no eddy
diffusivity)
    kz_mol0:       1.0E-9  # Molecular diffusivity at infinite dilution [m2/s] (default = 1.0E-9 m2/s)
                           #   Cf. range (0.5-2.7)E-9 m2/s in Boudreau 1997, Table 4.8
                           #   This sets a single constant value for all variables that is subsequently corrected for viscosity and
tortuosity
    mu0_musw:      0.94    # Inverse relative viscosity of saline pore water (default = 0.94 from Boudreau 1997 Table 4.10)
                           #   This relates the diffusivity in saline pore water to the infinite-dilution diffusivity
                           #   assuming the approximation from Li and Gregory (1974), see Boudreau (1997) equation 4.107
    kz_bioturb_max:  1.0E-11 # Maximum diffusivity due to bioturbation in the sediments [m2/s] (default = 1.0E-11 m2/s)
                           #   Cf. range (1-100) cm2/yr = (0.3-30)E-11 m2/s cited in Soetaert and Middelburg (2009), citing
Middelburg et al. (1997)
                           #   This sets value for upper z_const_bioturb metres, then bioturbation diffusivity decays with scale
z_decay_bioturb.
    z_const_bioturb: 0.01   # "Mixed layer depth" in sediments over which bioturbation diffusivity = kz_bioturb_max [m]
(default = 0.02 m)
                           #   Cf. values 0.05 m and 0.01 m used by Soetaert and Middelburg (2009) for well-mixed and anoxic
conditions respectively
                           #   Meire et al. (2013) use 0.05 m as a constant value
    z_decay_bioturb: 0.01   # Decay scale of bioturbation diffusivity below z_const_bioturb [m] (default = 0.01 m, following
Soetaert and Middelburg, 2009)
    K_O2s:          5.0    # Half-saturation constant for the effect of oxygen on bioturbation and bioirrigation [uM] (default =
5.0 uM)
                           #   Bioturbation diffusivity and bioirrigation rate are modulated by a Michaelis-Menten function with
parameter K_O2s
    bioturb_across_SWI: 1   # 1 to allow (interphase) bioturbation diffusion across the SWI (default = 1)
                           #   Bioturbation across the SWI must be interphase mixing rather than the intraphase mixing assumed
within the sediments
```

```
#
#
##---Bioirrigation parameters-----------------------------------------------------------------
#
# Bioirrigation rate alpha = a1_bioirr*exp(-a2_bioirr*z_s), where z_s is depth below the SWI [m]
#
    a1_bioirr:      0.0    # Maximum rate of bioirrigation in the sediments [s^-1] (default = 0.E-5)
                           #   Schluter et al. (2000) infer a range (0-5) d^-1 = (0-6)E-5 s^-1 for a1
                           #   This range is also broadly consistent with the profiles of alpha inferred by Miele et al. (2001)
    a2_bioirr:      50.    # Decay rate with depth of bioirrigation rate [m^-1] (default = 50)
                           #   Schluter et al. (2000) infer a range (0-1) cm^1 = (0-100) m^-1 for a2
                           #   This range is also broadly consistent with the profiles of alpha inferred by Miele et al. (2001)
#
#
##---Sedimentation parameters-----------------------------------------------------------------
    w_binf:         1.0E-10 # Particulate background burial velocity deep in the sediments where phi = phi_inf [m/s] (default =
1.0E-10 m/s = 0.3 cm/year, but note that true values are highly variable)
                           #   Soetaert et al. (1996) propose a regression model as a function of water depth:
                           #   w = 982*D^-1.548, where D is water depth in [m] and w is in cm/year, e.g. for D = 100 m, w = 0.8
cm/year = 2.5E-10 m/s
                           #   Note: Shallow particulate and solute burial velocities are inferred by assuming steady state compaction
(Boudreau, 1997)
    dynamic_w_sed:  1      # 1 to enable time-dependent advective velocities in the sediments (default = 0)
                           #   This uses the modelled (reactive) particulate variables to correct the advective velocities in the
sediments (see calculate_sed)
                           #   w_binf and phi_inf then define constant background components of these velocities
#
#
##---Porosity parameters----------------------------------------------------------------------
#
#   Porosity phi = phi_inf + (phi_0-phi_inf)*exp(-z_s/z_decay_phi), where z_s is depth below the SWI [m]
#
    phi_0:          0.95   # Maximum porosity at the SWI (default = 0.95, following Soetaert et al., 1996)
    phi_inf:        0.80   # Minimum porosity deep in the sediments (default = 0.80, following Soetaert et al., 1996)
    z_decay_phi:    0.04   # Exponential decay scale for excess porosity in the upper sediments [m] (default = 0.04,
following Soetaert et al., 1996)
#
#
##---I/O options-----------------------------------------------------------------------------
    input_type: 2                       # input forcing type: 0 for sinusoidal changes, 1 to read from ascii, 2 to read from netCDF
(default)
    ncoutfile_name: BROM_Sleipner_out20.nc    # netCDF output file name
    outfile_name: finish.dat            # ascii output file name
    port_initial_state: 1               # 0 to use FABM default (default), 1 to read from ascii file (icfile_name)
    icfile_name: start19.dat            # ascii initial condition file name (needed if port_initial_state = 1)
#The following are only used if reading input from netCDF (input_type = 2)
#Note: NetCDF variables (temperature, salinity, diffusivity) must have either two dimensions (depth, time) or four
dimensions ((latitude, longitude, depth , time) or (longitude, latitude, depth, time))
    nc_set_k_wat_bbl: 1                 # 1 (default) to set the no. water column layers to agree with netCDF input
                                        # 0 to use the value k_wat_bbl set above by subsampling the netCDF input
                                        # Note that in both cases the water layer thickness is determined by the netCDF input,
overriding water_layer_thickness above
    nc_staggered_grid: 1                # 1 (default) to assume a staggered input grid, (t,s) at layer midpoints, kz on layer
interfaces (e.g. ROMS, GOTM)
    nc_bottom_to_top: 1                 # 1 (default) if netCDF variables are stored with vertical index increasing from
bottom to top (e.g. ROMS, GOTM)
    nc_z_increasing_upward: 1           # 1 if netCDF depth variables are increasing upward (e.g. if "depth" is negative)
(default = 0)
    ncinfile_name: nns_annual.nc        # netCDF input file name
    ncintime_name: time                 # netCDF time dimension name [units since nc_year0-01-01 00:00:00]
    nc_year0: 1998                      # reference year for netCDF time variable (default = 1970) WARNING: This MUST be
correctly specified
    ncinz_name: z                       # netCDF depth dimension name for layer midpoints (rho points) [m]
```

```
    ncinz2_name: z1                    # netCDF depth dimension name for layer interfaces (w points) [m]
    ncinlat_name: lat                  # netCDF latitude dimension name (needed if reading 4D variables)
    ncinlon_name: lon                  # netCDF longitude dimension name (needed if reading 4D variables)
    ncinlat_sel: 1                     # Chosen latitude index (1,2,...,nlat) (needed if reading from 4D variables with nlat > 1)
    ncinlon_sel: 1                     # Chosen longitude index (1,2,...,nlon) (needed if reading from 4D variables with nlon > 1)
#
#Below we specify the names of variables in netCDF input files
#Format is <BROM internal name>: <netCDF input name>
#Can also specify a constant scale factor "fac", e.g. to convert units, or correct bias.
#BROM internal variable = fac * netCDF input variable (BROM assumes fac = 1 if not specified here)
#This factor can also be used to apply a simple stoichiometric assumption in lieu of nutrient variable data
#E.g. ncinSis_name: NO3s            # netCDF input surface silicate variable name [uM] - here using nitrate
#    ncinSis_fac: 1.5               # scale factor for netCDF input surface silicate - here assuming "extended Redfield ratio" Si:N = 1.5 mol Si / mol N
#
#2D physical variables used for setting BROM forcings
#These must be arrays of size [no. water column layers (= k_wat_bbl) * no. of days for all available years]
    ncint_name: temp                   # netCDF input temperature variable name [degC]
    ncins_name: salt                   # netCDF input salinity variable name [psu]
    ncinkz_name: nus                   # netCDF input vertical diffusivity variable name [m2/s]
    ncinkz_fac: 1.0                    # scale factor for netCDF input vertical diffusivity (default = 1.0)
#
#1D physical variables used for setting BROM forcings
#These must be arrays of size [no. of days for all available years]
    ncinEair_name: Eair                # netCDF input shortwave irradiance in air at water surface [W/m2] (only used if use_Eair = 1)
    ncinEair_fac: 1.0                  # scale factor for netCDF input shortwave irradiance (default = 1.0) (only used if use_Eair = 1)
    ncinhice_name: hice                # netCDF input ice thickness variable name [m] (only used if use_hice = 1)
    ncinhice_fac: 1.0                  # scale factor for netCDF input ice thickness (default = 1.0) (only used if use_hice = 1)
#
#Biogeochemical variables used for setting Dirichlet BCs at surface or bottom (bctype = 3)
#These must be arrays of size [1 * no. of days in repeated period (= days_in_yr)]
    ncinNH4s_name: NH4s                # netCDF input surface ammonium variable name [uM]
    ncinNH4s_fac: 1.0                  # scale factor for netCDF input surface ammonium (default = 1.0)
    ncinNO3s_name: NO3s                # netCDF input surface nitrate variable name [uM]
    ncinNO3s_fac: 1.0                  # scale factor for netCDF input surface nitrate (default = 1.0)
    ncinPO4s_name: PO4s                # netCDF input surface phosphate variable name [uM]
    ncinPO4s_fac: 1.0                  # scale factor for netCDF input surface phosphate (default = 1.0)
    ncinSis_name: Sis                  # netCDF input surface silicate variable name [uM]
    ncinSis_fac: 1.0                   # scale factor for netCDF input surface silicate (default = 1.0)
    ncinAlks_name: ATs                 # netCDF input surface alkalinity variable name [uM]
    ncinAlks_fac: 1.0                  # scale factor for netCDF input surface alkalinity (default = 1.0)
#
#Biogeochemical variables used for setting horizontal mixing fluxes
#NOTE: These must be arrays of size [no. water column layers (= k_wat_bbl) * no. of days in repeated period (= days_in_yr)]
#NOTE: The depth indexing must agree with temperature and salinity inputs
#NOTE: The layer index of the mixing variable is the layer with which it mixes in the internal BROM grid
#    This is does not necessarily reflect the actual depth of the mixing variable in its external location
#NOTE: This information is only used if hmix_<variable name> is > 0, see above
    ncinNH4hmix_name: NH4_N            # netCDF input horizontal mixing ammonium variable name [uM]
    ncinNH4hmix_fac: 1.0               # scale factor for netCDF input horizontal mixing ammonium (default = 1.0)
    ncinNO3hmix_name: NO3_N            # netCDF input horizontal mixing nitrate variable name [uM]
    ncinNO3hmix_fac: 1.0               # scale factor for netCDF input horizontal mixing nitrate (default = 1.0)
    ncinPO4hmix_name: PO4_N            # netCDF input horizontal mixing phosphate variable name [uM]
    ncinPO4s_fac: 1.0                  # scale factor for netCDF input horizontal mixing phosphate (default = 1.0)
    ncinSihmix_name: NO3_N             # netCDF input horizontal mixing silicate variable name [uM]
    ncinSihmix_fac: 1.5                # scale factor for netCDF input horizontal mixing silicate (default = 1.0)
    ncinO2hmix_name: O2_N              # netCDF input horizontal mixing oxygen variable name [uM]
    ncinO2hmix_fac: 1.0                # scale factor for netCDF input horizontal mixing oxygen (default = 1.0)
#
```

```
#Horizontal mixing rates
#NOTE: This must be an array of size [no. water column layers (= k_wat_bbl) * no. of days in repeated period (=
days_in_yr)]
#NOTE: The depth indexing must agree with temperature and salinity inputs
#NOTE: This information is only used if hmix_<variable name> is > 0, see above
   ncinhmix_rate_name: hmix_rate          # netCDF input horizontal mixing rates [day^-1]
   ncinhmix_rate_fac: 1.0                 # scale factor for netCDF input horizontal mixing rate (default = 1.0)
#
#
##---Options for run-time output to screen-----------------------------------------------------------
   show_maxmin: 0                         # 1 to show the profile maximum and minimum of each variable at the end of each
day (default = 0)
   show_kztCFL: 0                         # 1/2 to show the max/profile of total vertical diffusivity and associated Courant-
Friedrichs-Lewy number at the end of each day (default = 0)
   show_wCFL: 0                           # 1/2 to show the max/profile of vertical advection and associated Courant-Friedrichs-
Lewy number at the end of each day (default = 0)
   show_nan: 0                            # 1 to show the profile concentration output on NaN-termination for the offending
variable (default = 1)
   show_nan_kztCFL: 2                     # 1/2 to show the max/profile of total vertical diffusivity and associated Courant-
Friedrichs-Lewy number on NaN-termination (default = 1)
   show_nan_wCFL: 1                       # 1/2 to show the max/profile of vertical advection and associated Courant-
Friedrichs-Lewy number on NaN-termination (default = 1)
#
#
## References
# Boudreau B.P., 1997. Diagenetic Models and Their Implementation, Springer-Verlag, Berlin.
# Holzbecher, E., 2002. Advective flow in sediments under the influence of compaction. Hydrological Sciences 47(4), 641-
649.
# Link JS, Griswold CA, Methratta ET, Gunnard J, Editors. 2006. Documentation for the Energy Modeling and Analysis
eXercise (EMAX). US Dep. Commer., Northeast Fish. Sci. Cent. Ref. Doc. 06-15; 166 p.
# Meile, C., Koretsky, C.M., Cappellen, P.V., 2001. Quantifying bioirrigation in aquatic sediments: An inverse modeling
approach. Limnol. Oceanogr. 46(1), 164–177.
# Meire, L., Soetaert, K.E.R., Meysman, F.J.R, 2013. Impact of global change on coastal oxygen dynamics and risk of
hypoxia. Biogeosciences 10, 2633–2653.
# Mobley, C.D., Boss, E.S., 2012. Improved irradiances for use in ocean heating, primary production, and photo-oxidation
calculations. Applied Optics 51(27), 6549-6560.
# Schluter, M., Sauter, E., Hansen, H., Suess, E., 2000. Seasonal variations of bioirrigation in coastal sediments: Modelling
of field data. Geochimica et Cosmochimica Acta 64(5), 821–834.
# Soetaert, K., Herman, P.M.J., Middelburg, J.J., 1996. A model of early diagenetic processes from the shelf to abyssal
depths. Geochimica et Cosmochimica Acta 60(6), 1019-1040.
# Soetaert, K., Middelburg, J.J., 2009. Modeling eutrophication and oligotrophication of shallow-water marine systems: the
importance of sediments under stratified and well-mixed conditions. Hydrobiologia 629:239–254.
# Wimbush, M., 2012: The Physics of The Benthic Boundary Layer, in The Benthic Boundary Layer, edited by I. McCave.
```

Appendix D: run-time input file for BROM-biogeochemistry (fabm.yaml)

```
# IMPORTANT !!!!    <TAB> is NOT allowed here, used <Space> only !!!!
# Each entry must have 6 spaces before the parameter name
require_initialization: true
instances:
#-------------------------------------------------------------------------
  niva_brom_eqconst:
#-------------------------------------------------------------------------
  niva_brom_carb:
    initialization:
      Alk: 2200.
      DIC: 2100.
    coupling:
      Kc0: niva_brom_eqconst/Kc0
      Kc1: niva_brom_eqconst/Kc1
```

```
    Kc2: niva_brom_eqconst/Kc2
    Kw: niva_brom_eqconst/Kw
    Kb: niva_brom_eqconst/Kb
    Kp1: niva_brom_eqconst/Kp1
    Kp2: niva_brom_eqconst/Kp2
    Kp3: niva_brom_eqconst/Kp3
    Knh4: niva_brom_eqconst/Knh4
    Kh2s: niva_brom_eqconst/Kh2s
#     Kh2s2: niva_brom_eqconst/Kh2s2
    KSi: niva_brom_eqconst/KSi
    kso4: niva_brom_eqconst/kso4
    kflu: niva_brom_eqconst/kflu
    tot_free: niva_brom_eqconst/tot_free
#    Constants calculated: Kc0 (Weiss, 1974), Kc1, Kc2 (Roy et al., 1993), Kw, Kp1,Kp2,Kp3 (DOE, 2004),
#                          Kb (Dickson,1990), KSi(Millero,1995), Knh4, Kh2s1(Luff et al, 2001), Kh2s2(Volkov 1984)
#                          dissociation for B, F according to (Dickson et al., 2007), more references in the code.
    PO4: niva_brom_bio/PO4
    NH4: niva_brom_bio/NH4
    DON: niva_brom_bio/DON
    Si: niva_brom_redox/Si
    H2S: niva_brom_redox/H2S
    Mn3: niva_brom_redox/Mn3
    Mn4: niva_brom_redox/Mn4
    Fe3: niva_brom_redox/Fe3
    SO4: niva_brom_redox/SO4
#-------------------------------------------------------------------------
  niva_brom_bio:
    initialization:
      O2: 200.
      Phy: 0.01
      Het: 0.01
      PON: 0.01
      DON: 0.0
      NO3: 5.
      PO4: 1.
      NH4: 0.0
    parameters:
# ---- Phy  ----------
      K_phy_gro: 4.7       # Maximum specific growth rate (1/d) =0.9-1.3 (Savchuk, 2002), =3.(Gregoire, Lacroix, 2001) >!0.5
worked for Berre!<
      Iopt: 25.           # Optimal irradiance (W/m2) =50 (Savchuk, 2002)
      bm: 0.12            # Coefficient for growth dependence on t
      cm: 1.4             # Coefficient for growth dependence on t
      K_phy_mrt: 0.20      # Specific rate of mortality, (1/d) =0.3-0.6 (Savchuk, 2002), =0.05 (Gregoire, Lacroix, 2001)
      K_phy_exc: 0.10      # Specific rate of excretion, (1/d) =0.01 (Burchard et al., 2006)
# ----Het -----------
      K_het_phy_gro: 1.1    #! Max.spec. rate of grazing of Zoo on Phy, (1/d), =0.9 (Gregoire, Lacroix, 2001), =1.5 (Burchard
et al., 2006)
      K_het_phy_lim: 0.5    #! Half-sat.const.for grazing of Zoo on Phy for Phy/Zoo ratio
      K_het_pom_gro: 0.50   #! Max.spec.rate of grazing of Zoo on POP and bacteria, (1/d), =1.2 (Burchard et al., 2006)
      K_het_pom_lim: 0.05   #! Half-sat.const.for grazing of Zoo on POP for POP/Zoo_ratio
      K_het_res: 0.02       #! Specific respiration rate =0.02 (Yakushev et al., 2007)
      K_het_mrt: 0.05       #! %! Maximum specific rate of mortality of Zoo (1/d) =0.05 (Gregoire, Lacroix, 2001)
      Uz: 0.5             #! Food absorbency for Zoo (nd) =0.5-0.7 (Savchuk, 2002)
      Hz: 0.5             #! Ratio betw. diss. and part. excretes of Zoo (nd), =0.5 (Gregoire, Lacroix, 2001)
      limGrazBac:  2.       #! Limiting parameter for bacteria grazing by Zoo, =2. (Yakushev et al., 2007)
# ----N -------------
      K_nox_lim: 0.1        #! Half-sat.const.for uptake of NO3+NO2 (uM) =0.5 (Gregoire, Lacroix, 2001)
      K_nh4_lim: 0.02       #! Half-sat.const.for uptake of NH4 (uM) =0.2 (Gregoire, Lacroix, 2001)
      K_psi: 1.46          #! Strength of NH4 inhibition of NO3 uptake constant (uM-1) =1.46_rk (Gregoire, Lacroix, 2001)
      K_nfix: 0.4          #! Maximum specific rate of N-fixation (1/d) =0.5 (Savchuk, 2002)
# ----P ------------
      K_po4_lim: 0.012      #! Half-sat. constant for uptake of PO4 by Phy
```

```
# ----Si------------
    K_si_lim: 0.1        #! Half-sat. constant for uptake of Si_lim by Phy
# ----Sinking-------
    Wsed: 5.0        #! Rate of sinking of detritus (m/d), =0.4 (Savchuk, 2002), =5. (Gregoire, Lacroix, 2001), =1-370
(Alldredge, Gotschalk, 1988)
    Wphy: 0.2        #! Rate of sinking of Phy (m/d), =0.1-0.5 (Savchuk, 2002)
    Whet: 1.         #! Rate of sinking of Het (m/d), =1. (Yakushev et al., 2007)
# ---- Stoichiometric coefficients ----
    r_n_p: 16.0      #! N[uM]/P[uM]
    r_o_n: 6.625     #! O2[uM]/N[uM]
    r_c_n: 8.0       #! C[uM]/N[uM]
    r_si_n: 1.0      #! Si[uM]/N[uM]
  coupling:
    NO2: niva_brom_redox/NO2
    H2S: niva_brom_redox/H2S
    Baan: niva_brom_redox/Baan
    Baae: niva_brom_redox/Baae
    Bhae: niva_brom_redox/Bhae
    Bhan: niva_brom_redox/Bhan
    Si: niva_brom_redox/Si
    Sipart: niva_brom_redox/Sipart
    DIC: niva_brom_carb/DIC
    Alk: niva_brom_carb/Alk
    Hplus: niva_brom_carb/Hplus
    Kp1: niva_brom_eqconst/Kp1
    Kp2: niva_brom_eqconst/Kp2
    Kp3: niva_brom_eqconst/Kp3
    Knh4: niva_brom_eqconst/Knh4
    KSi: niva_brom_eqconst/KSi
#-------------------------------------------------------------------------
 niva_brom_redox:
  initialization:
    Mn2: 0.0
    Mn3: 0.0
    Mn4: 0.0
    MnS: 0.0
    MnCO3: 0.0
    Fe2: 0.0
    Fe3: 0.0
    FeS: 0.0
    FeCO3: 0.0
    NO2: 0.0
    Si: 0.0
    Sipart: 0.0
    H2S: 0.0
    S0:  0.0
    S2O3: 0.0
    SO4: 25000.
    Baae: 0.01
    Bhae: 0.01
    Baan: 0.01
    Bhan: 0.01
    CaCO3: 5.0
    CH4: 0.001
    FeS2: 0.0
  parameters:
# ---- Model parameters ------
    Wbact: 0.4       #! Rate of sinking of bacteria (Bhae,Baae,Bhan,Baan) (1/d), (Yakushev et al.,2007)
    Wm: 7.0          #! Rate of accelerated sinking of particles with settled metal hydroxides (1/d), (Yakushev et al.,2007)
# specific rates of biogeochemical processes
#---- Mn---------
    K_mn_ox1: 0.1       #! Specific rate of oxidation of Mn2 to Mn3 with O2 (1/d).
    K_mn_ox2: 0.2       #! Specific rate of oxidation of Mn3 to Mn4 with O2 (1/d)
```

```
    K_mn_rd1: 0.5       #! Specific rate of reduction of Mn4 to Mn3 with H2S (1/d)
    K_mn_rd2: 1.0       #! Specific rate of reduction of Mn3 to Mn2 with H2S (1/d)
    K_mns: 1500.        #! Conditional equilibrium constant for MnS from Mn2 with H2S (M)
    K_mns_diss: 0.0005  #! Specific rate of dissolution of MnS to Mn2 and H2S (1/d)
    K_mns_form: 0.00001 #! Specific rate of formation of MnS from Mn2 with H2S (1/d)
    K_mnco3: 1.         #! Conditional equilibrium constant %  1.8e-11 (M) (Internet)     1 uM2 for Mn2+CO3->MnCO3
(Meysman,2003)
    K_mnco3_diss: 7.e-7 #! Specific rate of dissolution of MnCO3 (1/d) =6.8e-7 (2.5 X 10-1 yr-1 (Van Cappellen, Wang,
1996) !1x10-4 yr-1) (Hunter et al, 98)
    K_mnco3_form: 0.1e-4 #! Specific rate of formation of MnCO3 (1/d) =2.7e-7  (1. X 10-4 yr-1 (Van Cappellen, Wang,
1996)!1x10-4 yr-1) (Hunter et al, 98))
    K_mnco3_ox: 0.0027  #! Specific rate of oxidation of MnCO3 with O2 (1/d)=0.0027  ( 1x10^(-6) M/yr (Van Cappellen,
Wang, 1996).
    K_DON_mn: 0.001     #! Specific rate of oxidation of DON with Mn4 (1/d)
    K_PON_mn: 0.001     #! Specific rate of oxidation of PON with Mn4 (1/d)
    s_mnox_mn2: 0.01    #! threshold of Mn2 oxidation (uM Mn) (Yakushev et al.,2007)
    s_mnox_mn3: 0.01    #! threshold of Mn3 oxidation (uM Mn) (Yakushev et al.,2007)
    s_mnrd_mn4: 0.01    #! threshold of Mn4 reduciton (uM Mn) (Yakushev et al.,2007)
    s_mnrd_mn3: 0.01    #! threshold of Mn3 reduciton  (uM Mn) (Yakushev et al.,2007)
#---- Fe---------
    K_fe_ox1: 0.5       #!Specific rate of oxidation of Fe2 to Fe3  with O2 (1/d), =4. (Konovalov et al., 2006)
    K_fe_ox2: 0.001     #!0.1! Specific rate of oxidation of Fe2 to Fe3  with MnO2 (1/d) =0.74 (Konovalov et al., 2006);
3x10^6 1/(M yr) is estimated in Van Cappellen-Wang-96
    K_fe_rd: 1.2        #!0.5! Specific rate of reduction of Fe3 to Fe2  with H2S (1/day) *=0.05 (Konovalov et al., 2006)
    K_fes: 2510.0       #!FeS equilibrium constant (Solubility Product Constant) (uM)=2510  ( 2.51x10-6 mol cm-3,
Bektursuniva,11)
    K_fes_form: 5.e-4   #!Specific rate of precipitation of FeS from Fe2 with H2S (1/day)=1.e-5 (4x10-3 1/yr,
Bektursunova,11)
    K_fes_diss: 1.e-6   #!Specific rate of dissollution of FeS to Fe2 and H2S  (1/day)=3.e-6 (1x10-3 1/yr, Bektursunova,11)
    K_fes_ox: 0.001     #!Specific rate of oxidation of FeS with O2 (1/day)=0.001(3x10^5 1/(M yr),(Van Cappellen, Wang,
1996)
    K_DON_fe: 0.00005   #!-0.0003 ! %  Specific rate of oxidation of DON with Fe3 (1/day)
    K_PON_fe: 0.00001   #!-0.0001 ! %  Specific rate of oxidation of PON with Fe3 (1/day)
    K_fes2_form: 1.e-6  #!specific rate of FeS2 formation by FeS oxidation by H2S (1/day)=0.000009 (10^(-4) L/mol/s
(Rickard-97)
    K_fes2_ox: 4.38e-4  #!specific rate of pyrite oxidation by O2  (1/uM/d)=4.38x10^(-4) 1/micromolar/day (Wijsman et al
-2002).
    s_feox_fe2: 0.001   #!threshold of Fe2 reduciton
    s_ferd_fe3: 0.01    #!threshold of Fe3 reduciton  (uM Fe)
    K_feco3: 15.        #!10. !2.e-2 ! Conditional equilibrium constant %  1.8e-11 (M) (Internet)  1 uM2 for Mn2+CO3-
>FeCO3 (Meysman,2003)
    K_feco3_diss: 7.e-4 #!Specific rate of dissolution of FeCO3 (1/day)=6.8e-7   !2.5 X 10-1 yr-1 (Van Cappellen, Wang,
1996) !1x10-4 yr-1 (Hunter et al, 98)
    K_feco3_form: 3.e-4 #!Specific rate of formation of FeCO3 (1/day)=2.7e-7  !! 1. X 10-4 yr-1(Van Cappellen, Wang,
1996)!1x10-4 yr-1 (Hunter et al, 98)
    K_feco3_ox: 0.0027  #!Specific rate of oxidation of FeCO3 with O2 (1/day)=0.0027  ( 1x10^(-6) M/yr (Van Cappellen,
Wang, 1996).
#---- S---------
    K_hs_ox: 0.5        #! Specific rate of oxidation of H2S to S0  with O2 (1/d),  =0.1 (Gregoire, Lacroix, 2001)
    K_s0_ox: 0.02       #! 0.02 Specific rate of oxidation of S0 with O2 (1/d), (Yakushev, Neretin,1997)
    K_s2o3_ox: 0.01     #! Specific rate of oxidation of S2O3 with O2 (1/d), (Yakushev, Neretin,1997)
    K_so4_rd: 5.e-6     #! Specific rate of OM sulfate reduction with sulfate (1/d), (Yakushev, Neretin,1997)
    K_s2o3_rd: 0.001    #! Specific rate of OM sulfate reduction with thiosulfate (1/d) (Yakushev, Neretin,1997)
    K_s0_disp: 0.001    #! Specific rate of S0 dispropotionation (1/d) (Yakushev,2013)
    K_s0_no3: 0.9       #! Specific rate of oxidation of S0 with NO3 (1/d) (Yakushev,2013)
    K_s2o3_no3: 0.01    #! Specific rate of oxidation of S2O3 with NO3 (1/d) (Yakushev,2013)
    K_mnrd_hs: 1.0      #! half sat. of Mn reduction (uM S) (Yakushev,2013)
    K_ferd_hs: 1.0      #! half sat. of Fe reduction (uM S) (Yakushev,2013)
#---- N---------!
    K_DON_ox: 0.05      #! Specific rate of oxidation of DON with O2 (1/d) = 0.1(Savchuk, 2002)
    K_PON_ox: 0.002     #! Specific rate of oxidation of PON with O2 (1/d) =0.002 (Savchuk, 2002), =0.07 (Gregoire,
Lacroix, 2001)
    Tda: 13.0           #! Temperature control coefficient for OM decay (Burchard et al., 2006)
```

```
  beta_da: 20.0        #! Temperature control coefficient for OM decay (Burchard et al., 2006)
  K_omox_o2: 1.0       #! Half sat. of o2 for OM mineralization (uM) (Yakushev,2013)
  K_PON_DON: 0.1       #! Specific rate of Autolysis of PON to DON (1/d), =0.02 (Burchard et al., 2006)
  K_nitrif1: 0.01      #! Spec.rate of 1st st. of nitrification, (1/d), =0.01 (Yakushev,2013) =0.1(Savchuk, 2002) =0.1
(Gregoire, Lacroix, 2001)
  K_nitrif2: 0.1       #! Spec.rate of 2d st. of nitrification, (1/d), =0.1 (Yakushev,2013)
  K_denitr1: 0.16      #! Spec.rate of 1 stage of denitrif =0.16 (Yakushev, Neretin,1997),= 0.5(Savchuk, 2002),=
0.015(Gregoire, Lacroix, 2001)
  K_denitr2: 0.25      #! Spec.rate of 2 stage of denitrif =0.22 (Yakushev, Neretin,1997)
  K_omno_no3: 0.001    #! Half sat. of no3 for OM denitr. (uM N) (Yakushev,2013)
  K_omno_no2: 0.001    #! Half sat. of no2 for OM denitr. (uM N) (Yakushev,2013)
  K_hs_no3: 0.8        #! Spec.rate of thiodenitrification (1/d), =.015 (Gregoire, Lacroix, 2001)
  K_annamox: 0.8       #! Spec.rate of Anammox (1/d),  (Gregoire, Lacroix, 2001)
#---- O2--------!
  O2s_nf: 5.           #! threshold of O2  saturation for nitrification, (uM), =10. (Gregoire, Lacroix, 2001)
  O2s_dn: 10.0         #! threshold of O2 for denitrification, anammox, Mn reduction (uM O2), =40 (0.72 mgO2/l)
(Savchuk, 2002)
  s_omox_o2: 0.01      #! threshold of o2 for OM mineralization (uM O2) (Yakushev,2013)
  s_omno_o2: 25.0      #! threshold of o2 for OM denitrification (uM O2) (Yakushev,2013)
  s_omso_o2: 25.0      #! threshold of o2 for OM sulfate reduction (uM O2) (Yakushev,2013)
  s_omso_no3: 5.0      #! threshold of noX for OM sulfate reduction (uM O2) (Yakushev,2013)
  K_mnox_o2: 2.0       #! half sat. of Mn oxidation (uM O2) (Yakushev,2013)
#---- C--------!
  K_caco3_diss: 3.0    #! CaCO3 dissollution rate constant (1/d) (wide ranges are given in (Luff et al., 2001))
  K_caco3_form: 0.0002  #! CaCO3 precipitation rate constant (1/d) (wide ranges are given in (Luff et al., 2001))
  K_DON_ch4: 0.00014    #! Specific rate of methane production from DON (1/d) (Lopes et al., 2011)
  K_PON_ch4: 0.00014    #! Specific rate of methane production from PON (1/d) (Lopes et al., 2011)
  K_ch4_o2: 0.14       #! Specific rate of oxidation of CH4 with O2 (1/d) =0.14 (Lopes et al., 2011)
  K_ch4_so4: 0.0000274  #! Specific rate of oxidation of CH4 with SO4 (1/uM/day) (0.0274 m3 /mol-1 day-1 Lopes et al.,
2011)
  s_omch_so4: 30.      #! threshold of of SO4 for methane production from OM (uM) (Lopes et al., 2011)
#---- Si-------!
  K_sipart_diss: 0.080  #! Si dissollution rate constant (1/d), =0.008 (Popova, Srokosz, 2009)
#---- Bacteria-!
  K_Baae_gro: 0.1      #!  Baae maximum specific growth rate (1/d) (Yakushev, 2013)
  K_Baae_mrt: 0.005    #!  Baae specific rate of mortality (1/d) (Yakushev et al., 2013)
  K_Baae_mrt_h2s: 0.899  #!  Baae increased specific rate of mortality due to H2S (1/d) (Yakushev et al., 2013)
  limBaae: 2.0         #! Limiting parameter for nutrient consumprion by Baae (nd) (Yakushev, 2013)
  K_Bhae_gro:  0.5     #!  Bhae maximum specific growth rate (1/d) (Yakushev, 2013)
  K_Bhae_mrt:  0.01    #!  Bhae specific rate of mortality (1/d) (Yakushev, 2013)
  K_Bhae_mrt_h2s: 0.799  #!  Bhae increased specific rate of mortality due to H2S (1/d)  (Yakushev, 2013)
  limBhae: 5.0         #! Limiting parameter for OM consumprion by Bhae (nd) (Yakushev, 2013)
  K_Baan_gro: 0.2      #!  Baan maximum specific growth rate (1/d) (Yakushev, 2013)
  K_Baan_mrt: 0.005    #!  Baan specific rate of mortality (1/d) (Yakushev, 2013)
  limBaan: 2.0         #! Limiting parameter for nutrient consumprion by Baan (nd) (Yakushev, 2013)
  K_Bhan_gro: 0.15     #!  Bhan maximum specific growth rate (1/d) (Yakushev, 2013)
  K_Bhan_mrt: 0.01     #!  Bhan specific rate of mortality (1/d) (Yakushev, 2013)
  K_Bhan_mrt_o2: 0.899  #!  Bhan increased specific rate of mortality due to O2 (1/d) (Yakushev, 2013)
  limBhan: 2.0         #! Limiting parameter for OM consumprion by Bhan (nd) (Yakushev, 2013)
#---- Stoichiometric coefficients ----!
  r_fe_n: 26.5         #! Fe[uM]/N[uM] (Boudreau, 1996)
  r_mn_n: 13.25        #! Mn[uM]/N[uM] (Boudreau, 1996)
  f:  0.66             #! conversion factor relating solid and dissolved species concentrations
  r_fe3_p: 2.7         #! Fe[uM]/P[uM] partitioning coeff. for Fe oxide (Yakushev et al., 2007)
  r_mn3_p: 0.67        #! Mn[uM]/P[uM] complex stoichiometric coeff. for Mn(III) (Yakusheve al., 2007)
  r_fe3_si: 3.         #! Fe[uM]/Si[uM] partitioning coeff. for Fe oxide
  coupling:
  O2: niva_brom_bio/O2   #  O2: niva_oxydep/oxy
  NH4: niva_brom_bio/NH4
  NO3: niva_brom_bio/NO3
  PO4: niva_brom_bio/PO4
  PON: niva_brom_bio/PON
  DON: niva_brom_bio/DON
```

Wsed: niva_brom_bio/Wsed
Kp1: niva_brom_eqconst/Kp1
Kp2: niva_brom_eqconst/Kp2
Kp3: niva_brom_eqconst/Kp3
Knh4: niva_brom_eqconst/Knh4
Kh2s: niva_brom_eqconst/Kh2s
KSi: niva_brom_eqconst/KSi
Kc0: niva_brom_eqconst/Kc0
Alk: niva_brom_carb/Alk
DIC: niva_brom_carb/DIC
Hplus: niva_brom_carb/Hplus
Om_Ca: niva_brom_carb/Om_Ca
Om_Ar: niva_brom_carb/Om_Ar
CO3: niva_brom_carb/CO3
pCO2: niva_brom_carb/pCO2
Ca: niva_brom_carb/Ca

REFERENCES:

Alldredge, A.L. and Gotschalk, C., 1988. In situ settling behavior of marine snow. Limnology and Oceanography, 33(3), pp.339-351.

Boudreau, B. P.: A method-of-lines code for carbon and nutrient diagenesis in aquatic sediments, Comput. Geosci., 22(5), 479–496, doi:10.1016/0098-3004(95)00115-8, 1996.

Burchard H., Bolding K., Kühn W., Meister A., Neumann T. and Umlauf L., 2006. Description of a flexible and extendable physical–biogeochemical model system for the water column. Journal of Marine Systems, 61(3), 180-211.

Dickson AG. 1990. Thermodynamics of the dissociation of boric acid in synthetic seawater from 273.15 to 318.15 K. Deep-Sea Research Part a-Oceanographic Research Papers. 37:755-766

Dickson, A.G., Sabine, C.L. and Christian, J.R., 2007. Guide to Best Practices for Ocean CO2 Measurements.

DOE (1994) Handbook of methods for the analysis of the various parameters of the carbon dioxide system in sea water; version 2, A. G. Dickson & C. Goyet, eds., ORNL/CDIAC-74.

Gregoire M. and Lacroix G., 2001. Study of the oxygen budget of the Black Sea waters using a 3D coupled hydrodynamical–biogeochemical model. Journal of marine systems, 31(1), pp.175-202.

Konovalov, S.K., Murray, J.W., Luther, G.W., Tebo, B.M., 2006. Processes controlling the Redox budget for oxic/anoxic water column of the Black Sea. Deep Sea Research (II) 53: 1817-1841.

Link JS, Griswold CA, Methratta ET, Gunnard J, Editors. 2006. Documentation for the Energy Modeling and Analysis eXercise (EMAX). US Dep. Commer., Northeast Fish. Sci. Cent. Ref. Doc. 06-15; 166 p.

Millero FJ , 1995 Thermodynamics of the carbon dioxide system in the oceans. Geochimica et Cosmochimica Acta 59 (4), 661-677

Luff R., Haeckel M., and Wallmann K. 2001. Robust and fast FORTRAN and MATLAB libraries to calculate pH distributions in marine systems, Comput. Geosci., 27, 157–169

Popova EE, Srokosz MA. 2009. Modelling the ecosystem dynamics at the Iceland-Faeroes Front: Biophysical interactions, J. Mar. Syst., 77(1-2), 182–196, doi:10.1016/j.jmarsys.2008.12.005, 2009.

Savchuk O. 2002. Nutrient biogeochemical cycles in the Gulf of Riga: scaling up field studies with a mathematical model. J. Mar. Syst. 32: 253-280.

Volkov II. 1984. Geokhimiya Sery v Osadkakh Okeana (Geochemistry of Sulfur in Ocean Sedi-ments), Nauka, Moscow, USSR.

Van Cappellen P., Wang, Y. F. 1996: Cycling of iron and manganese in surface sediments: A general theory for the coupled transport and reaction of carbon, oxygen, nitrogen, sulfur, iron, and manganese, Am. J. Sci., 296(3), 197–243, doi:10.2475/ajs.296.3.197, 1996.

Weiss RF. 1974 Carbon dioxide in water and seawater: the solubility of a non-ideal gas.Marine Chemistry 2:203-215.

Yakushev E., Neretin L., 1997. One-dimensional modelling of nitrogen and sulphur cycles in the aphotic zones of the Black Sea and Arabian Sea. Global Biogeochem. Cycles 11 Ž3.,401–414.

Yakushev EV, Pollehne F., Jost G., Kuznetsov I., Schneider B., Umlauf L. 2007. Analysis of the water column oxic/anoxic interface in the Black and Baltic seas with a numerical model, Mar. Chem., 107(3), 388–410.

Yakushev E. 2013. RedOx Layer Model: A Tool for Analysis of the Water Column Oxic/Anoxic Interface Processes. In: E.V.Yakushev (ed.) Chemical Structure of Pelagic Redox Interfaces: Observation and Modeling, Hdb Env Chem (2013) 22: 203–234, DOI 10.1007/698_2012_145, Springer-Verlag Berlin Heidelberg

Formatted: German (Germany)

Formatted: Space After: 0 pt, Line spacing: single

References

Alldredge, A. L. and Gotschalk, C.: In situ settling behavior of marine snow, Limnol. Ocean., 33(3), 339–35, doi:10.4319/lo.1988.33.3.0339, 1988.

Almroth, E., Tengberg, A., Andersson, J. H., Pakhomova, S. and Hall, P. O. J.: Effects of resuspension on benthic fluxes of oxygen, nutrients, dissolved inorganic carbon, iron and manganese in the Gulf of Finland, Baltic Sea, Cont. Shelf Res., 29(5-6), 807–818, doi:10.1016/j.csr.2008.12.011, 2009.

Arndt, S. and Regnier, P.: A model for the benthic-pelagic coupling of silica in estuarine ecosystems: sensitivity analysis and system scale simulation, Biogeosciences, 4(3), 331–352, doi:10.5194/bg-4-331-2007, 2007.

Bektursunova, R. and L'Heureux, I.: A reaction-transport model of periodic precipitation of pyrite in anoxic marine sediments, Chem. Geol., 287(3-4), 158–170, doi:10.1016/j.chemgeo.2011.06.004, 2011.

Berner, R. A.: Principles of Chemical Sedimentology, McGraw-Hill Inc., 1971.

Berner, R. A.: Early Diagenesis: A Theoretical Approach. [online] Available from: http://books.google.com/books?id=weRFglCVBkUC&pgis=1, 1980.

Blackford, J. C., Allen, J. I. and Gilbert, F. J.: Ecosystem dynamics at six contrasting sites: A generic modelling study, J. Mar. Syst., 52(1-4), 191–215, doi:10.1016/j.jmarsys.2004.02.004, 2004.

Blackwelder, P., Hood, T., Alvarez-Zarikian, C., Nelsen, T. A. and McKee, B.: Benthic foraminifera from the necop study area impacted by the Mississippi River plume and seasonal hypoxia, Quat. Int., 31, 19–36, doi:10.1016/1040-6182(95)00018-E, 1996.

~~Bolding, K., Burchard, H., Pohlmann, T. and Stips, A.: Turbulent mixing in the Northern North Sea: A numerical model study, in Continental Shelf Research, vol. 22, pp. 2707–2724., 2002.~~

Boudreau, B. P.: A method-of-lines code for carbon and nutrient diagenesis in aquatic sediments, Comput. Geosci., 22(5), 479–496, doi:10.1016/0098-3004(95)00115-8, 1996.

Boudreau, B. P.: Diagenetic models and their ~~impletation: modelling~~implementation. Modelling transport and reactions in aquatic sediments~~. Springer Verlag, Berlin, Heidelberg, NY, 414 pp~~., 1997.

Boudreau, B. P. and Jorgensen, B. B.: The Benthic Boundary Layer: Transport Processes and Biogeochemistry, 1st ed., edited by B. P. Boudreau and B. B. Jorgensen, Oxford University Press;, 2001.

Brigolin, D., Lovato, T., Rubino, A. and Pastres, R.: Coupling early-diagenesis and pelagic biogeochemical models for estimating the seasonal variability of N and P fluxes at the sediment-water interface: Application to the northwestern Adriatic coastal zone, J. Mar. Syst., 87(3-4), 239–255, doi:10.1016/j.jmarsys.2011.04.006, 2011.

Bruggeman, J. and Bolding, K.: A general framework for aquatic biogeochemical models, Environ. Model. Softw., doi:10.1016/j.envsoft.2014.04.002, 2014.

~~Calvert, S. E. and Pedersen, T. F.: Geochemistry of Recent oxic and anoxic marine sediments: implications for the geological record, Mar. Geol., 113, 67–88, 1993.~~

Burchard, H., Bolding, K., Kühn, W., Meister, A., Neumann, T. and Umlauf, L.: Description of a flexible and extendable physical-biogeochemical model system for the water column, J. Mar. Syst., 61(3-4 SPEC. ISS.), 180–211, doi:10.1016/j.jmarsys.2005.04.011, 2006.

Butenschön, M., Zavatarelli, M. and Vichi, M.: Sensitivity of a marine coupled physical biogeochemical model to time resolution, integration scheme and time splitting method, Ocean Model., 52-53, 36–53, doi:10.1016/j.ocemod.2012.04.008, 2012.

Butenschön, M., Clark, J., Aldridge, J. N., Allen, J. I., Artioli, Y., Blackford, J., Bruggeman, J., Cazenave, P., Ciavatta, S., Kay, S., Lessin, G., van Leeuwen, S., van der Molen, J., de Mora, L., Polimene, L., Sailley, S., Stephens, N. and Torres, R.: ERSEM 15.06: a generic model for marine biogeochemistry and the ecosystem dynamics of the lower trophic levels, Geosci. Model Dev. Discuss., 8(8), 7063–7187, doi:10.5194/gmdd-8-7063-2015, 2015.

Field Code Changed

Formatted: Normal, Space Before: 5 pt, After: 5 pt, No widow/orphan control, Don't adjust space between Latin and Asian text, Don't adjust space between Asian text and numbers

Butenschön, M., Clark, J., Aldridge, J. N., Icarus Allen, J., Artioli, Y., Blackford, J., Bruggeman, J., Cazenave, P., Ciavatta, S., Kay, S., Lessin, G., Van Leeuwen, S., Van Der Molen, J., De Mora, L., Polimene, L., Sailley, S., Stephens, N. and Torres, R.: ERSEM 15.06: A generic model for marine biogeochemistry and the ecosystem dynamics of the lower trophic levels, Geosci. Model Dev., 9(4), 1293–1339, doi:10.5194/gmd-9-1293-2016, 2016.

Canfield, D. E., Kristensen, E. and Thamdrup, B.: Aquatic geomicrobiology., Adv. Mar. Biol., 48, 1–599, doi:10.1016/S0065-2881(05)48011-6, 2005.

Van Cappellen, P. and Wang, Y. F.: Cycling of iron and manganese in surface sediments: A general theory for the coupled transport and reaction of carbon, oxygen, nitrogen, sulfur, iron, and manganese, Am. J. Sci., 296(3), 197–243, doi:10.2475/ajs.296.3.197, 1996.

Cerco, C. F., Noel, M. R. and Kim, S.-C.: Three-dimensional Management Model for Lake Washington, Part II: Eutrophication Modeling and Skill Assessment, Lake Reserv. Manag., 22(2), 115–131, doi:10.1080/07438140609353889, 2006.

Cooper, D. C. and Morse, J. W.: The Chemistry of Offatts Bayou, Texas: A Seasonally Highly Sulfidic Basin, Estuaries, 19(3), 595, doi:10.2307/1352520, 1996.

Couture, R. M., Shafei, B., Van Cappellen, P., Tessier, A. and Gobeil, C.: Non-steady state modeling of arsenic diagenesis in lake sediments, Environ. Sci. Technol., 44(1), 197–203, doi:10.1021/es902077q, 2010.

Dade, W. B., Hogg, A. J. and Boudreau, B. P.: Physics of Flow Above the Sediment- Water Interface, in The Benthic Boundary Layer, edited by B. P. Boudreau and B. B. Jorgensen, pp. 4–43, Oxford University Press;, New York., 2001.

Davison, W.: Iron and manganese in lakes, Earth-Science Rev., 34, 119–163, 1993.

Debolskaya, E. I., Yakushev, E. V. and Kuznetsov, I. S.: Analysis of the hydrophysical structure of the Sea of Azov in the period of the bottom anoxia development, J. Mar. Syst., 70(3-4), 300–307, doi:10.1016/j.jmarsys.2007.02.027, 2008.

Diaz, R. J. and Rosenberg, R.: Spreading dead zones and consequences for marine ecosystems., Science, 321(5891), 926–929, doi:10.1126/science.1156401, 2008.

Dickson, A. G.: The development of the alkalinity concept in marine chemistry, Mar. Chem., 40(1-2), 49–63, doi:10.1016/0304-4203(92)90047-E, 1992.

Fennel, K., Hetland, R., Feng, Y. and Dimarco, S.: A coupled physical-biological model of the Northern Gulf of Mexico shelf: Model description, validation and analysis of phytoplankton variability, Biogeosciences, 8(7), 1881–1899, doi:10.5194/bg-8-1881-2011, 2011.

Glud, R. N.: Oxygen dynamics of marine sediments, Mar. Biol. Res., 4(4), 243–289, doi:10.1080/17451000801888726, 2008.

Gregoire, M. and Lacroix, G.: Study of the oxygen budget of the Black Sea waters using a 3D coupled hydrodynamical – biogeochemical model, J. Mar. Syst., 2001.

Sen Gupta, B. K., Turner, R. E. and Rabalais, N. N.: Seasonal oxygen depletion in continental-shelf waters of Louisiana: Historical record of benthic foraminifers, Geology, 24(3), 227–230, doi:10.1130/0091-7613(1996)024<0227:SODICS>2.3.CO;2, 1996.

He, Y., Stanev, E. V., Yakushev, E. and Staneva, J.: Black Sea biogeochemistry: Response to decadal atmospheric variability during 1960-2000 inferred from numerical modeling, Mar. Environ. Res., 77, 90–102, doi:10.1016/j.marenvres.2012.02.007, 2012.

Hunter, K. S., Wang, Y. and Cappellen, P. Van: Kinetic modeling of microbially-driven redox chemistry of subsurface environments: coupling transport, microbial metabolism and geochemistry, J. Hydrol., 209(1–4), 53–80, doi:http://dx.doi.org/10.1016/S0022-1694(98)00157-7, 1998.

Jorgensen, B., Bang, M. and Blackburn, T.: Anaerobic mineralization in marine sediments from the Baltic Sea-North Sea transition, Mar. Ecol. Prog. Ser., 59, 39–54, doi:10.3354/meps059039, 1990.

Jourabchi, P., Van Cappellen, P. and Regnier, P.: Quantitative interpretation of pH distributions in aquatic sediments: A reaction-transport modeling approach, Am. J. Sci., 305(9), 919–956, doi:10.2475/ajs.305.9.919, 2005.

Formatted: Normal, Space Before: 5 pt, After: 5 pt, No widow/orphan control, Don't adjust space between Latin and Asian text, Don't adjust space between Asian text and numbers

Jourabchi, P., Meile, C., Pasion, L. R. and Van Cappellen, P.: Quantitative interpretation of pore water O2 and pH distributions in deep-sea sediments, Geochim. Cosmochim. Acta, 72(5), 1350–1364, doi:10.1016/j.gca.2007.12.012, 2008.

Kamyshny, A., Yakushev, E., Jost, G. and Podymov, O.: Chemical Structure of Pelagic Redox Interfaces. The Handbook of Environmental Chemistry., edited by E. Yakushev, Springer Berlin Heidelberg., 2013.

Kappler, A., Emerson, D., Edwards, K., Amend, J. P., Gralnick, J. A., Grathwohl, P., Hoehler, T. and Straub, K. L.: Microbial activity in biogeochemical gradients - New aspects of research, Geobiology, 3(3), 229–233, doi:10.1111/j.1472-4669.2005.00053.x, 2005.

~~Katsev, S. and Dittrich, M.: Modeling of decadal scale phosphorus retention in lake sediment under varying redox conditions, Ecol. Modell., 251, 246–259, doi:10.1016/j.ecolmodel.2012.12.008, 2013.~~

~~Katsev, S., Chaillou, G., Sundby, B. and Mucci, A.: Effects of progressive oxygen depletion on sediment diagenesis and fluxes: A model for the lower St. Lawrence River Estuary, Limnol. Oceanogr., 52(6), 2555–2568, doi:10.4319/lo.2007.52.6.2555, 2007.~~

Konovalov, S. K., Murray, J. W., Luther, G. W. and Tebo, B. M.: Processes controlling the redox budget for the oxic/anoxic water column of the Black Sea, Deep. Res. Part II Top. Stud. Oceanogr., 53(17-19), 1817–1841, doi:10.1016/j.dsr2.2006.03.013, 2006.

Lancelot, C., Spitz, Y., Gypens, N., Ruddick, K., Becquevort, S., Rousseau, V., Lacroix, G. and Billen, G.: Modelling diatom and Phaeocystis blooms and nutrient cycles in the Southern Bight of the North Sea: The MIRO model, Mar. Ecol. Prog. Ser., 289, 63–78, doi:10.3354/meps289063, 2005.

Lee, J. Y., Tett, P., Jones, K., Jones, S., Luyten, P., Smith, C. and Wild-Allen, K.: The PROWQM physical-biological model with benthicpelagic coupling applied to the northern North Sea, J. Sea Res., 48(4), 287–331, doi:10.1016/S1385-1101(02)00182-X, 2002.

Lewis, E. and Wallace, D.: Program developed for CO2 system calculations, , 1–21, doi:4735, 1998.

~~Linke, P., Haeckel, M., von Deimling, J. S., Vielstädte, L., Schmidt, M., Karstens, J., Berndt, C., Herreilers, H., Lichtschlag, A., James, R., Connelly, D., Baumberger, T., Pedersen, R. B., Denny, A. R., Rapp, H. T., Thorseth, I. H., Molari, M., de Beer, D., Rehder, G., Kedzior, S., Beaubien, S. and de Vittor, C.: Fluxes of CO2 from natural seep sites and Sleipner storage site, ECO2 Project Office, Kiel, Germany. [online] Available from: http://oceanrep.geomar.de/26057/, 2014.~~

Lopes, F., Viollier, E., Thiam, A., Michard, G., Abril, G., Groleau, A., Prévot, F., Carrias, J.-F., Albéric, P. and Jézéquel, D.: Biogeochemical modelling of anaerobic vs. aerobic methane oxidation in a meromictic crater lake (Lake Pavin, France), Appl. Geochemistry, 26(12), 1919–1932, doi:http://dx.doi.org/10.1016/j.apgeochem.2011.06.021, 2011.

Luff, R. and Moll, A.: Seasonal dynamics of the North Sea sediments using a three-dimensional coupled sediment-water model system, Cont. Shelf Res., 24(10), 1099–1127, doi:10.1016/j.csr.2004.03.010, 2004.

Luff, R., Haeckel, M. and Wallmann, K.: Robust and fast FORTRAN and MATLAB libraries to calculate pH distributions in marine systems, Comput. Geosci., 27(2), 157–169, doi:10.1016/S0098-3004(00)00097-2, 2001.

~~Madison, A. S., Tebo, B. M., Mucci, A., Sundby, B. and Luther, G. W.: Abundant porewater Mn(III) is a major component of the sedimentary redox system., Science, 341(6148), 875–8, doi:10.1126/science.1241396, 2013.~~

McCarthy, M. J., McNeal, K. S., Morse, J. W. and Gardner, W. S.: Bottom-water hypoxia effects on sediment-water interface nitrogen transformations in a seasonally hypoxic, shallow bay (Corpus Christi Bay, TX, USA), Estuaries and Coasts, 31(3), 521–531, doi:10.1007/s12237-008-9041-z, 2008.

Meile, C., Koretsky, C. M. and Van Cappellen, P.: Quantifying bioirrigation in aquatic sedimnets: An inverse modeling approach, Limnol. Ocean., 1(46), 164–177, 2001.

Formatted: Normal, Space Before: 5 pt, After: 5 pt, No widow/orphan control, Don't adjust space between Latin and Asian text, Don't adjust space between Asian text and numbers

Formatted: Normal, Space Before: 5 pt, After: 5 pt, No widow/orphan control, Don't adjust space between Latin and Asian text, Don't adjust space between Asian text and numbers

Formatted: Normal, Space Before: 5 pt, After: 5 pt, No widow/orphan control, Don't adjust space between Latin and Asian text, Don't adjust space between Asian text and numbers

Formatted: Normal, Space Before: 5 pt, After: 5 pt, No widow/orphan control, Don't adjust space between Latin and Asian text, Don't adjust space between Asian text and numbers

Meire, L., Soetaert, K. E. R. and Meysman, F. J~~., Risgaard-Petersen, N., Malkin, S. Y. and Nielsen, L. P.: The geochemical fingerprint~~. R.: Impact of ~~microbial long-distance electron~~global change on coastal oxygen dynamics and risk of hypoxia, Biogeosciences, 10(4), 2633–2653, doi:10.5194/bg-10-2633-2013, 2013.

Meysman, F. J. R., Boudreau, B. P. and Middelburg, J. J.: Modeling reactive transport in ~~the seafloor~~sediments subject to bioturbation and compaction, Geochim. Cosmochim. Acta, ~~152, 122–142, 2015~~69(14), 3601–3617, doi:10.1016/j.gca.2005.01.004, 2005.

Millero, F. J.: Thermodynamics of the carbon dioxide system in the oceans, Geochim. Cosmochim. Acta, 59(4), 661–677, doi:10.1016/0016-7037(94)00354-O, 1995.

Mobley, C. D. and Boss, E. S.: Improved irradiances for use in ocean heating, primary production, and photo-oxidation calculations, Appl. Opt., 51(27), 6549–6560, doi:10.1364/AO.51.006549, 2012.

Morgan, J. J.: Manganese speciation and redox kinetics in natural waters, in Chemical speciation and reactivity in water chemistry and water technology: Asumposium in honor of James J. Morgan, vol. 40, pp. 475–478., 2000.

Morse, J. W. and Eldridge, P. M.: A non-steady state diagenetic model for changes in sediment biogeochemistry in response to seasonally hypoxic/anoxic conditions in the "'dead ~~zone"~~zone' of the Louisiana shelf, Mar. Chem., 106(1-2 SPEC. ISS.), 239–255, doi:10.1016/j.marchem.2006.02.003, 2007.

~~National Oceanographic Data Center (NODC): National Oceanographic Data Center (NODC), [online] Available from: http://www.nodc.noaa.gov/, n.d.~~

~~Nielsen, L. P., Risgaard-Petersen, N., Fossing, H., Christensen, P. B. and Sayama, M.: Electric currents couple spatially separated biogeochemical processes in marine sediment., Nature, 463(7284), 1071–1074, doi:10.1038/nature08790, 2010.~~

~~Pakhomova, S. V, Kononets, M. Y., Yudin, M. V, Vershinin, A. V and Rozanov, A. G.: Studies on the fluxes of dissolved metal forms through the water-bottom interface in vistula lagoon of the Baltic sea, Oceanology, 44(4), 481–488, 2004.~~

~~Pakhomova, S. V., Kononets, M. Y., Yudin, M. V. and Rozanov, A. G.: Studies on the Fluxes of Dissolved Forms of Iron and Manganese through the Water–Bottom Interface on the Northeastern Shelf of the Black Sea, Oceanology, 43(4), 493–497, 2003.~~

Munhoven, G.: Mathematics of the total alkalinity-pH equation-Pathway to robust and universal solution algorithms: The SolveSAPHE package v1.0.1, Geosci. Model Dev., 6(4), 1367–1388, doi:10.5194/gmd-6-1367-2013, 2013.

Pakhomova, S. V., Hall, P. O. J., Kononets, M. Y., Rozanov, A. G., Tengberg, A. and Vershinin, A. V.: Fluxes of iron and manganese across the sediment-water interface under various redox conditions, Mar. Chem., 107(3), 319–331, doi:10.1016/j.marchem.2007.06.001, 2007.

Paraska, D. W., Hipsey, M. R. and Salmon, S. U.: Sediment diagenesis models: Review of approaches, challenges and opportunities, Environ. Model. Softw., 61, 297–325., doi:10.1016/j.envsoft.2014.05.011, 2014.

Pavlidou, A., Kontoyiannis, H., Anagnostou, C., Siokou–Frangou, I., Pagou, K., Krasakopoulou, E., Assimakopoulou, G., Zervoudaki, S., Zeri, C., Chatzianestis, J. and Psyllidou-Giouranovits, R.: Biogeochemical Characteristics in the Elefsis Bay (Aegean Sea, Eastern Mediterranean) in Relation to Anoxia and Climate Changes, in The Handbook of Environmental Chemistry, edited by E. (NIVA) Yakushev, pp. 161–201, Springer Berlin Heidelberg., 2013.

Pearson, T. H. and Rosenberg, R.: Macrobenthic succession in relation to organic enrichment and pollution of the marine environment, 1978.

Popova, E. E. and Srokosz, M. A.: Modelling the ecosystem dynamics at the Iceland-Faeroes Front: Biophysical interactions, J. Mar. Syst., 77(1-2), 182–196, doi:10.1016/j.jmarsys.2008.12.005, 2009.

Queirós, A. M., Norling, K., Amaro, T., Nunes, J., Cummings, D., Yakushev, E., Sorensen, K., Harris, C.,

Formatted: Normal, Space Before: 5 pt, After: 5 pt, No widow/orphan control, Don't adjust space between Latin and Asian text, Don't adjust space between Asian text and numbers

Formatted: Normal, Space Before: 5 pt, After: 5 pt, No widow/orphan control, Don't adjust space between Latin and Asian text, Don't adjust space between Asian text and numbers

Formatted: Normal, Space Before: 5 pt, After: 5 pt, No widow/orphan control, Don't adjust space between Latin and Asian text, Don't adjust space between Asian text and numbers

Formatted: Normal, Space Before: 5 pt, After: 5 pt, No widow/orphan control, Don't adjust space between Latin and Asian text, Don't adjust space between Asian text and numbers

Woodward, M., Danovaro, R., Rastelli, E., Alve, E., Vittor, C. De, Karuza, A., Cibic, T., Monti, M., Ingrosso, G., Fornasaro, D., Beaubien, S. E., Guilini, K., Vanreu, A., Bigalke, N. and Widdicombe, S.: Potential impact of CCS leakage on marine communities., 2014.

Rabalais, N. N., Turner, R. E. and Scavia, D.: Beyond Science into Policy: Gulf of Mexico Hypoxia and the Mississippi River, Bioscience, 52(2), 129, doi:10.1641/0006-3568(2002)052[0129:BSIPGO]2.0.CO;2, 2002.

Reed, D. C., Slomp, C. P. and Gustafsson, B. G.: Sedimentary phosphorus dynamics and the evolution of bottom-water hypoxia: A coupled benthic-pelagic model of a coastal system, Limnol. Oceanogr., 56(3), 1075–1092, doi:10.4319/lo.2011.56.3.1075, 2011.

Richards, F.: Anoxic basins and fjords, in Chemical Oceanography, edited by J. Riley and G. Skirrow, pp. 611–645, Academic Press, London., 1965.

Richardson, K. and Jørgensen, B. .: Eutrophication: Definition, History and Effects., 1996.

Rickard, D. and Luther, G. W.: Kinetics of pyrite formation by the H2S oxidation of iron (II) monosulfide in aqueous solutions between 25 and 125°C: The mechanism, Geochim. Cosmochim. Acta, 61(1), 135–147, doi:10.1016/S0016-7037(96)00322-5, 1997.

Roden, E. E. and Tuttle, J. H.: Sulfide release from estuarine sediments underlying anoxic bottom water, Limnol. Oceanogr., 37(4), 725–738, doi:10.4319/lo.1992.37.4.0725, 1992.

Roy, R. N., Roy, L. N., Vogel, K. M., Porter-Moore, C., Pearson, T., Good, C. E., Millero, F. J. and Campbell, D. M.: The dissociation constants of carbonic acid in seawater at salinities 5 to 45 and temperatures 0 to 45°C, Mar. Chem., 44(2-4), 249–267, doi:10.1016/0304-4203(93)90207-5, ~~1993~~1993a.

Roy, R. N., Roy, L. N., Vogel, K. M., Porter-Moore, C., Pearson, T., Good, C. E., Millero, F. J. and Campbell, D. M.: The dissociation constants of carbonic acid in seawater at salinities 5 to 45 and temperatures 0 to 45C, Mar. Chem., 44(2-4), 249–267, doi:10.1016/0304-4203(93)90207-5, 1993b.

Rutgers Van Der Loeff, M. M. and Boudreau, B. P.: The effect of resuspension on chemical exchanges at the sediment-water interface in the deep sea - A modelling and natural radiotracer approach, J. Mar. Syst., 11(3-4), 305–342, doi:10.1016/S0924-7963(96)00128-5, 1997.

Savchuk, O. and Wulff, F.: Biogeochemical Transformations of Nitrogen and Phousphorus in the Environment. Coupling Hydrodynamic and Biogeochemical Processes in Models for the Baltic Proper, , (2), 79 pp BT – Systems Ecology Contributions, 1996.

Savchuk, O. P.: Nutrient biogeochemical cycles in the Gulf of Riga: Scaling up field studies with a mathematical model, J. Mar. Syst., 32(4), 253–280, doi:10.1016/S0924-7963(02)00039-8, 2002.

Schippers, A. and Jorgensen, B. B.: Biogeochemistry of pyrite and iron sulfide oxidation in marine sediments, Geochim. Cosmochim. Acta, 66(1), 85–92, doi:10.1016/S0016-7037(01)00745-1, 2002.

Schlüter, M., Sauter, E., Hansen, H. P. and Suess, E.: Seasonal variations of bioirrigation in coastal sediments: Modelling of field data, Geochim. Cosmochim. Acta, 64(5), 821–834, doi:10.1016/S0016-7037(99)00375-0, 2000.

Sell, K. S. and Morse, J. W.: Dissolved Fe2+ and ∑ell Behavior in Sediments Seasonally Overlain by Hypoxic-to-anoxic Waters as Determined by CSV Microelectrodes, Aquat. Geochemistry, 12(2), 179–198, doi:10.1007/s10498-005-4574-2, 2006.

Soetaert, K. and Middelburg, J. J.: Modeling eutrophication and oligotrophication of shallow-water marine systems: The importance of sediments under stratified and well-mixed conditions, Hydrobiologia, 629(1), 239–254, doi:10.1007/s10750-009-9777-x, 2009.

Soetaert, K., Herman, P. M. J. and Middelburg, J. J.: A model of early diagenetic processes from the shelf to abyssal depths, Geochim. Cosmochim. Acta, 60(6), 1019–1040, doi:10.1016/0016-7037(96)00013-0, 1996.

Soetaert, K., Middelburg, J. J., Herman, P. M. J. and Buis, K.: On the coupling of benthic and pelagic biogeochemical models . Earth-Science On the coupling of benthic and pelagic biogeochemical models, , (April 2016), 173–201, doi:10.1016/S0012-8252(00)00004-0, 2000.

Soetaert, K., Herman, P. M. J., Middelburg, J. J., Heip, C., Smith, C. L., Tett, P. and Wild-allen, K.: Numerical modelling of the shelf break ecosystem : reproducing benthic and pelagic measurements, , 48, 3141–3177, 2001.

Soetaert, K., Hofmann, A. F., Middelburg, J. J., Meysman, F. J. R. and Greenwood, J.: The effect of

Formatted: Normal, Space Before: 5 pt, After: 5 pt, No widow/orphan control, Don't adjust space between Latin and Asian text, Don't adjust space between Asian text and numbers

Formatted: Normal, Space Before: 5 pt, After: 5 pt, No widow/orphan control, Don't adjust space between Latin and Asian text, Don't adjust space between Asian text and numbers

Formatted: Normal, Space Before: 5 pt, After: 5 pt, No widow/orphan control, Don't adjust space between Latin and Asian text, Don't adjust space between Asian text and numbers

Formatted: Normal, Space Before: 5 pt, After: 5 pt, No widow/orphan control, Don't adjust space between Latin and Asian text, Don't adjust space between Asian text and numbers

biogeochemical processes on pH (Reprinted from Marine Chemistry, vol 105, pg 30-51, 2007), Mar. Chem., 106(1-2), 380–401, doi:10.1016/j.marchem.2007.06.008, 2007.

Sohma, A., Sekiguchi, Y., Kuwae, T. and Nakamura, Y.: A benthic-pelagic coupled ecosystem model to estimate the hypoxic estuary including tidal flat-Model description and validation of seasonal/daily dynamics, Ecol. Modell., 215(1-3), 10–39, doi:10.1016/j.ecolmodel.2008.02.027, 2008.

Stanev, E. V., He, Y., Staneva, J. and Yakushev, E.: The Black Sea biogeochemistry: focus on temporal and spatial variability of oxygen, Biogeosciences Discuss., 11(1), 281–336, doi:10.5194/bgd-11-281-2014, 2014.

~~Sternbeck, J~~Tebo, B. M.: Manganese~~ cycling~~(II) oxidation in ~~a eutrophic lake - Rates and pathways, Aquat. Geochemistry, ~~the suboxic zone of the Black Sea, Deep Sea Res. Part A. Oceanogr. Res. Pap., 38(1~~(4), 399–426~~), S883–S905, doi:10.~~1007/BF00702741, 1996~~1016/S0198-0149(10)80015-9, 1991.

Thorpe, S. A.: The Turbulent Ocean, Cambridge University Press., 2005.

Umlauf, L., Burchard, H. and Bolding, K.: General ocean turbulence model. Source code documentation, Balt. Sea Res. Inst. Warn. Tech. Rep, 63, 346, 2005.

Volkov, I. I.: Geokhimiya Sery v Osadkakh Okeana (Geochemistry of Sulfur in Ocean Sediments~~),~~)., Nauka, Moscow~~,~~., 1984.

~~Vershinin, A.V., Rozanov, A.G.. Chemical Exchange across the Sediment – Water interface in oceans and seas, GEOS, Moscow, 2002. – 164 p.~~

Wanninkhof, R.: Relationship between wind speed and gas exchange over the ocean revisited, Limnol. Oceanogr., 12, 351–362, doi:10.4319/lom.2014.12.351, 2014.

Wersin, P.: The Fe(II)-CO2-H2O system in anoxic natural waters: equilibria and surface chemistry, Swiss Fed. Inst. Technol., 1990.

Wijsman, J. W. M., Herman, P. M. J., Middelburg, J. J. and Soetaert, K.: A Model for Early Diagenetic Processes in Sediments of the Continental Shelf of the Black Sea, Estuar. Coast. Shelf Sci., 54, 403–421, doi:10.1006/ecss.2000.0655, 2002.

Wolf-Gladrow, D. a., Zeebe, R. E., Klaas, C., Körtzinger, A. and Dickson, A. G.: Total alkalinity: The explicit conservative expression and its application to biogeochemical processes, Mar. Chem., 106(1-2 SPEC. ISS.), 287–300, doi:10.1016/j.marchem.2007.01.006, 2007.

Wollast, R.: Rate and mechanism of dissolution of carbonates in the system CaCO3-MgCO3 Publisher: Source: Aquatic chemical kinetics: reaction rates of processes in natural waters p.. Subject(s): Chemistry, in Aquatic Chemical Kinetics: Reaction Rates of Processes in Natural Waters, edited by W. Stumm, pp. 431–445, Wiley., 1990.

Yakushev~~.~~, E.: RedOx Layer Model: A Tool for Analysis of the Water Column Oxic/Anoxic Interface Processes~~. In: E.V.Yakushev (ed.)~~, in Chemical Structure of Pelagic Redox Interfaces: Observation and Modeling, ~~Hdb Env Chem (2013) 22:~~edited by E. V. Yakushev, pp. 203–234, Springer-Verlag Berlin Heidelberg~~,~~., 2013.

Yakushev, E., Pakhomova, S., Sørenson, K. and Skei, J.: Importance of the different manganese species in the formation of water column redox zones: Observations and modeling, Mar. Chem., 117(1-4), 59–70, doi:10.1016/j.marchem.2009.09.007, 2009.

Yakushev, E. ~~Yakushev, E. and Debolskaya, E.: Particulate manganese as a main factor of oxidation of hydrogen sulfide in redox zone of the Black Sea, in Konstantin Fedorov Memorial Symposium. Oceanic Fronts and Related Phenomena, pp. 18–22., 1998.~~

V and Neretin, L. N.: One-dimensional modeling of nitrogen and sulfur cycles in the aphotic zones of the Black and Arabian Seas, Global Biogeochem. Cycles, 11(3), 401–414, doi:10.1029/97GB00782, 1997.

Yakushev, E. V., Pollehne, F., Jost, G., Kuznetsov, I., Schneider, B. and Umlauf, L.: Redox Layer Model (ROLM): A Tool for Analysis of the Water Column Oxic/anoxic Interface Processes, Warnemunde., 2006.

Yakushev, E. V., Pollehne, F., Jost, G., Kuznetsov, I., Schneider, B. and Umlauf, L.: Analysis of the water

Formatted: Normal, Space Before: 5 pt, After: 5 pt, No widow/orphan control, Don't adjust space between Latin and Asian text, Don't adjust space between Asian text and numbers

Formatted: Normal, Space Before: 5 pt, After: 5 pt, No widow/orphan control, Don't adjust space between Latin and Asian text, Don't adjust space between Asian text and numbers

Formatted: Normal, Space Before: 5 pt, After: 5 pt, No widow/orphan control, Don't adjust space between Latin and Asian text, Don't adjust space between Asian text and numbers

Formatted: Normal, Space Before: 5 pt, After: 5 pt, No widow/orphan control, Don't adjust space between Latin and Asian text, Don't adjust space between Asian text and numbers

Formatted: Normal, Space Before: 5 pt, After: 5 pt, No widow/orphan control, Don't adjust space between Latin and Asian text, Don't adjust space between Asian text and numbers

Formatted: English (U.S.)

Formatted: Normal, Space Before: 5 pt, After: 5 pt, No widow/orphan control, Don't adjust space between Latin and Asian text, Don't adjust space between Asian text and numbers

column oxic/anoxic interface in the Black and Baltic seas with a numerical model, Mar. Chem., 107(3), 388–410, doi:10.1016/j.marchem.2007.06.003, 2007.

Yakushev, E. V., Chasovnikov, V. K., Murray, J. W., Pakhomova, S. V., Podymov, O. I. and Stunzhas, P. a.: Vertical hydrochemical structure of the black sea, Handb. Environ. Chem. Vol. 5 Water Pollut., 5 Q(July 2007), 277–307, doi:10.1007/698_5_088, 2008.

Yakushev, E. ~~., Pakhomova, S., Sørenson, K. and Skei, J.: Importance of the different manganese species in the formation of water column redox zones: Observations and modeling, Mar. Chem., 117(1–4), 59–70, doi:10.1016/j.marchem.2009.09.007, 2009.~~

~~Yakushev, E.~~ V., Kuznetsov, I. S., Podymov, O. I., Burchard, H., Neumann, T. and Pollehne, F.: Modeling the influence of oxygenated inflows on the biogeochemical structure of the Gotland Sea, central Baltic Sea: Changes in the distribution of manganese, Comput. Geosci., 37(4), 398–409, doi:10.1016/j.cageo.2011.01.001, 2011.

Yakushev, E. V., Debolskaya, E. I., Kuznetsov, I. S. and Staalstrøm, A.: Modelling of the Meromictic Fjord Hunnbunn (Norway) with an Oxygen Depletion Model (OxyDep), edited by E. V. Yakushev, Handb. Environ. Chem., (July 2011), doi:10.1007/698, 2013a.

Yakushev, E. V., Sorensen, K. and Sørensen, K.: On seasonal changes of the carbonate system in the Barents Sea: observations and modeling, Mar. Biol. Res., 9(9), 822–830, doi:Doi 10.1080/17451000.2013.775454, 2013b.

Yu, L., Fennel, K., Laurent, A., Murrell, M. C., and Lehrter, J. C.: Numerical analysis of the primary processes controlling oxygen dynamics on the Louisiana shelf, Biogeosciences, 7(12), 2063–2076, 2015.

Zeebe, R. E. and Wolf-Gladrow, D.: CO2 in Seawater: Equilibrium, Kinetics, Isotopes, Elsevier., 2001.

Formatted: Normal, Space Before: 5 pt, After: 5 pt, No widow/orphan control, Don't adjust space between Latin and Asian text, Don't adjust space between Asian text and numbers

Formatted: Normal, Space Before: 5 pt, After: 5 pt, No widow/orphan control, Don't adjust space between Latin and Asian text, Don't adjust space between Asian text and numbers

Table 1. State variables of BROM~~. Concentrations are presented in micromoles for chemical variables and in micromoles of nitrogen for biological variables.~~

N	Notation	Name	Units	N	Notation	Name	Units
	N	**Nitrogen**			**O ~~- oxygen~~**	**Oxygen**	
1	NH_4	Ammonia	µM N	19	O_2	~~dissolved~~Dissolved oxygen	µM ~~O~~O_2
2	NO_2	Nitrite	µM N		**S ~~- sulfur~~**	**Sulfur**	
3	NO_3	Nitrate	µM N	20	H_2S	~~hydrogen~~Hydrogen sulfide	µM S
4	PON	Particulate organic nitrogen	µM N	21	S^0	~~total~~Total elemental sulfur	µM S
5	DON	Dissolved organic nitrogen	µM N	22	S_2O_3	~~thiosulfate~~Thiosulfate and sulfites	µM S
	P	**Phosphorus**		23	SO_4	~~sulfate~~Sulfate	µM S

~~**N - nitrogen**~~

~~NH_4~~	~~ammonia~~	~~µM N~~
~~NO_2~~	~~nitrite~~	~~µM N~~
~~NO_3~~	~~nitrate~~	~~µM N~~
~~PON~~	~~particulate organic nitrogen~~	~~µM N~~
~~DON~~	~~dissolved organic nitrogen~~	~~µM N~~

~~**P - phosphorus**~~

6	PO_4	~~phosphate~~Phosphate	µM P		**C**	**Carbon**	
	Si ~~- silicate~~	**Silicon**		24	DIC	Dissolved inorganic carbon	µM C
7	Si	~~dissolved~~Dissolved silicon	µM Si	25	CH_4	Methane	µM C
8	Si_part	~~particulate~~Particulate silicon	µM Si	26	$CaCO_3$	Calcium carbonate	µM Ca
	Mn ~~- manganese~~	**Manganese**				**Alkalinity**	
~~MnII~~9	Mn^{2+}	~~dissolved~~Dissolved bivalent manganese	µM Mn	27	Alk	Total alkalinity	µM
~~MnIII~~10	Mn^{3+}	~~dissolved~~Dissolved trivalent manganese	µM Mn				
~~MnIV~~11	Mn^{4+}	~~particulate~~Particulate quadrivalent manganese	µM Mn			**Ecosystem parameters**	

~~MnS~~	~~manganese sulfide~~	~~µM Mn~~

~~$MnCO_3$~~	~~manganese carbonate~~	~~µM Mn~~
~~**Fe – iron**~~		
~~FeII~~	~~dissolved bivalent iron~~	~~µM Fe~~
~~FeIII~~	~~particulate trivalent iron~~	~~µM Fe~~
~~FeS~~	~~iron sulfide~~	~~µM Fe~~
~~FeS_2~~	~~iron pyrite~~	~~µM Fe~~
~~**C – carbon**~~		
~~DIC~~	~~dissolved inorganic carbon~~	~~µM C~~
~~**Ca – calcium**~~		
~~$CaCO_3$~~	~~Calcium carbonate~~	~~µM Ca~~
~~**Alkalinity**~~		
~~Alk~~	~~total alkalinity~~	~~µM~~
~~**Biological parameters**~~		

12	MnS	Manganese sulfide	µM Mn	28	Phy	~~phototrophic~~Phototrophic producers	µM N
13	$MnCO_3$	Manganese carbonate	µM Mn	29	Het	~~pelagic~~Pelagic and benthic heterotrophs	µM N
	Fe	**Iron**		30	Bhae	~~aerobic~~Aerobic heterotrophic bacteria	µM N
14	Fe^{2+}	Dissolved bivalent iron	µM Fe	31	Baae	~~aerobic~~Aerobic autotrophic bacteria	µM N
15	Fe^{3+}	Particulate trivalent iron	µM Fe	32	Bhan	~~anaerobic~~Anaerobic heterotrophic bacteria	µM N
16	FeS	Iron monosulfide	µM Fe	33	Baan	~~anaerobic~~Anaerobic autotrophic bacteria	µM N
17	FeS_2	Pyrite	µM Fe				
18	$FeCO_3$	Ferrous Carbonate	µM Fe				

Inserted Cells
Inserted Cells
Inserted Cells
Inserted Cells
Inserted Cells
Formatted: Space Before: 0 pt, Line spacing: Multiple 1,15 li
Formatted: Space Before: 0 pt, Line spacing: Multiple 1,15 li
Formatted: Space Before: 0 pt, Line spacing: Multiple 1,15 li
Formatted: Space Before: 0 pt, Line spacing: Multiple 1,15 li
Formatted: Space Before: 0 pt, Line spacing: Multiple 1,15 li
Formatted: Space Before: 0 pt, Line spacing: Multiple 1,15 li

Table 2. Parameterization of the biogeochemical processes

2.1. Nutrients

Name of Process, reference, reaction	Parameterization in the model
Nitrogen	
~~Autolysis~~Autolysis (Savchuk and Wulff, 1996)	~~AutolysisN~~ ~~K_{PON}~~Autolysis = K_PON_DON***PON**
Mineralization at oxic conditions (Richards, 1965) $(CH_2O)_{106}(NH_3)_{16}H_3PO_4 + 106O_2 \rightarrow$ $106CO_2 + 16NH_3 + H_3PO_4 + 106H_2O$	~~DcDM_O2 = K_{DON_ox} * DON * Fox * $(1 + f_t^D(t))$~~ ~~DcPM_O2 = K_{PON_ox} * PON * Fox * $(1 + f_t^D(t))$~~ ~~where Fox = $\frac{O_2}{O_2 + K_{omox O_2}}$~~ ; $f_t^D(t) = B_{da}\frac{t^2}{t^2 + t_{da}^2}$ -DcDM_O2 = K_DON_ox * **DON** * $\frac{\mathbf{O_2}}{\mathbf{O_2}+K\_omox\_o2}$ * $(1 + beta\_da\ \frac{t^2}{t^2+tda^2})$ DcPM_O2 = K_PON_ox * **PON** * $\frac{\mathbf{O_2}}{\mathbf{O_2} + K\_omox\_o2}$ * $(1 + beta\_da\ \frac{t^2}{t^2 + tda^2})$
Nitrification 1 stage (Canfield et al., 2005): $NH_4^+ + 1.5O_2 \rightarrow NO_2^- + 2H^+ + H_2O$	Nitrif1 = K_nitrif1 * $\mathbf{NH_4}$ * $\mathbf{O_2}$ * 0.5 * $(1. + \tanh(\mathbf{O_2} - O2s\_nf))$
Nitrification 2 stage (Canfield et al., 2005): $NO_2^- + 0.5\ O_2 \rightarrow NO_3^-$	Nitrif2 = K_nitrif2 * $\mathbf{NO_2}$ * $\mathbf{O_2}$ * 0.5 * $(1. + \tanh(\mathbf{O_2} - O2s\_nf))$
Anammox (Canfield et al., 2005): $NO_2^- + NH_4^+ \rightarrow N_2 + 2H_2O$	Anammox = K_anammox * $\mathbf{NO_2}$ * $\mathbf{NH_4}$ * $\left(1 - 0.5 * \left(1 + \tanh(\mathbf{O_2} - O2s\_dn)\right)\right)$
POM denitrification 1st stage: (Anderson et al., 1982)	Denitr1_PM = K_denitr1 * F_dnox * $\frac{\mathbf{NO_3}}{\mathbf{NO_3} + K\_omno\_no3}$ * **PON**

Formatted: Font: 9 pt
Formatted: Space Before: 0 pt, After: 10 pt
Formatted: Space Before: 0 pt, After: 0 pt
Formatted Table
Formatted: Font: 10 pt, Not Superscript/ Subscript
Formatted: Font: 10 pt, Bold
Formatted: Font: 10 pt
Formatted: Space Before: 0 pt, After: 0 pt
Formatted Table
Formatted: Font: 10 pt
Formatted: Font: 10 pt
Formatted: Space Before: 0 pt, After: 0 pt
Formatted: Font: 10 pt
Formatted: Font: 10 pt
Formatted: Font: 10 pt
Formatted: Space Before: 0 pt, After: 0 pt
Formatted: Space Before: 0 pt, After: 0 pt
Formatted: Font: 10 pt

$0.5CH_2O + NO_3^- \rightarrow NO_2^- + 0.5H_2O + 0.5CO_2$ 2d stage: (Anderson et al., 1982) $0.75CH_2O + H^+ + NO_2^- \rightarrow 0.5N_2 + 1.25H_2O + 0.75CO_2$	$\text{Denitr2\_PM} = \text{K\_denitr2} * \text{F\_dnox} * \frac{\mathbf{NO_2}}{\mathbf{NO_2} + \text{K\_omno\_no2}} * \mathbf{PON}$ where $\text{F\_dnox} = 1 - 0.5 * (1 + \tanh(\mathbf{O_2} - \text{O2s\_dn}))$ $\text{DcPM\_NOX} = \frac{16}{212} * \text{Denitr1\_PM} + \frac{16}{141.3} * \text{Denitr2\_PM}$
DOM denitrification (Anderson et al., 1982)	$\text{Denitr1\_DM} = \text{K\_denitr1} * \text{F\_dnox} * \frac{\mathbf{NO_3}}{\mathbf{NO_3} + \text{K\_omno\_no3}} * \mathbf{DON}$ $\text{Denitr2\_DM} = \text{K\_denitr2} * \text{F\_dnox} * \frac{\mathbf{NO_2}}{\mathbf{NO_2} + \text{K\_omno\_no2}} * \mathbf{DON}$ where $\text{F\_dnox} = 1 - 0.5 * (1 + \tanh(\mathbf{O_2} - \text{O2s\_dn}))$ $\text{DcDM\_NOX} = \frac{16}{212} * \text{Denitr1\_DM} + \frac{16}{141.3} * \text{Denitr2\_DM}$
Phosphate	
Complexation with Mn(III) (Yakushev et al., 2007):	mn_p_compl= (mn_ox2+mn_rd2-mn_ox1-mn_rd1)/ r_mn_p
Complexation with Fe(III) (Yakushev et al., 2007):	fe_p_compl= (fe_rd-fe_ox1-fe_ox2+4.*DcDM_Fe+4.*DcPM_Fe)/r_fe_p
Silicate	
Dissolution of particulate Si (Popova and Srokosz, 2009):	sipart_diss = **Si_part** * K_sipart_diss
Complexation with Fe(III):	fe_si_compl= (fe_rd-fe_ox1-fe_ox2+4.*DcDM_Fe+4.*DcPM_Fe)/r_fe_si

1

2.2. Redox metals and sulfur

Name of Process, reference, reaction	Parameterization in the model
Manganese	
Manganese(II) oxidation (Canfield et al., 2005) $4Mn^{2+} + O_2 + 4H^+ + 4H^{3+} + 2H_2O$	~~$mn\_ox = 0.5 * \left(1 + \tanh\left(Mn^{2+} - s_{mnox_{mnz}}\right)\right) * K_{mn_{ox}} * Mn^{2+} * \frac{O_z}{(O_z + k_{mnoxO_z})}$~~ mn_ox1 $= 0.5 * (1 + \tanh(\mathbf{Mn^{2+}} - s\_mnox\_mn2)) * K\_mn\_ox1 * \mathbf{Mn^{2+}} * \frac{\mathbf{O_2}}{(\mathbf{O_2} + K\_mnox\_o2)}$
Manganese (III) oxidation (Tebo et al., 1997) $2Mn^{3+} + 3H_2O + 0.5O_2 + 0_2 + 6H^+$	~~$mn\_ox2 = 0.5 * \left(1 + \tanh\left(Mn^{3+} - s_{mnox_{mnz}}\right)\right) * K_{mn_{ox_z}} * Mn^{3+} * \frac{O_z}{(O_z + k_{mnox_{O_z}})}$~~ mn_ox2 $= 0.5 * (1 + \tanh(\mathbf{Mn^{3+}} - s\_mnox\_mn2)) * K\_mn\_ox2 * \mathbf{Mn^{3+}} * \frac{O_2}{(O_2 + K\_mnox\_o2)}$
~~Manganese (IV) reduction~~ Manganese (IV) reduction (Canfield et al., 2005) $2MnO_2 + 7H^+ + HS^- + H^{3+} + 4H_2O + S^0$	~~$mn\_rd = 0.5 * \left(1 + \tanh\left(Mn^{4+} - s_{mnrd_{mn4}}\right)\right) * K_{mn_{rd}} * Mn^{4+} * \frac{H_2S}{(H_2S + k_{mnrdHS})}$~~ mn_rd1 $= 0.5 * (1 + \tanh(\mathbf{Mn^{4+}} - s\_mnrd\_mn4)) * K\_mn\_rd1 * \mathbf{Mn^{4+}} * \frac{\mathbf{H_2S}}{(\mathbf{H_2S} + K\_mnrd\_hs)}$
Manganese (III) reduction $2Mn^{3+} + HS^- + HS^{2+} + S^0 + H^+$	~~$mn\_rd2 = 0.5 * \left(1 + \tanh\left(Mn^{3+} - s_{mnrd_{mn3}}\right)\right) * K_{mn_{rd_z}} * Mn^{3+} * \frac{H_2S}{(H_2S + k_{mnrdHS})}$~~ mn_rd2 $= 0.5 * (1 + \tanh(\mathbf{Mn^{3+}} - s\_mnrd\_mn3)) * K\_mn\_rd2 * \mathbf{Mn^{3+}} * \frac{\mathbf{H_2S}}{(\mathbf{H_2S} + K\_mnrd\_hs)}$

Formatted: Space Before: 0 pt, After: 0 pt
Formatted: Font: 10 pt
Formatted Table
Formatted: Font: 10 pt
Formatted: Space Before: 0 pt, After: 0 pt
Formatted: Font: 10 pt
Formatted: Font: 10 pt
Formatted: Font: Times New Roman, 10 pt
Formatted: Font: 10 pt
Formatted: Font: 10 pt
Formatted: Font: 10 pt
Formatted ...
Formatted: Font: 10 pt
Formatted: Font: 10 pt
Formatted ...
Formatted: Font: 10 pt
Formatted: Font: 10 pt
Formatted: Font: 10 pt
Formatted ...
Formatted ...
Formatted: Font: 10 pt
Formatted: Font: 10 pt
Formatted: Font: 10 pt
Formatted ...
Formatted ...
Formatted: Font: 10 pt
Formatted: Font: 10 pt

~~MnS formation/dissollution (Davison, 1993)~~ MnS formation/dissollution (Davison, 1993) : $Mn^{2+}+HS^{-}\leftrightarrow MnS + H^{+}$	~~mns_prec = $K_{mns_{form}}$ * max{0, (om_mns − 1)}~~ mns_form = K_mns_form * max(0, $\left(\frac{\mathbf{H_2S} * \mathbf{Mn^{2+}}}{\text{K\_mns} * \mathbf{H^{+}}} - 1\right)$) mns_diss = ~~$K_{mns_{diss}}$ * MnS~~K_mns_diss * **MnS** * max~~{~~(0, ~~(1 − om_mns)}~~ ~~where om_mns = $\frac{H_2S*Mn^{2+}}{K_{mns}*H^{+}}\left(1 - \frac{H_2S*Mn^{2+}}{K\_mns*H^{+}}\right)$)~~
$MnCO_3$ precipitation/dissolution ~~(Van Capellen, Wang, 1996)~~ ~~Mn^{2+} +CO_3 (Van Cappellen and Wang, 1996):~~ $Mn^{2+}+CO_3^{2-}\leftrightarrow$ □ □nCO_3	mnco3_prec = ~~$K_{mnco3_{form}}$ *~~ K_mnco3_pres * max~~{~~(0, ~~(om_mnco3 − 1)}~~ $\left(\frac{\mathbf{Mn^{2+}} * \mathbf{CO_3}}{\text{K\_mnco3}} - 1\right)$) mnco3_diss = ~~$K_{mnco3_{diss}}$ * $MnCO_3$ *~~ K_mnco3_diss * **$MnCO_3$** * max~~{~~(0, ~~(1 − om_{mnco_3})}~~ ~~where $om_{mnco_3} = \frac{Mn^{2+}*CO_3}{K_{mnco_3}}\left(1 - \frac{Mn^{2+}*CO_3}{\text{K\_mnco3}}\right)$)~~
~~$MnCO_3$ oxidation by O_2 (Morgan, 2005)~~ $MnCO_3$ oxidation by O_2 (Morgan, 2000): 2 $MnCO_3$ + ~~O_2 + 2H_2O −~~ 2 MnO_2 + 2HCO_3^{-} + 2H^{+}	~~mn_co3_ox = $K_{mnco3_{ox}}$ * $MnCO_3$ * O_2~~mnco3_ox = K_mnco3_ox * **$MnCO_3$** * **O_2**
Manganese reduction for PON (Boudreau, 1996): $(CH_2O)_{106}(NH_3)_{16}H_3PO_4$ + 212MnO_2+ 318CO_2 +106H_2O → 424HCO_3^{-}+ 212 Mn^{2+}+16NH_3 + H_3PO_4	DcPM_Mn = ~~max{0, K_{PONMn} * PON * $\frac{Mn^{4+}}{Mn^{4+}+0.5}$}~~ * (K_PON_mn * **PON** * $\frac{\mathbf{Mn^{4+}}}{\mathbf{Mn^{4+}}+0.5}$ * (1 − 0.5 * (1 + tanh~~(O2 − O_2s_{dn}))~~(**O_2** − O2s_dn))
Manganese reduction for DON (Boudreau, 1996):	DcDM_Mn = ~~max{0, K_{DONMn} * DON * $\frac{Mn^{4+}}{Mn^{4+}+0.5}$}~~ * (K_DON_mn * **DON** * $\frac{Mn^{4+}}{Mn^{4+}+0.5}$ * (1 − 0.5 * (1 + tanh~~(o2 − O_2s_{dn}))~~)(**O_2** − O2s_dn))

Formatted ... (×40)

Iron	
~~Fe (II) oxidation with O_2 (Van Cappelen, Wang, 1996)~~ ~~$4Fe^{2+} + O_2 + 10H_2O \rightarrow 4Fe(OH)_3 + 8H^+$~~ Fe (II) oxidation with O_2 (Van Cappelen and Wang, 1996): $4Fe^{2+} + O_2 + 10H_2O \rightarrow Fe(OH)_3 + 8H^+$	fe~~_ox~~_ox1 = 0.5 ∗ (1 + tanh(~~$Fe^{2+} - s_{feox_{Fe^{2+}}}$~~)) ∗ ~~$K_{fe_{ox}}$~~ ∗ ~~$O_2$~~ ∗ ~~$Fe^{2+}$~~**$Fe^{2+}$** − s_feox_fe2)) ∗ K_fe_ox1 ∗ **O_2** ∗ **Fe^{2+}**
~~Fe (II) oxidation with Mn oxide (Van Cappelen, Wang, 1996)~~ Fe (II) oxidation with Mn oxide (Van Cappelen and Wang, 1996): $2Fe^{2+} + MnO_2 + 4H_2O \rightarrow$ □□□□□□□□□$_3$ + Mn^{2+} + 2 H^+	~~fe_ox2 = 0.5 ∗ (1 + tanh(Fe^2+ − s_feox_Fe^2+)) ∗ K_fe_ox ∗ Mn^4+ ∗ Fe^2+~~fe_ox2 = 0.5 ∗ (1 + tanh(**Fe^{2+}** − s_feox_fe2)) ∗ K_fe_ox2 ∗ **Mn^{4+}** ∗ **Fe^{2+}**
~~Fe (III) reduction (Volkov, 1984)~~ Fe (III) reduction (Volkov, 1984): $2Fe(OH)_3 + HS^- + 5H^+ \rightarrow$ 5H(O^{2+} + S^0 + $6H_2O$	fe~~_rd = 0.5 ∗ (1. +tanh(Fe^3+ − s_ferd_Fe^3+)) ∗ K_fe_rd ∗ Fe^3+ ∗ H2S / (H2S + k_ferd_HS)~~**Fe^{3+}** − s_feox_fe3)) ∗ K_fe_rd ∗ **Fe^{3+}** ∗ **$\frac{H_2S}{H_2S + K\_ferd\_hs}$**
FeS formation/dissolition ~~(Bektursunova et al., 2011);~~ (Bektursunova and L'Heureux, 2011) : $Fe^{2+} + HS^- \leftrightarrow FeS + H^+$	~~fes_prec = K_fes_form = K_Fes_form ∗ max{(0, (om_Fes − 1)}~~ fes_prec = K_fes_form ∗ max{(0, **$\left(\frac{H_2S * Fe^{2+}}{K\_fes * H^+} - 1\right)$**) fes_diss = ~~$K_{Fes_{diss}}$~~K_fes_diss ∗ **FeS** ∗ max{(0, ~~(1 − om_fe)~~) ~~where om_Fes = $\frac{H_2S * Fe^{2+}}{K_{Fes} * H^+}\left(1 - \frac{H_2S * Fe^{2+}}{K\_fes * H^+}\right)$~~
~~FeS oxidation (Soetaert et al., 2007):~~ FeS oxidation (Soetaert et al., 2007):	fes~~_ox = K_Fes_ox ∗ O2 ∗ FeS~~K_fes_ox ∗ **O_2** ∗ **FeS**

Formatted: Font: 10 pt
Formatted: Space Before: 0 pt, After: 0 pt
Formatted: Font: 10 pt
Formatted: Font: 10 pt
Formatted: Font: 10 pt
Formatted: Space Before: 0 pt, After: 0 pt
Formatted ...
Formatted: Font: 10 pt
Formatted: Font: 10 pt
Formatted ...
Formatted ...
Formatted: Font: 10 pt
Formatted ...
Formatted: Font: 10 pt
Formatted ...
Formatted ...
Formatted: Font: 10 pt
Formatted ...
Formatted ...
Formatted ...
Formatted ...
Formatted: Font: 10 pt
Formatted ...
Formatted ...
Formatted ...
Formatted ...
Formatted ...
Formatted: Font: 10 pt
Formatted ...

$FeS + 2.25O_2 + 2.5H_2O \rightarrow Fe(OH)_3 + 2H^+ + SO_4^{2-}$	
Pyrite formation (Rickard and Luther, 1997; Soetaert et al., 2007): $FeS + H_2S \rightarrow FeS_2 + H_2$ ~~Pyrite formation (Rickard, 1997, Soetaert et al., 2007):~~ ~~$FeS + H_2S \rightarrow FeS_2 + H_2$~~	fes2_form = ~~$K_{FeS2_{form}} * H_2S * FeS$~~ K_fes2_form $* \mathbf{H_2S} * \mathbf{FeS}$
~~Pyrite oxidation by O_2 (Wijsman et al., 2002):~~ Pyrite oxidation by O_2 (Wijsman et al., 2002): $FeS_2 + 3.5O_2 + H_2O \rightarrow H^{2+} + 2SO_4^{2-} + 2H^+$	fes2_ox = K_~~$FeS2_{ox} * FeS_2 * O_2$~~ fes2_ox $* \mathbf{FeS_2} * \mathbf{O_2}$
$FeCO_3$ precipitation/dissolution (Van Cappellen and Wang, 1996): $Fe^{2+} + CO_3^- \leftrightarrow FeCO_3$	$feco3\_form = K\_feco3\_form * \max(0, \left(\frac{\mathbf{Fe^{2+}} * \mathbf{CO_3}}{K\_feco3} - 1\right))$ $feco3\_diss = K\_feco3\_diss * \mathbf{FeCO_3} * \max(0, \left(1 - \frac{\mathbf{Fe^{2+}} * \mathbf{CO_3}}{K\_feco3}\right))$
$FeCO_3$ oxidation by O_2 (Morgan, 2000): $2\ FeCO_3 + O_2 + 2H_2O \rightarrow 2\ FeO_2 + 2HCO_3^- + 2H^+$	$feco3\_ox = K\_feco3\_ox * \mathbf{FeCO_3} * \mathbf{O_2}$
Iron reduction for DON (Boudreau, 1996): $(CH_2O)_{106}(NH_3)_{16}H_3PO_4 + 424\ Fe(OH)_3 + 742CO_2 \rightarrow$ $848HCO_3^- + 424\ Fe^{2+} + 318\ H_2O + 16NH_3 + H_3PO_4$	~~$DcDM\_Fe = K_{DON_{Fe}} * DON * Fe^{3+} * \left(1. - 0.5 * \left(1 + \tanh\left(O_2 - O_{2_{s_{dn}}}\right)\right)\right)$~~ DcDM_Fe $= K\_DON\_fe * \mathbf{DON} * \mathbf{Fe^{3+}} * \left(1. - 0.5 * \left(1 + \tanh(\mathbf{O_2} - O2s\_dn)\right)\right)$
Iron reduction for PON (Boudreau, 1996):	~~$DcPM\_Fe = K_{PON_{Fe}} * PON * Fe^{3+} * \left(1. - 0.5 * \left(1 + \tanh\left(O_2 - O_{2_{s_{dn}}}\right)\right)\right)$~~ DcPM_Fe $= K\_PON\_fe * \mathbf{PON} * \mathbf{Fe^{3+}} * \left(1. - 0.5 * \left(1 + \tanh(\mathbf{O_2} - O2s\_dn)\right)\right)$
	~~**Nitrogen**~~

Formatted: Font: 10 pt
Formatted: Font: Times New Roman, 10 pt
Formatted: Space Before: 0 pt, After: 0 pt
Formatted ...
Formatted: Font: 10 pt
Formatted: Font: 10 pt, English (U.K.)
Formatted: Font: 10 pt, English (U.K.)
Formatted ...
Formatted: Font: 10 pt
Formatted: Font: 10 pt
Formatted: Font: 10 pt
Formatted ...
Formatted ...
Formatted: Font: 10 pt
Formatted: Font: 10 pt
Formatted ...
Formatted Table
Formatted: Font: 10 pt
Formatted: Font: 10 pt
Formatted ...
Formatted: Font: 10 pt
Formatted ...
Formatted: Font: 10 pt
Formatted: Font: 10 pt
Formatted ...
Formatted: Font: 10 pt
Formatted: Font: 10 pt
Formatted ...

Nitrification 1-stage (Canfield et al., 2005) $NH_4^+ + 1.5O_2 \rightarrow NO_2^- + 2H^+ + H_2O$	$nitrif1 = K_{N42} * NH_4 * O_2 * 0.5 * (1. + \tanh(O_2 - O_{2\_s\_nit}))$
Nitrification 2-stage (Canfield et al., 2005) $NO_2^- + 0.5\,O_2 \rightarrow NO_3^-$	$nitrif2 = K_{N23} * NO_2 * O_2 * 0.5 * (1. + \tanh\left(O_2 - O_{2_{s_{nit}}}\right))$
Anammox (Canfield et al., 2005) $NO_2^- + NH_4^+ \rightarrow N_2 + 2H_2O$	$anammox = K_{anammox} * NO_2 * NH_4 * \left(1 - 0.5 * \left(1 + \tanh\left(O_2 - O_{2_{s_{dn}}}\right)\right)\right)$
POM and DOM denitrification (1st stage) (Anderson et al., 1982): $0.5CH_2O + NO_3^- \rightarrow NO_2^- + 0.5H_2O + 0.5CO_2$	$denitr1\_PM = K_{N32} * PON * Fdnox \frac{NO_3}{NO_3 + K_{omno_{NO3}}}$ $denitr1\_DM = K_{N32} * DON * Fdnox * \frac{NO_3}{NO_3 + K_{omno_{NO3}}}$ $denitr1 = denitr1\_PM + denitr1\_DM$ where $Fdnox = (1 - 0.5 * \left(1 + \tanh\left(O_2 - O_{2_{s_{dn}}}\right)\right))$

~~POM and DOM denitrification (2d stage) (Anderson et al., 1982)~~ ~~$0.75CH_2O + H^+ + NO_2^- \rightarrow 0.5N_2 + 1.25H_2O + 0.75CO_2$~~	~~$denitr2\_PM = K_{N24} * PON * Fdonx * \frac{NO_2}{NO_2 + K_{omno\_NO2}}$~~ ~~$denitr2\_DM = K_{N24} * DON * Fdnox * \frac{NO_2}{NO_2 + K_{omno\_NO2}}$~~ ~~$denitr2 = denitr2\_PM + denitr2\_DM$~~
~~Denitrification of POM and DOM (Richards, 1965)~~ ~~$(CH_2O)_{106}(NH_3)_{16}H_3PO_4 + 84.8HNO_3 \rightarrow 106CO_2 + 42.4N_2 + 148.4H_2O + 16NH_3 + H_3PO_4$~~	$DcPM\_NOX = \frac{16}{212} * Denitr1\_PM + \frac{16}{141.3} Denitr2\_PM$ $DcDM\_NOX = \frac{16}{212} * Denitr1\_DM + \frac{16}{141.3} Denitr2\_DM$
Sulfur	
S^0 disproportionation (Canfield et al., 2005): $4S^0 + 3H_2O \rightarrow 2H_2S + S_2O_3^{2-} + 2H^+$	~~$disprop = K_{dispro} * S^0$~~ $s0\_disp = K\_s0\_disp * \mathbf{S^0}$
~~Sulphide oxidation with O_2 (Volkov, 1984):~~ Sulphide oxidation with O_2 (Volkov, 1984): $2H_2S + O_2 \rightarrow 2S^0 + 2H_2O$	$hs\_ox = ~~K_{HS_{ox}} * H_2S * O_2~~ K\_hs\_ox * \mathbf{H_2S} * \mathbf{O_2}$
~~S^0 oxidation with O_2 (Volkov, 1984):~~ S^0 oxidation with O_2 (Volkov, 1984): $2S^0 + O_2 + H_2O \rightarrow S_2O_3^{2-} + 2H^+$	$s0\_ox = ~~K_{S^0\_ox} * S^0 * O_2~~ K\_s0\_ox * \mathbf{S^0} * \mathbf{O_2}$
~~S^0 oxidation with NO_3 (Kamyshny et al., 2013):~~	$s0\_no3 = ~~K_{S^0_{NO_3}} * NO_3 * S^0~~ K\_s0\_no3 * \mathbf{NO_3} * \mathbf{S^0}$

Formatted: Space Before: 0 pt, After: 0 pt
Formatted: Font: 10 pt
Formatted Table
Formatted: Font: 10 pt
Formatted: Font: 10 pt
Formatted: Space Before: 0 pt, After: 0 pt
Formatted: Font: 10 pt
Formatted: Font: 10 pt
Formatted: Font: Times New Roman, 10 pt
Formatted: Font: 10 pt
Formatted: Font: 10 pt
Formatted: Font: Times New Roman, 10 pt
Formatted: Font: 10 pt
Formatted: Font: 10 pt
Formatted: Space Before: 0 pt, After: 0 pt
Formatted: Font: 10 pt
Formatted: Font: 10 pt
Formatted: Font: 10 pt
Formatted: Font: 10 pt
Formatted: Font: 10 pt
Formatted: Space Before: 0 pt, After: 0 pt
Formatted: Font: 10 pt
Formatted: Font: 10 pt
Formatted: Font: 10 pt
Formatted: Font: 10 pt

S^0 oxidation with NO_3 (Kamyshny et al., 2013): $4S^0 + 3NO_3^- + 7H_2O \rightarrow 4SO_4^{2-} + 3NH_4^+ + 2H^+$	
~~S_2O_3 oxidation with O_2: (Volkov, 1984):~~ S_2O_3 oxidation with O_2: (Volkov, 1984): $S_2O_3^{2-} + 2O_2 + 2OH^- \rightarrow 2SO_4^{2-} + H_2O$	s2o3_ox = ~~$K_{s23\_ox} * S_2O_3 * O_2$~~K_s2o3_ox $* \mathbf{S_2O_3} * \mathbf{O_2}$
~~S_2O_3 oxidation with NO_3: (Kamyshny et al., 2013)~~ S_2O_3 oxidation with NO_3: (Kamyshny et al., 2013) $S_2O_3^{2-} + NO_3^- + 2H_2O \rightarrow 2SO_4^{2-} + NH_4^+$	s2o3_no3 = ~~$K_{s23\_NO_3} * NO_3 * S_2O_3$~~K_s2o3_no3 $* \mathbf{NO_3} * \mathbf{S_2O_3}$
~~Thiodenitrification (Volkov, 1984, Schippers and Jorgensen, 2002):~~ ~~$5H_2S + 8NO_3^- + 2OH^- \rightarrow 5SO_4^{2-} + 4N_2 + 6H_2O$~~Thiodenitrification: (Schippers and Jorgensen, 2002; Volkov, 1984) $5H_2S + 8NO_3^- + 2OH^- \rightarrow 5SO_4^{2-} + 4N_2 + 6H_2O$	~~sulfido = KT $* H_2S * NO_3$~~hs_no3 = K_hs_no3 $* \mathbf{H_2S} * \mathbf{NO_3}$
POM ~~sulfatereduction~~sulfate reduction 1st and 2d stages (Boudreau, 1996): $(CH_2O)_{106}(NH_3)_{16}H_3PO_4 + 53SO_4^{2-} \rightarrow 106HCO_3^- + 16NH_3 + H_3PO_4 + 53H_2S$	~~s4rd_PM = $K_{s4_{rd}} * Fsox * Fsnx * SO_4 * PON$~~ ~~s23rd_PM = $K_{s23_{rd}} * Fsox * Fsnx * S_2O_3 * PON$~~ ~~where:~~ ~~Fsox = (~~so4_rd_PM = K_so4_rd $*$ F_sox $*$ F_snx $* \mathbf{SO_4} * \mathbf{PON}$ s2o3_rd_PM = K_s2o3_rd $*$ F_sox $*$ F_snx $* \mathbf{S_2O_3} * \mathbf{PON}$ F_sox = 1.~~—~~ $- 0.5 * (1. + \tanh(\mathbf{O_2} - s_{omso_{o_2}}))\mathbf{O_2} -$ s_omso_o2))

Formatted ... (×30)

	Fsnx = (F_snx = 1. − 0.5 ∗ (1. +tanh(NO3 − s_omso_no))) **NO_3** − s_omso_no3)) DcPM_SO4 = 16/53 ∗ (s4rdPM + s23rdPM)16/53 ∗ (so4_rd_PM + s2o3_rd_PM)
DOM sulfatereductionsulfate reduction 1st and 2d stages (Boudreau, 1996):	s4rd_DM = $K_{s4_{rd}}$ ∗ Fsox ∗ Fsnx ∗ SO_4 ∗ DON s23rd_DM = $K_{s23_{rd}}$ ∗ Fsox ∗ Fsnx ∗ S_2O_3 ∗ DON so4_rd_DM = K_so4_rd ∗ F_sox ∗ F_snx ∗ **SO_4** ∗ **DON** s2o3_rd_DM = K_s2o3_rd ∗ F_sox ∗ F_snx ∗ **S_2O_3** ∗ **DON** DcDM_SO4 = 16/53 ∗ (s4rdDM + s23rdDM)16/53 ∗ (so4_rd_PM + s2o3_rd_PM)

Carbon and Alkalinity

Carbonate system	Carbonate system equilibration was parameterized using the standard approach (i.e. Lewis, E. and Wallace,, 1998)
$CaCO_3$ precipitation/dissolution (Luff et al., 2001) $Ca^{2+} + CO_3^{2-} \leftrightarrow CaCO_3$	caco3_prec = $K_{CaCO_{3_{prec}}}$ ∗ max{0, (om_$CaCO_3$ − 1)} caco3_diss = $K_{CaCO_{3_{diss}}}$ ∗ $CaCO_3$ ∗ max{0, (1 − om_$CaCO_3$)}$^{4.5}$ om_$CaCO_3$ = $\frac{Ca^{2+} * CO_3}{K_{CaCO_3}}$
Alkalinity changes	In addition to the standard Alkalinity components (i.e. Dickson, 1992), there were parameterized changes due to consumption or producing of a proton (see the text for details) in biogeochemical reactions and the 'nutrient H+ compensation principle for OM production and decay (Wolf-Gladrow et al., 2007): dAlk = Nitrif1 + (Denitr2_PM +Denitr2_DM) + 2*(s4_rd + s23_rd) + mn_ox 3*mn_ox2 + 3*mn_rd mn_rd2 2*mns_prec + 2*mns_diss - 2*mnco3_prec + 2*mnco3_diss + 26.5*(DcDM_Mn +DcPM_Mn) - 2*fe_ox - fe_ox2 + 2*fe_rd fes_prec + fes_diss 2*fes_ox 2*fes2_ox + 53*(DcDM_Fe +DcPM_Fe) 0.5*Disprop + s0_ox

Formatted: Font: 10 pt
Formatted: Font: 10 pt
Formatted: Font: Times New Roman, 10 pt
Formatted: Font: 10 pt
Formatted: Font: 10 pt
Formatted: Font: Times New Roman, 10 pt
Formatted: Font: 10 pt
Formatted: Space Before: 0 pt, After: 0 pt
Formatted: Font: 10 pt
Formatted: Font: 10 pt
Formatted: Font: 10 pt
Formatted: Font: Times New Roman, 10 pt
Formatted: Font: 10 pt
Formatted: Space Before: 0 pt, After: 0 pt
Formatted: Font: 10 pt
Formatted: Font: 10 pt

	~~0.5*s0_no3 – s23_ox – 0.4*sulfido – 2*$CaCO_3$_prec + 2*$CaCO_3$~~
	~~**Silicate**~~
~~Dissolution of particulate Si (Popova, Srokosz, 2009)~~	~~sipart_diss = Si_{part} * $K_{si_{part}diss}$~~

2.3. Carbon and Alkalinity

Name of Process, reference, reaction	Parameterization in the model
$CaCO_3$ formation/dissolution (Luff et al., 2001): $Ca^{2+} + CO_3^{2} \leftrightarrow CaCO_3$	$caco3\_form = K\_caco3\_form * \max(0, \left(\frac{\mathbf{Ca^{2+}} * \mathbf{CO_3}}{K\_caco3} - 1\right))$ $caco3\_diss = K\_caco3\_diss * \mathbf{CaCO_3} * \max(0, \left(1 - \frac{\mathbf{Ca^{2+}} * \mathbf{CO_3}}{K\_caco3}\right))^{4.5}$
CH_4 formation from PON, methanogenesis (Boudreau, 1996) : $(CH_2O)_{106}(NH_3)_{16}H_3PO_4$ $53CO_2 + 53CH_4 + 16NH_3 + H_3PO_4$	$DcPM\_CH4 = K\_PON\_ch4 * F\_sox * F\_snx * F\_ssx * \mathbf{CH_4} * \mathbf{PON}$ $F\_sox = 1 - 0.5 * (1. + \tanh(\mathbf{O_2} - s\_omso\_o2))$ $F\_snx = 1 - 0.5 * (1. + \tanh(\mathbf{NO_3} - s\_omso\_no3))$ $F\_ssx = 1 - 0.5 * (1. + \tanh(\mathbf{SO_4} - s\_omch\_so4))$
CH_4 formation from DON, methanogenesis (Boudreau, 1996)	$DcDM\_CH4 = K\_DON\_ch4 * F\_sox * F\_snx * F\_ssx * \mathbf{CH_4} * \mathbf{DON}$
CH_4 oxidation by O_2 (Boudreau, 1996) : $CH_4 + 2O_2 + \rightarrow CO_2 + 2H_2O$	$ch4\_o2 = K\_ch4\_o2 * \mathbf{CH_4} * \mathbf{O_2}$

Alkalinity changes (Dickson, 1992; Wolf-Gladrow et al., 2007)	$$\begin{aligned} dAlk = & -Nitrif1 + Denitr2\_PM + Denitr2\_DM + 2 * (so4_{rd} + s2o3_{rd}) + mn\_ox1 - 3 \\ & * mn\_ox2 + 3 * mn\_rd1 - mn\_rd2 - 2 * mns\_form + 2 * mns\_diss - 2 \\ & * mnco3\_form + 2 * mnco3\_diss + 26.5 * (DcDM_{Mn} + DcPM_{Mn}) - 2 * fe\_ox1 \\ & - fe\_ox2 + 2 * fe\_rd - fes\_form + fes\_diss - 2 * fes\_ox - 2 * fes2\_ox + 53 \\ & * (DcDM_{Fe} + DcPM_{Fe}) - 0.5 * Disprop + s0\_ox - 0.5 * s0\_no3 - s2o3\_ox \\ & - 0.4 * hs\_no3 - 2 * caco3\_form + 2 * caco3\_diss + GrowthPhy * \left(\frac{LimNO3}{LimN}\right) \\ & - GrowthPhy * \left(\frac{LimNH4}{LimN}\right) \end{aligned}$$

1
2

2.4. Ecosystem processes

Name of Process, reference, reaction	Parameterization in the model
Phytoplankton	

~~Irradiance changing with depth~~ ~~$Iz = Io * e^{(-k_{Erlov}*z)} * e^{(-kc*turbid*0.0001)}$~~

Influence of the irradiance on photosynthesis	$LimLight = (Iz/Iopt) * e^{(1-Iz/Iopt)}$
Influence of temperature on photosynthesis	$LimT = e^{(bm*t-cm)}$
Dependence of photosynthesis on P	~~$LimP = \frac{(PO_4/Phy)^2}{(KPO_4*NkP)^2+(PO_4/Phy)^2}$~~ $LimP = \frac{(\mathbf{PO_4/Phy})^2}{(K\_po4\_lim*r\_n\_p)^2+(\mathbf{PO_4/Phy})^2}$
Dependence of photosynthesis on NO_3	~~$LimNO_3 = \frac{((NO_3+NO_2)/Phy)^2}{KNO_3^2+((NO_3+NO_2)/Phy)^2}$~~ $LimNO_3 = \frac{((\mathbf{NO_3+NO_2})/\mathbf{Phy})^2}{K\_nox\_lim^2+((\mathbf{NO_3+NO_2})/\mathbf{Phy})^2} exp(-K\_psi \frac{(\mathbf{NH_4/Phy})^2}{K\_nh4\_lim^2+(\mathbf{NH_4/Phy})^2})$
Dependence of photosynthesis on NH_4	~~$LimNH_4 = \frac{(NH_4/Phy)^2}{KNH_4^2+(NH_4/Phy)^2}$~~ $LimNH_4 = \frac{(\frac{\mathbf{NH_4}}{\mathbf{Phy}})^2}{K\_nh4\_lim^2+(\frac{\mathbf{NH_4}}{\mathbf{Phy}})^2}(1 - exp(-K\_psi \frac{(\mathbf{NH_4/Phy})^2}{K\_nh4\_lim^2+(\mathbf{NH_4/Phy})^2}))$
Influence of N on photosynthesis	$LimN = LimNO_3 + LimNH_4$
Growth of phytoplankton	$GrowthPhy =$ ~~KNF~~ $K\_phy\_gro * LimLight * LimT * min(LimP, LimN) *$ ~~Phy~~ $\mathbf{Phy}$
Excretion rate ~~phyto.~~of phytoplankton	$ExcrPhy =$ ~~$K_{FD} * Phy$~~ $K\_phy\_exc * \mathbf{Phy}$
~~Phy~~Phytoplankton mortality rate	$MortPhy = ($ ~~KFP~~ $K\_phy\_mrt + 0.45 * (0.5 - 0.5 * tanh($ ~~O_2~~ $\mathbf{O_2} - 60)) + 0.45 * (0.5 - 0.5 * tanh($ ~~O_2~~ $\mathbf{O_2} - 20))) *$ ~~Phy~~ $\mathbf{Phy}$
Heterotrophs	

Grazing of ~~Het~~Heterotrophs	$\text{Grazing} = \text{GrazPhy} + \text{GrazPOP} + \text{GrazBact}$
Grazing of Het$_n$ on ~~Phy~~phytoplankton	~~$\text{GrazPhy} = \text{KFZ} * \text{Het} * \frac{(\text{Phy}/(\text{Het}+0.0001))^2}{\text{K}_{\text{PY}}{}^2 + (\text{Phy}/(\text{Het}+0.0001))^2}\text{GrazPhy}$~~ $= \text{K\_het\_phy\_gro} * \mathbf{Het} * \frac{(\mathbf{Phy}/(\mathbf{Het}+10^{-4}))^2}{\text{K\_het\_phy\_lim}^2 + (\mathbf{Phy}/(\mathbf{Het}+10^{-4}))^2}$
Grazing of Het$_n$ on detritus	~~$\text{GrazPOP} = \text{KPZ} * \text{Het} * \frac{(\frac{\text{PON}}{\text{Het}+0.0001})^2}{(\text{KPP})^2 + (\frac{\text{PON}}{\text{Het}+0.0001})^2}\text{GrazPOP}$~~ $= \text{K\_het\_pom\_gro} * \mathbf{Het} * \frac{(\frac{\mathbf{PON}}{\mathbf{Het}+10^{-4}})^2}{\text{K\_het\_pom\_lim}^2 + (\frac{\mathbf{PON}}{\mathbf{Het}+10^{-4}})^2}$
Grazing of Het$_n$ on bacteria	$\text{GrazBact} = \text{GrazBaae} + \text{GrazBaan} + \text{GrazBhae} + \text{GrazBhan}$
Grazing of Het$_n$ on bacteria autotrophic aerobic	~~$\text{GrazBaae} = \text{KPZ} * \text{Het} * \frac{(\text{Baae}/(\text{Het}+0.0001))^2}{\text{limGrazBac}^2 + (\text{Baae}/(\text{Het}+0.0001))^2}\text{GrazBaae}$~~ $= \text{K\_het\_pom\_gro} * \mathbf{Het} * \frac{(\mathbf{Baae}/(\mathbf{Het}+10^{-4}))^2}{\text{limGrazBac}^2 + (\mathbf{Baae}/(\mathbf{Het}+10^{-4}))^2}$
Grazing of Het$_n$ on bacteria autotrophic anaerobic	~~$\text{GrazBaan} = 0.5 * \text{KPZ} * \text{Het} * \frac{(\text{Baan}/(\text{Het}+0.0001))^2}{\text{limGrazBac}^2 + (\text{Baan}/(\text{Het}+0.0001))^2}\text{GrazBaan}$~~ $= 0.5 * \text{K\_het\_pom\_gro} * \mathbf{Het} * \frac{(\mathbf{Baan}/(\mathbf{Het}+10^{-4}))^2}{\text{limGrazBac}^2 + (\mathbf{Baan}/(\mathbf{Het}+10^{-4}))^2}$

Formatted: Font: 10 pt
Formatted: Space Before: 0 pt, After: 0 pt
Formatted: Font: 10 pt
Formatted: Font: 10 pt
Formatted: Space Before: 0 pt, After: 0 pt
Formatted: Font: 10 pt
Formatted: Font: 10 pt
Formatted: Font: Times New Roman, 10 pt
Formatted: Font: 10 pt
Formatted: Space Before: 0 pt, After: 0 pt
Formatted: Font: 10 pt
Formatted: Font: Times New Roman, 10 pt
Formatted: Font: 10 pt
Formatted: Space Before: 0 pt, After: 0 pt
Formatted: Font: 10 pt
Formatted: Font: 10 pt
Formatted: Space Before: 0 pt, After: 0 pt
Formatted: Font: 10 pt
Formatted: Font: Times New Roman, 10 pt
Formatted: Font: 10 pt
Formatted: Space Before: 0 pt, After: 0 pt
Formatted: Font: 10 pt
Formatted: Font: 10 pt

Grazing of Het$_{ae}$ on bacteria heterotrophic aerobic	~~$GrazBhae = KPZ * Het * \frac{(Bhae/(Het + 0.0001))^2}{limGrazBac^2 + (Bhae/(Het + 0.0001))^2} GrazBhae$~~ $= K\_het\_pom\_gro * \mathbf{Het} * \frac{(\mathbf{Bhae}/(\mathbf{Het} + 10^{-4}))^2}{limGrazBac^2 + (\mathbf{Bhae}/(\mathbf{Het} + 10^{-4}))^2}$
Grazing of Het$_{an}$ on bacteria heterotrophic anaerobic	~~$GrazBhan = 1.3 * KPZ * Het * \frac{(Bhan/Het + 0.0001)^2}{limGrazBac^2 + (Bhan/Het + 0.0001)^2} GrazBhan$~~ $= 1.3 * K\_het\_pom\_gro * \mathbf{Het} * \frac{(\mathbf{Bhan}/\mathbf{Het} + 0.0001)^2}{limGrazBac^2 + (\mathbf{Bhan}/\mathbf{Het} + 10^{-4})^2}$
Respiration rate of Het$_{ae}$	$RespHet = $ ~~$KZN * Het$~~ $K_het_res * \mathbf{Het} * (0.5 + 0.5 * $ ~~$\tanh(O_2 - 20)$~~ $\tanh(\mathbf{O_2} - 20))$
Mortality of Het$_{ae}$	~~$MortHet = Het * (0.25 + 0.3 * (0.5 - 0.5 * \tanh(O_2 - 20)) + 0.45 * (0.5 + 0.4 * \tanh(H_2S - 10)))$~~ MortHet $= \mathbf{Het} * (0.25 + 0.3 * (0.5 - 0.5 * \tanh(\mathbf{O_2} - 20)) + 0.45 * (0.5 + 0.4 * \tanh(\mathbf{H_2S} - 10)))$
Bacteria	
Growth rate of Bacteria aerobic autotrophic	~~$ChemBaae = (Nitrif1 + Nitrif2 + mn_{ox} + fe_{ox} + s23_{ox} + s0_{ox} + anammox) * k\_Baae\_gro * Baae * \min(\frac{(NH_4 / ((Baae + 0.0001)^2}{limBaae^2 + (NH_4 / (Baae + 0.0001))^2}, \frac{(PO_4 / (Baae + 0.0001))^2}{limBaae^2 + (PO_4 / (Baae + 0.0001))^2})$~~ ChemBaae $= (Nitrif1 + Nitrif2 + mn\_ox1 + fe\_ox1 + s2o3\_ox + s0\_ox + anammox) * k_{Baae_{gro}} * \mathbf{Baae} * \min(\frac{(\mathbf{NH_4} / ((\mathbf{Baae} + 10^{-4})^2}{limBaae^2 + (\mathbf{NH_4} / (\mathbf{Baae} + 10^{-4}))^2}, \frac{(\mathbf{PO_4} / (\mathbf{Baae} + 10^{-4}))^2}{limBaae^2 + (\mathbf{PO_4} / (\mathbf{Baae} + 10^{-4}))^2})$

Formatted: Font: 10 pt
Formatted: Space Before: 0 pt, After: 0 pt
Formatted: Font: 10 pt
Formatted: Font: Times New Roman, 10 pt
Formatted: Font: 10 pt
Formatted: Space Before: 0 pt, After: 0 pt
Formatted: Font: 10 pt
Formatted: Font: Times New Roman, 10 pt
Formatted: Font: 10 pt
Formatted: Space Before: 0 pt, After: 0 pt
Formatted: Font: 10 pt
Formatted: Font: 10 pt
Formatted: Font: 10 pt
Formatted: Font: 10 pt
Formatted: Font: 10 pt
Formatted: Space Before: 0 pt, After: 0 pt
Formatted: Font: 10 pt
Formatted: Space Before: 0 pt, After: 0 pt
Formatted: Font: 10 pt
Formatted: Font: 10 pt
Formatted: Space Before: 0 pt, After: 0 pt
Formatted: Font: Times New Roman, 10 pt

Rate of mortality of Bacteria aerobic autotrophic	$\text{MortBaae} = \sout{K_{Baae_{mrt}} + K_{Baae_{mrt_{h2s}}}} * \text{K\_Baae\_mrt} + \text{K\_Baae\_mrt\_h2s} * 0.5 * \sout{(1 - \tanh(1 - H_2S)) * Baae^2}\left(1 - \tanh(1 - \mathbf{H_2S})\right) * \mathbf{Baae}^2$
Growth rate of Bacteria aerobic heterotrophic	$\text{HetBhae} = \sout{(DcPM_{O2} + DcDM_{O2}) *} (\text{DcPM\_O2} + \text{DcDM\_O2}) * \text{K\_}\sout{Bhae_{gro} * Bhae *} \frac{\sout{(DON/(Bhae+0.0001))^2}}{\sout{limBhae^2} + (\mathbf{DON}/(\mathbf{Bhae}+10^{-4}))^2}\text{Bhae\_gro} * \mathbf{Bhae} * \frac{(\mathbf{DON}/(\mathbf{Bhae}+10^{-4}))^2}{\text{limBhae}^2+(\mathbf{DON}/(\mathbf{Bhae}+10^{-4}))^2}$
Rate of mortality of Bacteria aerobic heterotrophic	$\text{MortBhae} = \sout{K_{Bhae_{mrt}} + K_{Bhae_{mrt_{h2s}}} * Bhae}\text{K\_Bhae\_mrt} + \text{K\_Bhae\_mrt\_h2s} * \mathbf{Bhae} * 0.5 * (1 - \tanh(1 - \sout{H_2S}\mathbf{H_2S}))$
Growth rate of Bacteria anaerobic autotrophic	$\sout{\text{ChemBaan} = (mn_{rd} + mn_{rd2} + fe_{rd} + hs_{ox} + \text{sulfido}) * \text{K\_Baan}_{gro} * \text{Baan} * \min\left(\frac{(\text{NH4}/(\text{Baan} + 0.0001))^2}{\text{limBaan}^2 + (\text{NH4}/(\text{Baan} + 0.0001))^2}\right)}\text{ChemBaan} = (\text{mn\_rd1} + \text{mn\_rd2} + \text{fe\_rd} + \text{hs\_ox} + \text{hs\_no3}) * \text{K\_Baan\_gro} * \mathbf{Baan} * \min\left(\frac{(\mathbf{NH4}/(\mathbf{Baan} + 10^{-4}))^2}{\text{limBaan}^2 + (\mathbf{NH4}/(\mathbf{Baan} + 10^{-4}))^2}\right)$
Rate of mortality of Bacteria anaerobic autotrophic	$\text{MortBaan} = \sout{k\_Baan_{mrt} * Baan}\text{K\_Baan\_mrt} * \mathbf{Baan}$
Growth rate of Bacteria anaerobic heterotrophic	$\sout{\text{HetBhan} = (DcPM_{NOX} + DcDM_{NOX} + DcPM_{SO_4} + DcDM_{SO_4} + DcPM_{Mn} + DcDm_{Mn} + DcPM_{Fe} + DcDM_{Fe}) * K\_Bhan_{gro} * Bhan * \frac{(DON/(Bhan + 0.0001))^2}{limBhan^2 + (DON/(Bhan + 0.0001))^2}}\text{HetBhan} = (\text{DcPM\_NOX} + \text{DcDM\_NOX} + \text{DcDM\_Mn} + \text{DcPM\_Mn} + \text{DcDM\_Fe} + \text{DcPM\_Fe} + \text{DcDM\_SO4} + \text{DcPMSO4} + \text{DcDM\_CH4} + \text{DcPM\_CH4}) * \text{K\_Bhan\_gro} * \mathbf{Bhan} * \frac{(\mathbf{DON}/(\mathbf{Bhan} + 10^{-4}))^2}{\text{limBhan}^2 + (\mathbf{DON}/(\mathbf{Bhan} + 10^{-4}))^2}$

Formatted: Font: 10 pt
Formatted: Font: 10 pt
Formatted: Space Before: 0 pt, After: 0 pt
Formatted: Font: Times New Roman, 10 pt
Formatted: Font: 10 pt
Formatted: Font: 10 pt
Formatted: Space Before: 0 pt, After: 0 pt
Formatted: Font: 10 pt
Formatted: Font: Times New Roman, 10 pt
Formatted: Font: 10 pt
Formatted: Space Before: 0 pt, After: 0 pt
Formatted: Font: 10 pt
Formatted: Font: 10 pt
Formatted: Font: 10 pt
Formatted: Space Before: 0 pt, After: 0 pt
Formatted: Font: 10 pt
Formatted: Font: 10 pt
Formatted: Space Before: 0 pt, After: 0 pt
Formatted: Font: 10 pt
Formatted: Font: 10 pt
Formatted: Space Before: 0 pt, After: 0 pt
Formatted: Font: 10 pt

Rate of mortality of Bacteria anaerobic heterotrophic	MortBhan $= \sim\!\!\sout{k_{Bhan_{mrt}} + K_{Bhan_{mrt}O_2} * Bhan}$K_Bhan_mrt + K_Bhan_mrt_o2 $*$ **Bhan** $*$ $(0.5 + 0.5 * \tanh(1 - \sim\!\!\sout{O_2}\mathbf{O_2}))$
Summarized OM mineralization	$\sout{Dc_{OM_{total}} = DcDM_{O_2} + DcPM_{O_2} + DcPM_{NOX} + DcDM_{NOX} + DcDM_{Mn} + DcPM_{Mn} + DcDM_{Fe} + DcPM_{Fe} + DcDM_{SO_4} + DcDM_{SO_4}}$Dc_OM_total = DcDM_O2 + DcPM_O2 + DcPM_NOX + DcDM_NOX + DcDM_Mn + DcPM_Mn + DcDM_Fe + DcPM_Fe + DcDM_SO4 + DcPM_SO4 + 0.5 $*$ (DcDM_CH4 + DcPM_CH4)

Formatted: Font: 10 pt

Formatted: Font: 10 pt

Formatted: Space Before: 0 pt, After: 0 pt

Formatted: Font: 10 pt

Formatted: Font: 10 pt

Formatted: Space Before: 0 pt, After: 0 pt

Formatted: Font: 10 pt

Table 3. Parameters names, notations, values and units of the coefficients used in the model

Table 3.1. Nutrients and oxygen

Parameter	Notation	Units	
Manganese			
Specific rate of Mn(II) to Mn(III) oxidation with O_2	$K_{\_mn\_ox}$	d^{-1}	
Specific rate of Mn(IV) to Mn(III) reduction with H_2S	$K_{\_mn\_rd}$	d^{-1}	0.5
Specific rate of Mn(III) to Mn(IV) oxidation with O_2	$K_{\_mn\_ox2}$	d^{-1}	0.2
Specific rate of Mn(III) to Mn(II) reduction with H_2S	$K_{\_mn\_rd2}$	d^{-1}	1.0
Specific rate of formation of MnS from Mn(II) and H_2S	$K_{\_mns\_form}$	d^{-1}	$1*10^{-5}$
Specific rate of dissolution of MnS to Mn(II) and H_2S	K_{mns_diss}	d^{-1}	$5*10^{-4}$
Conditional equilibrium constant for MnS	$K_{\_mns}$	M	1500
Conditional equilibrium constant for $MnCO_3$	$K_{\_mnco3}$	M	15.
Specific rate of $MnCO_3$ dissolution	$K_{\_mnco3\_diss}$	d^{-1}	$7*10^{-4}$
Specific rate of $MnCO_3$ formation	$K_{\_mnco3\_form}$	d^{-1}	$3*10^{-4}$
Specific rate of DON Oxidation with Mn(IV)	$K_{\_DON\_Mn}$	d^{-1}	$1*10^{-3}$
Specific rate of PON Oxidation with Mn(IV)	$K_{\_PON\_Mn}$	d^{-1}	$1*10^{-3}$
Threshold value of Mn(II) oxidation	$s_{\_mnox\_mn2}$	µM Mn	0.01
Threshold value of Mn(III) oxidation	$s_{\_mnox\_mn3}$	µM Mn	0.01
Threshold value of Mn(IV) reduction	$s_{\_mnrd\_mn4}$	µM Mn	0.01
Threshold value of Mn(III) reduction	$s_{\_mnrd\_mn3}$	µM Mn	0.01
Iron			
Specific rate of Fe(II) to Fe(III) oxidation with O_2	$K_{\_fe\_ox}$	d^{-1}	0.5
Specific rate of Fe(II) to Fe(III) oxidation with MnO_2	$K_{\_fe\_ox2}$	d^{-1}	$1*10^{-3}$
Specific rate of Fe(III) to Fe(II) reduction with H_2S	$K_{\_fe\_rd}$	d^{-1}	0.5
Conditional equilibrium constant for FeS	$K_{\_FeS}$	µM	2510
Specific rate of FeS formation from Fe(II) and H_2S	$K_{\_Fes\_form}$	d^{-1}	$5*10^{-4}$
Specific rate of DON oxidation with Fe(III)	$K_{\_DON\_Fe}$	d^{-1}	$5*10^{-5}$
Specific rate of PON oxidation with Fe(III)	$K_{\_PON\_Fe}$	d^{-1}	$1*10^{-5}$
Specific rate of FeS_2 formation by reaction of FeS with H_2S	$K_{\_FeS2\_form}$	d^{-1}	$1*10^{-6}$
Specific rate of FeS_2 oxidation with O_2	$K_{\_FeS2\_ox}$	d^{-1}	$4.4*10^{-4}$
Threshold value of Fe(II) reduction	$s_{\_feox\_fe2}$	µM Fe	$1*10^{-3}$
Threshold value of Fe(III) reduction	$s_{\_ferd\_fe3}$	µM Fe	0.01

Formatted: Font: 9 pt
Formatted: Font: 9 pt
Formatted: Font: 9 pt
Formatted: Line spacing: Multiple 1,15 li
Formatted: Justified, Line spacing: Multiple 1,15 li
Inserted Cells

~~**Sulfur**~~		
~~Specific rate of H_2S oxidation to S^0 of with O_2~~	~~$K_{\_hs\_ox}$~~	~~d^{-1}~~
~~Specific rate of S^0 oxidation of with O_2~~	~~$K_{\_s0\_ox}$~~	~~d^{-1}~~
~~Specific rate of S^0 oxidation of with NO_3~~	~~$K_{\_S0\_NO3}$~~	~~d^{-1}~~
~~Specific rate of S_2O_3 oxidation with O_2~~	~~$K_{\_s23\_ox}$~~	~~d^{-1}~~
~~Specific rate of S_2O_3 oxidation with NO_3~~	~~$K_{\_s23\_NO3}$~~	~~d^{-1}~~
~~Specific rate of Sulfate reduction with sulfate~~	~~$K_{\_s4\_rd}$~~	~~d^{-1}~~
~~Specific rate of sulfate reduction with thiosulfate~~	~~$K_{\_s23\_rd}$~~	~~d^{-1}~~
~~Specific rate of S^0 disproportionation~~	~~K_{dispro}~~	~~d^{-1}~~
Nitrogen		
Specific rate of DON oxidation of with O_2	K_DON_ox	d^{-1}
Specific rate of PON oxidation of with O_2	K_PON_ox	d^{-1}
Temperature control threshold coefficient for OM decay	Tda	^oC
Temperature control coefficient for OM decay	beta_da	-
Half-saturation constant of O_2 for OM mineralization	K_omox_o2	µM
Specific rate of ~~decomposition of~~autolysis, PON to DON	K_PON_DON	d^{-1}
~~Strength of ammonium inhibition of nitrate uptake constant~~	~~K_{psi}~~	-
Half saturation constant for uptake of NO_3+NO_2	~~K_{NO3}~~K_nox_lim	µM
Half saturation constant for uptake of NH_4	~~K_{NH4}~~K_nh4_lim	µM
Strength of NH4 inhibition of NO3 uptake constant	K_psi	-
Specific rate of the 1st stage of nitrification	~~K_{N42}~~K_nitrif1	d^{-1}
Specific rate of the 2d stage of nitrification	~~K_{N23}~~K_nitrif2	d^{-1}
Specific rate of 1st stage of denitrification	~~K_{N32}~~K_denitr1	d^{-1}
Specific rate of 2d stage of denitrification	~~K_{N24}~~K_denitr2	d^{-1}
Half-saturation of ~~NO_2~~NO_3 for OM denitrification	k_omno_no3	µM N
Half-saturation of NO_2 for OM denitrification	k_omno_no2	µM N
Specific rate of thiodenitrification	~~K_T~~K_hs_no3	μM^{-1} d^{-1}
Specific rate of anammox	~~$K_{annamox}$~~K_annamox	d^{-1}
Oxygen		
Half-saturation constant for nitrification	O2s_nf	µM
Half-saturation constant for denitrification anammox, Mn reduction	O2s_dn	µM
Threshold value of O_2 for OM mineralization	s_omox_o2	µM
Threshold value of O_2 for OM denitrification	s_omno_o2	µM
Threshold value of O_2 for OM sulfate reduction	s_omso_o2	µM

Formatted: Centered, Line spacing: Multiple 1,15 li
Inserted Cells
Formatted Table
Formatted: Line spacing: Multiple 1,15 li
Inserted Cells
Formatted: Line spacing: Multiple 1,15 li
Inserted Cells
Formatted: Line spacing: Multiple 1,15 li
Formatted: Line spacing: Multiple 1,15 li
Formatted: Line spacing: Multiple 1,15 li
Formatted: Line spacing: Multiple 1,15 li
Formatted Table
Formatted: Line spacing: Multiple 1,15 li
Inserted Cells
Formatted: Line spacing: Multiple 1,15 li
Formatted: Line spacing: Multiple 1,15 li
Formatted: Line spacing: Multiple 1,15 li
Formatted Table
Inserted Cells
Formatted: Line spacing: Multiple 1,15 li
Formatted: Line spacing: Multiple 1,15 li
Inserted Cells
Formatted: Line spacing: Multiple 1,15 li
Formatted: Line spacing: Multiple 1,15 li
Formatted: Line spacing: Multiple 1,15 li
Formatted: Line spacing: Multiple 1,15 li
Formatted: Line spacing: Multiple 1,15 li

Threshold value of NO for OM sulfate reduction	s_omso_no3	µM	5	5 (Yakushev, 2013)
Stoichiometric coefficients				
N/P	r_n_p	-	16	(Richards, 1965)
O/N	r_o_n	-	6.625	(Richards, 1965)
C/N	r_c_n	-	8	(Richards, 1965)
Si/N	r_si_n	-	1	(Richards, 1965)
Fe/N	r_fe_n	-	26.5	(Boudreau, 1996)
Mn/N	r_mn_n	-	13.25	(Boudreau, 1996)
Phosphorus				
Half-saturation constant for uptake of PO_4 by phytoplankton	~~K_{PO4}~~K_po4_lim	µM		
Fe/P ratio in ~~during co-precipitation~~complexes with Fe oxides	r_fe_p	-		
Mn/P ratio in complexes with Mn(III)	r_mn_p	-		
~~**Oxygen**~~				
~~Half-saturation constant for nitrification~~	~~O_{2s_nf}~~	~~µM~~		
~~Half-saturation constant for denitrification~~	~~O_{2s_dn}~~	~~µM~~		
~~Threshold value of O_2 for OM mineralization~~	~~s_omox_o2~~	~~µM~~		
~~Threshold value of O_2 for OM denitrification~~	~~s_omno_o2~~	~~µM~~		
~~Threshold value of O_2 for OM sulfate reduction~~	~~s_omso_o2~~	~~µM~~	~~25~~	
~~Threshold value of NO for OM sulfate reduction~~	~~s_omso_no~~	~~µM~~	~~5~~	
~~Half saturation constant of Mn oxidation~~	~~k_mnoxO2~~	~~µM O~~	~~2~~	
~~**Calcium**~~				
~~Specific rate of $CaCO_3$ dissolution~~	~~K_CaCO3_diss~~	~~d^{-1}~~	~~3~~	
~~Specific rate of $CaCO_3$ precipitation~~	~~K_CaCO3_prec~~	~~d^{-1}~~	~~$1*10^{-4}$~~	
Silicon				
Specific rate of Si dissolution	K_~~Si~~sipart_diss	d^{-1}		
~~**Bacteria**~~				
~~Baae maximum specific growth rate~~	~~k_Baae_gro~~	~~d^{-1}~~		
~~Baae specific rate of mortality~~	~~k_Baae_mrt~~	~~d^{-1}~~		
~~Baae increased specific rate of mortality due to H_2S~~	~~k_Baae_mrt_h2s~~	~~d^{-1}~~		
~~Bhae maximum specific growth rate~~	~~k_Bhae_gro~~	~~d^{-1}~~		
~~Bhae specific rate of mortality~~	~~k_Bhae_mrt~~	~~d^{-1}~~		
~~Bhae increased specific rate of mortality due to H_2S~~	~~k_Bhae_mrt_h2s~~	~~d^{-1}~~		
~~Baan maximum specific growth rate~~	~~k_Baan_gro~~	~~d^{-1}~~		

Formatted: Font: 10 pt
Formatted: Centered, Line spacing: Multiple 1,15 li
Formatted: Font: Bold
Formatted Table
Formatted: Line spacing: Multiple 1,15 li
Inserted Cells
Formatted: Line spacing: Multiple 1,15 li
Formatted: Line spacing: Multiple 1,15 li
Formatted: Centered, Line spacing: Multiple 1,15 li
Formatted Table
Formatted: Highlight
Inserted Cells
Formatted: Right: -0,04 cm, Line spacing: Multiple 1,15 li, Adjust space between Latin and Asian text, Adjust space between Asian text and numbers
Formatted: Highlight
Formatted: Not Superscript/ Subscript
Formatted: Not Superscript/ Subscript
Formatted: Highlight
Formatted: Justified, Line spacing: Multiple 1,15 li, Tab stops: Not at 1,3 cm
Formatted: Line spacing: Multiple 1,15 li
Formatted: Highlight

~~Baan specific rate of mortality~~	~~k_{Baan_mrt}~~	~~d^{-1}~~	~~$5*10^{-3}$~~
~~Bhan maximum specific growth rate~~	~~k_{Bhan_gro}~~	~~d^{-1}~~	~~0.1~~
~~Bhan specific rate of mortality~~	~~k_{Bhan_mrt}~~	~~d^{-1}~~	~~$5*10^{-3}$~~
~~Bhan increased specific rate of mortality due to O_2~~	~~$k_{Bhan\_mrt\_o2}$~~	~~d^{-1}~~	~~0.899~~
~~**Phytoplankton**~~			
~~Maximum specific growth rate~~	~~K_{NF}~~	~~d^{-1}~~	~~2.6~~
~~Extinction coefficient~~	~~K_Erlov~~	~~m^{-1}~~	~~0.05~~
~~Surface irradiance~~	~~I_0~~	~~$W\ m^{-2}$~~	~~80~~
~~Optimal irradiance~~	~~I_{opt}~~	~~$W\ m^{-2}$~~	~~25~~
~~1st coefficient for growth dependence on t~~	~~bm~~	~~$°C^{-1}$~~	~~0.12~~
~~2d coefficient for growth dependence on t~~	~~cm~~	~~-~~	~~1.4~~
~~Attenuation constant for the self-shading effect~~	~~Kc~~	~~$m^2\ mmol\ N^{-1}$~~	~~0.03~~
~~Specific respiration rate~~	~~K_{FN}~~	~~d^{-1}~~	~~0.05~~
~~Specific rate of mortality~~	~~K_{FP}~~	~~d^{-1}~~	~~0.10~~
~~Specific rate of excretion~~	~~K_{FD}~~	~~d^{-1}~~	~~0.05~~
~~**Heterotrophs**~~			
~~Maximum specific rate of grazing of Het on Phy~~	~~K_{PZ}~~	~~d^{-1}~~	~~1.0~~
Half-saturation constant for ~~the grazing~~uptake of ~~Het on Phy for Phy/Het ratio~~Si by phytoplankton	~~K_{FV}~~K_si_lim	~~-~~	
~~Maximum specific rate of grazing of Het on POP~~	~~K_{PZ}~~	~~d^{-1}~~	
~~Specific respiration rate~~	~~K_{ZN}~~	~~d^{-1}~~	
~~Half-saturation constant for the grazing of Het on POP in dependence to ratio POP/Het~~Fe/P ratio in complexes with Fe oxides	~~K_{pp}~~r_fe_si	~~-~~	
~~Maximum specific rate of mortality of Het~~	~~K_{ZP}~~	~~d^{-1}~~	
~~Food absorbency for Heterotrophs~~	~~U_z~~	~~-~~	~~0.5~~
~~Ratio between dissolved and particulate excretes of Heterotrophs~~	~~H_z~~	~~-~~	~~0.5~~
~~Limiting parameter for bacteria grazing by Het~~	~~limGrazBac~~	~~-~~	~~2~~
~~Limiting parameter for bacteria anaerobic heterotrophic~~	~~limBhan~~	~~-~~	~~2~~
~~Limiting parameter for bacteria aerobic heterotrophic~~	~~limBhae~~	~~-~~	~~5~~
~~Limiting parameter for bacteria anaerobic autotrophic~~	~~limBaan~~	~~-~~	~~2~~
~~Limiting parameter for bacteria aerobic autotrophic~~	~~limBaae~~	~~-~~	~~1~~

Formatted: Highlight
Inserted Cells
Formatted: Highlight
Formatted: Line spacing: Multiple 1,15 li
Formatted: Highlight
Formatted: Line spacing: Multiple 1,15 li
Inserted Cells

Sinking			
Rate of sinking of Phy	W_{Phy}	$m\ d^{-1}$	0.1
Rate of sinking of Het	W_{Het}	$m\ d^{-1}$	1.0
Rate of sinking of bacteria (Bhe,Bae,Bha,Baa)	W_{Bact}	$m\ d^{-1}$	0.4
Rate of sinking of detritus (POP, PON)	W_{sed}	$m\ d^{-1}$	5
Rate of accelerated sinking of particles with settled Mn hydroxides	W_{M}	$m\ d^{-1}$	7

Table

Formatted: Font: 10 pt, English (U.S.)

Formatted: Justified, Space After: 0 pt

~~**Table 4. Rates of biogeochemical production/consumption of the model compartments**~~

3.2. Redox metals and sulfur

Parameter	Notation	Units	Value	Reference ranges
Manganese				
~~**Oxygen (O_2)**~~Specific rate of Mn(II) oxidation to Mn(III) with O_2	K_mn_ox1	d^{-1}	0.1	~~R_{O2} = (GrowthPhy*DcDM_O2*DcPM_O2/(RespHet+OkN)*0.5*mn_ox+0.25*mn_ox2+0.25*fe_ox*2.*mns_ox*2.*fes_ox*0.5*hs_ox+0.5*s0_ox*s23_ox*1.5*Nitrif1*0.5*Nitrif2*(DcDM_O2+DcPM_O2)/(GrowthPhy+RespHet+OkN)~~0.18-1.9 M/yr; (Tebo, 1991) 2 d^{-1}; (Yakushev et al., 2007)
~~**Phosphate (PO_4)**~~Specific rate of Mn(IV) reduction to Mn(III) with H_2S	~~R_{PO4}=(DcDM_O2+DcPM_O2+DcPM_NOX+DcDM_NOX+DcDM_SO4+DcPM_SO4+DcDM_Mn+DcPM_Mn+DcDM_Fe+DcPM_Fe*Chemos/(ChemosA+GrowthPhy+RespHet)/NkP*(fe_ox+fe_ox2~~	d^{-1}	0.5	22 d^{-1}; (Yakushev et al., 2007)

Inserted Cells

Formatted: Font: Bold

Inserted Cells

Inserted Cells

Formatted: Justified, Don't adjust space between Latin and Asian text, Don't adjust space between Asian text and numbers

Formatted: Justified, Right: -0,04 cm

Formatted: Right: -0,04 cm, Tab stops: 1,3 cm, Left

Inserted Cells

Formatted: Justified, Don't adjust space between Latin and Asian text, Don't adjust space between Asian text and numbers

		~~)/2.7 (mn_ox +mn_rd)/0.67 +fe_rd /2.7+(mn_ox2 + mn_rd2) /0.67~~K_mn_rd1			
~~Particulate Organic Nitrogen (PON)~~		~~R_{PON}= autolis DcPM_O2 DcPM_NOX DcPM_SO4 DcPM_Mn DcPM_Fe +MortBaut +MortBautA +MortBhet +MortBhetA +MortPhy +MortHet +Grazing *(1. Uz)*(1. Hz) GrazPOP~~			
~~Dissolved Organic Phosphorus (DON)~~		~~R_{DON}= autolis DcDM_O2 DcDM_NOX DcDM_ DcDM_Mn DcDM_Fe Hetero HeteroA+ExcrPhy +Grazing *(1. Uz)*Hz~~			
~~Ammonia (NH_4)~~	~~R_{NH4}= DcDM_O2 +DcPM_O2 +DcPM_NOX +DcDM_NOX + DcDM_Mn +DcPM_Mn +DcDM_Fe +DcPM_Fe +DcDM_SO4 +DcPM_SO4 Nitrif1 anammox +RespHet GrowthPhy *(LimNH4 /LimN) Chemos ChemosA~~ Specific rate of Mn(III) oxidation to Mn(IV) with O_2	K_mn_ox2	d^{-1}	0.2	18 d^{-1}; (Yakushev et al., 2008)
~~Nitrite (NO_2)~~		~~R_{NO2}= Nitrif1 Nitrif2 +Denitr1 Denitr2 anammox GrowthPhy *(LimNO3 /LimN) (NO2 /(NO2 + NO3))~~			
~~Nitrate (NO_3)~~		~~R_{NO3}= Nitrif2 Denitr1 sulphido *1.25 GrowthPhy *(LimNO3 /LimN) (NO3 /(NO2 + NO3))~~			
~~Hydrogen sulphide (H_2S)~~Specific rate of Mn(III) reduction to Mn(II) with H_2S		~~R_{H2S}= 0.5 mn_rd 0.5 mn_rd2 0.5 fe_rd~~	d^{-1}	1	0.96-3.6 M/yr; (Tebo, 1991); 2 d^{-1}; (Yakushev et al., 2007)

Deleted Cells
Formatted Table
Inserted Cells
Inserted Cells
Formatted: Justified, Don't adjust space between Latin and Asian text, Don't adjust space between Asian text and numbers
Inserted Cells
Inserted Cells
Formatted: Justified, Don't adjust space between Latin and Asian text, Don't adjust space between Asian text and numbers
Formatted: Right: -0,04 cm, Tab stops: 1,3 cm, Left
Inserted Cells
Inserted Cells
Inserted Cells

	~~*hs_ox - fes_form - mns_form +0.5 Disprop - sulphido +s23_rd*~~ K_mn_rd2			
~~**Elemental sulphur (S^0)**~~Specific rate of formation of MnS from Mn(II) and H_2S	K_mns_form	d^{-1}	~~*RS0 = hs_ox +0.5 mn_rd +0.5 mn_rd2+0.5 fe_rd - s0_ox - Disprop - S_{0_NO3}*~~ $1*10^{-5}$	
~~**Thiosulphate (S_2O_3)**~~Specific rate of dissolution of MnS to Mn(II) and H_2S	K_mns_diss	d^{-1}	~~*R_{S2O3} = 0.5 s0_ox 0.5 s23_ox +0.25*~~	

Formatted: Font: Not Bold

Inserted Cells

Formatted: Don't adjust space between Latin and Asian text, Don't adjust space between Asian text and numbers

Formatted: Justified, Right: -0,04 cm

Formatted: Font: Not Italic

Formatted: Don't adjust space between Latin and Asian text, Don't adjust space between Asian text and numbers

Formatted: Justified, Right: -0,04 cm

			~~*Dispr op +0.5 s4_rd -0.5 s23_rd -S 23_NO3*~~ 5*10^{-4}	
Solubility product for MnS	K_mns	M	1500	
Solubility product for $MnCO_3$	K_mnco3	M	1	
Specific rate of $MnCO_3$ formation	K_mnco3_form	d^{-1}	3*10^{-4}	10^{-4} – 10^{-2} mol/g yr; (Wersin, 1990); (Wollast, 1990)
Specific rate of $MnCO_3$ dissolution	K_mnco3_diss	d^{-1}	7*10^{-4}	10^{-2} – 10^{3} yr^{-1}; (Wersin, 1990; Wollast, 1990)
~~**Sulphate (SO_4)**~~Specific rate of MnCO3 oxidation	~~*R_{SO4} = sulphido_s4_rd +s23_ox +fes_ox +mns_ox*~~ K_mnco3_ox	d^{-1}	27*10^{-4}	
Specific rate of DON Oxidation with Mn(IV)	K_DON_Mn	d^{-1}	1*10^{-3}	1*10^{-3} (Yakushev et al., 2007)
Specific rate of PON Oxidation with Mn(IV)	K_PON_Mn	d^{-1}	1*10^{-3}	1*10^{-3} (Yakushev et al., 2007)
~~**Bivalent manganese (**~~Threshold value of Mn(II)~~**)**~~ oxidation	s_mnox_mn2	µM Mn	~~*R_{Mn2} = mn_ox*~~	1*10^{-2} (Yakushev et al., 2007)

Formatted: Font: Not Italic

Inserted Cells

Formatted: Don't adjust space between Latin and Asian text, Don't adjust space between Asian text and numbers

Inserted Cells

Inserted Cells

Formatted: Right: -0,04 cm, Tab stops: 1,3 cm, Left

Formatted: Font: Not Bold

Inserted Cells

Inserted Cells

Inserted Cells

Formatted: Don't adjust space between Latin and Asian text, Don't adjust space between Asian text and numbers

Formatted: Justified, Right: -0,04 cm

			~~+mn_rd2_mns_form +mns_ox +fe_ox2 +2.DcDM_Mn +2.DcPM_Mn~~ 1*10^{-2}	
Threshold value of Mn(III) oxidation	s_mnox_mn3	µM Mn	1*10^{-2}	1*10^{-2} (Yakushev et al., 2007)
~~**Quadrivalent manganese (**~~Threshold value of Mn(IV)~~**)**~~) reduction	s_mnrd_mn4	µM Mn	~~R_{Mn4} = mn_ox2 mn_rd fe_ox2 2.DcDM_Mn 2.DcPM_Mn~~	1*10^{-2}(Yakushev et al., 2007)

Inserted Cells

Formatted: Font: Not Bold

Formatted: Don't adjust space between Latin and Asian text, Don't adjust space between Asian text and numbers

Inserted Cells

Formatted: Justified, Right: -0,04 cm

Inserted Cells

			$1*10^{-2}$	
**~~Trivalent manganese (~~Threshold value of Mn(III~~))~~ reduction	~~R_{Mn3} = mn_ox - mn_ox2 + mn_rd - mn_rd2~~ s_mnrd_mn3	µM Mn	$1*10^{-2}$	$1*10^{-2}$ (Yakushev et al., 2007)
~~Manganese sulphide (MnS)~~Half saturation constant of Mn oxidation	~~R_{MnS} = mns_form - mns_ox~~K_mnox_o2	µM O_2	2	2 (Yakushev et al., 2007)
Iron				
~~Bivalent iron (Fe(II))~~Specific rate of Fe(II) to Fe(III) oxidation with O_2	~~R_{Fe2} = fe_ox - fe_ox2 +fe_rd - fes_form +fes_ox +4. DcDM_Fe +4. DcPM_Fe~~ K_fe_ox1	d^{-1}	0.5	$2*10^9$ M/yr; (Boudreau, 1996); 4 d^{-1}; (Yakushev et al., 2007)
~~Trivalent iron (Fe(III))~~Specific rate of Fe(II) to Fe(III) oxidation with MnO_2	~~R_{Fe3} = fe_ox +fe_ox2 - fe_rd -4. DcDM_Fe - 4. DcPM_Fe~~ K_fe_ox2	d^{-1}	$1*10^{-3}$	10^4–10^8 M/yr; (Boudreau, 1996); 1 d^{-1}; (Yakushev et al., 2007)
Specific rate of Fe(III) to Fe(II) reduction with H_2S	K_fe_rd	d^{-1}	0.5	$1*10^4$ M/yr;(Boudreau, 1996); 0.05d^{-1}; (Yakushev et al., 2007)

Formatted: Don't adjust space between Latin and Asian text, Don't adjust space between Asian text and numbers

Formatted: Font: Not Bold

Formatted: Right: -0,04 cm, Tab stops: 1,3 cm, Left

Inserted Cells

Formatted: Don't adjust space between Latin and Asian text, Don't adjust space between Asian text and numbers

Formatted: Font: Not Bold

Formatted: Right: -0,04 cm, Tab stops: 1,3 cm, Left

Formatted: Font: Not Italic

Formatted: Right: -0,04 cm

Formatted: Font: Bold

Formatted: Right: -0,04 cm, Tab stops: 1,3 cm, Left

Inserted Cells

Inserted Cells

Inserted Cells

Formatted: Right: -0,04 cm

Formatted: Right: -0,04 cm, Tab stops: 1,3 cm, Left

Solubility product for FeS		K_fes	µM	2510	
~~**Iron sulphide (FeS)**~~Specific rate of FeS formation from Fe(II) and H_2S		~~R_{FeS} =~~ K_fes_form ~~*fes_ox*~~	d^{-1}	$5*10^{-4}$	$5*10^{-6}$–10^{-3} M/yr; (Boudreau, 1996; Hunter et al., 1998); (Bektursunova and L'Heureux, 2011)
~~**Dissolved Inorganic Carbon (DIC)**~~	~~R_{DIC} = *(DcDM_O2+DcPM_O2+DcPM_NOX+DcDM_NOX +DcDM_SO4+DcPM_SO4+ DcDM_Mn +DcPM_Mn +DcDM_Fe +DcPM_Fe Chemos ChemosA GrowthPhy+RespHet) CkN*~~Specific rate of FeS dissolution to Fe(II) and H_2S	K_fes_diss	d^{-1}	$1*10^{-6}$	$1*10^{-3}$ yr^{-1} (Hunter et al., 1998); (Bektursunova and L'Heureux, 2011)
~~**Total alkalinity (Alk)**~~Specific rate of FeS oxidation with O_2		~~R_{Alk} = *dAlk*~~K_fes_ox	d^{-1}	$1*10^{-3}$	$2*10^{7}$–$3*10^{5}$ M/yr; (Boudreau, 1996); (Van Cappellen and Wang, 1996)
~~**Phytoplankton (Phy)**~~Specific rate of DON oxidation with Fe(III)		$R_{Phy} = Grov$ K_DON_fe	d^{-1}	$5*10^{-5}$	$5*10^{-5}$ (Yakushev et al., 2007)
~~**Heterotrophs (Het)**~~Specific rate of PON oxidation with Fe(III)		~~R_{Het} = *Grazing*U_z MortHet K_{ZN}*Het*~~K_PON_fe	d^{-1}	$1*10^{-5}$	$1*10^{-5}$ (Yakushev et al., 2007)
~~**Aerobic heterotrophic bacteria (Bhe)**~~Specific rate of FeS_2 formation by reaction of FeS with H_2S		$R_{Bhe} = C_{Bhe}$ K_fes2_form	d^{-1}	$1*10^{-6}$	$8.9*10^{-6}$M/day; (Rickard and Luther, 1997)
~~**Aerobic autotrophic bacteria (Bae)**~~Specific rate of FeS_2 oxidation with O_2		$R_{Bae} = C_{Bae}$ K_fes2_ox	d^{-1}	$4.4*10^{-4}$	
~~**Anaerobic heterotrophic bacteria (Bha)**~~Threshold value of Fe(II) reduction		$R_{Bha} = C_{Bha}$ s_feox_fe2	µM Fe	$1*10^{-3}$	$1*10^{-3}$(Yakushev et al., 2007)
~~**Anaerobic autotrophic bacteria (Baa)**~~Threshold value of Fe(III) reduction			µM	$1*10^{-2}$	$1*10^{-2}$(Yakushev et al., 2007)

Formatted ...
Inserted Cells ...
Formatted ...
Formatted ...
Inserted Cells ...
Inserted Cells ...
Formatted ...
Formatted ...
Deleted Cells ...
Formatted Table ...
Formatted ...
Inserted Cells ...
Formatted ...
Formatted ...
Formatted ...
Formatted ...
Formatted ...
Formatted ...
Formatted ...
Formatted ...
Formatted ...
Formatted ...
Formatted ...
Formatted ...
Formatted ...
Formatted ...
Formatted ...
Formatted ...
Formatted ...
Formatted ...
Formatted ...
Formatted ...

	$R_{Baa} = C_{Baa}$ Fes_ferd_fe3			
Solubility product for $FeCO_3$	K_feco3	d^{-1}	15	
Specific rate of $FeCO_3$ dissolution	K_feco3_diss	d^{-1}	$7*10^{-4}$	$2.5*10^{-1}$–10^{-2} yr^{-1}; (Wersin, 1990; Wollast, 1990)
Specific rate of $FeCO_3$ formation	K_feco3_form	d^{-1}	$3.4*10^{-4}$	10^{-6}–10^{-2} mol/g yr; (Boudreau, 1996; Wersin, 1990; Wollast, 1990)
Specific rate of $FeCO_3$ oxidation with O_2	K_feco3_ox	d^{-1}	$2.7*10^{-3}$	
Sulfur				
Specific rate of H_2S oxidation to S^0 of with O_2	K_hs_ox	d^{-1}	0.5	0.5 (Yakushev et al., 2007)
Specific rate of S^0 oxidation of with O_2	K_s0_ox	d^{-1}	$2*10^{-2}$	$2*10^{-2}$(Yakushev et al., 2007)
Specific rate of S^0 oxidation of with NO_3	K_s0_no3	d^{-1}	0.9	0.9 (Yakushev et al., 2007)
Specific rate of S_2O_3 oxidation with O_2	K_s2o3_ox	d^{-1}	$1*10^{-2}$	$1*10^{-2}$(Yakushev et al., 2007)
Specific rate of S_2O_3 oxidation with NO_3	K_s2o3_no3	d^{-1}	$1*10^{-2}$	$1*10^{-2}$(Yakushev et al., 2007)
Specific rate of OM reduction with sulfate	K_so4_rd	d^{-1}	$5*10^{-6}$	$5*10^{-6}$(Yakushev et al., 2007)
Specific rate of OM reduction with thiosulfate	K_s2o3_rd	d^{-1}	$1*10^{-3}$	$1*10^{-3}$(Yakushev et al., 2007)
Specific rate of S^0 disproportionation	K_s0_disp	d^{-1}	$1*10^{-3}$	$1*10^{-3}$(Yakushev et al., 2007)
Half-saturation of Mn reduction	K_mnrd_hs	µM S	1	1 (Yakushev et al., 2007)
Half-saturation of Fe reduction	K_ferd_hs	µM S	1	1 (Yakushev et al., 2007)

Formatted: Font: Times New Roman, Bold

Table 5. Modelled and observed* ranges of porewater concentration of studied components and its benthic fluxes.

Table 3.3. Carbon

Parameter	Notation	Units	Value	Reference ranges
Specific rate of $CaCO_3$ dissolution	water column concentration, µMK_caco3_diss / porewater concentration, µM	benthic flux, mmol m^{-2} d^{-1} / d^{-1}	3	wide ranges are given in (Luff et al., 2001)

	modelled	observed	modelled	observed	modelled	observed
O_2Specific rate of $CaCO_3$ formation	0 – 320K_caco3_prec		0 – 360 d^{-1}			0 – 2*10-4 / -4 – -13wide ranges are given in (Luff et al., 2001)
Solubility product constant for CaCO3	K_caco3					Calculated as a function of T, S (Roy et al., 1993b)
NO_3Specific rate of CH_4 formation from DON	0 – 26K_DON_ch4	0 – 10	0 – 2	0 – d^{-1}	0.5 – 2	-0.5 2.*10-5 / (Lopes et al., 2011)
Specific rate of CH_4 formation from PON	K_PON_ch4			d^{-1}		1*10-5 / (Lopes et al., 2011)
NO_2Specific rate of CH_4 oxidation with O_2	0 – 0.3K_ch4_o2			0 – uM-1d-1	0 – 4.5.14	0 – 2.8 / -0.1 – 0.10.14 (Lopes et al., 2011) / –
NH_4Specific rate of CH_4 oxidation with SO_4	0.1 – 16K_ch4_so4			0 – 25uM-1d-1	80 – 3000.0000274	50 – 300(0.0274 m3 /mol-1 day-1 (Lopes et al., 2011) / 0.03 – 1 / -1 – 6

PO_4	0 – 4	0 – 6	5 – 50	5 – 100	0.01 – 0.2	-1 – 1.5
Si	0 – 300	1 – 150	200 – 1400	100 – 600	0.5 – 15	1.7 – 11
pH	7.0 – 8.3	6.9 – 8.4	6.6 – 7.3	7.1 – 7.9		
DIC	–	–	–	–	1 – 20	5 – 50
Alk	2200–2300	-2000 – 3300	3000–4900	2000–20000	-1 – 5	3 – 200
MnII	0 – 1.5	0 – 12	8 – 20	5 – 200	0.01 – 0.1	-3 – 20
FeII	0 – 1.5	0 – 1.6	8 – 40	0.5 – 100	0.01 – 0.1	0.03 – 1

Split Cells
Deleted Cells
Formatted Table
Inserted Cells
Inserted Cells
Formatted
Formatted
Formatted
Formatted
Formatted
Formatted
Formatted
Deleted Cells
Deleted Cells
Formatted
Formatted Table
Formatted
Formatted
Formatted
Formatted
Inserted Cells
Formatted
Formatted Table
Formatted
Deleted Cells
Deleted Cells
Formatted
Deleted Cells
Formatted
Formatted
Formatted
Formatted
Formatted
Formatted Table
Formatted
Formatted
Formatted
Formatted
Formatted
Formatted
Deleted Cells
Formatted
Deleted Cells
Formatted

Table *Pakhomova et al., 2007; Almroth et al., 2011; Queirós et al., 2014

Formatted: Font: Bold

Formatted: Line spacing: 1,15 li

3.4. Ecosystem parameters

Table 6. Typical concentrations (ranges of concentrations) of alkalinity in the seawater (in µM).

Parameter	Notation	Units	Value, µM, in oxic (/anoxic) conditions	Source/Reference ranges

Formatted: Font: 10 pt, I
Formatted: Justified, Spa pt
Formatted: Font: 9 pt
Formatted: Centered, Rig cm, Space Before: 0 pt, A
Inserted Cells
Formatted: Right: -0,04 Before: 0 pt, After: 0 pt

			ions	
Bacteria				
A_{TCO_2}Baae maximum specific growth rate	K_Baae_gro	d-1	$(HCO_3^-)^{+2}(CO_3^{-2})^{-1}$	2306*10-2 (Yakushevet al. ..2000

Formatted Table
Deleted Cells
Inserted Cells
Inserted Cells
Formatted: Left, Space B After: 0 pt, Don't adjust s between Latin and Asian te adjust space between Asia
Formatted: English (U.S.
Formatted: Justified, Rig cm, Space Before: 0 pt, A
Formatted: Right: -0,04 Before: 0 pt, After: 0 pt
Formatted: English (U.K.

					7)	)
~~A_B~~	~~$[B(OH)_4^-]$~~		~~100~~	~~Typical seawater (Millero, 2008; Dickson, 2012)~~		
~~A_{DOM}~~	~~DOC (15%~~Baae specific rate of ~~total)~~mortality			~~6-75K_~~Baae_mrt	~~Sea water (Cranfield~~ e	5 * 10-3	5* 10-3 (Yakushev et al., 2007)

Deleted Cells

Formatted: English (U.K.

Formatted: Left, Space B After: 0 pt, Don't adjust s between Latin and Asian te adjust space between Asia

Formatted: Right: -0,04 Before: 0 pt, After: 0 pt

Inserted Cells

Formatted Table

Inserted Cells

			t a l . , 2 0 0 5 , K e p k a y , 2 0 0 0) d - 1		
A_{TH2S}Baae increased specific rate of mortality due to H_2S		[H S -] K _ B	d - 1	< 0 / 5 0 . 8 9 9	Bla ck Sea (V olk ov et al., ,

Formatted: Left, Space B
After: 0 pt, Don't adjust s
between Latin and Asian te
adjust space between Asia

Inserted Cells

Formatted: Justified, Rig
cm, Space Before: 0 pt, A

Formatted: Right: -0,04
Before: 0 pt, After: 0 pt

	aae_mrt_h2s			2000) 0.899 (Yakushev et al., 2007)
A_{Si} Bhae maximum specific growth rate	$(Si(OH)_4)_3 K_{Bhae\_gro}$	10^{-40} d^{-1}	Blake Sea (Volkov et al.,	0.5 (Yakushev et al., 2007)

Formatted: Left, Space B
After: 0 pt, Don't adjust s
between Latin and Asian te
adjust space between Asia

Formatted: Right: -0,04
Before: 0 pt, After: 0 pt

Inserted Cells

			2000)0.5		
A_{TPO4}Bhae specific rate of mortality	K_Bhae_mrt	d-1	(HpO4-1+2fpO4-1—fH3pO4	2/72*10-2(Yakushevet al..,	Blaek Sea (Volkov et al., 20

Inserted Cells

Inserted Cells

Formatted: Left, Space B
After: 0 pt, Don't adjust s
between Latin and Asian te
adjust space between Asia

Formatted Table

Formatted: Right: -0,04
Before: 0 pt, After: 0 pt

Formatted: Justified, Rig
cm, Space Before: 0 pt, A

Deleted Cells

			12*10-2	007)	00)
ATNH3Bhae increased specific rate of mortality due to H_2S	tNH3 tK_Bhae_mrt_h2s	<2/5d-1	Blaek Sea (Volkov et al., 2000	0.799 (Yakushev et al., 2007)	

Formatted: Left, Space B
After: 0 pt, Don't adjust s
between Latin and Asian te
adjust space between Asia

Formatted: Right: -0,04
Before: 0 pt, After: 0 pt

Inserted Cells

				0.799	
A_{THF}	[HF] (total F)	68	Typical seawater (Millero, 2008; Dickson, 2012)		
[OH⁻]	[OH⁻]	8	Typical seawater (Millero, 2008; Dickson, 2012)		
[H⁺]Baan maximum specific growth rate	[H]	d⁻	0.	Typic	

Formatted: Left, Space B
After: 0 pt, Don't adjust s
between Latin and Asian te
adjust space between Asia

Inserted Cells

Formatted: Justified, Rig
cm, Space Before: 0 pt, A

Formatted: Right: -0,04
Before: 0 pt, After: 0 pt

	~~*~~ ~~)~~ ~~(~~ ~~pH~~ ~~=~~ ~~8~~ ~~.~~ ~~1~~ ~~5~~ ~~1~~ ~~NBS~~ ~~)~~ K_Baan_gro	1	~~0~~ ~~0~~ ~~7~~ 12	~~al sea water (Mille ro, 1979)~~ 0.12 (Yakushev et al., 2007)
Baan specific rate of mortality	K_Baan_mrt	d-1	1.2*10-2	1.2*10-2 (Yakushev et al., 20

Formatted: Not Superscr

				07)
A_{TSO4}Bhan maximum specific growth rate	[HSO4=]K_Bhan_gro	d-1	0.0015-0.019	Typical seawater (Hoffmann et al., 2008) 0.19 (Yakushev et al., 2007)
Bhan specific rate of mortality	K_Bhan_mrt	d-1	7*10-3	7*10-3 (Yakushev et al., 2007)
Bhan increased specific rate of mortality due to O_2	K	d	0	0.8

Inserted Cells

Formatted: Left, Space B After: 0 pt, Don't adjust s between Latin and Asian te adjust space between Asia

Formatted: Justified, Rig cm, Space Before: 0 pt, A

Formatted: Right: -0,04 Before: 0 pt, After: 0 pt

Formatted: English (U.S.

	_Bhan_mrt_o2	-1	.899	99 (Yakushev et al., 2007)
Limiting parameter for bacteria grazing by Het	limGrazBac	-	2	2 (Yakushev et al., 2007)
Limiting parameter for bacteria anaerobic heterotrophic	limBhan	-	2	2 (Yakushev et al., 2007)
Limiting parameter for bacteria aerobic heterotrophic	limBha	-	5	5 (Yakushev et

	e			al., 2007)
Limiting parameter for bacteria anaerobic autotrophic	limBaan	-	2	2 (Yakushev et al., 2007)
Limiting parameter for nutrient consumption by Baae	limBaae	-	2	2 (Yakushev et al., 2007)
Phytoplankton				
Maximum specific growth rate	K_phy_gro	d^{-1}	4.8	0.9 - 1.3 (Savchuk, 2002), 3.0 (Gregoire and La

				croix, 2001)
Optimal irradiance	I_{opt}	$W m^{-2}$	25	50 (Savchuk, 2002)
1st coefficient for growth dependence on t	b_m	$°C^{-1}$	0.12	
2d coefficient for growth dependence on t	c_m	-	1.4	
Specific rate of mortality	K_{phy_mrt}	d^{-1}	0.15	0.3 - 0.6 (Savchuk, 2002), 0.05 (Gregoire and Lacroix, 2001)

Specific rate of excretion	K	d^{-1}	0.05	0.01 (Burchard et al., 2006)
Heterotrophs				
Maximum specific rate of grazing of Het on Phy	K_het_phy_gro	d^{-1}	1.0	0.9 (Gregoire and Lacroix, 2001), 1.5 (Burchard et al., 2006)
Half-saturation constant for the grazing of Het on Phy for Phy/Het ratio	K_het_	-	1.1	1 (Yakushev et

	phy_lim			al., 2007)
Maximum specific rate of grazing of Het on POM	K_het_pom_gro	d-1	0.7	1.2 (Burchard et al., 2006)
Specific respiration rate	K_het_res	d-1	0.02	1 (Yakushev et al., 2007)
Half-saturation constant for the grazing of Het on POM in dependence to ratio POM/Het	K_het_p	-	0.2	0.2 (Yakushev et al.,

	om_lim			2007)
Maximum specific rate of mortality of Het	K_het_mrt	d^{-1}	0.05	0.05(Gregoire and Lacroix, 2001)
Food absorbency for Heterotrophs	Uz	-	0.5	0.5 - 0.7 (Savchuk, 2002)
Ratio between dissolved and particulate excretes of Heterotrophs	Hz	-	0.5	0.5 (Gregoire and Lacroix, 2001)

Formatted: Font: Bold

Formatted: Level 2, Line Multiple 1,15 li

Table. 3.5. Sinking

Parameter	Notation	Units	Value	Reference ranges
Rate of sinking of Phy	Vphy	m d^{-1}	1	0.1-0.5 (Savchuk, 2002)
Rate of sinking of Het	Vhet	m d^{-1}	1	1 (Yakushev et al., 2007)
Rate of sinking of bacteria (Bhae, Baae, Bhan, Baan)	Vbact	m d^{-1}	0.4	0.5 (Yakushev et al., 2007)
Rate of sinking of detritus (PON)	Vsed	m d^{-1}	6	0.4 (Savchuk, 2002), 1-370 (Alldredge and Gotschalk, 1988)
Rate of sinking of inorganic particles (Fe and Mn hydroxides, carbonates)	Vm	m d^{-1}	8	6-18 (Yakushev et al., 2007)

Table 4. Rates of biogeochemical production/consumption of the model compartments

Formatted: Caption;Figu

Table 4.1. Nutrients and oxygen

Parameter	Rate
O_2	$R\,O_2 = (GrowthPhy - RespHet - DcDM\_O2 - DcPM\_O2) * r\_o\_n - 0.25 * mn\_ox1 - 0.25 * mn\_ox2 - 0.25 * fe\_ox1 - 0.5 * hs\_ox - 0.5 * s0\_ox - 0.5 * s2o3\_ox - 0.5 * mns\_ox - 1.5 * Nitrif1 - 0.5 * Nitrif2 - 2.25 * fes\_ox - 3.5 * fes2\_ox - 0.5 * mnco3\_ox + feco3\_ox - 2 * ch4\_o2$
Particulate Organic Nitrogen (PON)	$R\,PON = MortBaae + MortBaan + MortBhae + MortBhan + MortPhy + MortHet + Grazing * (1 - Uz) * (1 - Hz) - GrazPOP) - autolysis - DcPM\_O2 - DcPM\_NOX - DcPM\_SO4 - DcPM\_Mn - DcPM\_Fe - 0.5 * DcPM\_CH4$
Dissolved Organic Nitrogen (DON)	$R\,DON = autolysis - DcDM\_O2 - DcDM\_NOX - DcDM\_SO4 - DcDM\_Mn - DcDM\_Fe - 0.5 * DcPM\_CH4 - HetBhae - HetBhan + ExcrPhy + Grazing * (1 - Uz) * Hz$
NH_4	$R\,NH_4 = Dc\_OM\_total - Nitrif1 - anammox + 0.75 * s0\_ox + s2o3\_ox - ChemBaae - ChemBaan + RespHet - GrowthPhy * \frac{LimNH4}{LimN}$
NO_2	$R\,NO_2 = Nitrif1 - Nitrif2 + Denitr1 - Denitr2 - anammox - GrowthPhy * \frac{LimNO3}{LimN} * \frac{\mathbf{NO_2}}{\mathbf{NO_2} + \mathbf{NO_3} + 10^{-5}}$

NO_3	$R\,NO_3 = Nitrif2 - Denitr1 - 1.6 * hs\_no3 - 0.75\ s0\_ox - s2o3\_ox - GrowthPhy * \left(\frac{LimNO_3}{LimN}\right) ** \left(\frac{\mathbf{NO_3} + 10^{-5}}{\mathbf{NO_2} + \mathbf{NO_3} + 10^{-5}}\right)$
PO_4	$R\,PO_4 = \frac{GrowthPhy + RespHet + Dc\_OM\_total - ChemBaae - ChemBaan}{r\_n\_p} + fe\_p\_compl + mn\_p\_compl$
Si	R Si= (ExcrPhy-GrowthPhy)*r_si_n +fe_si_compl
Si particulate	$R\ Si\ part = -K\_sipart\_diss * \mathbf{Si\ part} + (MortPhy + GrazPhy) * r\_si\_n)$

Formatted: English (U.S.

Table ~~FIGURES:~~

4.2. Redox metals and sulfur

Parameter	Rate
Mn(II)	$R\,Mn2 = mn\_rd2 - mn\_ox1 + mns\_diss - mns\_form - mnco3\_form + mnco3\_diss + 0.5 * fe\_ox2 + (DcDM\_Mn + DcPM\_Mn) * r\_mn\_n$
Mn(III)	$R\,Mn3 = mn\_ox1 - mn\_ox2 + mn\_rd1 - mn\_rd2$
Mn(IV)	$RMn4 = mn\_ox2 - mn\_rd1 - 0.5 * fe\_ox2 + mnco3\_ox - (DcDM\_Mn + DcPM\_Mn) * r\_mn\_n$
MnS	$R\,MnS = mns\_form - mns\_diss$
$MnCO_3$	$R\,MnCO_3 = mnco3\_form - mnco3\_diss - mnco3\_ox$
Fe(II)	$R\,Fe2 = fe\_rd - fes\_form - fe\_ox1 - fe\_ox2 + fes\_diss - feco3\_form + feco3\_diss + fes2\_ox + 4 * r\_fe\_n * (DcDM\_Fe + DcPM\_Fe)$
Fe(III)	$R\,Fe3 = fe\_ox1 + fe\_ox2 - fe\_rd + fes\_ox + feco3\_ox - 4 * r\_fe\_n * (DcDM\_Fe + DcPM\_Fe)$
FeS	$R\,FeS = fes\_form - fes\_diss - fes\_ox - fes2\_form$
FeS_2	$R\,FeS_2 = fes2\_form - fes2\_ox$
$FeCO_3$	$R\,FeCO_3 = feco3\_form - feco3\_diss - feco3\_ox$

H_2S	$R\,H_2S = 0.5 * s0\_disp - hs\_no3 + s2o3\_rd - fes2\_form - 0.5 * mn\_rd1 - 0.5 * mn\_rd2 - 0.5 * fe\_rd - hs\_ox + fes\_diss - fes\_form + mns\_diss - mns\_form$
S^0	$R\,S^0 = hs\_ox + 0.5 * mn\_rd1 + 0.5 * mn\_rd2 + 0.5 * fe\_rd - s0\_ox - s0\_disp - s0\_no3$
S_2O_3	$R\,S_2O_3 = 0.5 * s0\_ox - s2o3\_ox + 0.25 * s0\_disp + 0.5 * so4\_rd - 0.5 * s2o3\_rd - s2o3\_no$
SO_4	$R\,SO_4 = hs\_no3 - so4\_rd + 0.5 * s2o3\_ox + s0\_no3 + 2 * s2o3\_no3 + fes\_ox + 2 * fes2\_ox$

Table 4.3. Carbon and alkalinity

Parameter	**Rate**
DIC	$R\,DIC = caco3\_diss - caco3\_form - mnco3\_form + mnco3\_diss + mnco3\_ox - feco3\_form + feco3\_diss + feco3\_ox + (Dc\_OM\_total - ChemBaae - ChemBaan - GrowthPhy + RespHet) * r\_c\_n$
$CaCO_3$	$R\,CaCO3 = caco3\_form - caco3\_diss$
CH_4	$R\,CH4 = ch4\_form - ch4\_ox$
Total alkalinity	$R\,Alk = dAlk$

Table 4.4. Ecosystem parameters

Parameter	**Rate**
Phytoplankton	$R\,Phy = GrowthPhy - MortPhy - ExcrPhy - GrazPhy$
Heterotrophs	$R\,Het = Uz * Grazing - MortHet - RespHet$
Aerobic heterotrophic bact.	$R\,Bhae = HetBhae - MortBhae - GrazBhae$
Aerobic autotrophic bact.	$R\,Baae = ChemBaae - MortBaae - GrazBaae$
Anaerobic heterotrophic bact.	$R\,Bhan = HetBhan - MortBhan - GrazBhan$
Anaerobic autotrophic bact.	$R\,Baan = ChemBaan - MortBaan - GrazBaan$

.

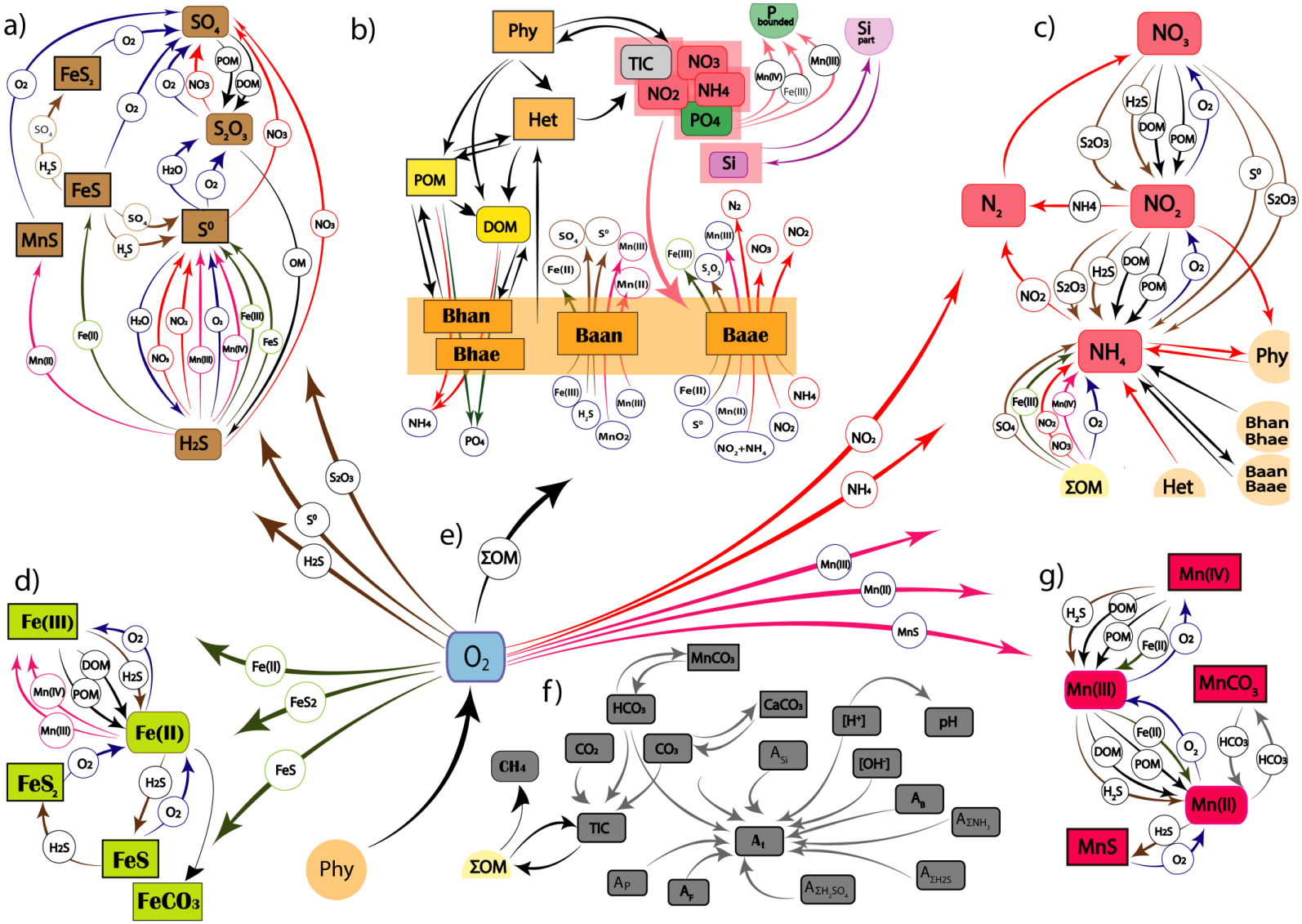

Figure 1. Flow-chart of biogeochemical processes represented in the Benthic RedOx Model (BROM~~.~~), showing the transformation of sulphur species (a), the ecological block (b), the transformation of nitrogen species (c), the transformation of iron species (d), the processes affecting dissolved oxygen (e), the carbonate system and alkalinity (f), and the transformation of

Formatted: Caption;Figu

manganese species (g).

~~Figure 2.~~

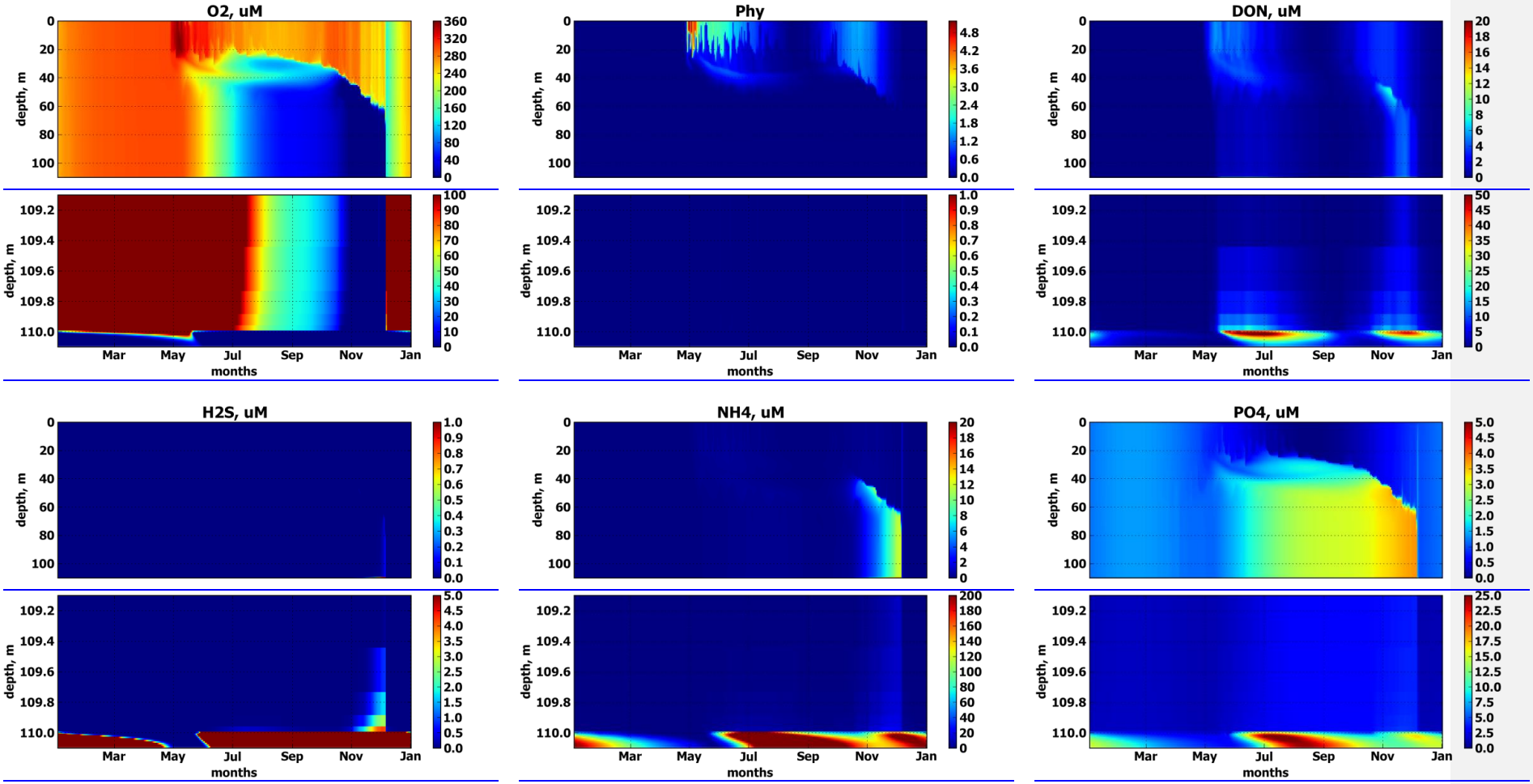

Figure 2. Simulated seasonal variability of the selected modelled chemical parameters (µM), in the water column (top panels) and in the benthic boundary layer and sediments (bottom panels).

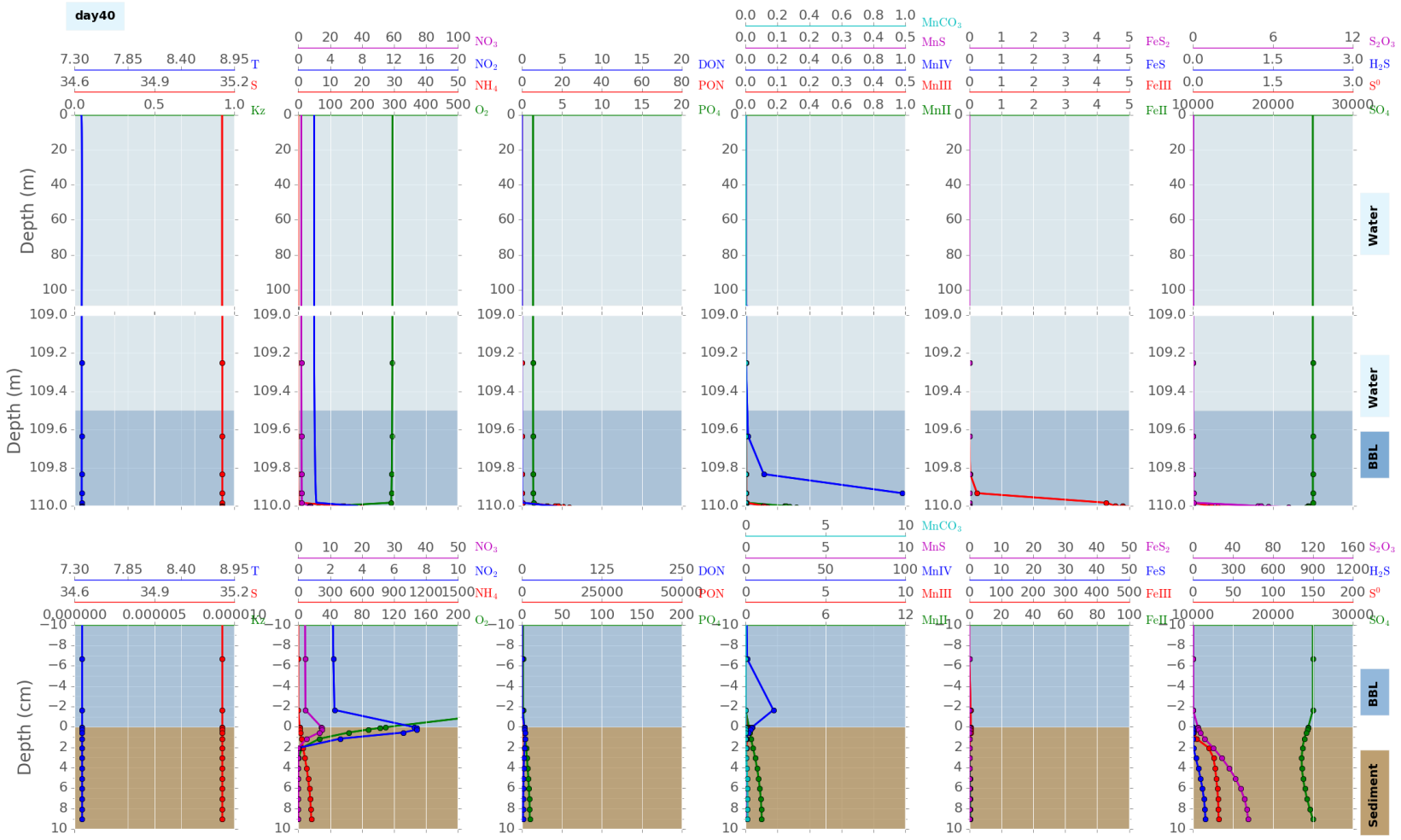

Figure 3. Vertical distributions of the modelled chemical parameters (µM), biological parameters (µM N), temperature (°C), salinity (PSU) and vertical ~~transport coefficient~~diffusivity (10^{-3} m^2s^{-1}) ~~in~~during the winter period of well-mixed conditions ~~(day 90) in~~, showing the water column ~~0-90 m (white background), the 50 cm thick BBL (90-90.5 m, (~~light ~~grey background)~~blue), the benthic boundary layer (dark blue),~~ and ~~12 cm upper sediment pore water (90.5-90.62, dark grey background~~the sediments (light brown).

Formatted: Superscript
Formatted: Caption;Figu
Formatted: Superscript
Formatted: Superscript
Formatted: Superscript

~~Figure 3.~~

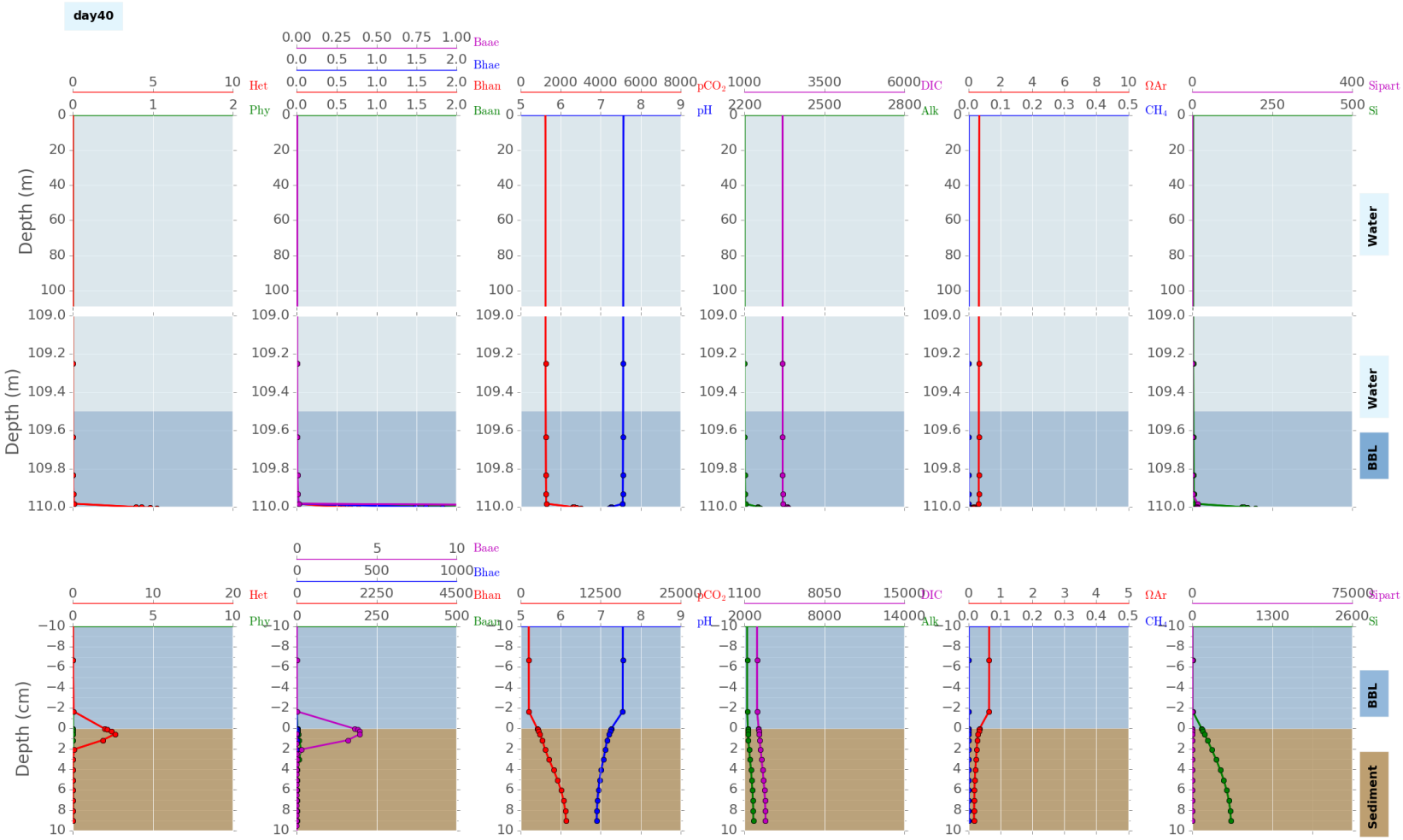

Figure 3 contd. Vertical distributions of the modelled chemical parameters (µM) and biological parameters (µM N) during the winter period of well-mixed conditions, showing the water column (light blue), the benthic boundary layer (dark blue), and the sediments (light brown).

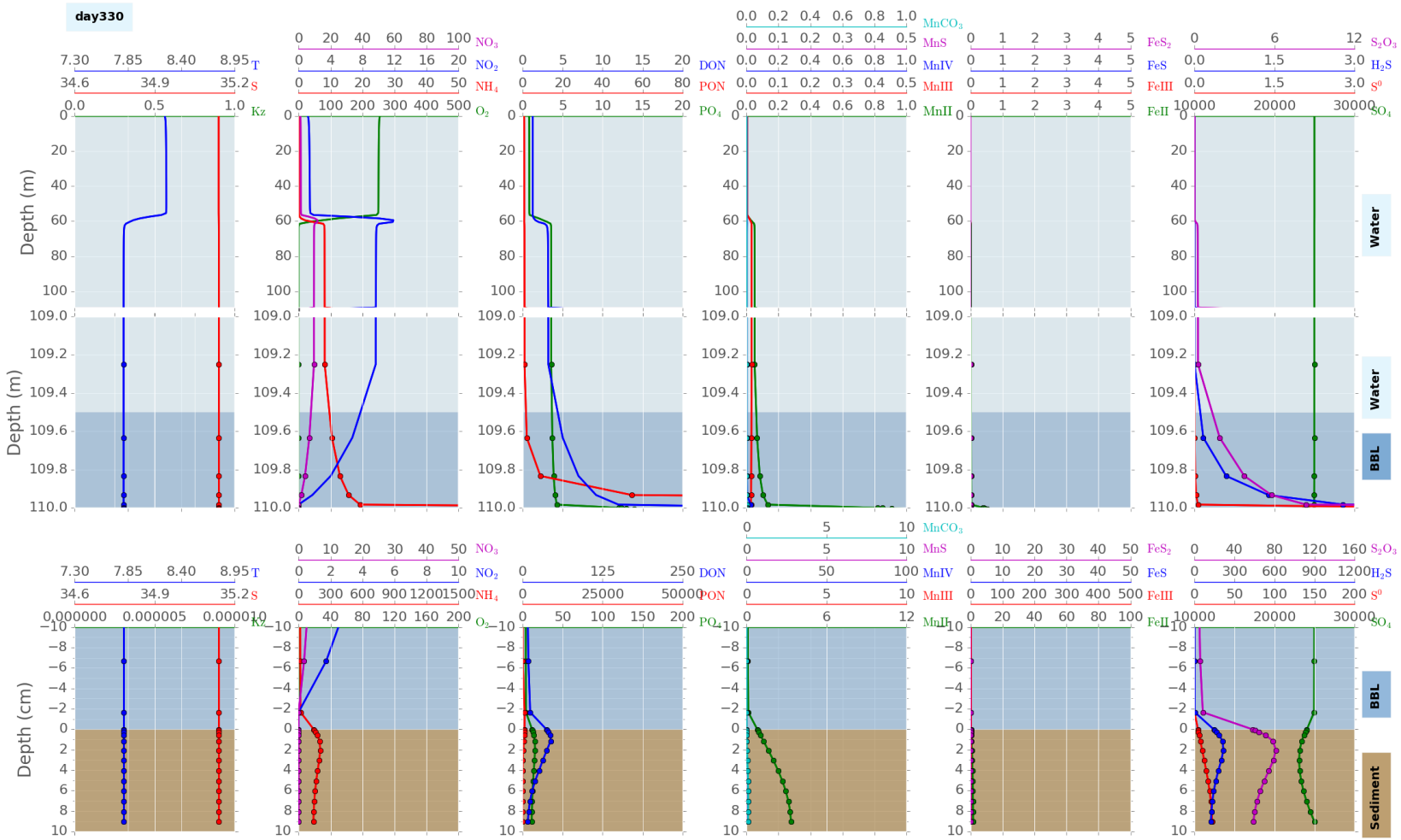

Figure 4. **Vertical distributions of the modelled chemical parameters (µM), biological parameters (µM N), temperature (°C), salinity (PSU) and vertical ~~transport coefficient~~diffusivity (10^{-3} $m^2 s^{-1}$) ~~in~~during the period of ~~organic matter production and formation of pycnocline (day 215) in~~bottom anoxia, showing the water column ~~0-90 m (white background~~(light blue), the ~~50 cm thick BBL (90-90.5 m, light grey background) and 12 cm upper sediment pore water (90.5-90.62,~~ benthic boundary layer (dark ~~grey background),~~ blue), and the sediments (light brown).

Formatted: Superscript
Formatted: Caption;Figu
Formatted: Superscript
Formatted: Superscript
Formatted: Superscript

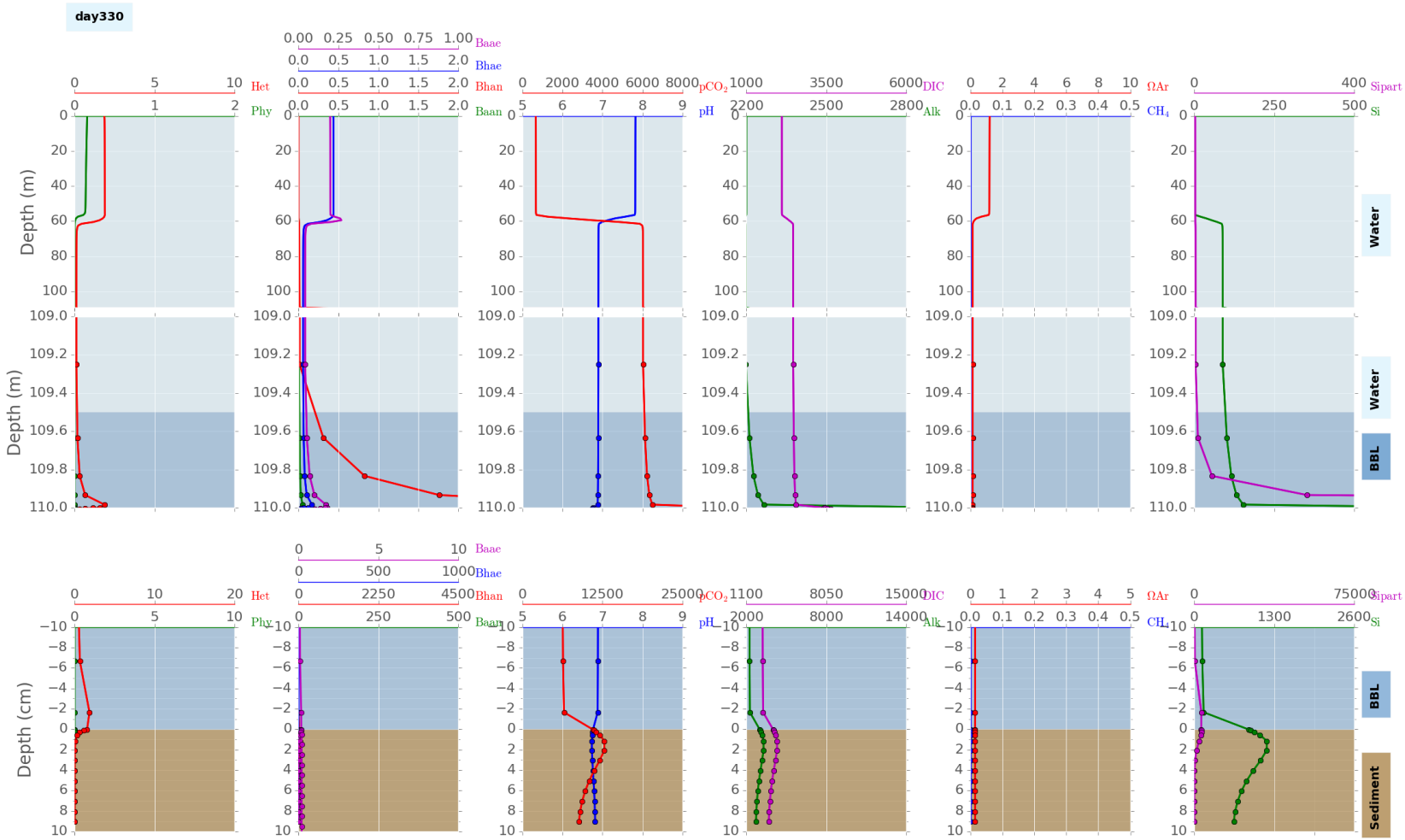

Figure 4.~~.~~ contd. Vertical distributions of the modelled chemical parameters (µM~~),~~) and biological parameters (µM N~~), temperature (oC), salinity (PSU) and vertical transport coefficient (10 3m2s 1) in~~) during the period of ~~stagnation and~~ bottom anoxia ~~(day 300) in~~, showing the water column ~~0 90 m (white background~~(light blue~~)~~, the ~~50 cm thick BBL (90 90.5 m, light grey background) and 12 cm upper sediment pore water (90.5 90.62, dark grey background).~~benthic boundary layer (dark blue), and the sediments (light brown).

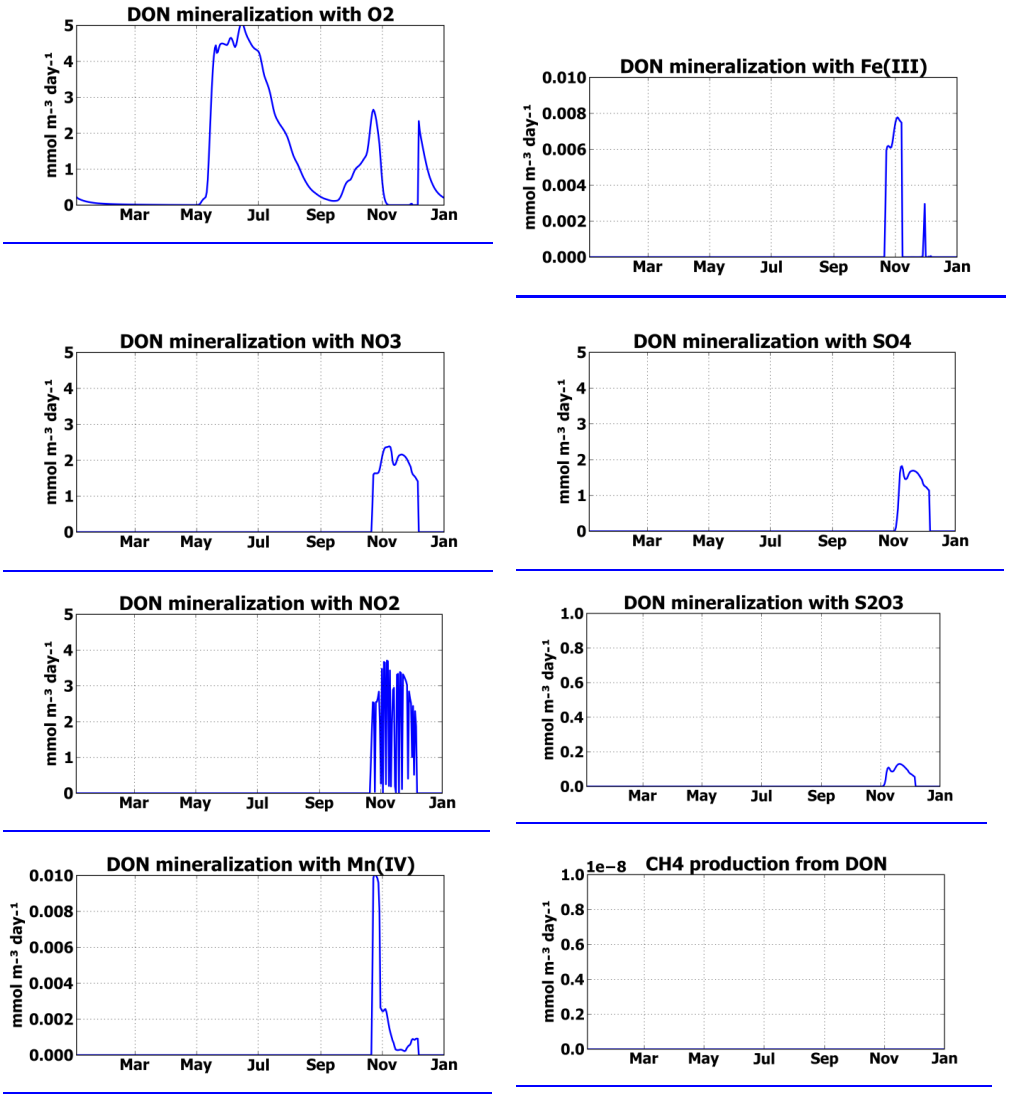

Figure 5. ~~Vertical distributions of the modelled carbonate system parameters in the winter well-mixed conditions (day 90), in the period of organic matter production and formation of pycnocline (day 215) in the period of stagnation and bottom anoxia (day 300) in the water column 0-90 m (white background), the 50-cm thick BBL (90-90.5 m, light grey background) and 12 cm upper sediment pore water (90.5-90.62, dark grey background).~~

~~Figure 6.~~ Simulated seasonal variability of ~~the modelled chemical parameters (μM), biological parameters (μM N), temperature (oC), salinity (PSU) and vertical transport coefficient (10-3m2s-1). The dotted line corresponds to the sediment-BBL boundary and the dashed line to the BBL-water column boundary.~~

~~**Figure 7. Simulated seasonal variability of vertical fluxes of**~~**biogeochemical transformation rates just above the sediment water interface, showing the rates of DON mineralization with oxygen, nitrate, nitrite, Mn(IV), ~~Mn(III),~~ Fe(III), SO4, S2O3, and CH4 production from DON. Units are mmol m^{-3} d^{-1}.**

Formatted: Left: 1,65 cm, Right: 1,65 cm, Top: 1 cm, Bottom: 2,36 cm, Width: 21 cm, Height: 29,7 cm, Header distance from edge: 0 cm, Footer distance from edge: 1,3 cm, From text: 0,4 cm

Formatted: Left, Space After: 10 pt, Line spacing: Multiple 1,15 li

Formatted: Don't adjust space between Latin and Asian text, Don't adjust space between Asian text and numbers

Formatted: Font: MS Shell Dlg 2, 8 pt

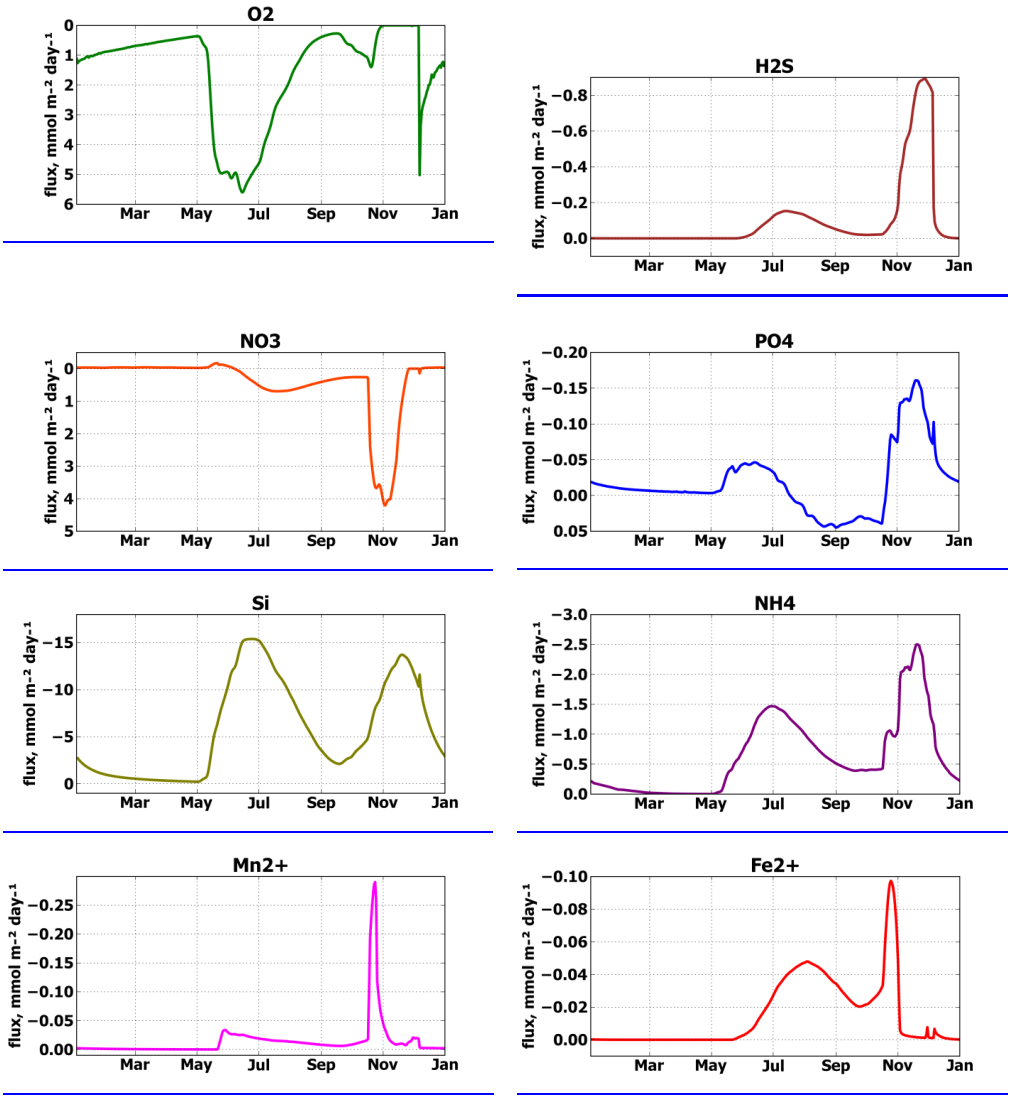

Figure 6. Simulated seasonal variability of vertical diffusive fluxes from the benthic boundary layer to the sediments of oxygen, hydrogen sulphide, ~~phosphate~~nitrate, silicate, ammonia, ~~thiosulphate and elemental sulphur, directed upwards (^) or downwards (v) in mmol m2 d-1.~~

~~**Figure 8. Modelled vertical distributions of O2, pH, calcite saturation (Om_Ca) and Bioturbation (Bt) in day 90, winter: top row for (I) absence of bioturbation,(Mn(II) baseline rates of bioturbation Kz_bio=1. 10-11 m2s-1and Fe(II). Positive fluxes are downward and (III) overpriced rate of bioturbation Kz_bio=10. 10-11 m2s-1. Left column correspond to baseline chemosynthesis (A) k_Baan_gro = 0.012negative fluxes are upward. Units are mmol m^{-2} d^{-1} and increased chemosynthesis (B) k_Baan_gro = 0.060 d-1.~~**

Formatted: Font: MS Shell Dlg 2, 8 pt

Formatted: Don't adjust space between Latin and Asian text, Don't adjust space between Asian text and numbers

Formatted: Caption;Figur/Tabell-Nr

Formatted: Superscript

~~TABLES~~

~~Table 1. State variables of BROM. Concentrations are presented in micromoles for chemical variables and in micromoles of nitrogen for biological variables.~~

~~Table 2. Parameterization of the biogeochemical processes~~

~~Table 3.Parameters names, notations, values and units of the coefficients used in the model~~

~~**Table 4. Rates of biogeochemical production/consumption of the model compartments**~~

~~Table 5. Modelled and observed* ranges of porewater concentration of studied components and its benthic fluxes.~~

~~**Table 6. Typical concentrations (ranges of concentrations) of alkalinity in the seawater (in µM).**~~

Formatted: Line spacing: Multiple 1,15 li

Formatted: Font: Bold

Formatted: Font: Bold

Formatted: Level 2, Line spacing: Multiple 1,15 li

Formatted: Caption;Figur/Tabell-Nr

Formatted: English (U.S.)

Formatted: Caption;Figur/Tabell-Nr